UNIVERSIDAD DE CANTABRIA

PROGRAMA DE DOCTORADO EN BIOLOGÍA MOLECULAR Y BIOMEDICINA

TESIS DOCTORAL

Mecanismos epigenéticos en la diferenciación eritroide y linfoide: el regulador transcripcional CTCF y fármacos epigenéticos

PHD THESIS

Epigenetic mechanisms in erythroid and lymphoid differentiation: CTCF transcriptional regulator and epigenetic drugs

Realizada por: Lorena García Gaipo

Dirigida por: Mª Dolores Delgado Villar y Javier León Serrano

Escuela de Doctorado de la Universidad de Cantabria

Santander 2019

La **Dra. M. Dolores Delgado Villar**, Catedrática de Bioquímica y Biología Molecular de la Facultad de Medicina de la Universidad de Cantabria y el **Dr. Javier León Serrano,** Catedrático de Bioquímica y Biología Molecular de la Facultad de Medicina de la Universidad de Cantabria.

CERTIFICAN:

Que la Licenciada Lorena García Gaipo, ha realizado bajo su dirección el presente trabajo de Tesis Doctoral titulado “Mecanismos epigenéticos en la diferenciación eritroide y linfoide: el regulador transcripcional CTCF y fármacos epigenéticos” (“Epigenetic mechanisms in erythroid and lymphoid differentiation: CTCF transcriptional regulator and epigenetic drugs”).

Consideramos que este trabajo reúne los requisitos de originalidad y calidad científica necesarios para su defensa como Memoria de Doctorado por la interesada, al objeto de poder optar al grado de Doctor en Biología Molecular y Biomedicina de la Universidad de Cantabria.

Y para que conste y surta los efectos oportunos, firmamos el presente certificado.

Santander, 23 de septiembre de 2019

Fdo. Mª Dolores Delgado Villar Fdo. Javier León Serrano

Esta Tesis ha sido realizada en el Instituto de Biomedicina y Biotecnología de Cantabria (IBBTEC) perteneciente a la Universidad de Cantabria (UC) y al Consejo Superior de Investigaciones Científicas (CSIC), en Santander (Cantabria, España).

La financiación para la realización de esta Tesis doctoral ha sido proporcionada por el Ministerio de Economía y Competitividad. Proyectos: SAF2014-53526-R “Oncoproteínas MYC y CTCF en el control transcripcional de la diferenciación hematopoyética y en linfoma” y SAF2017-88026-R “Interacciones funcionales de MYC y CTCF en células de linfoma B agresivo y precursores hematopoyéticos”. CoIPs: Javier León Serrano y Mª Dolores Delgado Villar.

La autora de esta Tesis ha disfrutado de un contrato predoctoral para la formación de doctores (referencia BES-2015-074537), concedido por el Ministerio de Economía y Competitividad.

AGRADECIMIENTOS

Hace ya siete años que, mirando la lista de los posibles trabajos de fin de máster, me decidí a hablar con Dolores Delgado para hacer mi trabajo con ella y su grupo, y esa ha sido una de las mejores decisiones que he tomado en mi vida. Sin apenas experiencia en un laboratorio, ella me acogió en su grupo y me dio la oportunidad de descubrir el increíble mundo de la investigación.

Si ya me sentía afortunada con todo lo que aprendí durante el TFM, mucho más cuando surgió la oportunidad de poder realizar la tesis con Dolores y Javier como directores. Volver a ese laboratorio en el que tanto aprendí y disfruté fue una gran alegría.

Agradecer enormemente a Dolores toda su confianza, esfuerzo y dedicación. Gracias por enseñarme tanto y por apoyarme en todos esos momentos de crisis en los que no entendíamos que podía estar pasando y parecía que nada tenía solución. Gracias por todas esas veces que me decías que te diera la lata y te insistiera para reunirnos y sobre todo por ser tú la que me insistía en hablar si veías que a mí se me olvidaba decírtelo. Gracias por ser más que una jefa, porque sé que estas para cualquier cosa que necesite tanto profesional como personal.

Gracias también a Javier, por sus consejos y su apoyo. Por sacar siempre tiempo para mí como para el resto del grupo, a pesar de su ajetreada vida. Gracias por transmitir tu pasión por la ciencia, pero también por el cine o la música.

Muchas gracias a los dos, porque juntos habéis conseguido crear un grupo de trabajo en el que es imposible estar mejor. Porque a un grupo así siempre apetece venir a trabajar.

Gracias también a los profesores del Departamento de Biología Molecular por hacerme un hueco en las prácticas de Bioquímica. Gracias a todos los grupos que han formado y forman parte de los “lab meetings” o “cáncer club”. Por todos los consejos e ideas que habéis aportado para mejorar mi trabajo.

Como ya he dicho, da gusto venir a trabajar a este grupo y una parte importante es toda la gente que se ha ido cruzando en mi camino. Encontrarme

con Lucía, una cara conocida, cuando empecé fue toda una suerte. Gracias porque sé que he sido muy pesada preguntándote de todo, pero tú siempre has tenido tiempo para ayudarme. Pero, sobre todo, gracias por hacerme reír, por tu risa contagiosa y nuestros ataques de risa, muchas veces en los momentos más inoportunos. Muchas gracias a Rosa, gracias por todo lo que me has ayudado y enseñado, sobre todo con las CD34. Gracias por todo tu apoyo no solo en temas del laboratorio. Muchas gracias a María, porque se hizo cargo de mí cuando llegue al laboratorio sin tener idea de nada y me aguantó siguiéndola y preguntándola constantemente, tanto que muchas veces ya intuía que la quería preguntar algo sin ni siquiera yo decir nada. Gracias a Judit y Ester, con las que más tiempo he pasado en este laboratorio. Gracias por vuestra ayuda y consejos. También quiero dar las gracias a todos aquellos con lo que he coincidido en el laboratorio, aunque fuera poco tiempo.

Muchas gracias al grupo “cafes random”, por hacer que el café de media mañana sea el momento relax del día, por hacer que esté lleno de risas y grandes historias.

Gracias también a todas las personas de otros grupos, a los Nachos, a los Pieros... por ayudarnos con cualquier duda y por dejarnos “robarles” material cuando nos urgía. Gracias especiales a Maria Aramburu por toda su ayuda con las citometrías y por hacerme huecos cuando parecía imposible encontrarlos. Gracias a todo el personal del IBBTEC, por toda su ayuda.

Sin duda alguna a los que más tengo que agradecer es a mis padres, gracias por todo el esfuerzo que habéis hecho para que yo pudiera estudiar lo que realmente me gustaba. Gracias por apoyarme cuando el futuro parecía algo negro y gracias por alegraros casi más que yo cuando empecé esta aventura. Muchas a gracias a mi hermana, Carmen, que, aunque no entiende lo que hago porque ella lo que no ve no lo cree, siempre la tengo a mi lado.

Muchas gracias a todos los que forman parte mi vida. A los lebaniegos que siempre están ahí, que durante estos últimos meses no han parado de preguntarme como lo llevaba y de animarme. A los santanderinos, que, aunque sé que les tengo un poco abandonados, siempre están cuando les necesito. Y a los leoneses que hicieron que mis años en León estén llenos de recuerdos inolvidables y que estudiar Biología fuera mucho más sencillo con ellos al lado.

Por último, muchas gracias a Diego, porque nuestra aventura empezó poco antes que la de la tesis y gracias a ti todo ha sido mucho más fácil. Gracias por escucharme (o hacer que me escuchabas) cuando te contaba mis problemas con los experimentos, aunque no entendieras nada de nada. Gracias por querer avanzar en nuestra aventura juntos y por todo lo que está por venir.

Muchas gracias a todos.

ABBREVIATIONS

ABC	Activated B-cell subtype
ac	Acetylation
AID	Activation-induced deaminase
ALL	Acute Lymphoblastic Leukemia
AML	Acute Myeloid Leukemia
APP	Amyloid Precursor Protein
Ara-C	1-β-D-arabinofuranosylcytosine or cytosine arabinoside
ASHM	Aberrant Somatic Hypermutation
BasoEB	Basophilic Erythroblast
BCL6	B-cell Lymphoma 6
BCL-xL	B-cell Lymphoma-extra-Large
BCR	B-cell receptor
BET	Bromodomain and Extraterminal domain
BETi	Bromodomain and Extraterminal domain Inhibitor
BFU-E	Burst Forming Unit-Erythroid
BL	Burkitt Lymphoma
BLIMP1	B-lymphocyte-induced maturation protein 1
bp	base pairs
BRD	Bromodomain
BSA	Bovine Serum Albumin
BTB/POZ	Domain for BR-C, tkk and bab/for Pox virus and Zinc Finger
CDK	Cyclin-Dependent Kinase
CDKN2A	Cyclin Dependent Kinase Inhibitor 2A
cDNA	Complementary DNA
CEN	Core Erythroid Network
CFU-E	Colony Forming Unit-Erythroid
CFU-GEMM	Colony forming unit-granulocyte, erythroid, macrophage and megakaryocyte

ChIA-PET	Chromatin Interaction Analysis with Paired-End Tag
ChIP seq	Chromatin immunoprecipitation followed by sequencing
ChIP	Chromatin Immunoprecipitation
Chr	Chromosome
CI	Combination Index
cKO	Conditional Knockout
CLL	Chronic Lymphocytic Leukemia
CLP	Common Lymphoid Progenitor
CMML	Chronic Myelomonocytic Leukemia
CMP	Common Myeloid Progenitor
CpG	Cytosine-phosphate-guanine
CSR	Class Switch Recombination
Ct	Cycle threshold
CTCF	CCCTC binding factor
CTCL	Cutaneous T-cell Lymphoma
CTS	CTCF binding site
DLBCL	Diffuse Large B-cell Lymphoma
DMEM	Dubelcco´s Modified Eagle Medium
DMSO	Dimethyl Sulphoxide
DNMT	DNA-Methyl Transferase
DNMTi	DNA-Methyl Transferase Inhibitor
Dox	Doxycycline
DZ	Dark Zone
EBV	Epstein-Barr Virus
EDTA	Ethylenediaminetetracetic acid
ENCODE	Encyclopedia of DNA Elements
EP	Erythroid Progenitor
EPO	Erythropoietin
EPO-R	EPO Receptor
ETS1	Erythroblastosis Oncogene 1
EV	Empty Vector
FBS	Fetal Bovine Serum

FDA	Food and Drug Administration
FISH	Fluorescence *In Situ* Hybridization
FL	Follicular Lymphoma
FLI1	Friend Leukemia Integration 1
FLT3L	FMS-like tyrosine kinase 3 ligand
FOG1	Friend Of GATA1
Fw	Foward
GATA	GATA-binding Factor
GC	Germinal Center
GCB	Germinal Center B-cell subtype
GMP	Granulocyte-Macrophage Progenitor
GPYA	Glycophorin-A
HAT	Histone Acetyl transferase
HDAC	Histone Deacetylase
HDACi	Histone Deacetylase Inhibitor
HEY1	Hairy/enhancer-of-split related with YRPW motif protein 1
HSC	Hematopoietic Stem Cell
HSS	DNA Hypersensitive Site
hTERT	Human Telomerase Reverse Transcriptase
IC_{50}	Half-maximal Inhibitory Concentration
ICR	Imprinted Control Region
Ig	Immunoglobulin
IL	Interleukin
IRF4	Interferon Regulatory Factor 4
IRF8	Interferon Regulatory Factor 8
kb	kilobase
kDa	kilodalton
KDM	Lysine Demethylase
KLF1	Kruppel-like Factor 1
KMT	Lysine Methyltransferase
KO	Knockout
LB	Luria-Bertani
LCR	Locus Control Region

LDB1	LIM Domain Binding 1
LMO2	LIM Domain Only 2
LZ	Light Zone
M	Molar
MDS	Myelodysplastic Syndrome
me	methylation
MEP	Megakaryocyte-erythroid Progenitor
MINE	MYC insulator element
MLL	Mixed Lineage Leukemia
MM	Multiple Myeloma
MOI	Multiplicity of Infection
MPP	Multipotent Progenitor
mRNA	messenger RNA
MYB	Myeloblastosis oncogene
NFE2	Nuclear Factor Erythroid 2
NFE2L2	Nuclear Factor Erythroid like 2
NK	Natural Killer
NP-40	Nonidet-P40 or octyl phenoxylpolyethoxylethanol
nt	nucleotides
OrthoEB	Orthochromatic Erythroblast
PAGE	Polyacrylamide Gel Electrophoresis
PARP	Poly(ADP-Ribose) Polymerase
PAX5	Paired Box 5
PBS	Phosphate Buffer Saline
PCR	Polymerase Chain Reaction
PEG	Polyethylene glycol
PolyEB	Polychromatic Erythroblast
PRDM1	Positive Regulatory Domain 1
PRMT	Protein Arginine Methyltransferase
ProEB	Proerythroblast
PTCL	Peripheral T-cell Lymphoma
PTM	Posttranslational Modifications
qPCR	Quantitative Polymerase Chain Reaction

R10F	RPMI-10% FBS
RB	Retinoblastoma
RBC	Red Blood Cell
rDNA	Ribosomal DNA
RET	Reticulocyte
RFP	Red Fluorescence Protein
RIPA	Radioimmunoprecipitation assay buffer
romid	Romidepsin
rpm	revolutions per minute
RPMI	Culture medium Roswell Park Memorial Institute
RT-qPCR	Reverse Transcriptase and Quantitative PCR
Rv	Reverse
s.e.m.	standard error of the mean
SAHA	Suberoylanilide Hydroxamic Acid
SCF	Stem Cell Factor
SCL	Stem Cell Leukemia
SDS	Sodium Dodecyl Sulfate
SFEM	Serum Free Expansion Medium
ShCTCF	Short hairpin RNA against CTCF
SHM	Somatic Hypermutation
shRNA	Short hairpin RNA
TAD	Topologically Associated Domain
TAL1	TAL BHLH Transcription Factor 1
T-ALL	T-cell Acute Lymphoblastic Leukemia
TBS-T	Tris Buffer Saline-Tween20
TCF3	Transcription Factor 3
TF	Transcription Factor
TFG- β	Transforming Growth Factor β
TPA	Terephthalic Acid
TPO	Thyroid peroxidase
TSS	Transcription Start Site
WHO	World Health Organization
XBP1	X-Box Binding Protein 1
ZF	Zinc Finger

LIST OF FIGURES

INTRODUCTION

MATERIALS AND METHODS

RESULTS

DISCUSSION

LIST OF TABLES

INTRODUCTION

MATERIALS AND METHODS

RESULTS

INDEX

INDEX

INTRODUCTION

1. INTRODUCTION

1.1. The transcriptional regulator CTCF

The CCCTC-binding factor (CTCF) is a highly conserved zinc finger DNA-binding protein. CTCF is implicated in many regulatory functions, including transcriptional activation or repression, chromatin insulation, chromatin looping and long-range interactions. CTCF is also involved in the epigenetic regulation of many genes.

CTCF was originally discovered by two independent groups in 1990 (Baniahmad et al., 1990; Lobanenkov et al., 1990). Lobanenkov et al, identified CTCF as a DNA-binding protein which interacts with three repeats of the CCCTC sequence in its DNA binding site at the chicken c-*MYC* promoter. CTCF was also characterized as a nuclear protein that bound to promoter sequences in human, mouse and avian *MYC* gene and suppressed the transcription of the c-*MYC* gene (Filippova et al., 1996; Klenova et al., 1993; Lobanenkov et al., 1990). In addition, CTCF was independently discovered as a silencer protein (NeP1) which bound to an AT-rich sequence of the chicken lysozyme silencer (Baniahmad et al., 1990; Burcin et al., 1997). Furthermore, it was described the ability of CTCF to interact with the amyloid precursor protein-β (APPβ) site of the human *APP* promoter (Vostrov and Quitschke, 1997) and with the FII site within the HS4 enhancer-blocking region of the chicken β-globin locus (Bell et al., 1999). CTCF was finally described a *multivalent* factor due its ability to recognize multiple target sites (Ohlsson et al., 2001).

1.1.1. The CTCF protein

Human *CTCF* gene maps at the 16q22.1 chromosome (Filippova et al., 1998), a region frequently deleted in several human malignancies (Lasko et al., 1991). *CTCF* gene encodes a 727 amino acids protein composed of three domains: the N-terminal domain (amino acids 1 to 265), a central DNA-binding

domain which contains 11 zinc finger motifs (amino acids 265 to 580) and the C-terminal domain (amino acids 580 to 727) (**Figure 1.1a**). The central domain consists in 10 ZFs of the C_2H_2 type and 1 ZF of the C_2HC type (Klenova et al., 1993). The 11 zinc finger motives are stabilized by zinc ions binding to cysteine and histidine residues to form a compact structure to recognize and interact with the major groove of the DNA (Klug and Schwabe, 1995). The 93% of the amino acids sequence of the avian and mammalian CTCF proteins are identical. However, in the zinc finger domain the identity increases up to 100% (Filippova et al., 1996).

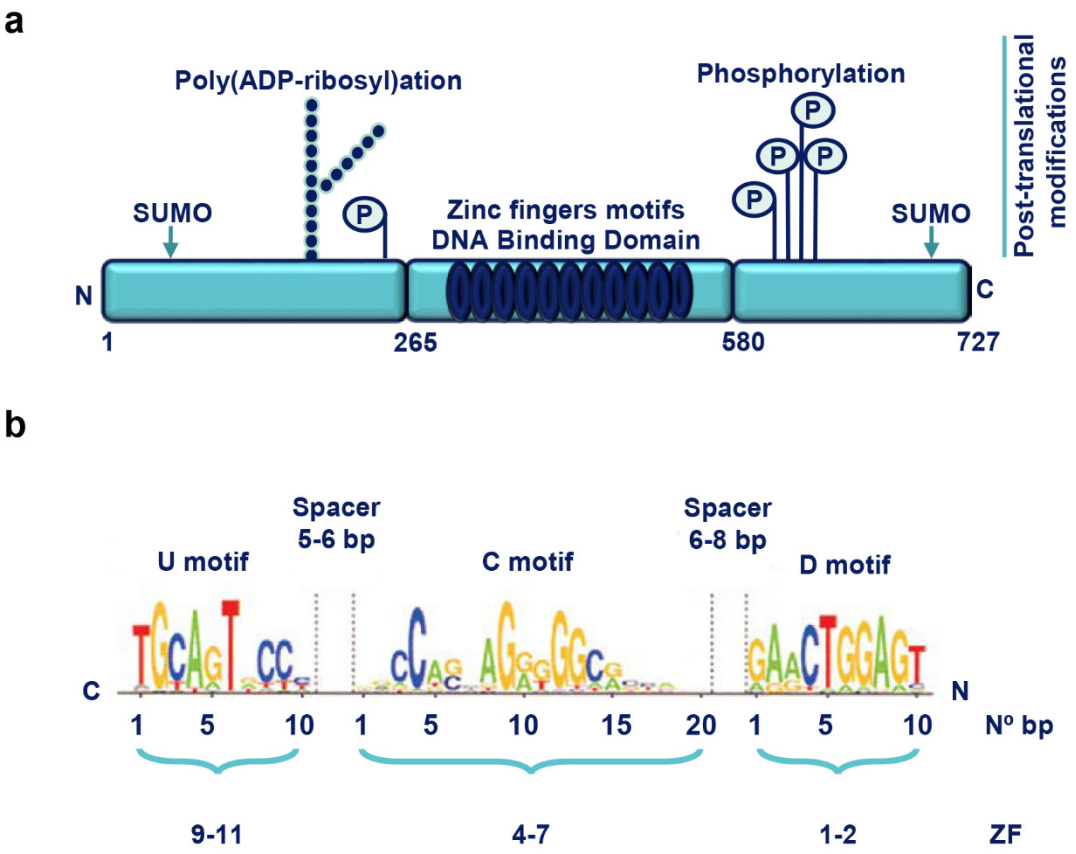

Figure 1.1. CTCF structure, post-translational modifications and binding motifs. *a) The scheme of the human CTCF proteins shows the N-terminal domain (amino acids 1 to 265), the central DNA-binding domain with the 11 zinc fingers (represented in dark blue) (amino acids 266 to 580) and the C-terminal domain (amino acids 581 to 727). The main post-translational modifications are also represented including phosphorylation (P), SUMOylation and poly(ADP-ribosyl)ation (Figure adapted from Ohlsson et al., 2010). B) CTCF DNA-binding consensus motifs D (downstream), C (core) and U (upstream). D motif is bound by fingers 1-2, C motif is bound by fingers 4-7 and the U motif is bound by fingers 9-11. Spacer sequences between DNA motifs are indicated in nucleotides (Figure adapted from Marshall et al., 2014).*

CTCF is expressed in various tissues and cells except primary spermatocytes (Klenova et al., 1993). CTCF is widely distributed within the nucleus (Klenova et al., 1993). CTCF can translocate to the nucleolus in myeloid cells and this localization is associated with cell differentiation and growth inhibition (Torrano et al., 2006). CTCF is also associated with centrosomes at metaphase (Rosa-Garrido et al., 2012; R. Zhang et al., 2004).

1.1.2. CTCF binding to DNA

CTCF is able to bind to many different DNA sequences called CTCF target sites (CTSs) using different combinations of the 11 zinc fingers. While the zinc finger domain was the major DNA binding region, the N-terminal and C-terminal domains also have a weak ability to interact with DNA (J. Guo et al., 2018).

Different groups of zinc fingers appear to be necessary for CTCF binding to some sequences but not necessary for others (Ohlsson et al., 2010). Initial studies revealed that mutations or deletions in the ZFs abolished CTCF binding and that only ZFs 4 to 7 were essential for binding to a core of 12 bp sequence found in different CTSs (Filippova et al., 2002, 1996; Renda et al., 2007). Kim et al, identified that ZFs 4 to 7 bound to a core of 15-20 bp motif in around 80% of CTCF target sites (Kim et al., 2007). Recent studies suggested that the ZFs recognize DNA fragments in groups: ZFs 4 to 7 target the CCCTC core motif (C), ZFs 1 to 2 recognize the downstream motif (D) and ZFs 9 to 11 the upstream motif (U) (Hashimoto et al., 2017; Nakahashi et al., 2013; Yin et al., 2017). The core motif is separated from the U motif by 5-6 nucleotides and from the D motif by 6-8 nucleotides. In the absence of the U motif, ZF 3 is important for binding and when D and U motifs are not present, ZFs 1-2 and 8 to 11 help to stabilize CTCF binding (Nakahashi et al., 2013). The linker regions between the zinc fingers are flexible to adopt multiple conformations and allow the recognition of different DNA sequences (Xu et al., 2018) (**Figure 1.1b**).

In the mammalian genome, CTCF is present at 40,000 to 80,000 sites depending on the cellular context (Chen et al., 2012). More than 70,000 CTSs were identified in different cell lines and near 50,000 CTSs showed cell-type

specific distribution (Wang et al., 2012). Most of the CTCF target sites are located in intergenic regions and sites upstream of transcription start sites (TSSs) while near the 15% are located near promoters and the 40% of CTSs are within introns and exons (Ong and Corces, 2014; Song and Kim, 2017).

1.1.3. Post-translational modifications of CTCF

Different post-translational modifications including poly(ADP-ribosyl)ation (PARylation), phosphorylation and SUMOylation, are important for the regulation of the CTCF activity (**Figure 1.1a**).

CTCF can suffer PARylation by the poly(ADP-ribose) polymerase enzymes. PARylation at Glu239 and Glu243 residues regulates CTCF activity as a chromatin insulator and is implicated in the control of imprinting (Yu et al., 2004). CTCF poly(ADP-ribosyl)ation also mediates its translocation to the nucleolus and ribosomal gene transcription inhibition (Torrano et al., 2006). PARylated CTCF is recruited to the sites of DNA damage with an important role in early DNA damage response (Han et al., 2017). Loss of CTCF PARylation is associated with cell proliferation and tumorigenesis (Docquier et al., 2009).

The protein kinase CK2 can phosphorylate CTCF at four serine residues of the SKKEDSSDSE motif in the C-terminal domain (Ser604, Ser609, Ser610 and Ser612) (El-Kady and Klenova, 2005; Klenova et al., 2001). Phosphorylation switches CTCF function from a transcription repressor to an activator of the *MYC* promoter (El-Kady and Klenova, 2005). A novel phosphorylation site in Ser224 was recently described, associated with the G2/M transition of the cell cycle (Del Rosario et al., 2019). CTCF is also phosphorylated during mitosis in Thr289, Thr317, Thr346, Thr374, Ser402, Ser461 and Thr518 which are situated in the linker sequences of the zinc fingers (Sekiya et al., 2017). These phosphorylations reduce CTCF DNA-binding activity (Sekiya et al., 2017). In myeloid cells, CTCF is differentially phosphorylated upon induction of cell differentiation (Delgado et al., 1999).

Finally, CTCF can be SUMOylated at the N-terminal and C-terminal domains (Lys74 and Lys589) by the small ubiquitin-like modifiers 1, 2 and 3 (MacPherson et al., 2009; Yu et al., 2004). SUMOylation is related with the repressive function of CTCF on the *MYC* P2 promoter (MacPherson et al., 2009). SUMOylation of CTCF at the N-terminal domain represses transactivation and chromatin decondensation (Kitchen and Schoenherr, 2010).

1.1.4. CTCF interacting partners

Interactions between CTCF and other proteins are important in the regulation of CTCF functions. CTCF partners interact with CTCF through different domains. Nowadays the number of proteins recognized to interact with CTCF is continuously increasing. CTCF partners can be grouped into several functional groups: basal transcription, DNA-binding, epigenetic modifiers/chromatin modelers, multifunctional proteins and architectural proteins (Arzate-Mejía et al., 2018; Zlatanova and Caiafa, 2009) (**Figure 1.2**).

CTCF can interact with basal transcription factors. CTCF interacts and recruits the largest subunit of the RNA polymerase II to regulate transcription and insulator functions (Chernukhin et al., 2007). The general transcription factor II-I (TFII-I) binds to CTCF in promoter-proximal regions and co-operate with CTCF to recruit the cyclin-dependent kinase 8 (CDK8) to the promoter regions and enhance transcription initiation (Peña-Hernández et al., 2015).

The DNA-binding proteins group includes different transcription factors (activators or repressors) and cofactors. The Class II transactivator (CIITA) and the regulatory factor X (RFX) bind to CTCF and activate the transcription of the major histocompatibility complex class II genes (Majumder et al., 2006). The methyl-CpG binding protein Kaiso mediates enhancer-blocking activity of CTCF (Defossez et al., 2005) and contributes to epigenetic silencing of the retinoblastoma protein (pRB) (De La Rosa-Velazquez et al., 2007). Smad3 protein binds to CTCF at the Igf2/H19 imprinted control region (Bergström et al., 2010). The Y-box DNA/RNA-binding protein (YB1) interacts with CTCF to repress transcriptionally *MYC* (Chernukhin et al., 2000) and to activate the serotonin

transporter 5-HTT (Klenova et al., 2004). The Ying Yang 1 protein (YY1) is a ZF transcription factor which cooperates with CTCF in the transactivation of *Tsix* gene (Donohoe et al., 2007). CTCF also interacts with the DNA-binding proteins HOXA10, MYOD, OCT1, OCT4 and RBPJ. Our group described the interaction of CTCF with the transcription factor UBF to regulate the ribosomal genes transcription (van de Nobelen et al., 2010).

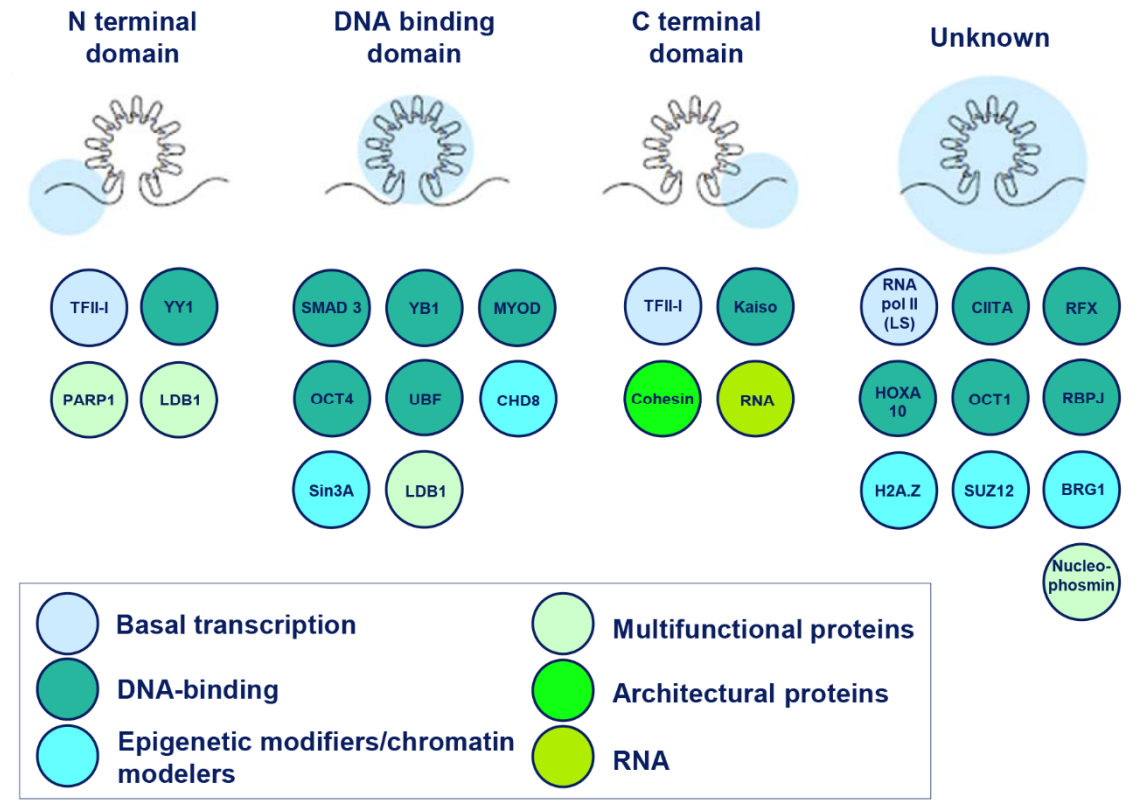

Figure 1.2. CTCF interacting partners and regions involved in the interactions. *CTCF partners are shown according to function: basal transcription, DNA-binding, epigenetic modifiers/chromatin modelers, multifunctional proteins, architectural proteins and RNA (color code are shown in the square). CTCF partners are located under the interacting CTCF domain: N terminal domain, DNA binding domain or C terminal domain (highlighting in blue). A number of proteins have been shown to interact with CTCF, although their binding has not been mapped to a specific domain (Figure adapted from Arzate-Mejía et al., 2018).*

The group of epigenetic modifiers and chromatin modelers includes structural proteins and enzymes. The chromodomain helicase DNA-binding protein 8 (CHD8) regulates CTCF-mediated intrachromosomal contacts (Ishihara et al., 2006). The histone variant H2A.Z that replaces H2A in nucleosomes was identified as a CTCF cofactor that co-localize with CTCF genome-wide (Barski et

al., 2007; Yusufzai et al., 2004). Sin3A recruits histones deacetylases and contributes to the transcriptional repressor activity of CTCF (Lutz et al., 2000). The Polycomb group repressor Suz12 has an important role in the regulation of the insulation function of CTCF at the H19 Imprinting Control Region (Li et al., 2008). Recently, it has been found that BRG1, the major ATPase subunit of the chromatin remodeling complex SWI/SNF, physically interacts with CTCF and mediates the effect of CTCF on transcription (Marino et al., 2019).

The multifunctional group includes proteins with different functions. PARP1 interacts with CTCF which is involved in the cross-talk between poly(ADP-ribosyl)ation and DNA methylation (Guastafierro et al., 2008). Nucleophosmin is a molecular chaperone which interacts with CTCF at insulator sites and regulates CTCF function (Yusufzai et al., 2004). The interaction between LDB1 transcription complex and CTCF provides a mechanism to recruit CTCF into erythroid lineage specific enhancer looping function (J. Lee et al., 2017).

Cohesin is the most important chromatin architectural protein interacting with CTCF. Genome wide analysis demonstrated that between 60-90% of cohesion sites are co-occupied by CTCF and the 55-80% of CTCF sites overlap with cohesin (Wendt et al., 2008). Cohesins regulate insulation function of CTCF and formation and maintenance of chromatin loops (Ing-Simmons et al., 2015; Wendt et al., 2008) (see next section).

Finally, CTCF can also directly bind to RNA and regulate gene expression (Saldaña-Meyer et al., 2014). Also, RNAs target CTCF to the X-inactivation center by long non-coding RNAs and induce homologous X-chromosome pairing (Kung et al., 2015).

1.1.5. Molecular functions of CTCF

Nowadays, the best known function of CTCF is the regulation of the global organization of chromatin architecture. However, CTCF has been implicated in many regulatory functions, including transcriptional activation or repression,

insulation ability and epigenetic regulation. The different CTCF molecular functions are briefly described below.

Transcriptional repressor and activator

CTCF was originally identified as a transcriptional repressor of chicken *lysozyme* gene and the chicken and human *MYC* gene (Burcin et al., 1997; Filippova et al., 1996; Klenova et al., 1993; Lobanenkov et al., 1990). CTCF represses these genes by the interaction with promoters and upstream silencers of the genes. The ZF region of CTCF binds to the corepressor SIN3A at the PAH3 domain and the C-terminal region and allows CTCF to repress transcription by the recruitment of histone deacetylase complexes (Lutz et al., 2000). As another example, the binding of CTCF to the *hTERT* gene inhibits the transcription of the telomerase catalytic subunit (Renaud et al., 2005).

Analysis of other CTCF target sites revealed that CTCF can also activates gene transcription. CTCF allows the activation of the *amyloid-β precursor protein* (*APP*) (Vostrov and Quitschke, 1997), the *CDKN2A* (*p19ARF*) tumor suppressor gene (Ohlsson et al., 2001), the *human interleukin 1 receptor-associated kinase-2* (*IRAK2*) promoter (Kuzmin et al., 2005) and the human *p16INK4a* (Witcher and Emerson, 2009).

In summary, the first function described for CTCF was the transcriptional regulation of genes, acting either as activator or repressor (**Figure 1.3a**).

Insulator binding factor

Chromatin insulators are DNA elements that prevent inappropriate interactions between neighboring genes. Insulators can block the interaction between promoters, enhancers and silencers when positioned between them (enhancer-blocking activity) or can avoid the spreading of heterochromatin into euchromatin (barrier activity) (Bushey et al., 2009) (**Figure 1.3b**).

CTCF is the only known insulator protein in vertebrates (for recent reviews see Arzate-Mejía et al., 2018; Liu et al., 2018; Merkenschlager and Nora, 2016).

The first relation between an enhancer-blocking element and CTCF was described by Bell et al who found that CTCF binds to the 5´HS4 insulator sequence upstream of the chicken *β-globin* locus (Bell et al., 1999). Subsequently, four CTCF-binding sites were discovered at the imprinted control region (ICR) of the *H19/Igf2* locus (Bell and Felsenfeld, 2000; Hark et al., 2000; Kanduri et al., 2000). More recently, a role of CTCF in the mediation of enhancer-promoter interactions was described (Guo et al., 2015). Recent studies revealed that BRD2 is recruited to CTCF sites and both cooperated as insulators to enforce architectural boundaries in the genome in order to block enhancer regulation (Hsu et al., 2017). Moreover, it was described that the activity of the IgH 3′ regulatory region (3´RR) is delayed by CTCF insulator in developing B cells (Braikia et al., 2017).

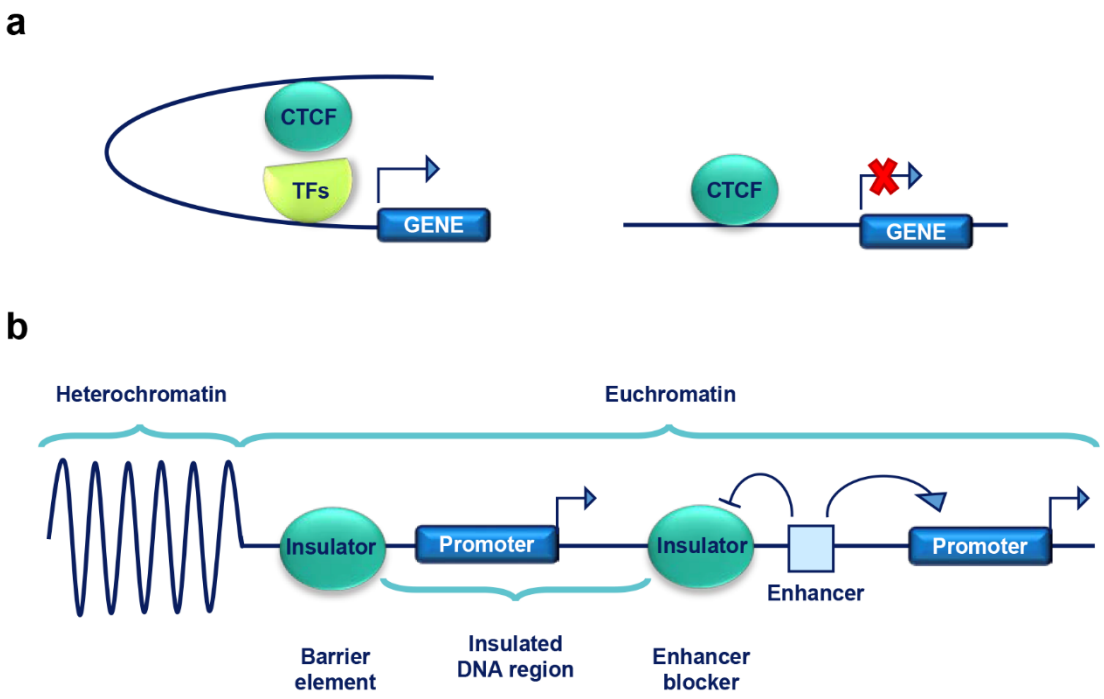

Figure 1.3. CTCF function as a transcription factor or insulator binding factor. *a) CTCF transcription factor can mediate both activation (left) and repression (right) of transcription of a number of genes. b) CTCF as an insulator binding factor. The enhancer blocking function is illustrated at the right. Enhancer blockers are located between promoters and enhancers. The barrier function is represented at the left. The barrier element avoids the spreading of heterochromatin into euchromatin.*

CTCF binds at barrier sites flanked by opposite chromatin states: highly condensed heterochromatin and less condensed euchromatin (Dixon et al.,

2012). CTCF binding sites are enriched at the boundaries between the repressive H3K27me3 and active H2AK5ac domains in cell-type specific patterns (Cuddapah et al., 2009). A recent study showed that CTCF binding to *CTRL2* region prevent the spread of heterochromatin markers as H3K27me3 to the *Herpes simplex virus 1* (*HSV-1*) LAT promoter/regulatory sequences (Lee et al., 2018).

The insulation function of CTCF is tightly related to its role in regulating the three-dimensional chromatin organization as it will be described in the next section.

Chromatin architecture regulator

The three-dimensional structure of the chromatin is important for the maintenance of genome stability, organization and regulation of gene expression (Szalaj and Plewczynski, 2018).

Genome is organized at different levels: the nucleosome, chromatin loops, topologically associating domains (TADs), chromosomal compartments and chromosome territories (**Figure 1.4**). The functional unit of chromatin is the nucleosome which consists of DNA wrapped around a core of two copies of each of the H2A, H2B, H3 and H4 histones. Post-translational modifications of histones and chromatin modifiers affect the accessibility of the DNA. Chromatin can form long-range interactions in which two distal DNA elements are brought close together forming a loop. Multiple loops form a chromosomal framework of insulated neighborhoods and form topologically associating domains. TADs are categorized based on the enrichment of specific epigenetic marks. Compartments are formed by interaction between different TADs with similar epigenetic signature. Finally, all compartments of a chromosome together form one territory (Rosa-Garrido et al., 2018; Stam et al., 2019; Zheng and Xie, 2019).

Eukaryotic genomes form long-range interactions that allow the formation of chromatin loops and TADs (Nora et al., 2012). TADs are regions of genome organization that allow interactions between genes and regulatory sequences in

the same TAD, but prevent interactions between sequences located in different TADs (Bickmore, 2013; Dixon et al., 2012). TADs are highly conserved through species and its organization is stable between cell types (Dixon et al., 2012).

Together, CTCF and cohesin are regulators of TAD formation and maintenance (Merkenschlager and Nora, 2016). CTCF and cohesin participate on gene regulation through the formation or stabilization of long-range chromatin loops. These CTCF / cohesin loops are distributed throughout the genome, creating a network of long-range interactions which includes loops that define the borders of TADs but also loops within the TADs (Phillips-Cremins et al., 2013; Seitan et al., 2013; Zuin et al., 2014). Highly transcribed genes, including housekeeping genes and architectural protein genes are contained in TAD borders (Nora et al., 2012). Only 15% of CTCF binding sites are present at TAD borders in mouse and human cells and that sites are frequently oriented convergent at TAD borders (de Wit et al., 2015; Guo et al., 2015; Vietri Rudan et al., 2015). However, most CTCF-binding sites (85%) are localized within TADs (Dixon et al., 2012).

Loop formation is highly dynamic and can be explained by the “loop extrusion” model. In this model, the cohesin complex extrude chromatin until it meets with CTCF chromatin barriers (Chen and Lei, 2019; Fudenberg et al., 2016; Haarhuis et al., 2017). CTCF binding to convergent CTCF binding sites (sites with consensus CTCF motifs pointing toward each other) seems to serve as a barrier to extrusion, where cohesin accumulates at CTCF-anchored loops (Haarhuis et al., 2017; Wutz et al., 2017). Depletion of CTCF or cohesin causes global loss of most loops and TADs (Nora et al., 2017; Wutz et al., 2017). Silencing or deletion of CTCF binding sites disrupts loop domain boundaries and allows abnormal interaction between enhancers and promoters and, consequently, the induction of aberrant gene activation (Flavahan et al., 2016; Denes Hnisz et al., 2016). A recent study shows that during transcription elongation, RNA polymerase II disrupts cohesin from CTCF sites and leads to local decompaction. Conversely, when the elongation is inhibited cohesin can accumulate at transcribed CTCF sites and mediate chromatin looping and 3D genome architecture (Heinz et al., 2018).

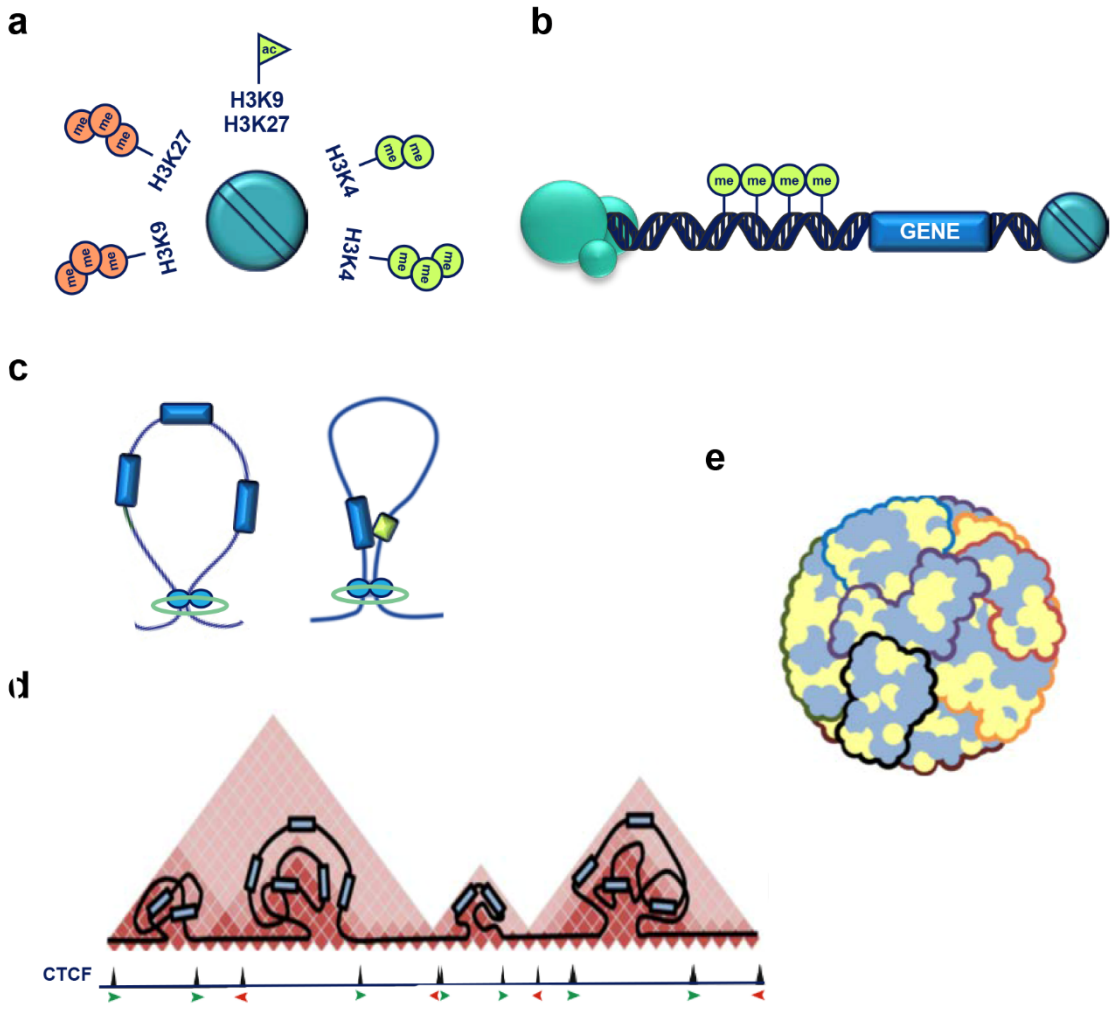

Figure 1.4. Chromatin organization. *a) The nucleosome is the functional unit of the chromatin. Different histone post-translational modifications regulates the accessibility to transcription factors or chromatin modifiers. b) Gene transcription is regulated by transcription factors and DNA methylation state. c) CTCF (blue balls) together with cohesins (green circles) mediates chromatin loop formation, facilitating or preventing enhancer-promoter interactions and other regulatory elements. d) Topologically associating domains (TADs) are regions of preferential chromatin interactions. TADs contain smaller subTADs and within them several chromatin loops are formed. CTCF is present at TADs borders. The direction of CTCF sites is indicated by the orientations of red and green arrows. e) Chromatin compartmentalization in active and inactive compartments (shown in yellow and blue, respectively) (Figure adapted from Rosa-Garrido et al., 2018).*

Epigenetic regulator

CTCF is involved in different aspects of epigenetic regulation. It can modulate the histone posttranslational modification status and DNA methylation at CpGs

from several genes. CTCF is also involved in the regulation of genomic imprinting and X-chromosome inactivation (Filippova, 2008).

Epigenetic marks in some promoters are related with the presence or the absence of CTCF and, therefore, influencing gene expression. For example, in the *Retinoblastoma* (*Rb*) promoter, CTCF bins to unmethylated DNA and blocks the spreading of the CpG methylation front (De La Rosa-Velázquez et al., 2007). Moreover, *PUMA* transcriptional repression by CTCF is associated with repressive histone marks since CTCF knockdown leads to the loss of the repressive mark H3K9me3 and increases PUMA levels (Gomes and Espinosa, 2010). In the case of *BAX* gene, it was described two CTSs on its promoter, which were enriched with open chromatin marks and unmethylated DNA, and the depletion of CTCF resulted in the activation of BAX and apoptosis (Méndez-Catalá et al., 2013).

CTCF prevents the spread of DNA methylation front which is important for the maintenance of methylation-free zones. Frequently, CpG methylation blocks CTCF binding (Engel et al., 2006). Methylation-dependent binding of CTCF at the imprinted control region (ICR) mediates imprinted expression of the *H19* and *Igf2* genes. ICR is methylated on the parental allele which prevents CTCF binding and allows *Igf2* expression by the interaction between the *Igf2* promoter and the distal enhancer. On the contrary, ICR is unmethylated on maternal alleles and allows the binding of CTCF which blocks the interaction between the *Igf2* gene and the distal enhancer activating *H19* gene (Bell and Felsenfeld, 2000). Similar CTCF-mediated mechanisms are also found at other imprinted control regions like *WT1* (Hancock et al., 2007) and *PLAGL1* (Iglesias-Platas et al., 2013).

CTCF is also implicated in the regulation of the X-chromosome inactivation. In mammals, one X chromosome is selected for inactivation. This process is controlled by the transcription of inactive x-specific transcript (*Xist*) and is blocked by the gene *Tsix* (Chao et al., 2002). Numerous CTCF binding sites are present in the imprinting center of the X chromosome inactivation (Xu et al., 2007). CTCF binding repress *Xist* expression and is required for *Tsix* transactivation and expression of the active X (Sun et al., 2013). The initiation and propagation of the

X-chromosome inactivation occurs in DNA unmethylated and CpG methylation is necessary for the maintenance of stable silencing (Sado, 2004).

Finally, CTCF is implicated in the epigenetic regulation of important cancer associated genes (see below).

1.1.6. CTCF in human cancer

CTCF deregulation is associated with the development of different malignancies and genetic diseases. Among other mechanisms, mutations in the zinc finger domain or mutations in the CTCF binding sites are responsible for CTCF deregulation in tumors.

Human CTCF gene is located at chromosome 16q22.1, a region frequently associated with loss of heterozygosity in Wilm´s tumor, breast and prostate cancer (Filippova et al., 1998). Mutations or heterozygous deletion of CTCF have been found in early T-cell precursor acute lymphoblastic leukemia (Zhang et al., 2012). Nonsense mutations and missense DNA mutations have been identified in the 11 ZF region that inhibits CTCF binding to its target sites (Aulmann et al., 2003; Filippova et al., 2002; Tiffen et al., 2013).

Recurrent mutations happen frequently in CTCF binding sites adjacent to cancer associated genes or oncogenes (Ji et al., 2016). For example, isocitrate dehydrogenase (IDH) mutant gliomas present genome-wide hypermethylation which reduces CTCF binding to specific sites in the genome and leads to abnormal gene activation and carcinogenesis (Flavahan et al., 2016). Abnormal CTCF enrichment on the promoter region of *HOXA10* in breast cancer cells helps in the development of tumorigenesis by the inactivation of *HOXA10* expression (J. Y. Lee et al., 2017). In T-cell acute lymphoblastic leukemia (T-ALL) deletions of a loop boundary CTCF site in *TAL1* and *LMO2* oncogenes generates aberrant regulatory interactions that increase oncogene expression (D Hnisz et al., 2016). Recent studies support that CTCF/cohesin loop anchors can suffer continuous DNA breaks and that translocation breakpoint regions in some cancers are enriched at loop anchors (Canela et al., 2017).

Mutations in CTCF binding sites are related with aberrant gene expression and affect chromatin structure. CTCF/cohesin binding sites are frequently mutated in colorectal cancer (Katainen et al., 2015). Accumulation of mutations at A•T base pairs in CTCF binding sites are related with tumorigenesis and cellular defects such as aberrant gene expression, epigenetic changes and genetic instability (Katainen et al., 2015). Recently, Guo et al identified 11 mutation hotspots overlapping CTCF binding sites in gastric cancer which are associated with changes in the expression of neighboring genes (Y. A. Guo et al., 2018).

Finally, CTCF participates in the epigenetic regulation of cancer associated genes such as *RB*, *p53* or *BCL6*. CTCF binding protects the *RB* gene promoter against DNA methylation and contributes to an optimal chromatin conformation (De La Rosa-Velazquez et al., 2007). CTCF promotes *p53* transcription by maintaining an open chromatin state and protecting this region against repressive histone marks (Soto-Reyes and Recillas-Targa, 2010). Our group found that CTCF regulates epigenetically *BCL6* gene through the binding to the exon 1A of *BCL6* and this binding is associated with the presence of active histone marks and gene expression (Batlle-Lopez et al., 2015).

1.1.7. CTCF in cell differentiation

CTCF is also involved in the control of different developmental processes (reviewed in Arzate-Mejía et al., 2018). CTCF is crucial during early, postnatal and adult development. Depletion of CTCF in oocytes causes embryo lethality and nullizygous mice presented early embryonic lethality at the peri-implantation stage (Moore et al., 2012; Wan et al., 2008). CTCF is also important in brain development, synapse formation and dendritic development. For example, it was found a high number of brain-specific CTSs which were involved in the regulation of neural genes expression (Prickett et al., 2013). Gregor et al, identified de novo mutations in CTCF in individuals with intellectual disability (Gregor et al., 2013). A recent study showed that CTCF is essential for cardiogenesis, as the conditional removal of CTCF from cardiac progenitors in mouse embryos causes

severe cardiac defects and death, and CTCF mediates genomic interactions to coordinate cardiomyocyte differentiation in the developing heart (Gomez-Velazquez et al., 2017; Rosa-Garrido et al., 2018).

Importantly, CTCF is implicated in hematopoietic cell differentiation. Enforced expression of CTCF blocked dendritic cells maturation (Koesters et al., 2007). In T-cells, CTCF mediates inter-chromosomal interactions between genes related with T-cell differentiation like Oct-1 (Kim et al., 2014). Also, inactivation of CTCF in thymocytes impairs differentiation of αβ T cells (Heath et al., 2008). Our group has described that CTCF downregulation in BCL6-expressing cells reduces BCL6 expression and induces B-cell terminal differentiation toward plasma cells (Batlle-Lopez et al., 2015). Finally, CTCF also regulates erythroid cell differentiation, as described in the next section.

1.2. Erythroid cell differentiation

1.2.1. Hematopoiesis

Hematopoiesis is a tightly regulated process that involves the formation, development and differentiation of all the cellular components of the blood from the pluripotent hematopoietic stem cells (HSCs). Mature hematopoietic cells included myeloid and lymphoid lineages. The myeloid lineage comprises erythrocytes, megakaryocytes producing platelets, granulocytes (basophils, neutrophils and eosinophils), monocyte-macrophages and mast cells. The lymphoid lineage includes T-cells, B-cells and natural killer cells. Dendritic cells can derived from the myeloid or lymphoid lineage (Hoffmann et al., 2016; Iwasaki and Akashi, 2007) (**Figure 1.5**). Hematopoietic differentiation is regulated at different levels by cytokines, growth factors and hormones as well as specific transcriptional regulators (Miranda-Saavedra and Gottgens, 2008; Orkin and Zon, 2008).

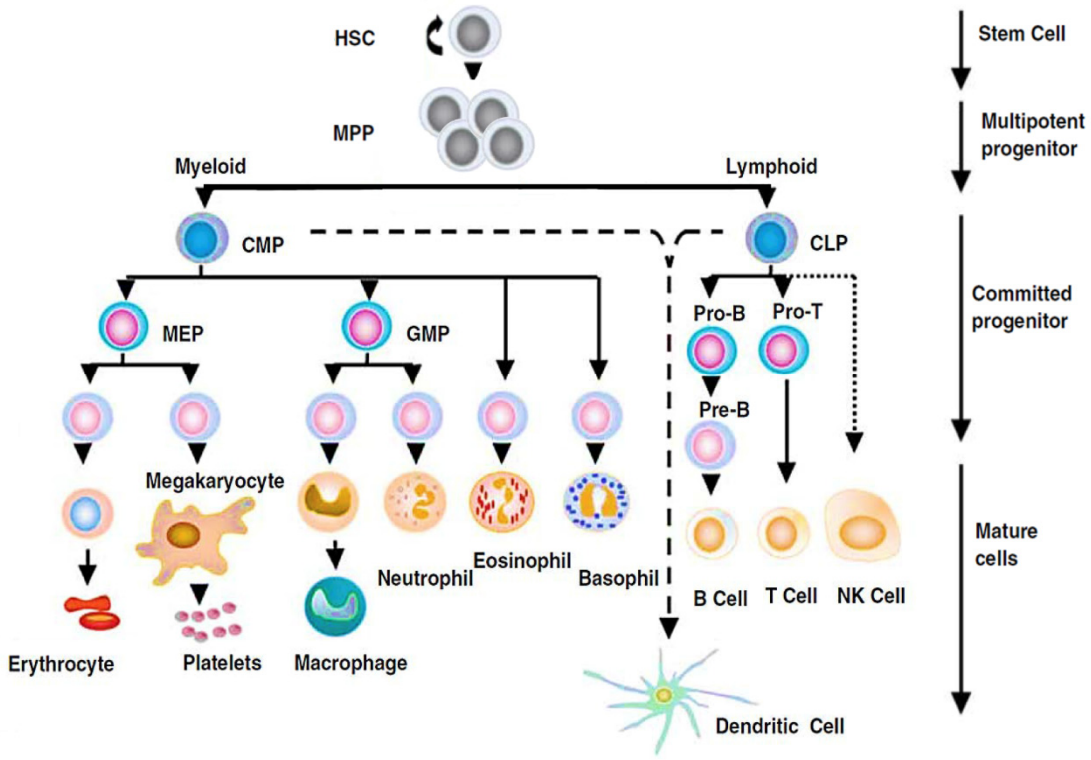

Figure 1.5. The hematopoietic hierarchy. *Representation of hematopoietic lineage pathways from hematopoietic stem cells (HSC) to mature blood cells. Abbreviations: HSC, hematopoietic stem cells; MPP, multipotent progenitor; CMP, common myeloid progenitor; CLP, common lymphoid progenitor; MEP, megakaryocyte-erythroid progenitor; GMP, granulocyte-macrophage progenitor. (Figure adapted from Larsson and Karlsson, 2005).*

Multipotent hematopoietic stem cells are undifferentiated cells with two essential properties, self-renewal and multipotent differentiation (Orkin and Zon, 2008). Stem cells renewal allows the production of new stem cells to maintaining the pool of HSCs. During multipotent differentiation, the stem cells produce, through several steps of differentiation, multipotent progenitors, committed progenitors and, finally, the different mature blood cells which are non-proliferative and lineage restricted cells (Orkin and Zon, 2008; Seita and Weissman, 2010) (**Figure 1.5**).

1.2.2. Erythropoiesis

Erythropoiesis is the process by which the red blood cells are formed. Red blood cells are necessary for transporting oxygen to tissues in the body

(Nikinmaa, 1997). During embryonic development, erythrocytes are produced in different organs by highly regulated and tightly orchestrated events (Barminko et al., 2015). In healthy adults, the bone marrow produces about $2x10^{11}$ erythrocytes per day that are released into the peripheral blood (Palis, 2014).

The erythroid cell differentiation from stem cells to erythrocytes takes place through different stages which are characterized based on cell morphology, colony forming capacity or marker expression analysis by flow cytometry (**Figure 1.6**). Hematopoietic stem cells firstly differentiate towards multipotent progenitors (MPPs) which give rise to common lymphoid progenitors (CLPs) or common myeloid progenitors (CMPs). CMPs further differentiate towards progenitors with restricted erythroid potential and reduce proliferative capacity which have the ability to generate megakaryocytes or erythrocytes (MEPs). MEPs differentiate to committed erythroid progenitors (EPs). The most immature erythroid progenitors are the burst forming unit-erythroid (BFU-E) that can form large colonies containing thousands of hemoglobinized cells (Dulmovits et al., 2017; Dzierzak and Philipsen, 2013). BFU-Es respond to erythropoietin (EPO), Stem Cell Factor (SCF), Interleukin-3 (IL-3), Interleukin-6 (IL-6) and corticosteroids (Hattangadi et al., 2011). BFU-Es then differentiate into mature erythroid progenitors known as colony-forming units-erythroid (CFU-E) which can form smaller colonies. Terminal erythroid differentiation is strongly dependent on EPO (Koury and Bondurant, 1988). During this process, cells become progressively smaller, the nucleus condensates and hemoglobin accumulates in the cytoplasm (Barminko et al., 2015; Nandakumar et al., 2016). The earliest morphologically identifiable erythroid precursor is the proerythroblast. It progressively differentiates into basophilic erythroblast, polychromatophilic erythroblast and orthochromatophilic erythroblast which form the reticulocyte upon enucleation (Chen et al., 2009). Finally, reticulocytes enter the blood stream where they mature into non-proliferative erythrocytes (Dzierzak and Philipsen, 2013) (**Figure 1.6**).

The expression of different cell-surface markers is characteristic of the different stages of erythroid cell differentiation. The expression of the transmembrane glycoproteins, CD34 and CD38, are characteristic of the first steps of erythropoiesis, from HSCs to MEPs. MEPs gradually lose CD34

expression and acquire CD71 (transferrin receptor) high expression (Sanada et al., 2016). The maturation of proerythroblasts to reticulocytes can be discerned by the loss of CD71 expression and the increase of CD235a (Glycophorin-A) expression (Nandakumar et al., 2016) (**Figure 1.6**).

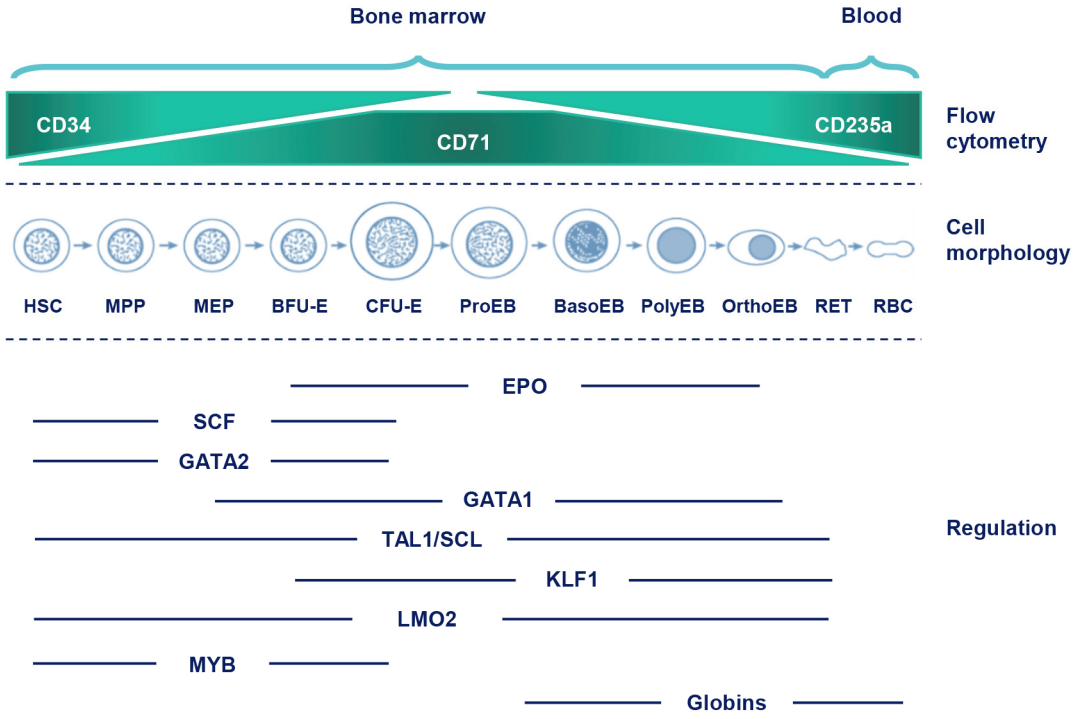

Figure 1.6. Erythroid cell differentiation. *Differentiation from hematopoietic stem cell to erythrocyte follows different stages based on surface marker expression (flow cytometry analysis), cell morphology and regulation by cytokines and transcription factor. Blue bars show the periods of expression for each cytokine, transcription factor and erythrocyte-related proteins. Abbreviations: HSC, hematopoietic stem cells; MPP, multipotent progenitor; MEP, megakaryocyte-erythroid progenitor; BFU-E, burst-forming unit-erythroid; CFU-E, colony-forming unit-erythroid; ProEB, proerythroblast; BasoEB, basophilic erythroblast; PolyEB, polychromatic erythroblast; OrthoEB, orthochromatic erythroblast; RET, reticulocyte; RBC, red blood cell. (Figure adapted from Koury, 2009).*

The main role of erythroid cells is the production of hemoglobin, the protein responsible for oxygen transport in the bloodstream. Loss of the erythroid nucleus in mammals is thought to provide more intracellular space for hemoglobin, allowing erythrocytes to specialize for efficient gas exchange (Ji et al., 2011). Different hemoglobins are synthesized in the embryo, fetus and adult which are adapted to their particular oxygen requirements. Hemoglobin is a tetramer which

consists in two α and two β globin chains associated with a heme group. In humans, the α locus and the β locus gene clusters controls the synthesis of hemoglobins. The α locus contains the embryonic ζ gene and the two adult α genes. The β locus consists of the ε, $^{G}\gamma$, $^{A}\gamma$, δ, and β genes (Stamatoyannopoulos, 2005).

1.2.3. Regulation of erythropoiesis by extracellular signals

Different cytokines and growth factors are involved in the regulation of the erythropoiesis (**Figure 1.6**). Erythropoietin (EPO) is the main regulator of the erythroid cell maturation. EPO acts on erythroid progenitors and early precursors by increasing proliferation and reducing apoptosis. CFU-E depends on EPO for survival and continued differentiation (Koury, 2016). EPO signaling is initiated by the binding to an specific receptor, the Epo receptor (EpoR) which is expressed on the surface of erythroid cells from BFU-Es to orthochromatic erythroblast (Constantinescu et al., 1999; Ingley et al., 2004). Binding of EPO to its receptor activates the cytoplasmic tyrosine kinase Janus Kinase 2 (JAK2) which activates a downstream signaling cascade via the signal transducer and activator of transcription 5 (STAT5), phosphoinositide-3-kinase (PI3K) and protein kinase B (PKB) pathways to maintain the proliferation and differentiation of erythroid progenitors. STAT5 maintains the viability of the cells during the late stages of maturation by the induction of the expression of the anti-apoptotic B-cell lymphoma-extra-large (BCL-xL) (Gregory et al., 1999; Ingley et al., 2004). Upon EPO stimulation, STAT5 and some transcription factors (GATA1, TAL1 and KLF1) co-occupy enhancers of numerous erythroid genes to induce erythropoiesis and, finally, the expression of globin genes and the enucleation of reticulocytes (Koulnis et al., 2014; Moore and von Lindern, 2018; Perreault and Venters, 2018). The importance of EPO has been demonstrated in $Epo^{-/-}$ or $EpoR^{-/-}$ mice, which are both embryonically lethal due to lack of mature erythrocytes (Suzuki et al., 2002).

Another important regulator during erythropoiesis is Stem Cell Factor (SCF), which binds to the cell growth factor receptor KIT to enhance growth and survival of early erythroid progenitors. SCF cooperates with EPO to induce erythroid cell

proliferation (Wang et al., 2008). Moreover, KIT maintains EpoR expression, which results in erythroid progenitor survival upon EPO stimulation (Kapur and Zhang, 2001).

In addition to EPO and SCF, other factors with positive effects on erythroid cell differentiation are insulin-like growth factor, activin or angiotensin II (Nandakumar et al., 2016). For example, insulin and Insulin-Like Growth Factor-I stimulate the proliferation of the late stage of primitive erythroid progenitor cells and mature erythroid progenitor cells and have anti-apoptotic effects on differentiating cells (Miyagawa et al., 2000). Finally, other factors that regulate negatively erythropoiesis are transforming growth factor β (TFGβ), growth and differentiation factor 11 (GDF11) or γ-interferon (Nandakumar et al., 2016).

1.2.4. Transcriptional regulation of erythropoiesis

Differentiation of the erythroid cells requires the expression of lineage-specific transcription factors (TFs). These transcription factors must be expressed at the correct time to control the commitment, proliferation and differentiation of red blood cells. There are some TFs essential for the development and maintenance of HSCs, others for the differentiation process and some TFs are involved in both processes. Different transcription factors such as GATA1, SCL/TAL1, LMO2, LDB1 and KLF1 are found forming protein complexes which allows the regulation of erythroid genes (Hattangadi et al., 2011; Nandakumar et al., 2016).

The GATA transcription factors, GATA1 and GATA2, are essential regulators of hematopoiesis (J. Gao et al., 2015). GATA2 is necessary for expansion, survival and maintenance of early hematopoietic progenitor cells (Bresnick et al., 2012; Tsai and Orkin, 1997). On the other hand, GATA1 has an essential role in the terminal differentiation and maturation of erythroid progenitors (Weiss and Orkin, 1995). *Gata1* and *Gata2* null mutant embryos die between E10 and E11 of gestation from severe anemia showing up the importance of both factors in erythropoiesis (Fujiwara et al., 1996; Tsai and Orkin, 1997).

A GATA factor switching was described during human erythropoiesis (Suzuki et al., 2013). During normal erythroid development, GATA2 is expressed in hematopoietic stem cells and hematopoietic progenitor cells like CMP, MEP and BFU-E and its expression is inhibited from CFU-E stage. GATA2 is replaced by GATA1 during terminal maturation, during this process the level of GATA2 decline whilst GATA1 increase. GATA1 expression is initiated at common myeloid progenitors (CMP) and is highly upregulated in MEPs and erythroblasts. Finally, GATA1 expression decrease during the maturation of red blood cells (Moriguchi and Yamamoto, 2014; Suzuki et al., 2013).

Both GATA factors can associate with the transcription factor Friend of GATA-1 (FOG-1) which is a GATA coregulator. In early erythroid cells, GATA2 and FOG1 association takes place before the GATA switch. It is remarkable that, when FOG1 is not present, GATA2 is not efficiently silenced (Pal et al., 2004). Within the MEP, FOG1 binds GATA1 to promote erythroid maturation (Mancini et al., 2012). Furthermore, FOG1 and GATA1 cooperation activates β-goblin expression (Welch et al., 2004).

GATA1 also acts in cooperation with other DNA-binding transcription factors like TAL1 and KLF1 and non-DNA-binding factors like LDB1 and LMO2 forming a complex known as “Core Erythroid Network” (CEN) to activate erythroid genes (Cantor and Orkin, 2002; Nandakumar et al., 2016) (**Figure 1.7**). GATA1, TAL1 and KLF1 are considered erythroid “master regulators” and the absence of any of them in mice results in severe anemia and death by mid-gestation (Nuez et al., 1995; Pevny et al., 1991; Porcher et al., 1996). High expression levels of TAL1/SCL are detected in HSC, myeloid progenitors, and mature myeloid cells (Porcher et al., 2017). TAL1/SCL expression increases during erythropoiesis promoting proliferation and differentiation and is absent from most mature myeloid and lymphoid cells (Begley et al., 1999). TAL1 directly binds to the LMO2 protein, which, in turn, interacts with LDB1. The expression of the transcription factor KLF1 (also called EKLF) is essential for the maturation of erythroblasts to erythrocytes and in the activation of *β-globin* gene expression during terminal erythroid differentiation (Miller and Bieker, 1993; Perkins et al., 2016). Also, KLF1 expression blocks megakaryocyte development and allows erythroid

development (Bouilloux et al., 2008; Frontelo et al., 2007). One important non-DNA-binding factor is LDB1 which is required for fetal and adult definitive erythropoiesis (Mukhopadhyay et al., 2003). LDB1 null mice do not produce red blood cells and die at approximately embryonic day 9.5 (Mukhopadhyay et al., 2003). On the other hand, LMO2 participates in the lineage-specific mechanism that regulates erythropoiesis. LMO2 null mice die around E9 by severe anemia and lack of any yolk sac hematopoiesis which suggest an essential role of LMO2 in early hematopoiesis (Warren et al., 1994).

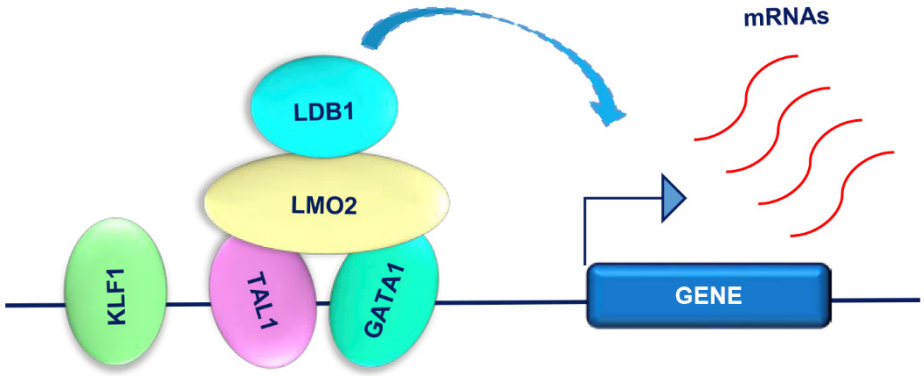

Figure 1.7. Core Erythroid Network (CEN). *The DNA-binding transcription factors, GATA1, TAL1 and KLF1, and the non-DNA-binding transcription factors, LMO2 and LDB1 act in cooperation forming the core erythroid network to activate erythroid gene transcription. (Figure adapted from Nandakumar et al., 2016).*

Outside the CEN, other transcription factors also have important roles in erythropoiesis. One of them is NFE2 which participates in the regulation of globin gene expression during erythroid differentiation (Sawado et al., 2001). Deletion of NFE2 results in reduced α- and β-globins in mature red cells (Shivdasani and Orkin, 1995). The proto-oncogen *c-MYB* is highly expressed in immature hematopoietic cells but its expression declines upon differentiation. To allow terminal differentiation, MYB expression has to be downregulated. Moreover, MYB transactivates *KLF1* and *LMO2* expression which enhances erythropoiesis (Bianchi et al., 2010), although MYB forced expression inhibits erythropoiesis (Shivdasani and Orkin, 1996). Other important factor is ETS1 which must be downregulated for optimal red blood cells maturation. Moreover, enforced

expression of ETS1 blocks erythrocyte maturation at the polychromatophilic stage (Lulli et al., 2006).

Finally, MYC transcription factor was shown to have pivotal roles in the regulation of hematopoiesis and erythropoiesis (Delgado and Leon, 2010). MYC is an erythropoietin early response gene and its expression is upregulated in response to erythropoietin stimulation (Spangler and Sytkowski, 1992). The first biological effect described for MYC was its ability to inhibit erythroid cell differentiation in a murine erythroleukemia-derived cell line (Coppola and Cole, 1986; Dmitrovsky et al., 1986; Prochownik and Kukowska, 1986). Our group described that MYC inhibits erythroid differentiation induced by Ara-C in K562 cells (Delgado et al., 1995). In addition, MYC also inhibits the erythroid differentiation induce by p27 in K562 cells and blocks the upregulation of erythroid specific genes and transcription factors that regulate the erythroid commitment like GATA1 and NFE2 (Acosta et al., 2008).

In conclusion, erythroid cell differentiation is a highly regulated process by the combination of transcription factors in a stage-specific manner. However, erythropoiesis is not only regulated by transcriptional mechanisms and regulation by microRNAs (reviewed in Azzouzi et al., 2012; Kim et al., 2019; Listowski et al., 2013), long non-coding RNAs (reviewed in Alvarez-Dominguez et al., 2014; Jeong and Goodell, 2016; Kulczyńska and Siatecka, 2016) and epigenetic mechanisms (reviewed in Ginder et al., 2008; Wozniak and Bresnick, 2008; Hattangadi et al., 2011; Perreault and Venters, 2018) are also important in erythroid cells differentiation and erythroid gene expression (**Figure 1.8**).

1.2.5. CTCF role in erythropoiesis

CTCF seems to have important functions in the regulation of erythroid cells differentiation. Previous results from our group revealed a possible role for CTCF in the regulation of erythroid differentiation. We described that CTCF mRNA and protein expression was modulated during differentiation in different erythroid, megakaryocytic, granulocytic and monocytic-like cells (Delgado et al., 1999). Also, overexpression of CTCF increased differentiation specifically into the

erythroid pathway while CTCF down-regulation inhibited the expression of erythroid markers like ε-globin (Torrano et al., 2005). More recently, the importance of CTCF in cell differentiation was pointed out on studies with CTCF-cKO mice which present functionally immature erythroid cells, severe anemia and rapid hematopoietic failure (Kim et al., 2017).

Several studies described that specific CTCF binding sites are required for correct chromatin contacts and transcription of the erythroid genes (**Figure 1.8**). In erythrocytes, interactions between enhancers and globin genes promoters take place within CTCF insulated subdomains (Hanssen et al., 2017; Splinter et al., 2006). The chicken, human and mouse β-globin loci are located in chromosomal regions of heterochromatin which are flanked by CTCF-binding sites and are associated with CTCF enhancer-blocking activity (Farrell et al., 2002; Ulianov et al., 2012). Human β-globin (*HBB*) gene contains a locus control region (LCR) which consists of five DNaseI hypersensitive sites (HSSs), among which HS1 to HS4 are enhancers and rich in binding sites for erythroid specific transcription factors (GATA1, NFE2 and EKLF), while HS5 carries CTCF binding sites (Palstra et al., 2003; Tanimoto et al., 2003). CTCF is involved in loop formation and long-range interactions during the activation of β-globin gene in erythroid cells (Splinter et al., 2006). Moreover, interaction between CTCF sites around the β-globin locus is dependent on erythroid transcription activator GATA1 (Kang et al., 2017). CTCF-dependent enhancer-blocking elements were also identified in the upstream region of the chicken α-globin domain (Valadez-Graham et al., 2004). Mahajan et al describe a pattern of CTCF recruitment at the α-globin locus and its rearrangement during erythropoiesis and suggested that CTCF can acts as an insulator before erythropoiesis and as a positive transcription factor upon erythropoiesis (Mahajan et al., 2009). Recently, it was reported the interaction between CTCF and LDB1, allowing the activation of a significant number of erythroid genes by LDB1-CTCF enhancer looping via CTCF sites within their promoters (J. Lee et al., 2017).

Despite the increasing information regarding the link of CTCF with erythropoiesis, the precise role of CTCF in this process is still unknown. Following

previous results from our lab, the first part of this Thesis was devoted to get insights into the regulation of erythroid differentiation by CTCF.

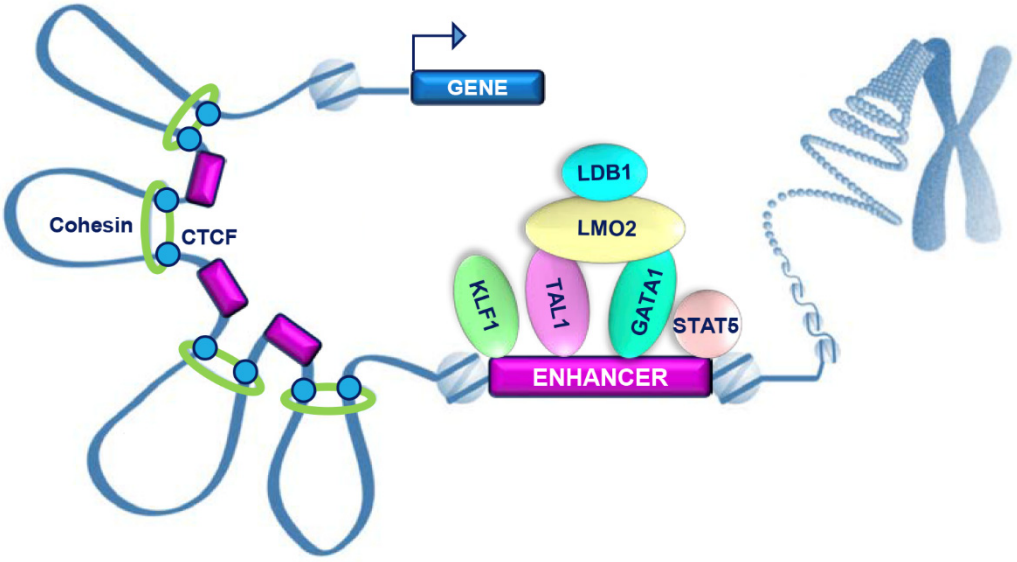

Figure 1.8. Transcriptional and epigenetic regulation of erythroid genes. *CTCF together with cohesin may participate in the formation of chromatin loops allowing the interaction of enhancers with erythroid master transcription factors such as GATA1, KLF1 and TAL1. EPO-EPOR signaling activates STAT5 that together with erythroid transcription factors bind to enhancers and direct erythropoiesis. Transcription factors, enhancers and chromatin looping work together during erythropoiesis activating the transcription of specific erythroid genes (Figure adapted from Perreault and Venters, 2018).*

1.3. B-cell differentiation and germinal centers

B-cells are produced in the bone marrow from hematopoietic stem cells which differentiate into progenitor stages with restricted potential. The development of immature B-cells can be defined by the differential expression of cell-surface markers and by the rearrangement status of immunoglobulin genes. Immature B-cells express IgM at their surface and migrate as naïve B-cells from the bone marrow to lymph nodes. Naïve B-cells become activated by interaction with $CD4^+$ T-cells and aggregate into primary follicles to form germinal centers (GCs) (Basso and Dalla-Favera, 2015; De Silva and Klein, 2015; Song and Matthias, 2018).

Germinal centers are dynamic and highly organized structures within normal lymph nodes and are essential for the formation of high affinity antibodies. GCs can be histologically differentiated in two zones with different functions, the dark zone (DZ) and the light zone (LZ) (**Figure 1.9**). The dark zone contains a large number of highly proliferating cells named centroblasts. After several rounds of proliferation, centroblasts undergo somatic hypermutation (SHM), a process that increases the affinity and the specificity of the immunoglobulin. Germinal center B-cells express the enzyme activation-induced deaminase (AID) which introduces mutations into the immunoglobulin genes to generate diverse clones which express antibodies with different affinity for the antigen. Then, the B-cells move to the light zone which contains a number of follicular dendritic cells presenting the immunizing antigen on their surface. B-cells in the light zone, called centrocytes, exit the cell cycle and are selected based on their affinity for the antigen. Centrocytes in which this selection fails, die by apoptosis. B-cells with high affinity can differentiate into antibody-secreting plasma cells or memory B-cells. Finally, B-cells with low affinity for the antigen, can re-enter to the dark zone and suffer additional cycles of SHM in order to increase their affinity (Bannard and Cyster, 2017; Basso and Dalla-Favera, 2015; Song and Matthias, 2018; Victora and Nussenzweig, 2012).

Germinal center reaction is controlled by a complex network of cellular signals that affect GC B-cell responses by activating or repressing specific transcriptional programs in order to coordinate proliferation, cell cycle exit, re-entry into the dark zone, cell differentiation and cell death by apoptosis.

1.3.1. Transcription factors regulating Germinal Center reaction

Multiple transcription factors act in concert to promote or repress specific steps of the germinal center development. Some factors like BCL6, PAX5 and BLIMP1 are consider to be master regulators of the GC or plasma cell differentiation. Many other factors like XBP1, MYC or IRF4 are also important for the GC reaction (**Figure 1.10**).

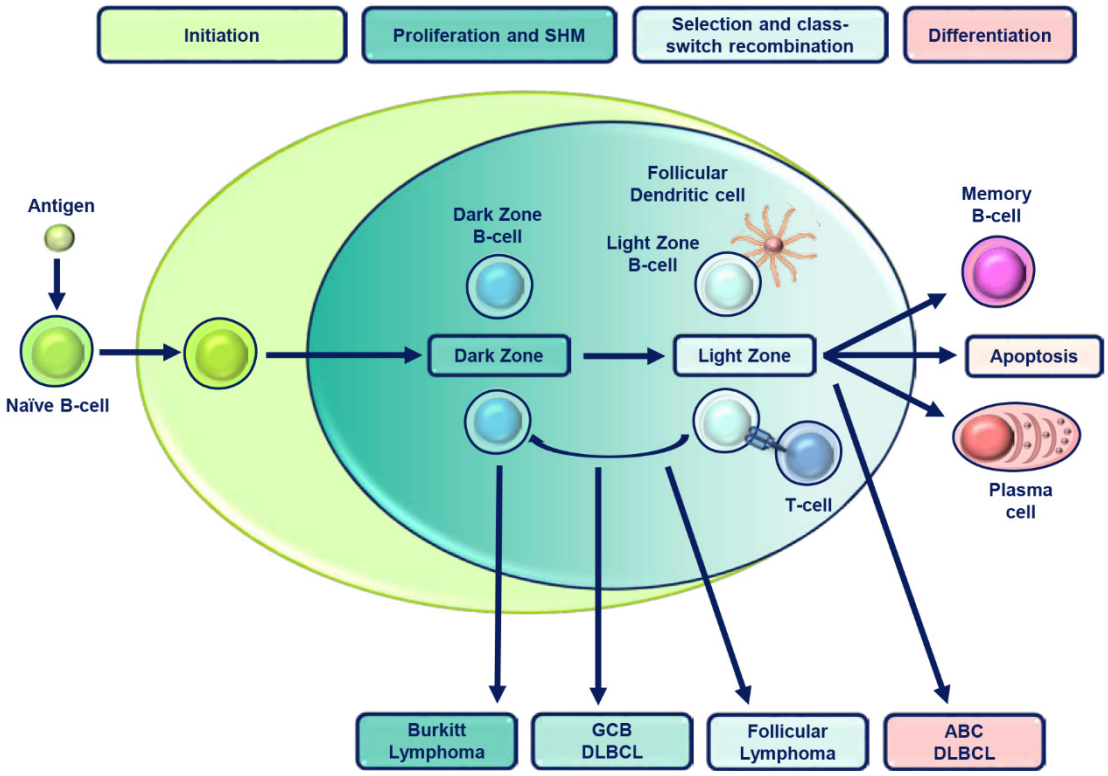

Figure 1.9. Germinal center reaction and GC-derived lymphomas. *Activated naïve B-cells are recruited into the follicles to form the germinal centers. Germinal center dark zone consists in highly proliferative B-cells that undergo somatic hypermutation (SHM). B-cells in the light zone stop proliferate and are selected based on their affinity for the antigen to differentiate into plasma cells or memory B-cells. Cells in which selection fails, die by apoptosis. A number of B-cells can re-enter to the dark zone to suffer new cycles of SHM. Different germinal center derived B-cell lymphomas are shown at the bottom. Arrows indicated their origin: Burkitt lymphoma from dark zone B-cells; GCB DLBCL and Follicular lymphoma from light zone B-cells; and ABC DLBCL from B-cells that are commited to plasma cell differentiation (Figure adapted from Basso and Dalla-Favera, 2015).*

BCL6

B-cell lymphoma 6 protein (BCL6) is a transcriptional repressor that belongs to the family of BTB/POZ proteins. BCL6 has an N-terminal BTB/POZ domain that mediates transcriptional repression and form multi-molecular complexes; a middle region which contains a second repression domain (RD2); and the C-terminal domain which contains six zinc fingers that bind to DNA and target proteins (Cardenas et al., 2017; Chang et al., 1996). BCL6 contains an autoregulatory binding site within the first exon which allows suppression of its own transcription (Kikuchi et al., 2000; Pasqualucci et al., 2003). Also, acetylation

inhibits BCL6 function by preventing the recruitment of corepressor complexes containing histone deacetylases (HDAC) (Bereshchenko et al., 2002). Our group has previously described that CTCF regulates epigenetically BCL6 expression by the binding to the exon 1A of *BCL6* and this binding is associated with the presence of active histone marks; on the contrary, the absence of CTCF lead the binding of BCL6 to its negative autoregulatory region and the recruitment of repressive histone marks (Batlle-Lopez et al., 2015).

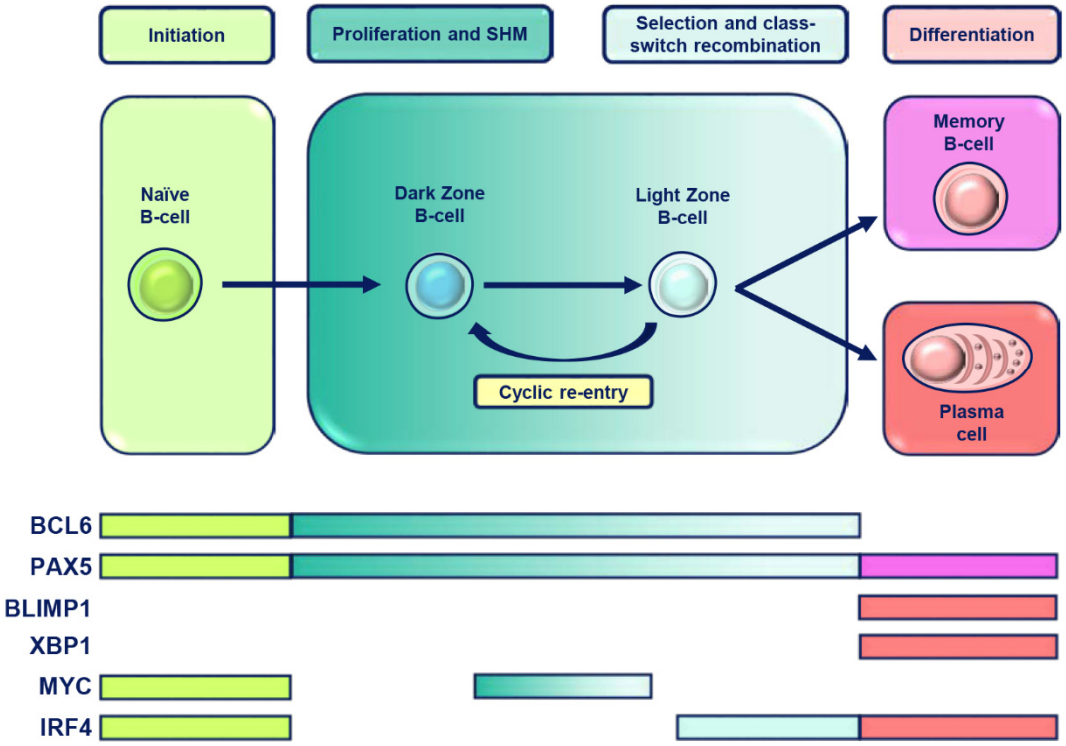

Figure 1.10. Transcriptional regulation of germinal center reaction. *Transcription factors are involved in the regulation of the different processes of the germinal center reaction from the initiation to the exit and differentiation. Color bars indicate the stages in which transcription factors are expressed. (Figure adapted from Basso and Dalla-Favera, 2015).*

BCL6 is essential for germinal center formation as BCL6-null mice fail to develop GCs and immunoglobulin affinity maturation (Ye et al., 1997). BCL6 is first detected in naïve B-cells in which upregulation of BCL6 is essential for initiation of GC reaction and for the migration of these cells to the center of the follicle (Kitano et al., 2011). BCL6 is induced and highly expressed in centroblasts

and its expression is maintained in most centrocytes (Cattoretti et al., 1995) (**Figure 1.10**). In the DZ, BCL6 acts predominantly as a transcriptional repressor, inhibiting genes involved in the DNA damage-sensing pathway, including TP53, ATR and CHEK1 and regulators of the cell cycle like p21 (Phan et al., 2005; Phan and Dalla-Favera, 2004; Ranuncolo et al., 2008, 2007). DNA damage-sensing and response pathway is functionally correlated with the regulation of apoptosis in which BCL6 affects pro- and antiapoptotic proteins such as BCL2 (Basso and Dalla-Favera, 2010). Also, BCL6 regulates other cellular pathways by modulating signaling through toll-like receptors, IFN-R, cytokines, TGF-R and WNT signaling (Basso and Dalla-Favera, 2010). BCL6 function in the DZ allows the maintenance of the GC phenotype by the establishment of a transcriptional program that facilitate the rapid proliferation of cells and tolerance of genomic damage during clonal expansion and somatic hypermutation. Moreover, BCL6 represses a number of genes required for the differentiation of B-cells into plasma cells, including PRDM1 and IRF4 (Tunyaplin et al., 2004). Finally, BCL6 expression has to be downregulated in order to allow B-cells to exit the GC and to differentiate and is undetectable in plasma cells (Basso et al., 2010).

PAX5

Paired Box Protein 5 (PAX5) is the master regulator of B-cell identity and is expressed during B-cell development, from pro-B cells to mature GC B-cells (Revilla et al., 2012) (**Figure 1.10**). Conditional inactivation of PAX5 in mature B-cells results in the loss of B-cell identity and reversion to a progenitor stage (Cobaleda et al., 2007). PAX5 forms a complex with AID and other proteins to contribute to directing AID to the Igh locus for class switch recombination (CSR) (Hauser et al., 2016). PAX5 represses XBP1 to prevent plasma cell differentiation and its downregulation is necessary for differentiation into committed Ig-secreting plasma cells (K. I. Lin et al., 2002; Nera et al., 2006).

BLIMP1

B-lymphocyte-induced maturation protein 1 (BLIMP1) is encoded by the PR domain zinc finger protein 1 (PRDM1) and is essential for promoting plasma cell differentiation and repressing the B-cell transcriptional program by the repression

of BCL6 (Shaffer et al., 2004a) (**Figure 1.10**). BLIMP1 is essential for the generation and maintenance of mature plasma cells, but is not required for the initiation of the plasmatic differentiation program (Shapiro-Shelef et al., 2003). BLIMP1 downregulates PAX5 which is necessary for the induction of XBP1 and the activation of the plasma cell program (K. I. Lin et al., 2002). BLIMP1 expression induces growth arrest and death at the earliest stages of B-cell development but induces maturation and the acquisition of an antibody-secreting phenotype at the later stages of B-cell differentiation (K.-I. Lin et al., 2002).

Other factors

X-bon binding protein (XBP1) is a transcription factor essential for upregulation of the secretory apparatus necessary for antibody production in plasma cells (Shaffer et al., 2004b). Studies using a B-cell specific knockout of *Xbp1* shown that, in its absence, plasma cells are formed but they are strongly impaired in their capacity to secrete high amounts of immunoglobulins (Hu et al., 2009).

MYC is transcription factor with important roles in cell growth and division. MYC is expressed at the initiation of the germinal center formation (Calado et al., 2014). MYC expression is suppressed in the highly proliferative germinal center centroblasts by BCL6, so B-cells in the dark zone are capable to proliferate in a MYC-independent manner (Dominguez-Sola et al., 2012). MYC expression is reactivated in a subset of B-cells from the light zone that are going to re-enter into the dark zone for further cycles of SHM (Dominguez-Sola et al., 2012).

Interferon regulatory factor 4 (IRF4) is required for the formation of the germinal centers and once they are formed and initiated, IRF4 expression is inhibited (Bollig et al., 2012). IRF4 induces BCL6 expression at the early phase of the germinal center formation and inhibits it at the end of the germinal center reaction (De Silva and Klein, 2015). IRF4 is also required for the initiation of the plasma cell differentiation program and its expression is induced in the B-cells of the light zone which present high affinity antibodies (Ochiai et al., 2013; Song and Matthias, 2018).

IRF8 is expressed in the germinal center initiation and contributes in the induction of BCL6 expression and also regulates SHM (Lee et al., 2006). MEF2B is expressed early during germinal center formation and induces BCL6 expression in germinal center precursor B-cells (Ying et al., 2013). MCL1 is the principal regulator of B-cell survival during germinal center formation (Vikstrom et al., 2010). BACH2 represses BLIMP1 and blocks plasma cell differentiation (Muto et al., 2010). Finally, BCL2 overexpression leads to increased plasma cells number and enhances B-cell ability for plasmatic differentiation (Smith et al., 2000; Taylor et al., 2015).

Deregulated expression of these genes, due to chromosomal translocations, mutations or genetic alterations, is associated with the development of different hematological malignancies, mainly lymphomas.

1.3.2. Germinal Center derived B-cell lymphomas

Lymphomas are a heterogeneous group of malignancies that arise from cells of the lymphoid lineage. Lymphomas can be classified depending on the cell origin in T-cell, B-cell or NK-cell. B-cell derived lymphomas are the most common lymphomas and comprise a group of genetically, phenotypically and clinically different neoplasias. In general, they are originated from lymphoid B-cells with uncontrolled growth during their maturation in the germinal center (Basso and Dalla-Favera, 2015; Küppers, 2005). Lymphomas can be originated at any stage of B-cell development, although the most common occur in B-cells following migration to germinal centers, where B-cells undergo proliferation and antibody diversification of immunoglobulin genes through somatic hypermutation and heavy chain class switching (Basso and Dalla-Favera, 2015) (**Figure 1.9**).

Genome-wide analysis revealed that B-cell lymphomas present numerous genetic alterations such as amplifications, deletions and point mutations which can alter the structure or transcriptional regulation of proto-oncogenes and tumor suppressor genes (Pasqualucci, 2019). Two additional types of genetic alterations are aberrant somatic hypermutation (ASHM) and chromosomal alterations. ASHM allows the introduction of point mutations in non-

immunoglobulin loci that are not targeted in normal GC B-cells (Pasqualucci et al., 2001). This phenomenon is uniquely associated with germinal center B-cell lymphomas. On the other hand, chromosomal alterations usually involve recombination between immunoglobulin loci and an oncogene locus. Translocations can derived from mistakes in the recombination-activating gene (RAG) mediated VDJ recombination as happens in translocations involving *IgH* and *BCL2* in Follicular Lymphoma (FL). Translocations can also derived from errors in the AID-mediated CSR process like, for example, immunoglobulin-*MYC* translocation in sporadic Burkitt Lymphoma (BL). Finally, AID-mediated SHM mechanism can generate DNA breaks and allows translocations as happens between immunoglobulin and *MYC* in endemic BL (Küppers and Dalla-Favera, 2001; Nussenzweig and Nussenzweig, 2010; Pasqualucci, 2019).

According to the latest World Health Organization (WHO) classification there are over 30 different subtypes of B-cell lymphomas (Swerdlow et al., 2016). Two important types of germinal center derived lymphomas are Burkitt Lymphoma (BL) and Diffuse Large B-cell Lymphoma (DLBCL).

Burkitt Lymphoma (BL)

Burkitt Lymphoma is an aggressive malignancy derived from germinal center dark zone B cells and included three variants: sporadic, endemic and immunodeficiency-associated (Schmitz et al., 2014). BL is also associated with Epstein-Barr virus which is present in almost all cases of endemic BL and in 25% to 40% of sporadic and immunodeficiency-associated cases (Magrath, 2012). Almost all cases of BL present a *MYC* translocation. The translocation between *MYC* gene on chromosome 8 and the immunoglobulin heavy chain gene on chromosome 14 is found in more than 80% of cases which allows the constitutive expression of *MYC* in BL. In the remaining 20% of BL cases, the translocation involves the kappa and lambda light-chain loci in chromosomes 2 and 22 (15% and 5% respectively) (Hecht and Aster, 2000). *BCL6* is expressed in all cases of Burkitt Lymphoma and contributes to proliferation and survival, but its role has not been thoroughly investigated.

Diffuse Large B-cell Lymphoma (DLBCL)

Diffuse large B-cell lymphoma is the most common aggressive B-lymphoma and accounts for ~ 40% of lymphoma cases. DLBCL can occur de novo or as a result of transformation from a more indolent lymphoma. It has been identified two major subtypes: GCB-DLBCL which derives from GC light zone B-cells that re-enter in the DZ and ABC-DLBCL which originate when B-cells are committed to plasmablastic differentiation prior to GC exit (Alizadeh et al., 2000) (**Figure 1.9**).

Each subtype presents exclusive genetic lesions. However, some oncogenic pathways are common in both subtypes like *BCL6* deregulation, inactivating mutations of *TP53* and mutations in genes implicated in the immune response (*B2M* and *CD58*), as well as alterations in chromatin modifiers which affects epigenetic regulation (*CREBBP*, *EP300* and *MLL2*). Deregulated *BCL6* (by mutation or chromosomal translocation) contributes to pathogenesis via several mechanisms, such as suppression of DNA damage response through p53 repression, increasing the proliferative phenotype and blocking terminal differentiation (Basso and Dalla-Favera, 2015; Pasqualucci, 2019; Pasqualucci and Dalla-Favera, 2015).

BCL6 is overexpressed in GCB-DLBCLs but translocation affecting *BCL6* locus occurs more frequently in the ABC-DLBCL subtype (24%) than in GCB DLBCL (10%). GCB subtype is characterized by alterations in the PI3K/AKT and JAK/STAT signaling pathways and has a higher frequency of *BCL2* and *EZH2* mutations. Chromosomal translocations involving *MYC* and *BCL2* are detected in 10% and 40% of cases, respectively. On the other hand, ABC subtype is characterized by the constitutive activation of the NF-κB pathway and the blockade of terminal plasma cell differentiation. They also present a higher frequency of *BCL6* rearrangements, *BCL2* amplifications and recurrent mutations of *CD79B*, *MYD88* and *PRDM1* (Basso and Dalla-Favera, 2015; Crombie and Armand, 2019; Pasqualucci, 2019).

Currently, treatments for aggressive B-cell lymphoma are based on nonspecific and highly toxic regimens such as chemotherapy, radiation or the monoclonal anti-CD20 antibody rituximab, but many patients are not cured (Coiffier et al., 2010). The recent findings about the genetic and molecular characteristics of the different lymphomas provide information for the development of new therapies. Novel agents that target oncogenic pathways and drug combinations are recently under clinical trials (Shaffer et al., 2012). For example, BET inhibitors and PI3K inhibitors are being using in Burkitt lymphoma (Delmore et al., 2011; Schmitz et al., 2012). In DLBCL, therapy with BCL2 and EZH2 inhibitors are already available (Anderson et al., 2014; Knutson et al., 2012). Thus, the identification of somatic mutations which are drivers and define the regulatory pathways to which lymphomas are development are the key to identify new approaches to therapy for patients with lymphomas.

1.4. Epigenetic therapy of lymphomas

1.4.1. Epigenetic modifications

Epigenetics is defined as heritable changes in gene expression that are not due to any alterations in the DNA sequence (Holliday, 1987). Epigenetic is based on the study of the chromatin modifications that include DNA methylation, posttranslational modifications of histone residues and chromatin remodeling (Ahuja et al., 2016). These mechanism are involved in the regulation of gene expression and in the control of essential biological processes like proliferation, survival, cell differentiation, genomic imprinting and X chromosome inactivation.

DNA methylation

DNA methylation occurs mainly in the cytosines of CpG dinucleotides. Regions with high density of CpGs are called CpG islands and they are often located in promoters. Hypermethylation in promoters is associated with repression of gene transcription while methylation in gene bodies is associated with active transcription (Jones, 2012; Kazanets et al., 2016).

Methylation is regulated by three DNA methyltransferases (DNMTs) enzymes: DNMT1, DNMT3A and DNMT3B (Cheng and Blumenthal, 2008). DNMT1 is a maintenance methyltransferase that methylates the newly synthesized hemimethylated DNA generated during DNA replication (Li et al., 1992). On the other hand, DNMT3A and DNMT3B are de novo methyltransferases which establish DNA methylation during early development (Okano et al., 1999).

The regulation of DNA methylation is important for embryonic development, genome instability and cell differentiation. During normal hematopoiesis, DMNTs are essential for hematopoietic stem cell self-renewal, niche retention and for the production of the different blood lineages (Celik et al., 2016; Gore and Weinstein, 2016). Loss of methylation by active DNA demethylation processes is carry out by the ten-eleven translocation (TET) proteins. These proteins are essential intermediates in both active and passive DNA demethylation and also promote DNA demethylation in collaboration with DNA repair enzymes (Ko et al., 2015).

Histone posttranslational modifications

Posttranslational modifications of histones at the N-terminal domain of the histone “tails” affects the local structure of chromatin. The most common histone modifications are acetylation, methylation and phosphorylation. PTMs can regulate chromatin structure and also provide binding sites for the recruitment of non-histone proteins. Histone modifications are involved in the regulation of many cellular processes like gene expression regulation, replication and DNA repair (Fardi et al., 2018; Kouzarides, 2007; Wang and Zhong, 2015).

Histone acetylation is associated with gene transcription and deacetylation with gene repression. Lysine acetylation neutralizes the positive charge of histones tails and their interaction with the negatively charged DNA. This generates a more open chromatin state that allows the binding of transcription factors and increased levels of gene transcription. On the contrary, histone deacetylation results in a more compacted chromatin and reduced transcriptional activity (Grunstein, 1997; Shahbazian and Grunstein, 2007). Histone acetyl

transferases (HATs) and histone deacetylases (HDACs) add and remove acetyl groups from histone residues and are critical regulators of gene expression. HATs include different families such as MYST, GNAT and CREBBP/EP300. On the other hand, there are 18 HDACs, divided in four families: Class I (HDAC 1, 2, 3 and 8), Class II (HDAC 4, 5, 6, 7, 9 and 10), Class III (sirtuins 1-7) and Class IV (HDAC 11). Both types of enzymes can target histones and non-histone proteins (Bannister and Kouzarides, 2011).

Histones are mainly methylated on arginine (R) and lysine (K) residues. Histone methylation can regulate gene transcriptional activation and repression. For example, methylation of H3K4, H3K36 and H3K79 is related with actively transcribed genes in euchromatin while methylation of H3K9, H3K27 and H3K20 is associated with silenced genes (Barski et al., 2007). In addition, the number of methyl groups (mono-, di- or trimethylation) is also related with the regulation of gene transcription, for example, the monomethylation of lysine in H3K9 activate transcription while its trimethylaton causes transcriptional inhibition (Barski et al., 2007). Histone methylation is mediated by lysine methyltransferases (KMTs) and protein arginine methyltransferases (PRMTs). Lysines can also be demethylated by lysine demethylases (KDMs) (Allis et al., 2007).

1.4.2. Epigenetic alterations in hematological malignancies

Alterations in epigenetic modifiers disturb the balance between gene activation and gene repression which result in aberrant gene expression and in uncontrolled cell proliferation. Epigenetic deregulation is found in cancer cells presenting global DNA hypomethylation, particularly in gene bodies and intergenic regions, which generate genome instability. This hypomethylation is accompanied by increased *de novo* methylation at many promoters of specific tumor suppressor genes, resulting in gene silencing (Ahuja et al., 2016; Esteller, 2008; Jones and Baylin, 2007).

Alterations in proteins related with DNA methylation are involved in hematological malignancies. Around 20% of patients with acute myeloid leukemia (AML) and acute lymphoblastic leukemia (ALL) present recurrent mutations in

DNMT3 (Ley et al., 2010; Neumann et al., 2013). Also, *TET2* inactivation through loss-of-function mutation or deletion is a frequent event in myeloid (AML and MDS) and lymphoid malignancies (T-cell lymphomas) (Solary et al., 2014).

HATs and HDACs have been found frequently mutated in hematological malignancies. Loss-of-function mutations in HATs are recurrent in lymphoid malignancies, occurring in up to 40% of DLBCL (Pasqualucci et al., 2011) and, with reduced frequency, in cutaneous T-cell lymphoma (Da Silva Almeida et al., 2015). Moreover, mutations and chromosomal translocations in CREBBP and EP300 histone acetyl transferases result in loss of HAT activity and transcriptional deregulation present in DLBCL, AML and ALL malignancies (Morin et al., 2011; Pasqualucci et al., 2011).

Mutations in histone methyltransferases and their aberrant activity have been reported in different hematological malignancies. *MLL1* (*KMT2A*) and *MLL2* (*KMT2B*) are members of the mixed-lineage leukemia (MLL) gene family which encode for histone methyltransferases. Mutations in *MLL2*, one of the most frequent mutated gene in B-cell lymphoma, leads to a global reduction in H3K4 methylation and is the most common mutated gene in B-cell lymphomas (Morin et al., 2011). Moreover, *MLL1* is frequently rearranged by chromosomal translocations in leukemias with poor prognosis (De Braekeleer et al., 2005).

Polycomb repressive complex 2 (PRC2) is a group of proteins which stablishes specific PTMs. EZH2 is the catalytic component of PRC2. EZH2 has H3K27 methyltransferase activity and is involved in gene transcriptional silencing (Schwartz and Pirrotta, 2008). Loss-of-function mutations of *EZH2* have been found in myeloid malignancies while mutations in B-cell lymphomas result in enzymatic hyperactivity which allows the inappropriate inhibition of tumor suppressor genes (Morin et al., 2010; Nikoloski et al., 2010).

Epigenetic alterations are starting to get used as biomarkers in hematological malignancies and some of them have been found to be associated with poor prognosis. Epigenetic modifications are reversible which make them important therapeutic targets.

1.4.3. Epigenetic drugs

In contrast to genetic alterations, which are hard to target, epigenetic modifications are potentially reversible and can be targeted with the therapeutic inhibition of a specific epigenetic drug. Some epigenetic drugs have been approved for the treatment of different hematological malignancies and novel drugs are currently being used in different clinical trials. Some examples will be describe below.

DNA methyltransferase inhibitors (DNMTi)

DNA methyltransferase inhibitors are analogs of cytidine nucleosides that are incorporated into the DNA or RNA of proliferating cells. DNMTis covalently sequester DNMTs and inhibit their enzymatic activity and target them for proteosomal degradation (Ghoshal et al., 2005).

Two DNMTis were approved by the Food and Drug Administration (FDA) for the treatment of myelodysplastic syndromes (MDS) characterized by global promoter hypermethylation. 5-azacytidine was the first epigenetic drug approved by the FDA (Kaminskas et al., 2005). It was proved to be efficient in patients with MDS in clinical trials, improving the response rate and increasing survival. Decitabina or 5-aza-2´-deoxycytidina has been also approved for the treatment of MDS (Lübbert et al., 2011). Additional DNMTS are being used in different clinical trials with promising results. Some example are azacytidine in MDS and chronic myelomonocytic leukemia (CMML) (Garcia-Manero et al., 2016); guadecitabine in MDS and AML (Issa et al., 2015; Kantarjian et al., 2017) and decitabine in MDS (Garcia-Manero et al., 2017).

Histone deacetylase inhibitors (HDACi)

Aberrant activity of HDACs has been implicated in cancer. Therefore, HDACs represent an important target for cancer treatment (Imai et al., 2016). HDAC inhibitors can induce cell cycle arrest which results in differentiation and/or apoptosis of tumor cells while normal cells remain relatively tolerant. The substrate of HDACs is not limited to histones, they also can deacetylate non-

histone proteins, which provides the opportunity for the use of HDAC inhibitors in regulating these transcription factor, oncoproteins, and/or signal transducers (Glozak et al., 2005).

Several classes of synthetic and natural HDAC (class I, II, and IV) inhibitors have been identified: hydroxamic acids, benzamides, short chain fatty acids, and cyclic peptides (Dimopoulos and Grønbæk, 2019; Qin et al., 2017). An overview of some HDAC inhibitors currently used in clinical trials is shown in **Table 1.1**.

Table 1.1. HDAC inhibitors. *Histone deacetylases inhibitors used in clinical trials involving hematological malignancies. Abbreviations: CTCL, cutaneous T-cell lymphoma; AML, acute myeloblastic leukemia; MDS, myelodysplastic syndrome; CLL, chronic lymphocytic leukemia. (Dimopoulos and Grønbæk, 2019).*

Chemical structure	Name	Specificity	Clinical Status
Hydroxamic acid derivatives	LBH589 (panobinostat)	Classes I, II and IV	Approved (multiple mieloma)
	SAHA (vorinostat)	Classes I, II and IV	Approved (CTCL)
	PXD-101 (belinostat)	Classes I, II and IV	Phase II (B-cell and T-cell lymphomas)
	ITF2357 (givinostat)	Classes I, II and IV	Phase II (polycythemia vera)
	4SC-201 (resminostat)	Classes I, II and IV	Phase II (Hodgkin lymphoma)
	LAQ824 (dacinostat)	Classes I, II and IV	Phase I (solid tumors)
	PCI24781 (abexinostat)	Classes I and II	Phase II (B-cell lymphomas)
	ACY-1215 (ricolinostat)	HDAC6	Phase II (multiple lymphoma)
	SB939 (pracinostat)	Classes I, II and IV	Phase II (AML, myelofibrosis)
Benzamide derivatives	MGCD0103 (mocetinostat)	Class I	Phase II (B-cell lymphomas)
	MS-275 (entinostat)	Class I	Phase II (B-cell lymphomas)
Cyclic peptides	Depsipeptide (romidepsin)	Class I	Approved (CTCL)
Short chain fatty acids	Valproate	Classes I and IIa	Phase II (MDS, AML)
	Butyrate	Classes I and IIa	Phase II (CLL, AML)

The FDA approved the use of some HDAC inhibitors for the treatment of different hematological malignancies. In 2006, SAHA (suberoylanilide hydroxamic acid) also known as Vorinostat, was the first HDAC inhibitor approved by the FDA for clinical use in patients with cutaneous T-cell lymphoma (CTCL) (Grant et al., 2007). Depsipeptide or Romidepsin, a cyclic peptide, was approved in 2009 for the treatment of CTCL (Vandermolen et al., 2011) and in 2011 for the

treatment of peripheral T-cell lymphoma (PTCL) (Barbarotta and Hurley, 2015). Belinostat (PXD-101), the third drug approved by FDA in 2014, has been used for the treatment of refractory or relapsed PTCL (Lee et al., 2015). Finally, panobinostat, a hidroxamic acid analog, was approved in 2015 for the treatment of multiple myeloma (MM) (Laubach et al., 2015).

Romidepsin is a natural product obtained from the bacteria *Chromobacterium violaceum* (Ueda et al., 1994). Romidepsin is a HDAC inhibitor, being especially active against class I HDACs. Within the cell, the disulfide bond of the peptide is reduced releasing thiol which interacts with zinc atoms in the binding pocket of the HDAC, inhibiting its activity. By the inhibition of HDAC, romidepsin blocks the removal of acetyl groups from the lysine residues of N-terminal histone tails maintaining a more open and transcriptionally active chromatin state in the cell (**Figure 1.11**). The cellular action of romidepsin results in enhanced histone acetylation, as well as the acetylation of other nuclear or cytoplasmic proteins, influencing in cell cycle regulation, apoptosis, DNA repair and autophagy (Smolewski and Robak, 2017). Romidepsin was shown to induce antiproliferative effects and apoptosis in many human cancer cell lines including leukemia, non-small cell lung cancer, breast cancer or colon cancer. Romidepsin was approved by the FDA for the treatment of CTCL and PTCLs but its effect on B-cell lymphomas and on BCL6 regulation has not been thoroughly investigated.

Bromodomain and extraterminal domain inhibitors (BETi)

BET proteins are a family of chromatin readers (BRD2, BRD3, BRD4 and BRDT). They can bind to acetylated histone tails and other acetylated proteins like transcription factors and act as regulators of RNA transcription and cell cycle progression (Fukazawa and Masumi, 2012). BET proteins are also related with cancer development. For example, BRD2 overexpression is associated with DLBCL and inhibition of BRD4 has antileukemic potential in AML (Genta et al., 2019).

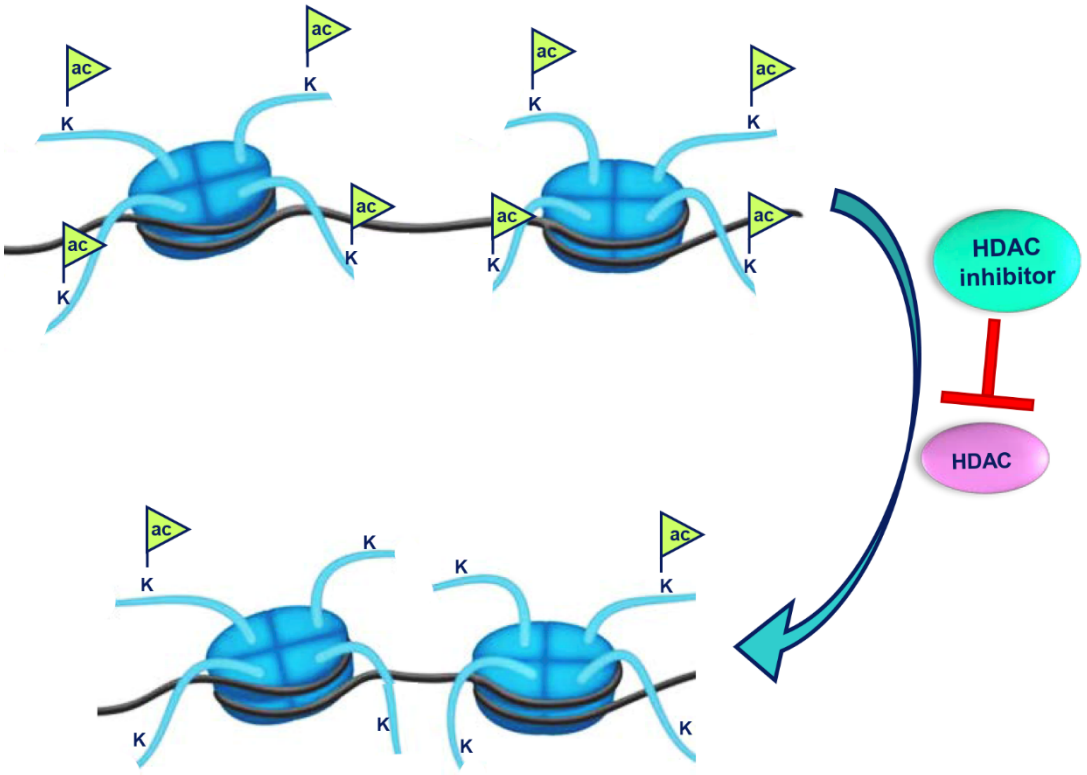

Figure 1.11. Mechanism of action of histone deacetylase inhibitors. *Histone acetylation is associated with open chromatin and gene transcription. Histone deacetylases remove acetyl groups from histone residues resulting in a compacted chromatin state and gene repression. Histone deacetylase inhibitors such as romidepsin, blocks the removal of acetylation. Abbreviations: K, lysine residue; ac, acetylation; HDAC, histone deacetylase.*

JQ1 is a potent and selective BET inhibitor which can competitively occupy the acetyl lysine recognition pocket of bromodomains and displace BRD4 from chromatin leading to cell cycle arrest and promotion of apoptosis (Delmore et al., 2011; Ramadoss and Mahadevan, 2018). JQ1 is being widely studied in many cancer cell lines and multiple animal models as a potential therapeutic agent. JQ1 is able to downregulate MYC levels in different human cancers such as lymphomas and leukemias (Cortiguera et al., 2015) (**Figure 1.12**). JQ1 induces transcriptional downregulation of *MYC* gene and, subsequently, leads to a downregulation of MYC-dependent target genes. MYC is transcriptionally regulated by multiple enhancers and super-enhancers that are dependent on BRD4. JQ1 displaces BRD4 from the super-enhancer regions leading to inhibition of *MYC* (Delmore et al., 2011; Lovén et al., 2013).

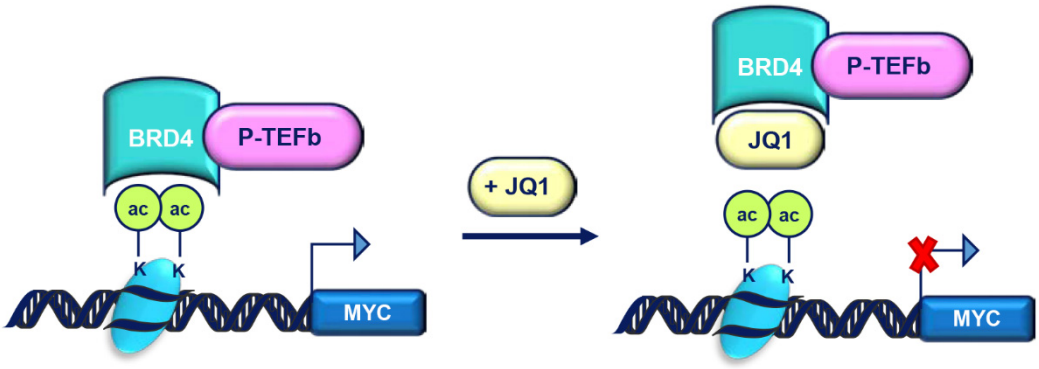

Figure 1.12. Mechanism of action of JQ1 inhibitor. *BRD4 interaction with acetylated histones activates MYC gene expression. JQ1 binds to BRD4, preventing this interaction and repressing MYC transcription. Abbreviations: K, lysine residues; ac, acetylation; BRD4, bromodomain-containing protein 4; pTEFb, positive transcription elongation factor b.*

Combination of therapies

Currently, therapy with a single epigenetic drug is not sufficient to achieve disease control with the exception of the drugs approved by the FDA. However, the combination of epigenetic drugs with standard or other epigenetic therapies seems to be efficient and helps to reduce the possible cytotoxicity of the drugs.

Several clinical trials show that the combination of chemotherapy with epigenetic drugs increases the sensitivity of the malignant cells to chemotherapy in lymphoid and myeloid cancers and also in myeloma (Dimopoulos et al., 2018; Mathur et al., 2017; Niitsu et al., 2001; Xue et al., 2016). For example, the combination of the HDACi sodium butyrate and chemotherapy has an apoptotic synergistic effect on Burkitt lymphoma cell lines (Dos Santos Ferreira et al., 2012). Treatment with HDAC inhibitors after low doses of DNMT inhibitors allows a synergistic reactivation of tumor suppressor genes and restoration of DNA-repair pathways of malignant cells in different hematological malignancies (Ahuja et al., 2016; Hassler et al., 2013; Momparler, 2003). Currently, a phase I/IIa clinical trial studies the effects of the combination of oral 5-azacitidine with romidepsin in patients with relapsed and refractory lymphoid malignancies (NCT01998035). In addition, synergistic effects between some BET bromodomain inhibitors and HDAC inhibitors have been found in different studies

in lymphoma and myeloma cells (Ramadoss and Mahadevan, 2018). Finally, several ongoing clinical trials investigate the effect of combining epigenetic therapy with immune checkpoint inhibitors (Ali et al., 2017).

In summary, many epigenetic drugs are currently been tested in several clinical trials, either as monotherapy or in combination with other drugs and therapies for the treatment of cancer.

2. AIMS

This Thesis is divided into two parts related to the regulation of hematopoietic cells differentiation. The first part refers to the control of erythroid differentiation by the transcriptional regulator CTCF. The second part deals with lymphomas produced by B-cells differentiation deregulation and its possible treatment with epigenetic drugs.

2.1. Erythroid cells differentiation: regulation by the CTCF factor

As it has been highlighted in the introduction, CTCF can interact with a high number of DNA sequences all over the genome and is involved in the regulation of gene transcription, chromatin insulation, epigenetic regulation and genome organization. Previous results from our group indicated a possible role of CTCF in the regulation of erythroid differentiation (Delgado et al., 1999), showing that overexpression of CTCF promotes erythroid cell differentiation (Torrano et al., 2005). Moreover, profiling analysis in K562 cells overexpressing CTCF revealed the differential expression of erythroid related genes (unpublished data). However, the underlying molecular events of these effects are unknown.

The general aim of the first part of this work is to gain further insight into CTCF function in the regulation of erythroid cell differentiation in human hematopoietic cells. For this purpose we stablished the following aims:

1. Analyze the effects of CTCF knock-down on K562 erythroid cell differentiation.
2. Explore the role of CTCF in the differentiation of human $CD34^+$ cells.
3. Identify erythroid transcription factors regulated by CTCF.
4. Study CTCF binding to regulatory regions of erythroid transcription factor genes upon induction of erythroid differentiation.
5. Analyze CTCF occupancy of *MYC* regulatory regions upon differentiation.

2.2. B-cells differentiation and lymphoma: regulation by epigenetic drugs

CTCF is also involved in the regulation of lineage-specific gene expression in lymphoid cells. Our group has demonstrated that CTCF affects plasma cell differentiation through the epigenetic regulation of *BCL6* in lymphoma cells (Batlle-Lopez et al., 2015). In contrast to genetic alterations, epigenetic modifications are potentially reversible and can be targeted with specific epigenetic drugs. Therapy with epigenetic drugs has an enormous potential in lymphoma-B treatment. Romidepsin is a histone deacetylase inhibitor that inhibits HDAC class I (Smolewski and Robak, 2017). We have previously demonstrated that romidepsin treatment induces apoptosis, cell cycle arrest and plasma cell differentiation in B-cells lymphoma (Cortiguera, MG and Garcia-Gaipo, L, submitted, see annex). On the other hand, JQ1 is a potent BET bromodomain inhibitor that is able to repress the expression of some genes such as *MYC* (Delmore et al., 2011). MYC deregulation is prevalent in lymphomas and is associated to a worse prognosis in lymphomas derived from the germinal center (Nguyen et al., 2017). Moreover, promising results combining HDAC with BET inhibitors have been recently reported (Ahuja et al., 2016; Ramadoss and Mahadevan, 2018).

The general aim of the second part is to investigate the effects of romidepsin in combination with JQ1 in the treatment of different aggressive B-cell lymphoma cells. For this purpose we stablished the following aims:

1. Study the effects of romidepsin and JQ1 combined treatment in cell proliferation, apoptosis and cell cycle.
2. Analyze the effect of romidepsin and JQ1 treatment on *BCL6* expression and B-cell differentiation.

MATERIALS AND METHODS

3. MATERIALS AND METHODS

3.1. Cell culture

3.1.1. Cell lines

Cells were grown in RPMI-1640 or DMEM basal media (Gibco) supplemented with 10% or 20% fetal bovine serum (Gibco), 150 µg/ml of gentamycin and 2 µg/ml of ciprofloxacin and confirmed to be mycoplasma free. Cells were maintained at 37°C in a humidified 5% CO_2 atmosphere. **Table 3.1** provides a list of cell lines used in this study.

Table 3.1. Cell lines used in this work

CELL LINE	PHENOTYPE	CULTURE MEDIUM	SOURCE / REFERENCE
Ramos	Burkitt-Lymphoma. EBV negative	RPMI-10F	Laboratory collection / Klein et al, 1975
DG75	Burkitt-Lymphoma. EBV negative	RPMI-10F	Laboratory collection / Ben-Bassat et al, 1977
Raji	Burkitt-Lymphoma. EBV positive	RPMI-10F	ATCC / Epstein et al, 1965
Toledo	GCB-DLBCL	RPMI-10F	ATCC / Martinez et al, 1993
LY03	ABC-DLBCL	RPMI-20F	Dr. A Piris CNIO / Martinez el at, 1993
K562	Human chronic myeloid leukemia	RPMI-10F	ATCC / Lozzio 1975
HeLa	Human cervical cancer	DMEM-10F	ATCC / Gey et al, 1952
HEK-293T	Human embryonic kidney with SV40 T antigen constitutive expression	DMEM-10F	Laboratory collection / Graham et al, 1977

3.1.2. Purification and culture of human $CD34^+$ cells

Primary $CD34^+$ cells were obtained from human umbilical cord blood kindly donated from the Banco de Sangre y Tejidos de Cantabria. Mononuclear cells were isolated by density gradient centrifugation on Ficoll-Paque Plus (GE Healthcare). For separation, fresh blood was diluted with phosphate-buffer saline (PBS) supplemented with 2 mM EDTA and 100 U/ml DNase was added. Diluted

blood was carefully layed over the Ficoll solution in a centrifuge tube. Tubes were centrifuged at 400 g for 35 min at 20°C without brake. Mononuclear cell layer was harvested from the interface and washed 2 times with PBS-2 mM EDTA. Mononuclear cells were frozen resuspended in freezing medium (90% fetal bovine serum and 10% DMSO) at -80°C.

$CD34^+$ cells were purified using a magnetic beads separation system (CD34 MIcroBead Kit Ultrapure and MACS Columns. Miltenyi Biotec)(Giani et al., 2016). Mononuclear cells were thawed and centrifuged for 5 min at 1200 rpm. Cell pellet was resuspended in a buffer containing PBS, 0.5% bovine serum albumin (BSA) and 2 mM EDTA (300 µl of buffer for each 10^8 cells). CD34 Microbeads and Blocking Reagent were added (100 µl of each for 10^8 cells) and samples were incubated for 30 min at 4°C. Cells were washed with 5 ml of buffer and centrifuged at 300 g for 10 min. Cell pellet was resuspended in 500 µl of buffer and cell suspension was added into a MACS Magnetic Column placed in a magnetic field of a MACS Separator. Column was previously equilibrated with 3 ml of buffer. Column was washed three times with 3 ml of buffer. Then, the column was removed from the magnetic separator and 5 ml of buffer were added to collect the cells. $CD34^+$ cells were immediately cultured in StemSpam™ SFEM II supplemented with StemSpam™ $CD34^+$ Expansion Supplement 10X (Flt3L, SCF, IL-3, IL-6 and TPO) (StemCell Technologies) up to three days. The purity of the isolated $CD34^+$ cells was evaluated by flow cytometry analysis (see below).

3.1.3. Induction and assessment of erythroid cell differentiation

Exponentially growing K562 cells ($2.5x10^5$ cell/ml) were treated with 1 µM 1-β-D-arabinofuranosylcytosine (Ara-C) (Sigma-Aldrich) or 0.5 or 1 µM Imatinib (LC Laboratories) up to 5 days to induce erythroid cell differentiation (Delgado et al., 1995; Gómez-Casares et al., 2013). Ara-C is incorporated into replicating DNA strands and inhibits DNA polymerase producing topoisomerase dysfunction and preventing DNA repair. Imatinib is an ATP-competitive inhibitor of Bcl-Abl tyrosine kinase that works by binding close to the ATP binding site, locking it in a closed conformation and inhibiting the enzyme activity. Both drugs are used for the treatment of chronic myeloid leukemia.

Expanded $CD34^+$ cells were treated with 3 or 6 U/ml Erythropoietin (EPO) (R&D Systems) up to 14 days to induce erythroid differentiation. Cells were collected at different time points and erythroid differentiation was analyzed by the expression of specific erythroid markers and the benzidine test.

Benzidine test is based on the catalytic reaction occurring between benzidine and hemoglobin in presence of H_2O_2. The benzidine test was carried out mixing $5x10^4$ cells resuspended in 20 µl of medium and 20 µl benzidine-H_2O_2 mixture (50:1 v/v). After 10 min of incubation on ice, blue cells (hemoglobin-containing cells) were counted in a Neubauer chamber. A minimum of 200 cells were counted using the ImageJ software and the number of hemoglobin producing cells (blue) over the number of non-hemoglobin producing cells (white) was determined and expressed as percentage of benzidine-positive cells.

Ara-C*: dissolved in distilled water; stock concentration: 100 mM; stored at -20°C.*
Imatinib*: dissolved in DMSO; stock concentration: 1 mM; stored at -20°C.*
Benzidine*: dissolved in 0.5 M acetic acid solution; stock concentration: 0.2% (Sigma); stored at 4°C protected from light.*

3.1.4. Colony forming unit assay

Expanded $CD34^+$ cells were plated in duplicated at a density of $2x10^3$ cells in 35-mm Petri dishes in 1.5 mL of a methylcellulose semisolid medium (Methocult; Stem Cell Technologies Inc.) mixed with StemSpam™ SFEM II supplemented with StemSpam™ $CD34^+$ Expansion Supplement 10X (Flt3L, SCF, IL-3, IL-6 and TPO) or with StemSpam™ $CD34^+$ Erythroid Expansion Supplement 100X (SCF, IL-3 and EPO). After 14 days of incubation, individual colonies were identified and counted using an inverted microscope.

3.1.5. Cell surface markers analysis

The purity of the isolated $CD34^+$ cells was evaluated by flow cytometry analysis. The CD34 antigen is a single chain transmembrane glycoprotein, expressed on human hematopoietic stem and progenitor cells. $1x10^6$ purified $CD34^+$ cells were harvested, centrifuge 3 min at 1500 rpm, resuspended in 100

µl of phosphate-buffered saline (PBS) and incubate with 10 µl of CD34 PE antibody (Miltenyi Biotec) for 30 min at room temperature in dark conditions. After incubation, cells were washed in PBS and analyzed by flow cytometry using the FACScan cytometer (BD Biosciences).

Erythroid differentiation was analyzed by flow cytometry. Glycophorin-A (CD235a) is a single-pass transmembrane glycoprotein, which is expressed on mature erythrocytes and erythroid precursor cells. It is one of the major sialoglycoprotein expressed on human red blood cells. $1x10^6$ cells were harvested, centrifuge 3 min at 1500 rpm, resuspended in 100 µl of phosphate-buffered saline (PBS) and incubated with 5 µl of anti-CD235a VioBlue (Miltenyi Biotec) for 30 min at room temperature in dark conditions. After incubation, cells were washed in PBS and analyzed by flow cytometry using the FACScan cytometer (BD Biosciences).

3.1.6. Epigenetic drugs

Lymphoma B-cells were treated with the histone deacetylase inhibitor romidepsin (kindly provided by Celgene) and/or the BET bromodomain inhibitor (+) JQ1 (Cayman Chemical).

To study the effects of the epigenetic drugs, exponentially growing cells ($3x10^5$ cells/ml) were treated with different drugs alone or in combination for several time points (24, 48 and 72 hours) at the indicated concentrations, depending on the experiment and cell line.

Romidepsin*: dissolved in DMSO; stock concentration: 100 mM; stored at -20°C.*
JQ1*: dissolved in DMSO; stock concentration: 1 mM; stored at -20°C.*

3.1.7. Cell proliferation and viability assays

Cells growing exponentially were counted using the NucleoCounter NC-100™ System (Chemometec) which identifies and counts cells containing staining DNA. The system consists in a NucleoCassette, which contains a

fluorescent dye (propidium iodide), the measurement chamber and two buffers. The Lysis Buffer (Reagent A100) is used for disruption of the plasma membranes and the Stabilizing buffer (Reagent B) raises the pH of the sample mixture and stabilize the cell nuclei. To obtain the total cell number, 100 µl of the sample were diluted with 100 µl of Reagent A and 100 µl of Reagent B and loaded into the NucleoCassette where the nuclei were stained with propidium iodide.

Metabolic activity was measured using the WST-1 reagent (Roche) which allows the quantification of the number of viable cells by the cleavage of tetrazolium salt WST-1 (4-[3-(4-Iodophenyl)-2-(4-nitrophenyl)-2H-5-tetrazolio]-1,3-benzene disulfonate) to formazan dye. The amount of formazan directly correlates to the number of metabolically active cells in the culture. Cells were grown for 3 days in T96 well plates with R10F at $2.5x10^5$ cells/ml in a final volume of 100 µl in each well. For each day, 10 µl of WST-1 reagent was added to the cell culture and incubated for 2-4 h at 37°C. The absorbance was measured at 405 nm in the microplate (ELISA) reader Multiskan™ FC Microplate Photometer (Thermo Scientific). Metabolic activity was expressed as percentages relative to the activity of the non treated cells (value = 100%).

Cell viability was assessed by the dye exclusion test with Trypan Blue (Sigma). In this test, 10 µl of cell suspension was mixed with 10 µl of Trypan Blue and applied to a Neubauer chamber. Stained (blue) and unstained cells were counted and the percentage of viable cells was calculated.

3.1.8. Calculation of IC_{50} values and drugs synergy

To determine the half maximal inhibitory concentration (IC_{50}) values and the combination index (CI) of the drugs, lymphoma B- cells were seeded in quadruplicates in T96 well plates and treated with different concentrations of romidepsin and JQ1. After 72 hours of treatment, metabolic activity was measured by WST-1 assay and IC_{50} values were determined with CompuSyn software. For determination of drug synergy, metabolic activity results were used according to the Chou-Talalay method (Chou, 2010; Chou and Talalay, 1984) using CompuSyn software to determine the combination index. The Chou-Talalay

method is based on the median-effect equation. Using this method, values < 1 represent synergistic effect of the two drugs, values equal to 1 indicate additive effect and values > 1 represent an antagonistic effect of the drugs.

3.1.9. Apoptosis analysis

Annexin V-PE Apoptosis detection Kit (Immunostep) was used for the detection of early apoptotic cells. The human vascular anticoagulant, Annexin V, is a phospholipids binding protein with high affinity for phosphatidylserine. In the early phases of apoptotic cell death, the distribution of phosphatidylserine changes and it appears in the external surface of the cell membrane. Staining of cells with Annexin-V allows the discrimination of intact cells (Annexin-V negative) and early apoptotic cells (Annexin-V positive).

Cells were treated with romidepsin and/or JQ1 for 24 and 48 h. $1x10^5$ cells were harvested, washed twice with PBS and resuspended in 100 µl of 1X Annexin V Binding Buffer. Five µl of Annexin V-PE were added. After incubation for 15 min at room temperature in the dark, 400 µl of Annexin V Binding Buffer were added and samples were analyzed by flow cytometry. The percentage of apoptotic cells was calculated using FACSDIVA™ software (BD Biosciences). The number of apoptotic cells was expressed as percentages relative to the apoptosis of the non treated samples (value = 100%).

The cleavage of poly(ADP-ribose)polymerase-1 (PARP1) indicative of apoptosis, was analyze by immunoblot, as described below.

Annexin V Binding Buffer: *10 mM Hepes/NaOH, pH 7.4, 140 mM NaCl and 2.5 mM $CaCl_2$; stored at 4ºC.*

3.1.10. Cell cycle analysis

Cell cycle measurement was carried out using propidium iodide staining as previously described (Albajar et al., 2011). Propidium iodide is a nucleic acid intercalating agent and fluorescent molecule used to stain DNA. Propidium iodide

staining allows the quantification of the number of cells in each cell cycle phase by flow cytometry.

Cells were treated with romidepsin and/or JQ1 for 24, 48 and 72 h. $1x10^6$ cells were harvested, centrifuge for 3 min at 1500 rpm and resuspended in 1.5 ml of phosphate-buffered saline (PBS). To fix the cells, 3.5 ml of pure cold ethanol was added in a drop-wise manner on a top of a vortex device at low velocity. Cells were incubated for at least 30 min (up to 3 days) on ice. After incubation, cell were washed with PBS and resuspended in 0.5 ml PBS-citrate Na-BSA 1X containing 200 µg/ml RNase and 10 µg/ml propidium iodide. The samples were incubated at 37°C in the dark for 30 min. The analysis was performed by flow cytometry (FACSDiva cytometer). Cell cycle distribution was analyzed by flow cytometry in the FACScan cytometer (BD Biosciences).

PBS-Citrate Na-BSA 10X*: 0.1 g sodium citrate, 1 g BSA dissolved in 10 ml PBS; stored at -20ºC.*

3.2. Lentiviral infection

3.2.1. Lentivirus production

Lentiviral particles were produced to transduce different cell lines in order to downregulate CTCF expression.

To produce the lentiviral particles, HEK293T cells were transfected using the PEI cationic lipids-based method. Three different plasmids were transfected:

- pCMV-VSV-G: envelope plasmid encoding the VSV-G gene.
- psPAX2: packaging plasmid encoding the HIV gag, pol, rev and tat genes.
- Short hairpin sequence lentiviral plasmid of interest: provides the psi packaging signal and the LTRs (Long Terminal Repeats) needed to integrate the construct in the genome of the infected cell.

The ratio amount for the mixture of the three different plasmids was 1:3:4 (VSV-G:PAX2:plasmid of interest, respectively) (**Table 3.2**). The following transfer plasmids were used: pLKO (Sigma-Mission®) and pTRIPZ (Dharmacon™ GE healthcare) (**Figure 3.1**). Cells were seeded in 150 mm plates at 70-80% of confluence. Total amount of transfected DNA (6:19:25 µg) was mixed with 1 ml of DMEM (without serum) and 100 µl PEI (Polysciences, Inc.). Mixture of DNA+PEI was added to the cells containing 15 ml of serum-free DMEM and, after 12 hours, the medium was replaced by 15 ml of complete medium.

Two days after transfection, supernatants containing lentivirus were collected and stored at 4°C and 15 ml of complete medium were added. 24 hours afterwards, supernatants were collected. Both supernatants were mixed, centrifuged 10 min at 1500 rpm and filtered through a 0.45 µm pore size sterile syringe filters (Merck Millipore). Next, PEG8000 (Sigma-Aldrich) was added to a final concentration of 15%. Mixture was homogenized by inversion and kept at 4°C for at least 6 hours. After that, the mixture was centrifuged for 30 min at 1500 rpm in order to concentrate the lentiviral particles. Supernatant was removed and the pellet containing lentivirus was resuspended in 150 µl serum-free medium, aliquoted and stored at -80°C.

***PEI**: dissolved in distilled water; stock concentration 1 µg/µl, pH: 7; Filtered with a 0.22 µm pore size sterile syringe filters; stored at -20°C.*
***PEG8000**: dissolved in PBS 1X; stock concentration 40% (w/v); autoclaved; stored at room temperature.*

Table 3.2. Plasmids used in this work.

PLASMID	CONSTRUCT	ORIGIN
pLKO Control	Lentiviral empty vector	Sigma-Mission®
pLKO shCTCF	Lentiviral shRNA for human *CTCF* gene	Sigma-Mission®
TRIPZ Control	TRIPZ Inducible lentiviral empty vector	Dharmacon™ GE Healthcare
TRIPZ Human CTCF shRNA V3THS_409881	Inducible lentiviral shRNA for human *CTCF* gene	Dharmacon™ GE Healthcare
pCMV-VSV-G	*VSV-G* gene encoding enveloped lentiviral protein	Addgene
psPAX2	*GAG* and *POL* genes enconding packaging lentiviral proteins	Addgene

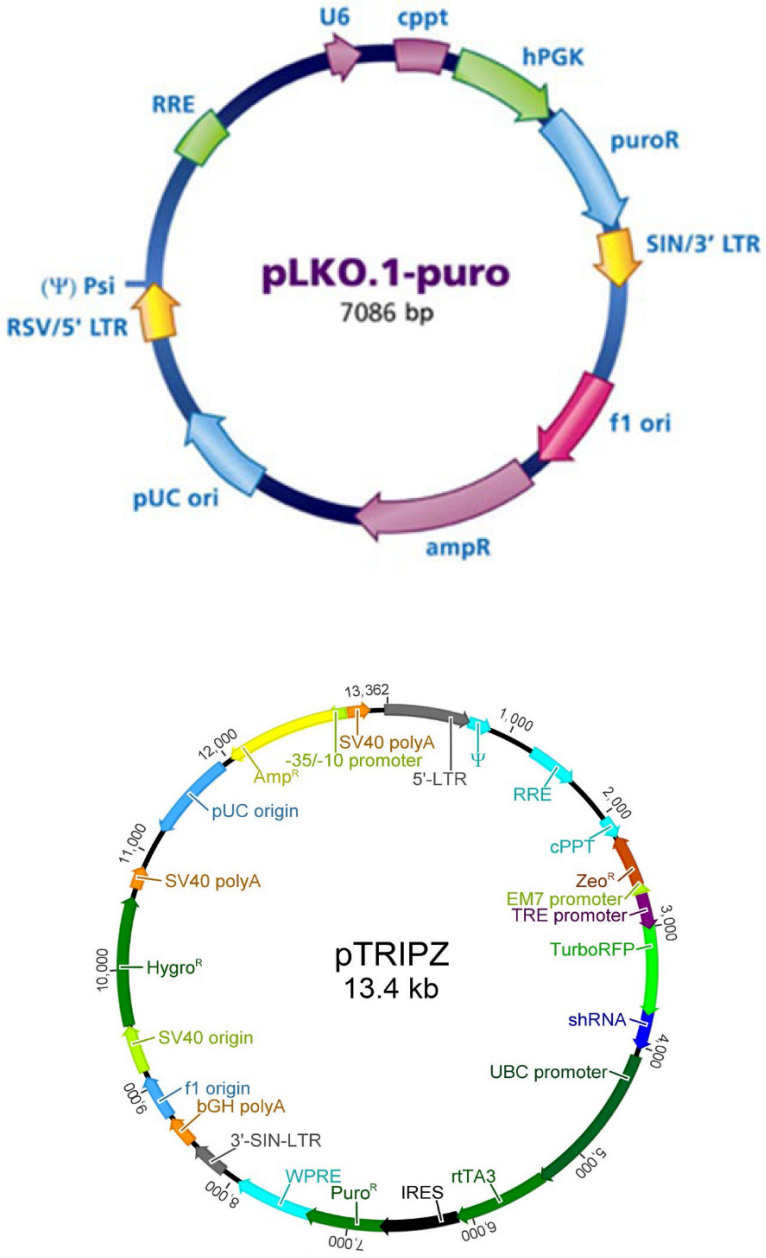

Figure 3.1. Detailed Vector Maps of the pLKO and pTRIPZ lentiviral vectors.

3.2.2. Lentivirus tittering

HeLa cells were used to titer lentivirus particles. Between 10^4 and $2x10^4$ cells were seeded on a 6-well plate and different volumes of the concentrated lentivirus (0.1, 0.5, 1 and 5 µl) were added in 1.5 ml of serum-free culture medium containing 3 µg/ml of Polibrene (Sigma-Aldrich). After 12 hours, 3 ml of complete medium were added and 48 hours after infection the selective antibiotic was

added (1 µg/ml of Puromycin; Sigma-Aldrich) to select the infected cells. Puromycin selection was controlled by using a control well without lentiviral particles. Puromycin selection was maintained until control cells die and the single-infected cells form colonies of more than 6-10 cells. Then, the medium was removed and the wells were washed twice with PBS. Cell colonies were stained with Crystal Violet solution and the number of cell colonies were counted under the microscope. The titer of the lentivirus was calculated as following:

$$\frac{\text{x number of colonies}}{\text{y µL of virus}} \text{ x } 10^3 = \text{C.F.U./ml}$$

Polybrene*: dissolved in distilled water; stock concentration: 5 mg/mL; stored at -20°C.*
Crystal Violet solution*: 1% acetic acid, 1% methanol, 1% (w:v) crystal violet dye.*

3.2.3. Cell transduction

For K562 cells transduction, a MOI (multiplicity of infection) from 3 to 5 was used. The MOI indicates the ratio of the number of virus particles to the number of target cells. $2.5x10^5$ cells/ml were seeded in half of the normal volume in serum-free medium and the corresponding amount of lentiviral particles. 5 µg/ml polybrene were added to the cells during transduction in order to increase the efficiency of the infection. After 12 hours, complete cell culture medium was added until the corresponding total volume and 48 hours after infection medium was removed and new medium, containing 1 µg/ml puromycin, was added to select the infected cell population.

For $CD34^+$ cells transduction, a MOI of 3 was used. 1.2 ml per well of 50 µg/ml retronectin were added in a 6-well plate and incubated for 2 hours at room temperature. Retronectin is a 63 kDa fragment of recombinant human fibronectin fragment that enhances the efficiency of lentiviral-mediated gene transduction. Then, retronectin was removed and 1.2 ml of PBS-2% BSA were added and incubated 30 min at room temperature. After that, wells were washed with PBS. The corresponding amount of viruses was added and incubated for 5 hours at 37°C. Lentivirus were removed and cells were resuspended in 1 ml of serum-free

medium. After 12 hours, StemSpam™ SFEM II supplemented with StemSpan™ CD34⁺ Expansion Supplement 10X (StemCell Technologies) was added until the corresponding total volume and 48 hours after infection medium was removed and new medium with 0.5 µg/ml puromycin was added to select the infected cell population.

Retronectin*: dissolved in PBS; stock concentration: 1 µg/µl; stored at -20ºC.*

3.3. DNA and RNA analysis

3.3.1. Plasmid DNA purification

Plasmid DNA for transfections was purified using the Plasmid Midi Kit (Qiagen). Twenty µl from the glycerol stock of the desire plasmid-containing bacteria was inoculated into 10 ml LB growth medium containing antibiotic (100 µg/ml ampicillin) and incubated for 6 hours in an orbital shaking incubator at 37°C and 160 rpm. After incubation, the culture was added to 200 ml LB growth medium containing the same selection antibiotic and grown over-night in the same conditions (37°C and 160 rpm). The following day, bacterial culture was centrifuged at 6000 rpm for 10 min at 4°C and plasmid DNA was purified following manufacturer's instructions. Plasmid DNA concentration was determined by measuring A_{260nm} using a microvolume spectrophotometer (Thermo Scientific™ NanoDrop 2000). All constructs used in this study were verified by DNA sequencing and/or restriction enzyme digestion.

3.3.2. RNA extraction and purification

Total RNA purification from cell cultures was performed using Trizol reagent (Invitrogen™). Between 2-5x10^6 cells were collected by centrifugation and lysed with 1 ml of Trizol reagent. After 5 min of incubation at room temperature, 0.2 ml of chloroform was added, gently mixed for 15 s, incubate 2-3 min at room temperature and centrifuged at 12000 rpm for 15 min at 4°C. The upper aqueous phase was collected and mixed in a new 1.5 ml tube with 0.5 ml of isopropanol.

The mixture was incubated 10 min at room temperature and centrifuged at 12000 rpm for 20 min at 4°C. Supernatant was discarded and the RNA pellet was washed with 75% ethanol and centrifuged at 7500 rpm for 5 min at 4°C. Ethanol supernatant was discarded and the pellet was allowed to dry at room temperature for 5-10 min. After drying, the RNA pellet was resuspended in 30 µl of RNAse-free water. Finally, RNA concentration was determined by measuring A_{260nm} using a microvolume spectrophotometer (Thermo Scientific™ NanoDrop 2000). RNA was stored at -80°C until used.

Alternatively, RNA purification from $CD34^+$ cells was performed using the RNeasy Mini Kit (Qiagen). One million cells were collected by centrifugation and lysed with 350 µl Buffer RLT. Lysates were mixed with 350 µl of 70% ethanol. The mixture was transferred to an RNeasy mini spin column and centrifuged for 15 s at ≥ 8000 g. Then, 700 µl Buffer RW1 was added to the column and centrifuged for 15 s at ≥ 8000 g. After that, 500 µl Buffer RPE was added to the column and centrifuged for 2 min at ≥ 8000 g. Finally, RNA was eluted in 30 µl RNase-free water and RNA concentration was determined by measuring A_{260nm} using a microvolume spectrophotometer (Thermo Scientific™ NanoDrop 2000). RNA was stored at -80°C until used.

3.3.3. Reverse transcription and quantitative polymerase chain reaction (RT-qPCR)

In order to analyze the expression of genes at mRNA level, quantitative real time PCR (RT-qPCR) was performed.

For reverse transcription reaction, complementary DNA (cDNA) was synthesized from 1 µg of RNA using the iScript cDNA Synthesis Kit (Bio-Rad) in a total volume of 20 µl, according to manufacturer´s instructions. The following protocol was set for the reaction: 5 min at 25°C, 20 min at 46°C and 1 min at 85°C. The obtained cDNA samples were stored at -20°C until used.

cDNA was amplified by quantitative PCR using specific primers for the gene of interest in order to analyze the expression of a specific mRNA. Primers were designed using the online Primer 3 software tool (http://bioinfo.ut.ee/primer3-0.4.0/) following the PCR standard guidelines: length 18 to 25 bp; GC content 40 to 65%; avoiding secondary structures; Tm: 50 to 65°C. PCR conditions were determined depending on the nature and complexity of the primers. Primer sequences and amplicon sizes used in RT-qPCR assays are shown in Table 3.3.

Quantitative PCR reaction mix was prepared (22 µl final volume used for two duplicate reactions) mixing 11 µl of 2X SyBR® Select Master Mix (Applied Biosystems), 1.3 µl of specific primers (0.3 µM; stock concentration 100 mM), 8.7 µl of distilled water and 1 µl of cDNA. Ten µl per well were loaded on a 96-well white PCR plate. Reaction mix without cDNA was used as negative control to detect possible amplification from contaminating DNA or primer dimers.

PCR was performed in the CFX Connect™ Real-Time PCR Detection System (Bio-Rad). The qPCR protocol for DNA amplification was the following: 95°C 10 min; (95°C 5 min; 55-65°C 30 s) 40 cycles; 95°C 1 min; 55°C 1 min. The protocol for real time melting curve was: (55°C 10 s decreasing by half a degree each cycle) 80 cycles.

Quantitative PCRs were analyzed with the CFX Manager™ software. Threshold cycles (Ct) were determined by default at the beginning of DNA amplification in the exponential phase. mRNA expression of genes of interest was normalized to mRNA expression of the ribosomal protein S14 using the comparative DeltaDeltaCt (ΔΔCt) method:

**deltaCt1 = Ct (target condition 1) - Ct (normalizer condition 1; S14).*
deltaCt2 = Ct (target condition 2) - Ct (normalizer condition 2; S14).
*** delta delta Ct: delta Ct1-delta Ct2*
****comparative expression level = 2 –ΔΔCt*
*****Standard deviation= √(SD1 2+SD2 2)*

Table 3.3. Primers used for RT-qPCR analysis

AMPLIFIED GENE	PRIMER SEQUENCES (5´ → 3´)	AMPLICON SIZE
CTCF	Fw: TTACACGTGTCCACGGCGTTC Rv: GCTTGTATGTGTCCCTGCTGGCA	365 bp
ETS1	Fw: TCCAGACAGACACCTTGCAG Rv: TGAGGCGATCACAACTATCG	153 bp
GATA1	Fw: CCAAGCTTCGTGGAACTCTC Rv: CCTGCCCGTTTACTGACAAT	202 bp
GATA2	Fw: CAAGATGAATGGGCAGAACC Rv: GCCATAAGGTGGTGGTTGTC	113 bp
GLYCOPHORIN-A	Fw: GAGAAAGGGTACAACTTGCC Rv: CATTGATCACTTGTCTCTGG	220 bp
HEY1	Fw. GACCGTGGATCACCTGA AA Rv. ATTCCCGAAATCCCAAACTC	123 bp
KLF1	Fw: CAGGTGTGATAGCCGAGACC Rv: CCGTGTGTTTCCGGTAGTG	241 bp
LMO2	Fw: CTGAGCTGCGACCTCTGTG Rv: CGCATTGTCATCTCATAGGC	164 bp
MYB	Fw: AGCAAGGTGCATGATCGTC Rv: GGGGGTGGAAGTTAAAGAAGG	157 bp
MYC	Fw: TCGGATTCTCTGCTCTCCTC Rv: CCTGCCTCTTTTCCACAGAA	157 bp
NFE2L2	Fw: CGGTATGCAACAGGACATTG Rv: AGAGGATGCTGCTGAAGGAA	246 bp
PAX5	Fw: AGACTTGTTCACACAGCAGCA Rv: AGATTGGCCTTCATGTCGTC	165 bp
PRDM1	Fw: CTGAGAGTGCACAGTGGAGA Rv: TGGGTCTTGAGATTGCTGGT	167 bp
RPS14	Fw: TATCACCGCCCTACACATCA Rv: GGGGTGACATCCTCAATCC	135 bp
XBP1	Fw: GGAGTTAAGACAGCGCTTGG Rv: GAGATGTTCTGGAGGGGTGA	168 bp
ε-GLOBIN	Fw: GCAAGAAGGTGCTGACTTCC Rv: TGCCAAAGTGAGTAGCCAGA	168 bp

3.4. Protein analysis

3.4.1. Western-Blot

Protein levels were analyzed by Western-Blot. Five to ten million cells were collected, washed in cold PBS and resuspended in RIPA lysis buffer. Cell lysates were incubated 30 min on ice. Then, samples were sonicated using the Bioruptor Plus sonication device (Diagenode) set at high power setting for 10 cycles (30 s ON, 30 s OFF). After sonication, cell lysates were centrifuged at 14000 rpm for 20 min at 4°C. Supernatant was placed on a new tube and protein concentration was measured using the Qubit 2.0 Fluorometer (Invitrogen) mixing 1 µl of the

protein extract with 199 µl of freshly prepared Qubit Working Solution (Invitrogen). Samples were incubated for 15 min protected from light at room temperature and finally, samples were read in the Qubit 2.0 Fluorometer.

5X Laemli buffer were mixed with 50 µg of protein and distilled water to 1X final concentration. The protein samples were heated for 4 min at 95°C and loaded in a polyacrylamide-SDS (SDS-PAGE) gel. The percentage of the SDS-PAGE gels varied from 8 to 15% depending on the molecular weight of the analyzed protein. Vertical electrophoresis was carried out in a Mini Protean III cuvette, (Bio-Rad) at constant voltage of 175 V for 1 hour, using electrophoresis running buffer. "Precision PlusProtein™ Dual Colors Standars" (Bio-Rad) were used to evaluate protein migration and separation during gel electrophoresis. Proteins were transferred to a nitrocellulose membrane (AmershamProtan Supported 0.45 NC, GE Healthcare Life Sciences) in a Mini-Trans Blot cell (Bio-Rad) using transfer buffer at constant amperage of 400 mA for 30 min to 1 hour depending on the molecular weight of the protein of interest. After the transference, the polyacrylamide-SDS gels were stained with Coomassie Brilliant Blue solution for 10 min at room temperature and distained with water until proteins bands were seen to check proteins load and integrity.

The membrane containing the proteins was incubated with shaking for 60 min at room temperature using TBS-T solution with 10% non-fat dry milk for blocking unspecific binding sites. Then, the membranes were incubated over-night or during 4 hours at 4°C in agitation with the specific primary antibody (**Table 3.4**) diluted in 1-5% BSA in TBS-T solution. Membranes were washed 3 times for 5 min each with TBS-T at room temperature on a shaker and incubated with the corresponding fluorescent secondary antibodies (**Table 3.5**) for 45 min diluted in 1% BSA in TBS-T. Finally, the membranes were washed 3 times for 5 min each with TBS-T solution.

Finally, the immunocomplexes were detected with an Odyssey Infrared Imaging System (Li-COR, Biosciences). For protein loading control, the blots were restained with anti-Actin or anti-Tubulin antibodies.

***RIPA lysis buffer**: 150 mM NaCl, 50 mM Tris-HCl pH 6.8; 0.5% NaDoc; 1% NP-40; 0.1% SDS; supplemented with protease inhibitor cocktail Set I (1:100; Calbiochem) and phosphatase inhibitor cocktail I (1:100; Sigma-Aldrich®) immediately before using; stock concentration: 1%; stored at 4°C.*

***Laemli buffer**: 100 mM Tris-HCl pH 6.8, 5% β-mercaptoethanol (v/v), 5% SDS (w/v), 0.1% bromophenol blue (w/v), 50% glycerol (v/v); stock concentration: 5X; stored at -20°C.*

***Running buffer**: 25 mM Trizma pH 8.3, 192 mM glycine and 0.1% SDS (w/v); stock concentration: 1X; stored at room temperature.*

***Transfer buffer**: 25 mM Trizma pH 8.3, 192 mM glycine and 10% methanol (v/v); stock concentration: 1X; stored at room temperature.*

***Coomassie Brillant Blue solution**: 0.025% Coomassie Brilliant Blue R-250 (w/v), 40% methanol (v/v) and 10% (v/v) glacial acetic acid; stock concentration: 1X; stored at room temperature.*

***TBS-T**: 20 mM Tris-HCl pH 7.5, 150 mM NaCl, 0.05% Tween 20 (v/v); stock concentration: 1X; stored at room temperature protected from light.*

Table 3.4. Primary antibodies used for Western-Blot

ANTIBODY	TYPE	ORIGIN	DILUTION
ACTIN (C-4)	Mouse monoclonal	Santa Cruz BT (sc-47778)	1:3000
BCL6 (N-3)	Rabbit polyclonal	Santa Cruz BT (sc-858)	1:1000
BCL-xL	Rabbit monoclonal	Cell Signaling (2764s)	1:1000
BLIMP1	Rabbit polyclonal	Cell Signaling (C14A4)	1:1000
CTCF	Mouse monoclonal	BD Bioscience (612149)	1:1000
CYCLIN-A (H-432)	Rabbit polyclonal	Santa Cruz BT (sc-751)	1:1000
GATA1 (C-20)	Goat polyclonal	Santa Cruz BT (sc-1233)	1:1000
LMO2	Rabbit polyclonal	Abcam (ab72841)	1:2000
MYC	Rabbit polyclonal	Cell Signaling (9402s)	1:3000
P21	Rabbit monoclonal	Cell Signaling (2947s)	1:1000
P27	Rabbit monoclonal	Cell Signaling (3686s)	1:1000
PARP1 (H-250)	Rabbit polyclonal	Santa Cruz BT (sc-7150)	1:1000
TUBULIN	Rabbit polyclonal	Laboratory of Nick Cowan, NY, USA	1:3000
γ-GLOBIN (51-7)	Mouse monoclonal	Santa Cruz BT (sc-21756)	1:1000
γ-H2A.X (Ser139)	Mouse monoclonal	Millipore (05-636)	1:1000

Table 3.5. Secondary antibodies used for Western-Blot

ANTIBODY	TYPE	ORIGIN	DILUTION
Anti-Goat IRDye®680	Donkey polyclonal	LI-COR (926-68074)	1:10000
Anti-Goat IRDye®800	Donkey polyclonal	LI-COR (926-32214)	1:10000
Anti-Mouse IRDye®680	Donkey polyclonal	LI-COR (926-68072)	1:10000
Anti-Mouse IRDye®800	Donkey polyclonal	LI-COR (926-32212)	1:10000
Anti-Rabbit IRDye®680	Donkey polyclonal	LI-COR (926-68073)	1:10000
Anti-Rabbit IRDye®800	Donkey polyclonal	LI-COR (926-32213)	1:10000

3.5. ENCODE analysis of CTCF binding and interactions

The Encyclopedia of DNA Elements (ENCODE) project was used to predict and analyze possible CTCF binding sites (CTSs) to erythroid genes and *MYC* gene. ENCODE is a Genome Browser, which contains a broad collection of model organism assemblies and annotations developed by University of California Santa Cruz (UCSC) and the other members of the International Human Genome Project consortium (https://genome.ucsc.edu/).

All analyses were done using the Feb. 2009 GRCh37/hg19 assembly of the human genome. CTCF ChIP-seq peak files for the K562 cell line were taken from the ENCODE project. The identified CTSs were then utilized for designing primers and performing chromatin immunoprecipitation (ChIP) to confirm CTCF binding. ENCODE analysis for the binding of cohesin (Rad21 subunit) was also carried out. ENCODE project also shows the locations of CTCF mediated chromatin interactions determined by ChIA-PET techniques (Chromatin Interaction Analysis with Paired-End Tag) sequencing.

3.6. Chromatin Immunoprecipitation (ChIP)

ChIP experiments were performed using the Pierce™ Magnetic ChIP Kit (Thermo Scientific). Four million cells were used for each immunoprecipitation.

Cells were fixed with 1% formaldehyde (Thermo Scientific 16% Formaldehide solution Methanol-free) diluted in PBS and incubated for 10 min at room temperature by shaking. To stop the fixation, glycine was added to a final concentration of 1X (stock solution: 10X) and incubated for 5 min at room temperature by shaking. Cells were collected by centrifugation (5 min at 1500 rpm) and washed twice with cold PBS. Cell pellets were resuspended in 200 µl of Membrane Extraction Buffer supplemented with protease and phosphatase inhibitors and incubated on ice for 10 min. The nuclei were collected by centrifugation (3 min at 9000 g) and resuspended in 200 µl of MNase Digestion Buffer Working Solution. MNase (10 U/µl) were diluted in MNase Digestion Buffer Working Solution (1:10) and 1 µl was added and incubate for 15 min at 37°C. After incubation, 20 µl of MNase Stop Solution was added to stop the reaction, samples were incubate on ice for 5 min and centrifuged at 9000 g for 5 min. Nuclei were resuspended in 100 µl of 1X IP Dilution Buffer supplemented with protease and phosphatase inhibitors and sonicated using the Bioruptor Plus sonication device (Diagenode) set at high power setting for 10 cycles (30 s ON, 30 s OFF). The supernatant containing the digested chromatin was collected by centrifugation at 9000 g for 5 min. Ten µl of the sample was used as the 10% total input sample and 90 µl were taken to a final volume of 500 µl with 1X IP Dilution Buffer.

Chromatin immunoprecipitation was performed with a mixture of three CTCF antibodies (2 µl of each antibody) (**Table 3.6**) and lysates were incubated rotating over-night at 4°C. For each experiment, sample without antibody was used as negative control (beads).

Table 3.6. Antibodies used for ChIP experiments

ANTIBODY	IMMUNOGEN	TYPE	ORIGIN
CTCF	Human CTCF aa. 184-290	Mouse monoclonal	BD Bioscience (612149)
CTCF	Human CTCF aa. 659-675	Rabbit polyclonal	EMD Millipore/Merck
CTCF	Human CTCF aa. 650-700	Rabbit polyclonal	ABCAM

After incubation, 20 µl of the ChIP Grade Protein A/G Magnetic Beads was added to each immunoprecipitation and incubated for 2 h at 4°C by mixing. Afterwards, beads were collected with a magnet, the supernatant was discarded and beads were washed three times with 1 ml of IP Wash Buffer 1 and once with 1 ml of IP Wash Buffer 2 for 5 min each washed. Immunocomplexes were eluted from beads in 150 µl of 1X IP Elution Buffer for 30 min at 65°C. Then, beads were collected with a magnet and the supernatant containing the eluted complexes was treated with 6 µl of 5 M NaCl and 2 µl of 20 mg/ml Proteinase K. At this point, 150 µl of 1X IP Elution Buffer, 6 µl of 5 M NaCl and 2 µl of 20 mg/ml Proteinase K were added to input samples. Immunocomplexes and input samples were incubated for 1.5 h at 65°C.

To purify DNA, 750 µl of DNA Binding Buffer was added to each sample. The mixture was transferred to a DNA Clean-Up Column and centrifuged for 1 min at 10000 g. Then, 750 µl of DNA Column Wash Buffer was added to the column and centrifuged for 1 min at 10000 g. Finally, DNA was eluted in 50 µl of DNA Column Elution Solution by centrifugation at 10000 g for 1 min.

Immunoprecipitated DNA was analyzed by quantitative PCR using the CFX Connect™ Real-Time PCR Detection System (Bio-Rad). Quantitative PCR reaction mix was prepared (35 µl final volume used for two duplicate reactions) mixing 17.5 µl of 2X SyBR® Select Master Mix (Applied Biosystems), 2.1 µl of specific primers (0.3 µM; stock concentration 100 mM), 12.4 µl of distilled water and 3 µl of DNA. Fifteen µl per well were loaded on a 96-well white PCR plate. Primers were designed using the online Primer 3 software tool (http://bioinfo.ut.ee/primer3-0.4.0/) (**Table 3.7**). Quantitative PCR protocol was the same described in RT-qPCR section.

Immunoprecipitated DNA was normalized to total DNA (input) using the comparative DeltaCt (ΔCt) method: $\Delta Ct = 2^{(Ct\ input\ -\ Ct\ immunoprecipitated\ sample)}$ where Ct is the number of cycles needed to rise the threshold. The fold enrichment was calculated relative to the control sample (no-antibody).

Table 3.7. Primers used for ChIP

AMPLIFIED GENE	LOCATION	PRIMER SEQUENCES (5´ → 3´)	AMPLICON SIZE
ETS1	43 kb upstream	Fw: GAGGTCCTTCCTCCTGGAAC Rv: ATGCAGCTATTGGGTTTTGC	184 bp
GATA2	5 kb upstream	Fw: TGCTTTGTCACTGCTGTTCC Rv: AAATTCAGTGGGATGCGTTC	198 bp
H4	rDNA repeats	Fw: CGACGACCCATTCGAACGTCT Rv: CTCTCCGGAATCGAACCCTGA	103 bp
H42.1	rDNA repeats	Fw: GCTTCTCGACTCACGGTTTC Rv: CCGAGAGCACGATCTCAAA	124 bp
HEY1	Exon 5 (+ 2.1 kb)	Fw: GCCACTGAGGAGAGCAGAG Rv: GACCGTCTTCGGACATCAC	234 bp
KLF1	Exon 2 (+ 1.4 kb)	Fw: GGTGGGAGCTCTTGGTGTAG Rv: CCCCTCCTTCCTGAGTTGTT	191 bp
LMO2	34 kb downstream	Fw: TTAAGGTGATGGCCAGAAGG Rv: TTTTCCAAGACGGGTGTCTC	162 bp
MYB	Intron 1 (+ 2.5 kb)	Fw: TCCAAGCAAGCCCTTATTGT Rv: ACAACCCAGGAACAAGCAAC	198 bp
MYC A/B	0.2 kb downstream MYC	Fw: CGGGGCTTTATCTAACTCGC Rv: TGGGCAAAGTTTCGTGGATG	220 bp
MYC N	2 kb upstream MYC	Fw: GTGCATCGGATTTGGAAGCT Rv: TTTTCTCTCCCTCCACCACC	157 bp
MYC SITE -10	10 kb upstream MYC	Fw: CTTCTCCCTAGCCCAGTTCC Rv: TGAATTGCCCTCATTGACCG	195 bp
MYC SITE -335	335 kb upstream MYC	Fw: ACCTCTGACCAATTGCCTGA Rv: GCTGAGCTCAAAGGACGATG	150 bp
MYC SITE -515	515 kb upstream MYC	Fw: TGGTGGAGAGAAGGATGCAG Rv: CCCTGTGGTCAATTGAGGGA	180 bp
MYC W	1.8 kb downstream MYC	Fw: AGCTGGCAAAAGGAGTGTTG Rv: AAAGTTTTGCGCCACCTGAA	221 bp
NFE2L2	Intron 1 (+ 10 kb)	Fw: GCAACAGATCAACAGCTCCA Rv: CACCCGGGGCTTCTAGTT	185 bp
TCF3	23 kb upstream	Fw: ACAGGGACAGATCCAACCAC Rv: AGGCTGGATTGGGATTGAG	155 bp

3.7. Statistical analysis

Data was represented as the mean of two to five independent experiments (in some cases performed in duplicate or triplicate). Error bars represent the standard error of the mean.

The significance of differences was determined by the unpaired Student's *t*-test. Results were considered statistically significant when $\rho < 0.05$ (* $\rho < 0.05$; ** $\rho < 0.01$; *** $\rho < 0.001$; **** $\rho < 0.0001$).

RESULTS

4. RESULTS

4.1. Function of CTCF in the control of erythroid differentiation

During erythroid cell differentiation, hematopoietic stem cells differentiate into different erythroid progenitors to finally form mature red blood cells. Erythropoiesis is a highly regulated process by different growth factors, cytokines and transcription factors.

The transcription factor CTCF has the ability to bind to a high number of DNA sequences all over the genome and participates in the regulation of gene transcription, chromatin insulation, epigenetic regulation and genome organization. Insulator activities nearby globin genes firstly indicated a role of CTCF in erythroid cell differentiation (Splinter et al., 2006). Previous results from our group indicated a possible role of CTCF in the regulation of erythroid differentiation (Delgado et al., 1999), showing that overexpression of CTCF promotes erythroid cell differentiation (Torrano et al., 2005). However, the underlying molecular events of these effects are unknown.

The aim of the first part of this work is to gain further insight into CTCF function in the control of erythroid cell differentiation and in the regulation of specific erythroid transcription factors in hematopoietic cells.

4.1.1. Cytosine arabinoside (Ara-C) and Imatinib induce erythroid cell differentiation in K562 cells

In order to study the role of CTCF in the control of erythroid differentiation, we first used the multipotent cell line K562 which derived from a human chronic myeloid leukemia in blast crisis. This cell line has the ability to differentiate into distinct hematopoietic lineages in response to specific differentiation inducers. For example, K562 can be differentiated into the erythroid lineage by treatment with cytosine arabinoside (Ara-C) (Delgado et al., 1995) or Imatinib (Gómez-Casares et al., 2013) (**Figure 4.1a**), into the megakaryocytic lineage with

staurosporine or into the monocytic-macrophagic pathway with TPA (Lerga et al., 1999). In this cellular model, CTCF seems to have a specific role in the erythroid differentiation (Torrano et al., 2005).

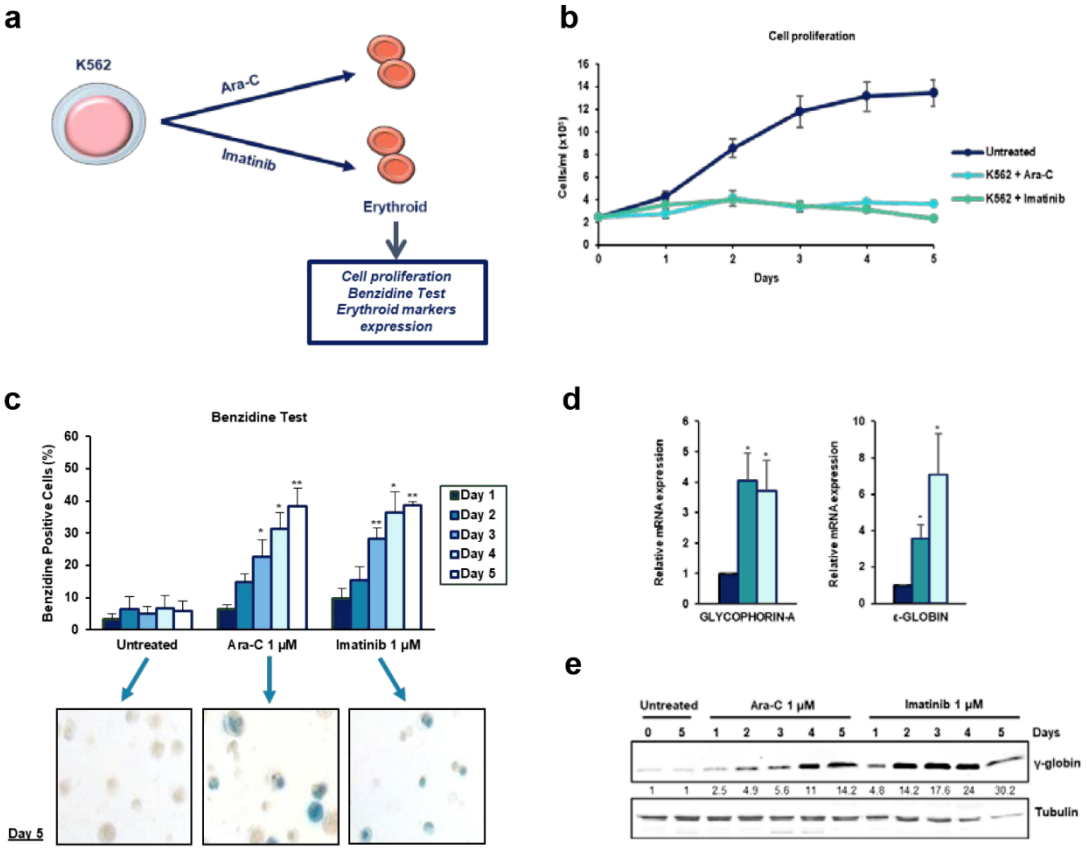

Figure 4.1. Ara-C and Imatinib induce erythroid differentiation of K562 cells. *a) Schematic representation of the differentiation assay. b) Cell proliferation curves for K562. 2.5x10^5 cells were seeded and treated with 1 µM Ara-C or 1 µM Imatinib. Cells were counted daily for 5 days. Bars indicate mean ± s.e.m of five independent experiments. c) Benzidine test of K562 cells treated with 1 µM Ara-C or 1 µM Imatinib for 5 days. Pictures taken during benzidine test evaluation are shown. In each experiment, a minimum of 200 cells were counted. Bars indicate mean ± s.e.m of three independent experiments; significance difference (*,p<0.05; **,p<0.01) from the untreated cells. d) Expression of glycophorin-A and ε-globin was analyzed by RT-qPCR after treatment with 1 µM Ara-C and 1 µM Imatinib for 72 hours. Expression was normalized against RPS14 levels. Bars indicate mean ± s.e.m of two to four independent experiments; significance difference (*,p<0.05) from the untreated cells. e) Protein expression of γ-globin analyzed by Western-Blot after treatment with 1 µM Ara-C and 1 µM Imatinib during 5 days. Tubulin levels were used as loading control. Densitometry values are shown at the bottom, normalized to the control.*

We first confirmed the effects of Ara-C and imatinib in the proliferation and differentiation of K562 cells. Erythroid cell differentiation is correlated with cell growth arrest while undifferentiation and stemness maintenance are associated to an active proliferative state. Erythroid differentiation was induced by treatment with 1 μM Ara-C and 1 μM Imatinib in K562 cells and number of cells were counted during the following five days to analyze cell proliferation. We observed that both treatments induced cell proliferation arrest in K562 cells compared to untreated cells (**Figure 4.1b**). Trypan blue assay was carried out to assess cell viability. Treatment with 1 μM Ara-C did not significantly affect cell viability, while treatment with 1 μM Imatinib decreased cell viability up to 50% after four days (data not shown). For that reason, we decided to reduce Imatinib concentration to 0.5 μM and time of treatment up to 72 hours in the following studies.

The presence of hemoglobin is exclusive of erythroid cells. Thus, we can assess the erythroid differentiation analyzing the hemoglobin production using the benzidine test. With this test, the cells which produce hemoglobin become blue in the presence of benzidine. K562 cells were treated with 1 μM Ara-C and 1 μM Imatinib and benzidine test was performed during 5 days (**Figure 4.1c**). We observed that cells treated with Ara-C and Imatinib showed a progressive increase in the percentage of hemoglobin producing cells after 5 days of treatment compared to untreated cells, indicating erythroid cell differentiation.

In order to confirm erythroid differentiation induction, we analyzed the expression of key erythroid markers. For that, K562 cells treated during 72 hours with Ara-C or Imatinib were harvested and mRNA expression was measured by RT-qPCR (**Figure 4.1d**). We analyzed the levels of glycophorin-A (GYPA), which is an erythrocyte membrane surface marker and ε-globin, which is an embryonic globin gene expressed in K562 and used as a specific erythroid marker. GYPA and ε-globin levels were significantly upregulated upon treatment with both drugs. We also analyzed by Western-Blot the expression of the fetal γ-globin protein upon induction of differentiation (**Figure 4.1e**). Ara-C and Imatinib treatments increased γ-globin protein levels within 5 days compared with untreated cells.

As mentioned before, CTCF is involved in the regulation of erythroid cell differentiation. CTCF was first described as a transcriptional regulator of *MYC* gene which also plays an important role in erythropoiesis. Our group has previously described that MYC inhibits erythroid differentiation induced by Ara-C in K562 cells (Delgado et al., 1995) and inhibition of MYC activity enhances erythroid differentiation (Cañelles et al., 1997). So, we analyzed CTCF and MYC mRNA and protein levels in K562 cells upon Ara-C and Imatinib treatment in order to analyze how their expression changes upon erythroid differentiation (**Figure 4.2**). We observed a significant downregulation of CTCF mRNA expression only with Ara-C, while CTCF protein levels were maintained quite stable along the differentiation process. A strong downregulation in MYC mRNA and protein levels was observed upon induction of differentiation with both treatments, as previously described (Delgado et al., 1999). These results are consistent with the role of MYC in cell proliferation and in the maintenance of an undifferentiated state. Taking all these results together we can confirmed the induction of erythroid differentiation of K562 cells upon Ara-C and Imatinib treatment.

4.1.2. CTCF knock-down inhibits erythroid differentiation induced by Ara-C and Imatinib in K562 cells

To study the importance of CTCF in erythropoiesis, we aimed to silence its expression in K562 cells and analyzed erythroid cell differentiation upon induction with Ara-C and Imatinib. First, we produced lentiviral particles containing a specific shRNA for *CTCF* gene (shCTCF) and for the corresponding empty vector pLKO (EV). K562 cells were infected with the lentiviral particles, selected for puromycin resistance for two days and CTCF downregulation was assessed by RT-qPCR and Western-Blot (**Figure 4.3a**).

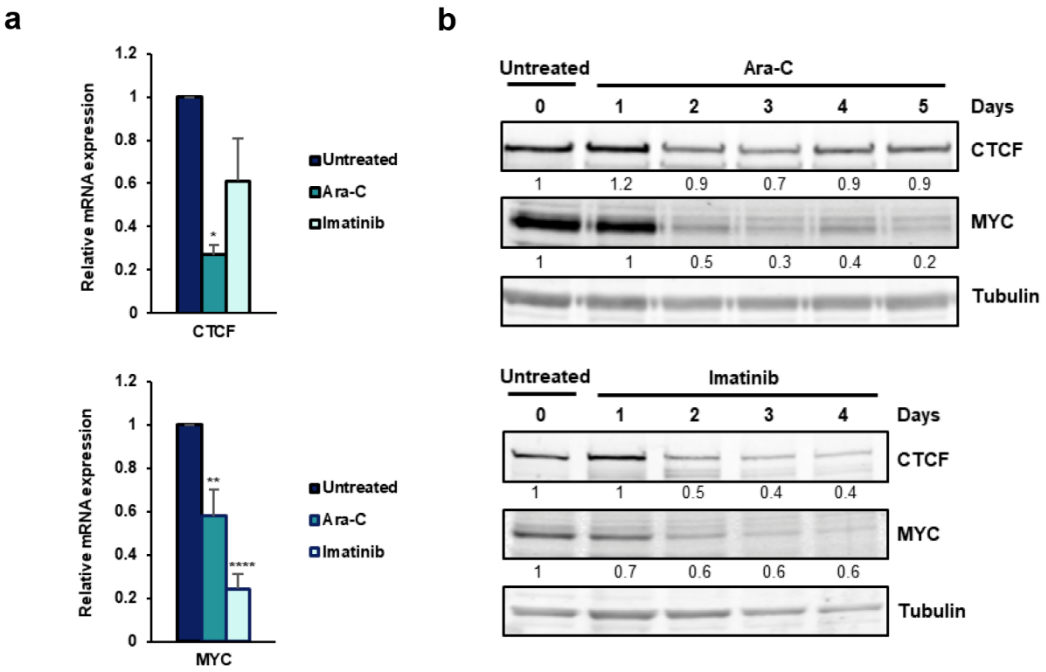

Figure 4.2. CTCF and MYC expression upon erythroid differentiation of K562. *a) Expression of CTCF and MYC was analyzed by RT-qPCR after treatment with 1 μM Ara-C or 1 μM Imatinib for 72 hours. Expression was normalized against RPS14 levels. Bars indicate mean ± s.e.m of two to five independent experiments; significance difference (*,p<0.05; **,p<0.01; ****,p<0.0001) from the untreated cells. b) Protein expression of CTCF and MYC analyzed by Western-Blot after treatment with 1 μM Ara-C or 1 μM Imatinib during 5 days. Tubulin levels were used as loading control. Densitometry values are shown at the bottom, normalized to the control.*

Once CTCF downregulation was confirmed, infected K562 cells were treated with 1 μM Ara-C or 0.5 μM Imatinib during 3 days to induce erythroid cell differentiation. We analyzed again CTCF protein levels by Western-Blot to confirm that CTCF downregulation was maintaining upon treatments (**Figure 4.3b**). Exponentially growing cells were counted daily for 3 days and growth curves were performed (**Figure 4.3c**). We found that both treatments reduced cell proliferation independently of CTCF downregulation. We also observed a slight reduction in cell proliferation when we reduced CTCF expression.

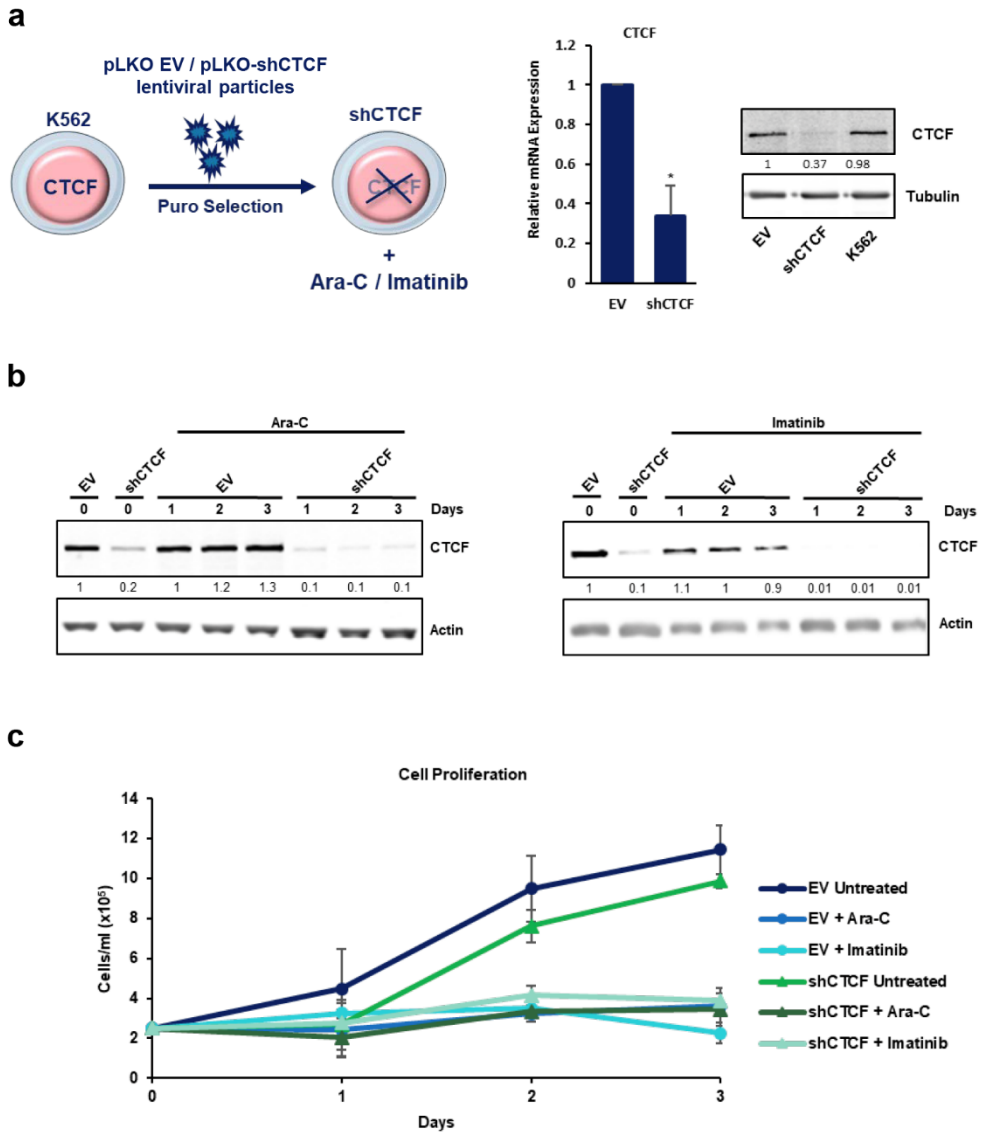

Figure 4.3. Downregulation of CTCF in K562 cells with the pLKO constitutive vector. *a) Schematic representation of the experimental workflow and validation of CTCF downregulation. Expression of CTCF was analyzed by RT-qPCR after infection of K562 cells with shCTCF or pLKO (EV) and selection with puromycin for two days. Expression was normalized against RPS14 levels. Bars indicate mean ± s.e.m of three independent experiments; significance difference (*,p<0.05) from the untreated cells. CTCF protein levels analyzed by Western-Blot in K562 cells infected as above. Tubulin levels were used as loading control. Densitometry values are shown at the bottom, normalized to the control. b) CTCF protein levels analyzed by Western-Blot after infection of K562 cells with shCTCF or pLKO EV and treated with 1 μM Ara-C or 0.5 μM Imatinib during 3 days. Actin levels were used as loading control. Densitometry values are shown at the bottom, normalized to the control. c) Cell proliferation curves for K562 infected with shCTCF or pLKO (EV). 2.5x10^5 cells were seeded after 2 days of puromycin selection and treated with 1 μM Ara-C or 0.5 μM Imatinib. Cells were counted daily for 3 days. Bars indicate mean ± s.e.m of two independent experiments.*

.

To verify that the downregulation of CTCF inhibits erythropoiesis, the expression of specific erythroid markers, γ-globin, GATA1 and LMO2, were analyzed by Western-Blot upon induction of cell differentiation (**Figure 4.4b**). As we shown before, γ-globin levels increased upon treatment with Ara-C and Imatinib in K562 cells infected with the empty vector, indicating erythroid differentiation. However, upon CTCF silencing, no increase in γ-globin protein levels was observed. Similar results were found when we analyzed GATA1 and LMO2 levels: they increased upon treatments with Ara-C and Imatinib but remained low when CTCF expression was reduced. These results were consistent with the benzidine test data.

Interestingly, when we compared the K562 cells infected with shCTCF with the ones infected with the EV prior to Ara-C or Imatinib treatment (Day 0 of treatment), we also observed a reduction in the percentage of benzidine positive cells (**Figure 4.4.a**) and in the expression of γ-globin, GATA1 and LMO2 protein levels (**Figure 4.4b**; Day 0). These results indicates that knock-down of CTCF not only inhibits erythroid differentiation induced by Ara-C and Imatinib, but also the spontaneous erythroid differentiation.

To sum up, downregulation of CTCF strongly decreases the percentage of hemoglobin producing cells and erythroid markers protein levels, indicating that CTCF knock-down could inhibit erythroid cell differentiation.

In order to confirm and extend these results, the pTRIPZ inducible lentiviral shRNA vector containing a tetracycline-inducible promoter reporter (tet-on system) was used. K562 cells were infected with pTRIPZ Empty Vector and pTRIPZ shCTCF lentiviral particles and selected for puromycin resistance to eliminate the uninfected cells (**Figure 4.5a**). Then induction with doxycycline was carried out for 3 days and the expression of the TurboRFP reporter (indicating the efficiency of infection) was checked by microscopy and quantified. We obtained more than the 83% of infected cells with the empty vector and more than the 78% with the shCTCF vector (**Figure 4.5b**). The next step was to confirm CTCF downregulation upon doxycycline induction, by RT-qPCR. Induction of

pTRIPZ shCTCF with doxycycline reduced CTCF mRNA levels more than the 60% (**Figure 4.5c**).

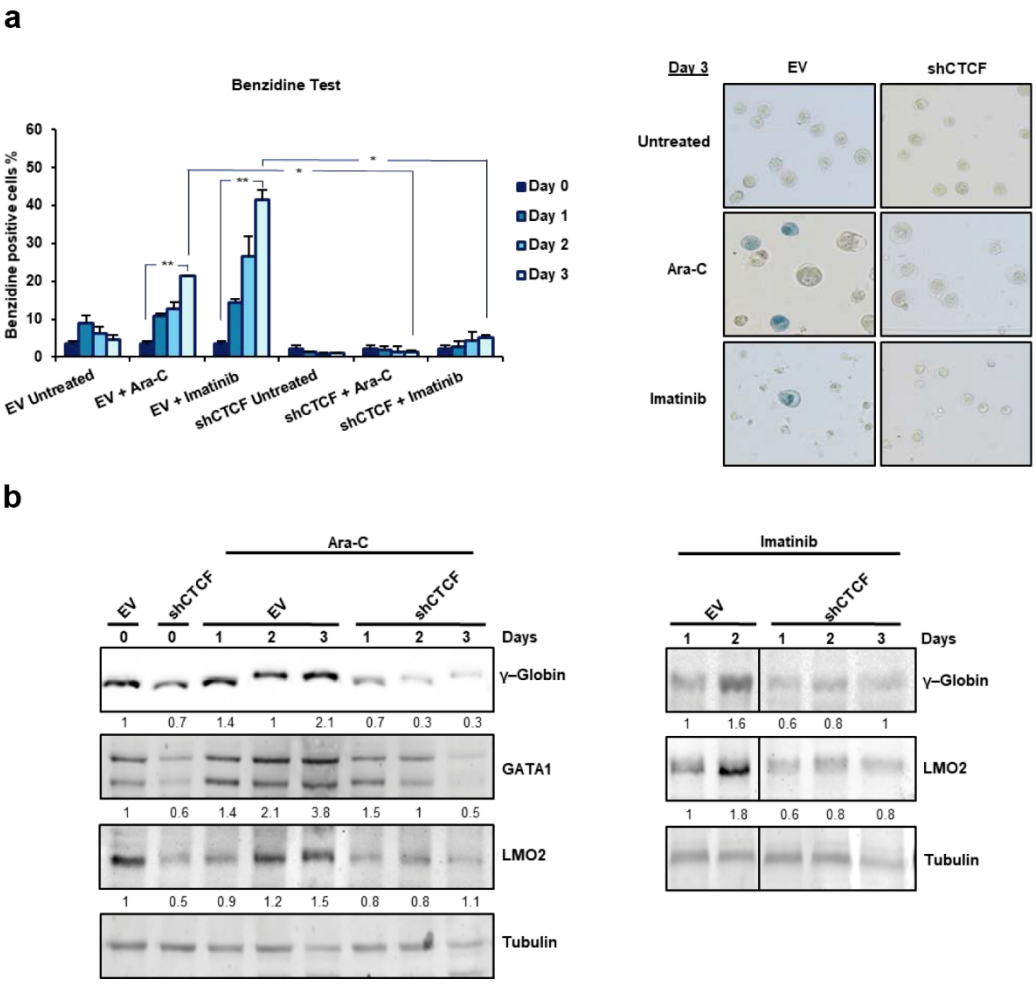

Figure 4.4. Constitutive CTCF downregulation inhibits erythroid differentiation of K562 cells. *a) Benzidine test of K562 cells infected with shCTCF or pLKO EV and treated with 1 μM Ara-C or 0.5 μM Imatinib during 3 days. Pictures taken during benzidine test evaluation are shown. In each experiment, a minimum of 200 cells were counted. Bars indicate mean ± s.e.m of three independent experiments; significance difference (*,p<0.05; **,p<001) from the untreated cells. b) Protein expression of γ-globin, GATA1 and LMO2 analyzed by Western-Blot after infection of K562 cells with shCTCF or pLKO EV and treated with 1 μM Ara-C or 0.5 μM Imatinib during 3 days. Tubulin levels were used as loading control. Densitometry values are shown at the bottom, normalized to control.*

Once confirmed that the inducible system worked, infected K562 cells were treated with 1 μM Ara-C or 0.5 μM Imatinib for 3 days to induce erythroid differentiation. Then, we analyzed CTCF protein levels by Western-Blot to confirm

that CTCF downregulation was maintaining upon treatments (**Figure 4.6a**). Number of cells were counted during 3 days of treatment to measure cell proliferation. As we observed before, Ara-C and Imatinib treatments inhibited cell proliferation independently of CTCF downregulation (data not shown).

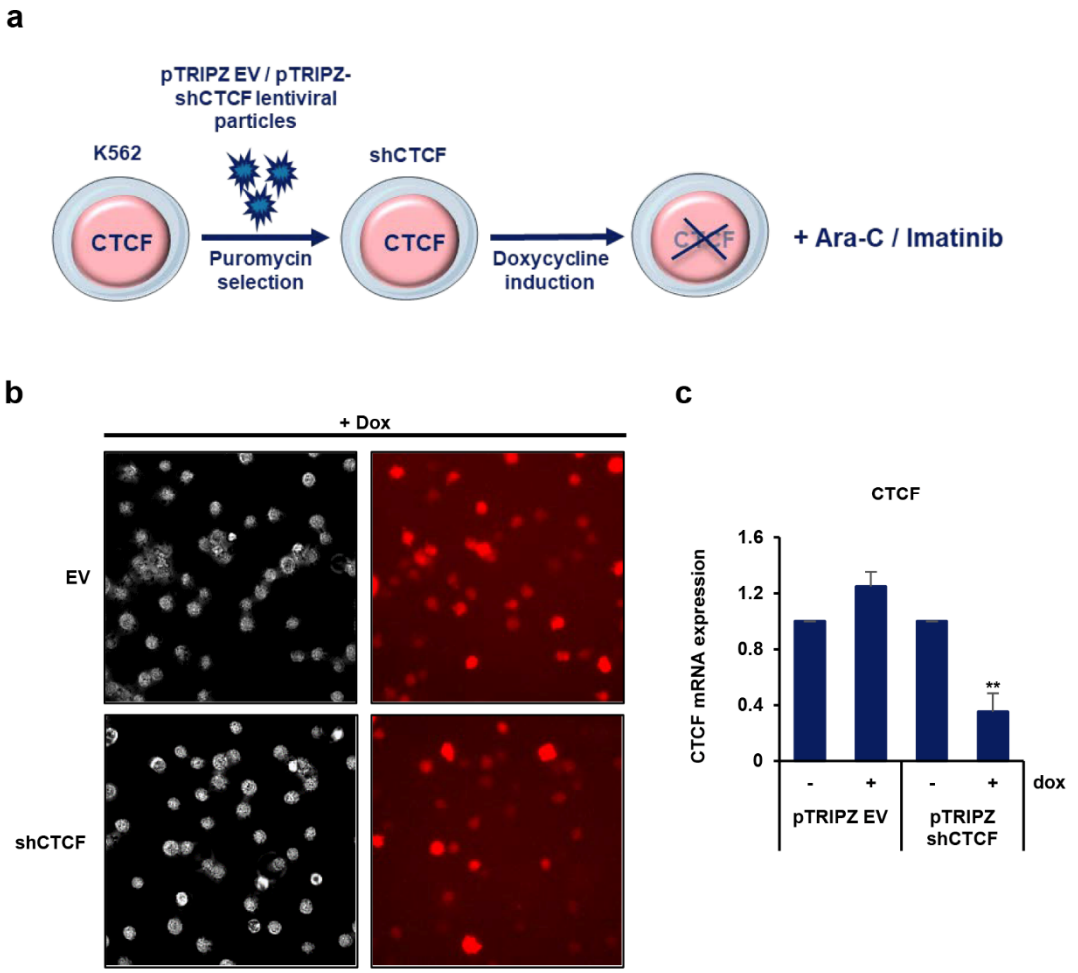

Figure 4.5. Downregulation of CTCF in K562 cells with the pTRIPZ inducible vector. *a) Schematic representation of the experimental workflow. b) Efficiency of infection checked by microscopy after three days with doxycycline induction. Bright field pictures show total cell number. Red cells represent infected cells. c) Validation of CTCF downregulation. Expression of CTCF was analyzed by RT-qPCR after infection of K562 cells with inducible shCTCF or pTRIPZ EV, two days of puromycin selection and three days of induction with 2 µg/ml doxycycline. Expression was normalized against RPS14 levels. Bars indicate mean ± s.e.m of three independent experiments; significance difference (**,p<0.01) from the untreated cells.*

Erythroid differentiation was assessed by the benzidine test to score hemoglobinized cells after three days of Ara-C or Imatinib treatment (**Figure**

4.6b). In cells infected with the EV without (-) and with (+) doxycycline induction, we observed and increase in the percentage of benzidine positive cells, as expected. Similar results were observed in K562 cells infected with shCTCF prior to doxycycline induction. However, in K562 cells with CTCF downregulation (i.e. upon doxycycline induction), the percentage of hemoglobinized cells was significantly reduced, indicating inhibition of erythroid cell differentiation. We also analyzed the expression of erythroid markers by Western-Blot (**Figure 4.6c**). γ-globin levels increased upon treatments with Ara-C and Imatinib in cells with normal expression of CTCF. However, in cells with shCTCF, lower increase in γ-globin protein levels was observed. Similar results were observed when GATA1 protein levels were analyzed.

These results obtained upon knock-down of CTCF with the inducible pTRIPZ system are consistent with the ones obtained with the constitutive pLKO system. Altogether, our results indicate that silencing of CTCF inhibits erythroid cell differentiation, therefore, CTCF seems to be essential for erythroid differentiation in K562 cells.

4.1.3. Erythropoietin (EPO) induces erythroid differentiation in primary CD34$^+$ cells

In view of the results observed with the K562 cell line, we decides to switch to a more physiological model as primary CD34$^+$ cells. While K562, is an immortalized leukemia cell line, CD34$^+$ cells are human hematopoietic stem/progenitor cells with the capacity to differentiate into myeloid or lymphoid lineage and, therefore, a more suitable model to study the role of CTCF in erythropoiesis. We purified CD34$^+$ cells from cord blood of newborns. First, we isolated the mononuclear cells by density gradient centrifugation on Ficoll and then we purified CD34$^+$ cells using magnetic beads. By flow cytometry analysis, a purity of more than 85% of CD34$^+$ cells was obtained. Finally, we treated them in culture with erythropoietin (EPO) to induce erythroid differentiation (**Figure 4.7a**). Two different concentrations of EPO (3 U/ml and 6 U/ml) were used to set up the system.

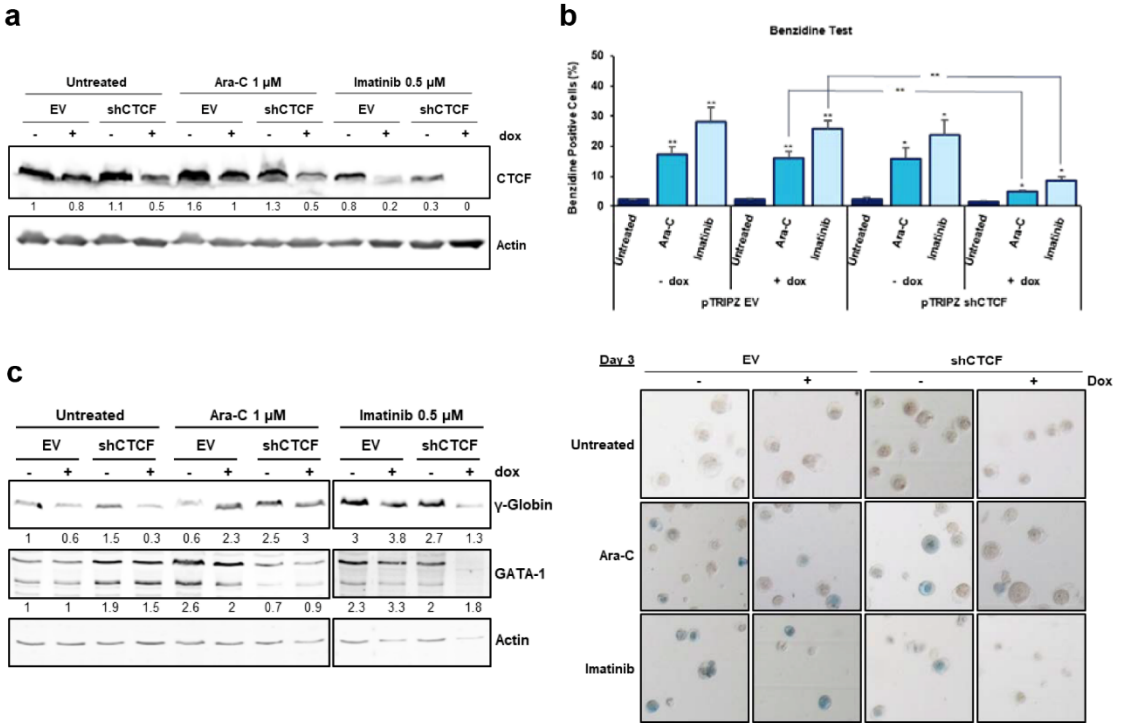

Figure 4.6. Inducible CTCF downregulation inhibits erythroid differentiation of K562 cells. *a) Protein expression of CTCF analyzed by Western-Blot after infection of K562 cells with inducible shCTCF or pTRIPZ EV and treated with 1 µM Ara-C or 0.5 µM Imatinib for 3 days. Actin levels were used as loading control. Densitometry values are shown at the bottom, normalized to the control. b) Benzidine test in K562 cells infected with inducible shCTCF or pTRIPZ EV and treated with Ara-C or Imatinib as in a). Pictures taken during benzidine test evaluation are shown. In each experiment, a minimum of 200 cells were counted. Bars indicate mean ± s.e.m of three independent experiments; significance difference (*,p<0.05; **,p<0.01) from the untreated cells. d) γ-globin and GATA1 protein expression analyzed by Western-Blot in K562 cells after infection with inducible shCTCF or pTRIPZ EV and treated with Ara-C or Imatinib as in a). Actin levels were used as loading control. Densitometry values are shown at the bottom, normalized to the control.*

Erythroid cell differentiation was analyzed first using the benzidine test after 5, 7 and 10 days of EPO induction (**Figure 4.7b**). We observed a significant increase in the percentage of hemoglobinized cells after treatment with both concentrations of EPO. To confirm erythroid cell differentiation we also analyzed the percentage of GYPA positive cells by flow cytometry (**Figure 4.7c**) and the expression of γ-globin and GATA1 proteins by Western-Blot (**Figure 4.7d**). An increase in the number of $GYPA^+$ cells and in the levels of γ-globin and GATA1 were observed upon EPO treatment. These results together confirmed that we set up the model system for erythroid cell differentiation in $CD34^+$ cells.

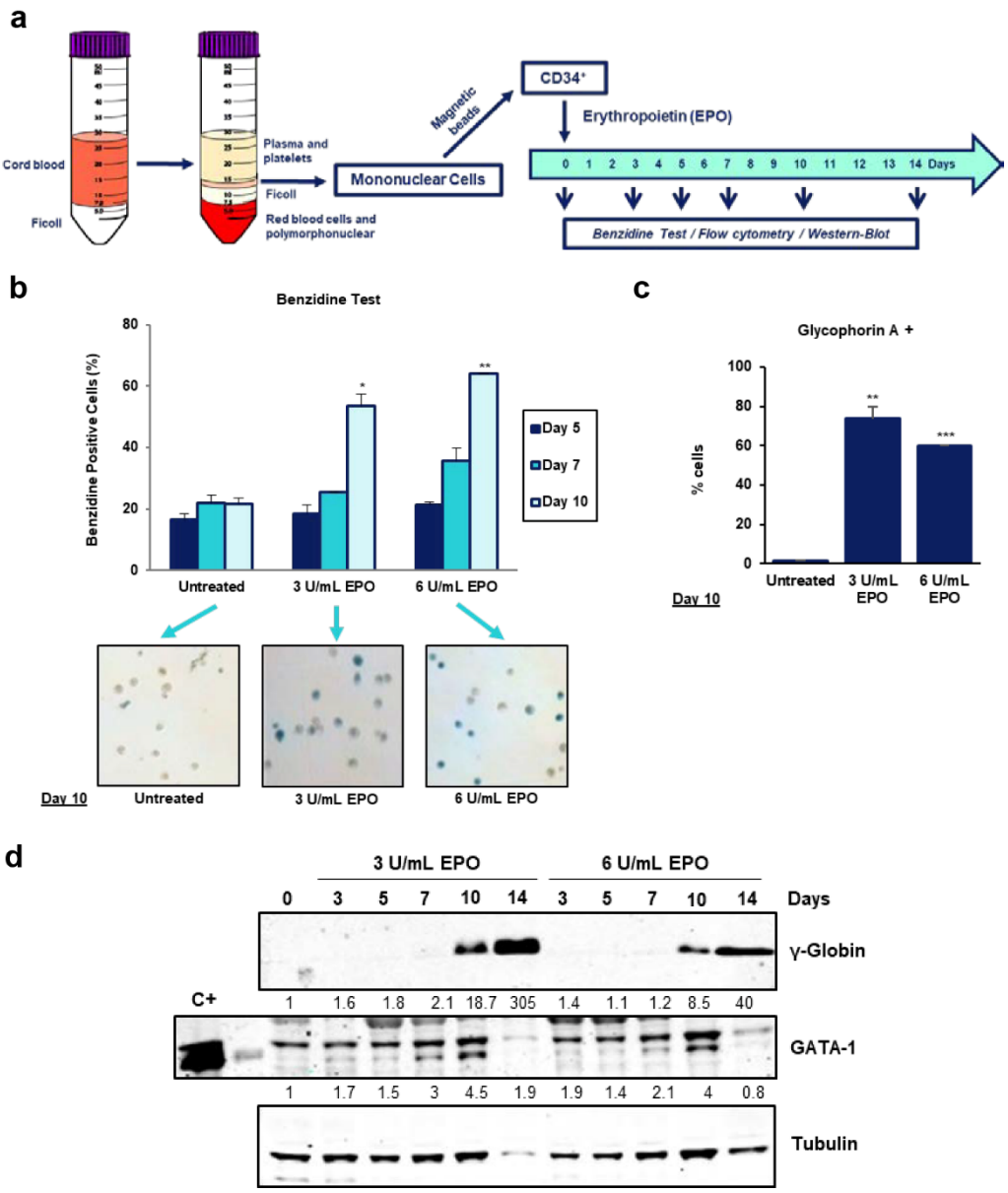

Figure 4.7. EPO induces erythroid differentiation of primary CD34⁺cells. *a) Schematic representation of CD34⁺ cells purification and induction of differentiation with EPO. b) Benzidine test of CD34⁺ cells treated with 3 U/ml and 6 U/ml EPO during 10 days. Pictures taken during benzidine test evaluation are shown. In each experiment, a minimum of 200 cells were counted. Bars indicate mean ± s.e.m of two independent experiments; significance difference (*,p<0.05; **,p<0.01) from the untreated cells. c) Glycophorin-A positive cells analyzed by flow cytometry after treatment of CD34⁺ cells with 3 U/ml and 6 U/ml EPO during 10 days. Bars indicate mean ± s.e.m of two independent experiments; significance difference (**,p<0.05; ***,p<0.001) from the untreated cells. d) Protein expression of γ-globin and GATA1 analyzed by Western-Blot after treatment of CD34⁺ cells with 3 U/ml and 6 U/ml EPO during 14 days. Tubulin levels were used as loading control. Densitometry values are shown at the bottom, normalized to the control. C+, 293T cells transfected with pCEFL-GATA1 as positive control.*

4.1.4. Downregulation of CTCF inhibits erythroid differentiation in CD34$^+$ cells

Once the conditions for CD34$^+$ cells purification and differentiation were established, we studied the effects of CTCF downregulation using both the constitutive and inducible lentiviral shRNA systems described in the previous section.

Isolated CD34$^+$ cells were infected with lentiviral particles containing the specific shRNA against CTCF (shCTCF) or with the pLKO empty vector (EV) and selected for puromycin resistance. After two days of puromycin selection, CTCF mRNA expression was analyzed to confirm CTCF downregulation (**Figure 4.8a**). We observed that the expression of CTCF was significantly reduced (around 50%) in shCTCF cells. CTCF protein levels could not be detected by Western-Blot in CD34$^+$ cells.

To study the effect of CTCF ablation in erythroid differentiation, CD34$^+$ cells infected with EV and with shCTCF were treated with EPO during 14 days and benzidine test was performed (**Figure 4.8b**). Upon EPO treatment, the fraction of benzidine positive cells gradually increase in EV-CD34$^+$ cells, indicating erythroid cell differentiation. However, CD34$^+$ cells infected with lentiviral particles containing shCTCF did not show an increase in benzidine positive cells. Upon CTCF downregulation, the fraction of benzidine positive cells was reduced by approximately 40% compared with the empty vector. These results were confirmed by measuring the percentage of Glycophorin-A (GYPA) positive cells and the expression of γ-globin and GATA1 proteins after EPO treatment. As shown **Figure 4.8c**, the percentage of GYPA$^+$ cells, analyzed by flow cytometry, increased with EPO treatment in cells infected with the empty vector whereas in cells with shCTCF, no increase in the percentage was observed. Protein levels of γ-globin and GATA1 were analyzed by Western-Blot (**Figure 4.8d**). We observed a high increase in γ-globin levels in cells infected with the empty vector. In contrast, upon CTCF known-down, a slightly increase can be revealed. Similar results were found with GATA1 protein levels.

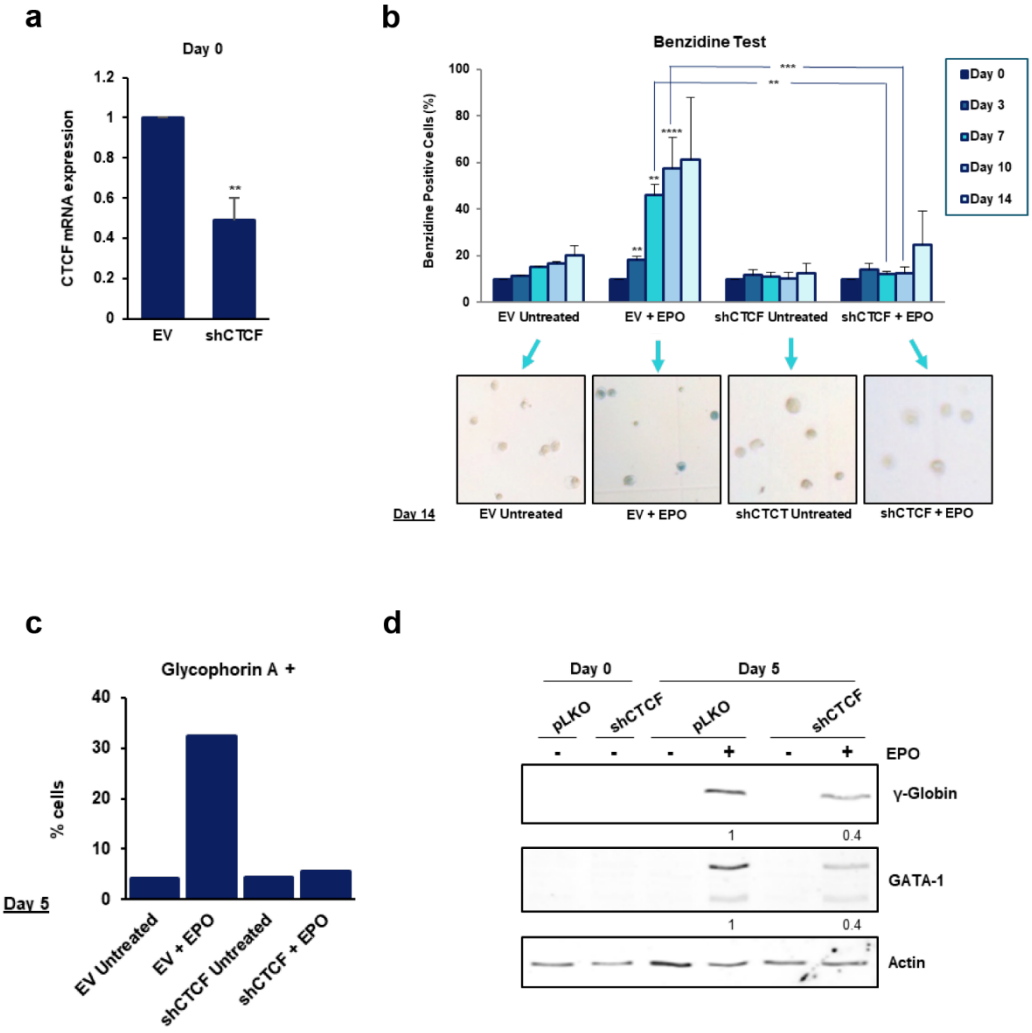

Figure 4.8. CTCF downregulation inhibits erythroid differentiation of CD34⁺cells. *a) Expression of CTCF was analyzed by RT-qPCR after infection of CD34⁺ cells with shCTCF or pLKO (EV) and puromycin selection for two days. Expression was normalized against RPS14 levels. Bars indicate mean ± s.e.m of three independent experiments; significance difference (**,p<0.01) from the EV. b) Benzidine test of CD34⁺ cells infected with shCTCF or pLKO (EV) and treated with EPO during 14 days. Pictures taken during benzidine test evaluation are shown. In each experiment, a minimum of 200 cells were counted. Bars indicate mean ± s.e.m of three independent experiments; significance difference (**,p<0.01; ***,p<0.001; ****,p<0.0001) from the EV untreated cells. c) Glycophorin-A positive cells analyzed by flow cytometry after infection with shCTCF or pLKO (EV) and treated with EPO during 5 days. d) Protein expression of γ-globin and GATA1 analyzed by Western-Blot of CD34⁺ cells after infection with shCTCF or pLKO (EV) and treated with EPO during 5 days. Actin levels were used as loading control. Densitometry values are shown at the bottom.*

Colony forming unit assay was also performed to analyze erythroid cell differentiation. Infected CD34⁺ cells, with EV or shCTCF, and treated with EPO,

were grown in methocult medium. Upon 14 days of incubation, individual colonies were identified and counted using an inverted microscope. We observed different types of colonies such us CFU-GEMM (Colony forming unit-granulocyte, erythroid, macrophage and megakaryocyte) and BFU-E (Burst forming unit-erythroid) (**Figure 4.9a**). After counting the number of colonies, we observed that CTCF downregulation dramatically reduced the number of erythroid colonies (**Figure 4.9b**).

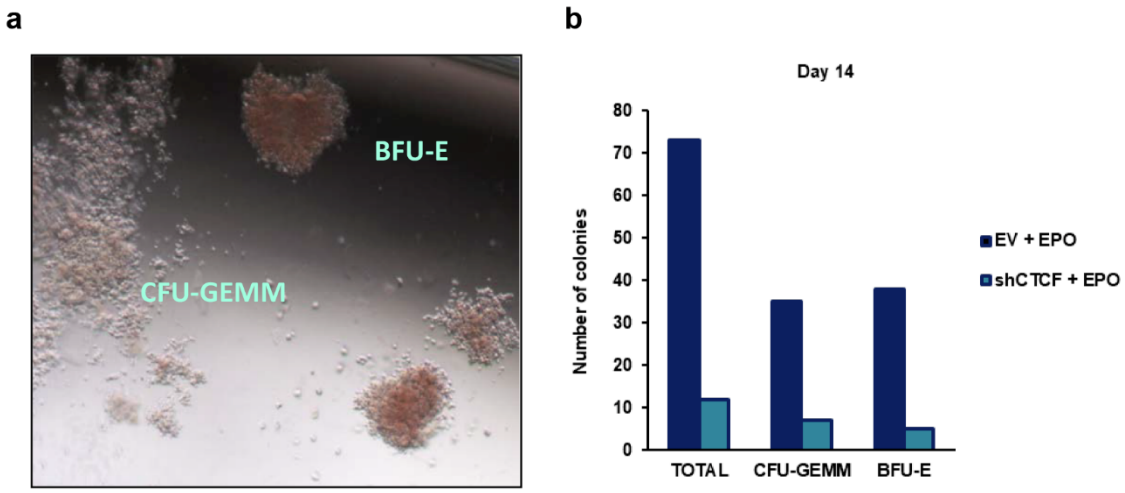

Figure 4.9. CTCF downregulation inhibits erythroid colony formation. *Infected CD34⁺ cells were treated with EPO and grown in methocult medium for 14 days. One representative experiment is shown. a) Erythroid colonies observed in the inverted microscope. CFU-GEMM; colony forming unit-granulocyte, erythroid, macrophage and megakaryocyte. BFU-E; Burst forming unit-erythroid. b) Number of erythroid colonies counted in the inverted microscope.*

Together, these findings reveal that CTCF downregulation inhibits erythroid cell differentiation in CD34⁺ primary cells. To confirm this result, we downregulated CTCF expression with the pTRIPZ doxycycline-inducible system. Isolated CD34⁺ cells were infected with pTRIPZ EV and pTRIPZ shCTCF lentiviral particles and selected for puromycin resistance. Then, treatment with doxycycline was carried out for 2 days to deplete CTCF. The efficiency of infection was confirmed by fluorescence and more than the 84% of the CD34⁺ cells were infected cells with both vectors (**Figure 4.10a**). CTCF downregulation upon doxycycline induction was confirmed by RT-qPCR. Induction of pTRIPZ

shCTCF by doxycycline reduced CTCF mRNA levels by more than the 65% (**Figure 4.10b**).

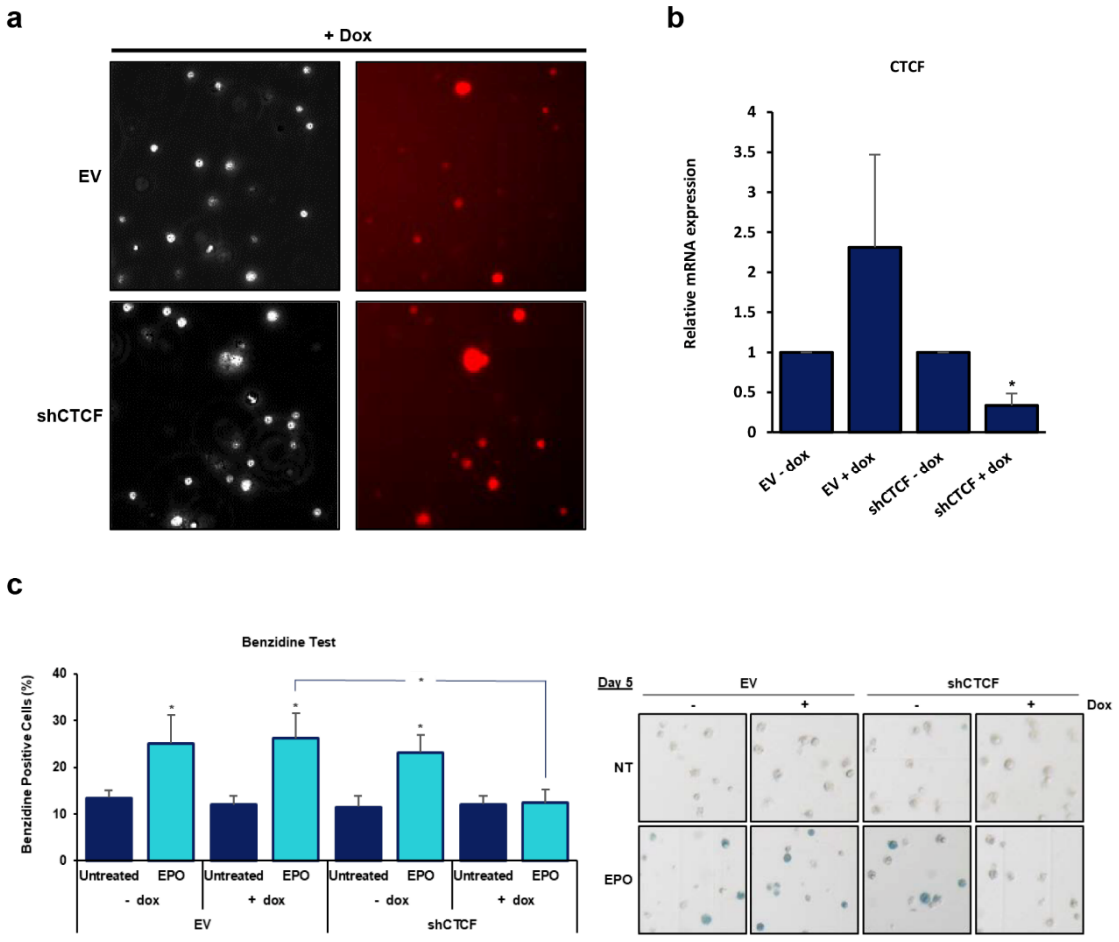

Figure 4.10. Inducible CTCF downregulation inhibits erythroid differentiation of CD34⁺ cells. *a) Efficiency of infection of CD34+ cells checked by microscopy after two days with doxycycline induction. Bright field pictures show total cell number. Red cells represent infected cells. b) Validation of CTCF downregulation. Expression of CTCF was analyzed by RT-qPCR after infection of CD34⁺ cells with inducible shCTCF or pTRIPZ EV, two days of puromycin selection and two days of induction with 2 µg/ml doxycycline. Expression was normalized against RPS14 levels. Bars indicate mean ± s.e.m of two independent experiments; significance difference (*,p<0.05) from the untreated cells. c) Benzidine test of CD34⁺ cells infected with inducible shCTCF or pTRIPZ EV and treated with EPO during 5 days. Pictures taken during benzidine test evaluation are shown. In each experiment, a minimum of 200 cells were counted. Bars indicate mean ± s.e.m of three independent experiments; significance difference (*,p<0.05) from the EV untreated cells without doxycycline induction.*

Finally, erythroid differentiation was analyzed by the benzidine test after five days of EPO treatment (**Figure 4.10c**). In cells infected with the EV without (-)

and with (+) doxycycline induction, we observed the expected increase in the percentage of benzidine positive cells. Similar results were observed in $CD34^+$ cells infected with shCTCF without doxycycline induction. However, in cells with downregulated CTCF (doxycycline induction), the percentage of benzidine positive cells was reduced indicating inhibition of erythroid differentiation.

To summarize, all these results together reveal that CTCF downregulation, with constitutive or inducible systems, inhibits erythroid cell differentiation in K562 cells and in primary $CD34^+$ cells indicating an important role of CTCF in the regulation of erythropoiesis.

4.1.5. CTCF binding *in vivo* to erythroid transcription factor genes

Once we have demonstrated that CTCF has an essential role in the erythroid differentiation, we aimed to analyze the molecular mechanisms in which CTCF could be involved in erythropoiesis. We hypothesized that CTCF could be regulating specific erythroid genes, therefore we analyzed the CTCF *in vivo* binding to the regulatory regions of selected genes encoding erythroid transcription factors and how the binding changes upon induction of erythroid differentiation.

Our group had previously described that overexpression of CTCF in K562 cells induces erythroid differentiation (Torrano et al., 2005). Torrano *et al* performed microarray analysis with the Affymetrix platform HG-U133 Plus2.0 comparing RNA from K562 control cells and K562 cells overexpressing CTCF (unpublished data) and focused the analysis in genes implicated in different aspects of the erythroid differentiation (**Table 4.1**). The analysis of transcriptomic data revealed the differential expression of genes encoding erythroid membrane proteins (glycophorin A and E, ankirin1, transmembrane glycoproteins), erythroid cytoskeletal proteins (spectrin alpha) and different hemoglobin components (hemoglobin alpha, beta, delta, and epsilon). Notably, a number of transcription factors that determine erythroid lineage differentiation seemed to be regulated by CTCF (**Table 4.1**). The microarray-based expression profiling data where consistent with the function of CTCF promoting erythroid differentiation.

Table 4.1. Erythroid related genes regulated by CTCF expression. *a) Affymetrix microarray analysis revealed erythroid genes upregulated by CTCF expression. b) Affymetrix microarray analysis revealed erythroid genes downregulated by CTCF expression. Data from Torrano, V. (unpublished).*

a

GENE	DESCRIPTION	FUNCTION
GYPA	Glycophorin A	Erythroid-specific membrane protein
GYPE	Glycophorin E	Erythroid-specific membrane protein
ANK1	Ankirin 1, erythrocytic	Erythroid-specific membrane protein
SPTA1	Spectrin alpha, erythrocytic 1	Erythrocyte cytoskeletal protein
HBA2	Hemoglobin, alpha 2, adult chain 2	Hemoglobin component
HBA1	Hemoglobin, alpha 1, adult chain 1	Hemoglobin component
HBB	Hemoglobin, beta adult chain	Hemoglobin component
HBD	Hemoglobin, delta	Hemoglobin component
HBZ	Hemoglobin,zeta	Hemoglobin component
HBE1	Hemoglobin, epsilon1	Hemoglobin component
HEMGN	Hemogen	**Hematopoietic nuclear protein.** Regulated by GATA1
ID1	Inhibitor of DNA binding 1	**Transcription factor.** Erythroid function
ID3	Inhibitor of DNA binding 3	**Transcription factor 3**. Induces erythroid differentiation
LMO2	LIM domain2 (rhombotin-like 1)	**Transcription factor**. TAL-1/SCL partner
TCF3	Transcription factor (E2A)	**Transcription factor**. TAL-1/SCL partner
NF-E2-like 2	Nuclear factor erythroid like 2	**Transcription factor**. Binds to beta-globin promoter
KLF1/EKLF	Erythroid Kruppel-like factor 1	**Transcription factor.** Activates beta-globin gene

b

GENE	DESCRIPTION	FUNCTION
CD44	Cluster of differentiation 44	Transmembrane glycoprotein
CD164	Cluster of differentiation 164	Transmembrane glycoprotein
MYB	Myeloblastosis oncogene	**Transcription factor**. Inhibitor of erythroid differentiation
HES 1	Hairy and enhancer of split 1	**Transcription factor. I**nhibits GATA1
HEY1	Hairy related transcription factor 1	**Transcription factor. I**nhibits erythroid differentiation
ID2	Inhibitor of DNA binding 2	**Transcription factor. I**nhibited during erythroid differentiation
GATA 2	GATA binding protein 2	**Transcription factor. I**nhibits erythroid differentiation
ETS1	Erythroblastosis oncogene 1	**Transcription factor.** Blocks erythroid differentiation
STAT5B	Signal transducer and activator of transcription B	**Transcription factor.** Antiapoptotic effect
VIM	Vimentin	Intermediate filament

In this Thesis work, we selected some important transcription factors implicated in erythroid differentiation such as LMO2, KLF1, GATA2 and MYB among others. We first analyzed their mRNA expression upon induction of erythroid cell differentiation with Ara-C or Imatinib (**Figure 4.11**). We observed a significant reduction in the expression in ETS1, MYB and GATA2 upon differentiation and an increase in the levels of LMO2 and KLF1. In the case of HEY1 and NFE2L2 their expression were slightly increased with Ara-C treatment and reduce with Imatinib treatment. In general, these results are in concordance with the role of those genes during differentiation (see Introduction).

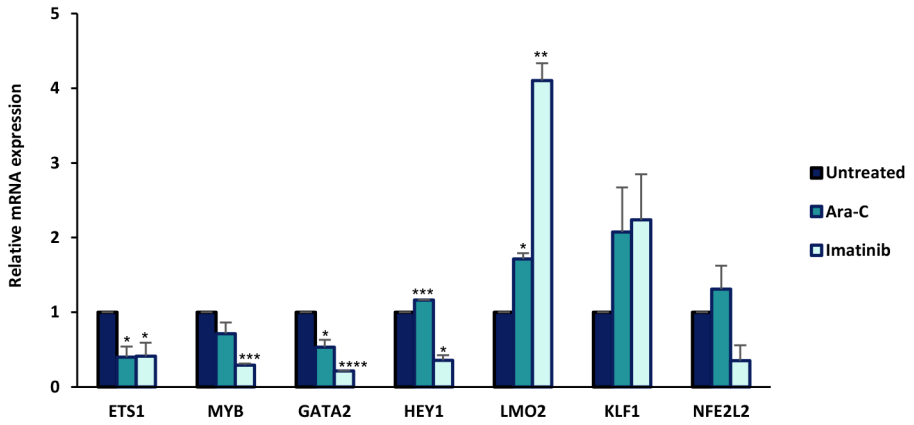

Figure 4.11. mRNA expression of erythroid genes upon differentiation. mRNA expression levels of *ETS1, MYB, GATA2, HEY1, LMO2, KLF1 and NFE2L2* analyzed by RT-qPCR in K562 cells upon treatment with 1 µM Ara-C for 72 hours or with 0.5 µM Imatinib 48 hours. Expression was normalized against RPS14 levels. Bars indicate mean ± s.e.m of two or three independent experiments; significance difference (*,p<0.05; **,p<0.01; ***,p<0.001; ****,p<0.0001) from the untreated cells.

We next asked if CTCF is regulating the expression of these erythroid related genes by binding directly to their regulatory sequences. For this, we performed chromatin immunoprecipitation (ChIP) assays to confirm the CTCF *in vivo* binding to a number of erythroid-related genes from **Table 4.11**: *ETS1*, *MYB*, *GATA2*, *HEY1*, *LMO2*, *KLF1*, *NFE2L2* and *TCF3*. The ChIP-seq data published in the Encyclopedia of DNA Elements (ENCODE) project (https://genome.ucsc.edu/) was analyzed to identify possible CTCF binding sites (CTSs) to the selected erythroid genes. For the study of CTCF binding in erythroid-differentiated cells, K562 cells were treated with 1 µM Ara-C for 48 and 72 hours followed by CTCF

immunoprecipitation with a mixture of three anti-CTCF antibodies. Then, chromatin enrichment was detected by real-time quantitative PCR using different sets of primer pairs. In all the experiments, positive and negative controls were used in order to check that ChIP was working. The H42.1 ribosomal DNA (rDNA) repeat was used as positive control and the H4 ribosomal DNA (rDNA) repeat as negative control (**Figure 4.12),** as previously described by our group (van de Nobelen et al., 2010). Samples incubated without antibody were used to check the specificity of the beads (samples referred as beads).

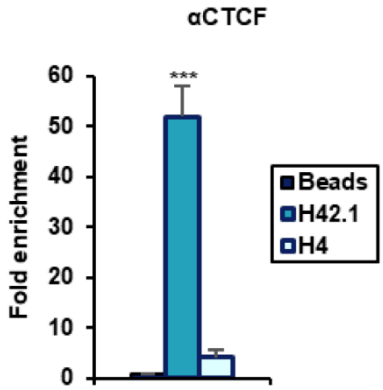

Figure 4.12. Positive and negative controls for ChIP assays. Binding of CTCF to H42.1 rDNA and H4 rDNA. Fold enrichment was determined by calculating the ratio of the amount of the target sequence in the immunoprecipitation over the amount of the target sequence in the input DNA. Each value was normalized with respect to the beads (no-antibody sample).

CTCF and cohesins participate on gene regulation through the formation or stabilization of long-range chromatin loops (see Introduction). To get further information of the possible loops formed by CTCF and cohesin (Rad21 subunit) for the regulation of the erythroid genes, we used the ENCODE platform to find chromatin interactions by Chromatin Interaction Analysis with Paired-End Tag (ChIA-PET). PET clusters indicate two different genomic regions in the chromatin interacting with each other for regulatory functions. ChIA-PET sequencing is a genome-wide high-throughput technology use to detect chromatin interactions associated with a specific protein of interest in the cell genome (Li et al., 2015). The ENCODE Project shows the locations of protein factor mediated chromatin interactions determined by ChIA-PET techniques. We analyzed the selected CTSs of the different erythroid transcription factors to look for possible PET clusters.

In summary, for the analysis of the erythroid genes mentioned above we performed: i) ENCODE analysis to predict possible CTSs; ii) ChIP assay in K562

cells to confirm *in vivo* binding of CTCF; iii) ChIP assays in K562 cells treated with Ara-C to analyzed how CTCF binding changes upon induction of differentiation; and iv) ENCODE analysis showing possible PET clusters.

ETS1

ETS1 (Erythroblastosis oncogene 1) is a transcription factor which inhibits erythroid differentiation and, during erythropoiesis, its expression has to be downregulated (Lulli et al., 2006). ENCODE analysis revealed a CTCF binding site 43 kb upstream *ETS1* gene (**Figure 4.13a, blue arrow**).

CTCF binding to the CTS found upstream *ETS1* gene was analyzed in K562 cells without induction of differentiation (untreated K562 cells). ChIP experiments revealed a high occupancy of CTCF at the analyzed CTS (**Figure 4.13b**). Once confirmed that CTCF is binding to the *ETS1* CTS, we analyzed the binding upon induction of erythroid differentiation with Ara-C (**Figure 4.13c**). ChIP assay showed a gradual increase in CTCF binding to *ETS1* upon differentiation with Ara-C.

From the ENCODE ChIA-PET data we analyzed the possible interactions that are formed around *ETS1* gene. The CTCF and cohesin (Rad21 subunit) binding sites were analyzed (**Figure 4.13d**). We observed two loops which bridge regions of CTCF occupancy. The loops are formed between the analyzed CTS upstream ETS1 and two CTS located downstream and both loops contain ETS1 gene. A scheme of the possible loop formed is also depicted, showing that CTCF could act as an insulator between *ETS1* and *FLI1* (another *ETS*-family gene) (**Figure 4.13d**).

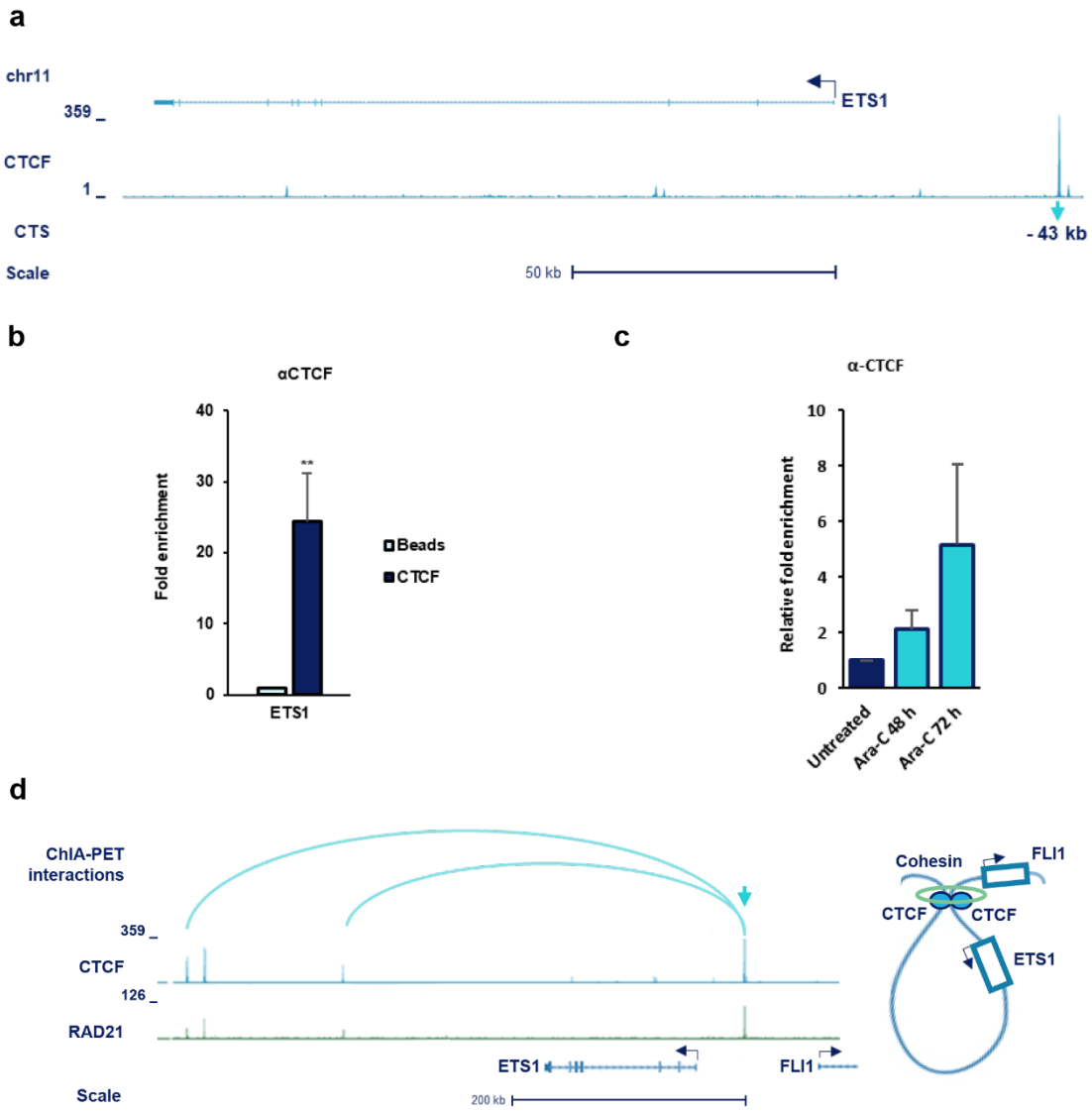

Figure 4.13. CTCF binding to ETS1 gene. *a) ENCODE analysis showing ChIP-seq profile of CTCF for ETS1 gene in chromosome 11 from K562 cell line. CTCF binding site is shown (blue arrow). b) ChIP analysis showing the binding of CTCF to the ETS1 CTS in K562 cells. The fold enrichment of the target sequence was determined as indicated in Materials and Methods section. Each value was normalized with respect to the beads (no-antibody). Bars indicate mean ± s.e.m of eight independent experiments; significance difference (**,p<0.01) from the beads. c) ChIP analysis showing the binding of CTCF to the ETS1 CTS in K562 cells upon treatment with 1 μM Ara-C for the indicated times. Each value was normalized with respect to the untreated cells. Bars indicate mean ± s.e.m of eight independent experiments. d) ChIA-PET interactions from the ETS1 CTS (blue arrow) are shown as blue arcs. ChIP-seq profiles of CTCF and RAD21 (left) and representation of possible loop (right) are shown. CTCF, blue balls; Cohesin (RAD21), green circle; genes, blue boxes.*

MYB

MYB (Myeloblastosys oncogene) is a crucial transcription factor in hematopoiesis and erythropoiesis. MYB is highly expressed in the hematopoietic stem and progenitor cells and downregulated during differentiation (Wang et al., 2018). Actually MYB was discovered in retrovirus inducing leukemia in chicken (Lipsick and Wang, 1999). ENCODE analysis showed a CTCF binding site in the Intron 1 (+ 2.5 kb) of the *MYB* gene (**Figure 4.14a, blue arrow**).

Binding of CTCF to the Intron 1 of *MYB* gene was determined in untreated K562 cells. ChIP experiments confirmed a high occupancy of CTCF to *MYB* gene (**Figure 4.14b**). Furthermore, CTCF binding upon treatment with Ara-C was analyzed (**Figure 4.14c**). ChIP assay revealed an increase in CTCF binding to *MYB* upon induction of differentiation.

From the ENCODE ChIA-PET data we analyzed the putative interactions that are formed around *MYB* gene, looking for the CTCF and cohesin (Rad21 subunit) binding sites. We observed a loop formed between the analyzed CTS in the Intron 1 of *MYB* and a CTS located upstream *MYB* gene (**Figure 4.14d**).

GATA2

GATA2 is a transcription factor expressed in hematopoietic stem and early progenitor cells and regulates their proliferation and maintenance. During erythroid differentiation, GATA2 expression is repressed by GATA1 (GATA switching) (Moriguchi and Yamamoto, 2014). According to ENCODE analysis, a CTCF binding site sited 5 kb upstream *GATA2* gene was found (**Figure 4.15a, blue arrow**).

ChIP assays in untreated K562 cells, revealed high CTCF occupancy in *GATA2* CTS (**Figure 4.15b**). Additionally, we analyzed changes in CTCF binding upon induction of erythroid differentiation (**Figure 4.15c**). We observed that treatment with Ara-C increased occupancy of CTCF upstream *GATA2*.

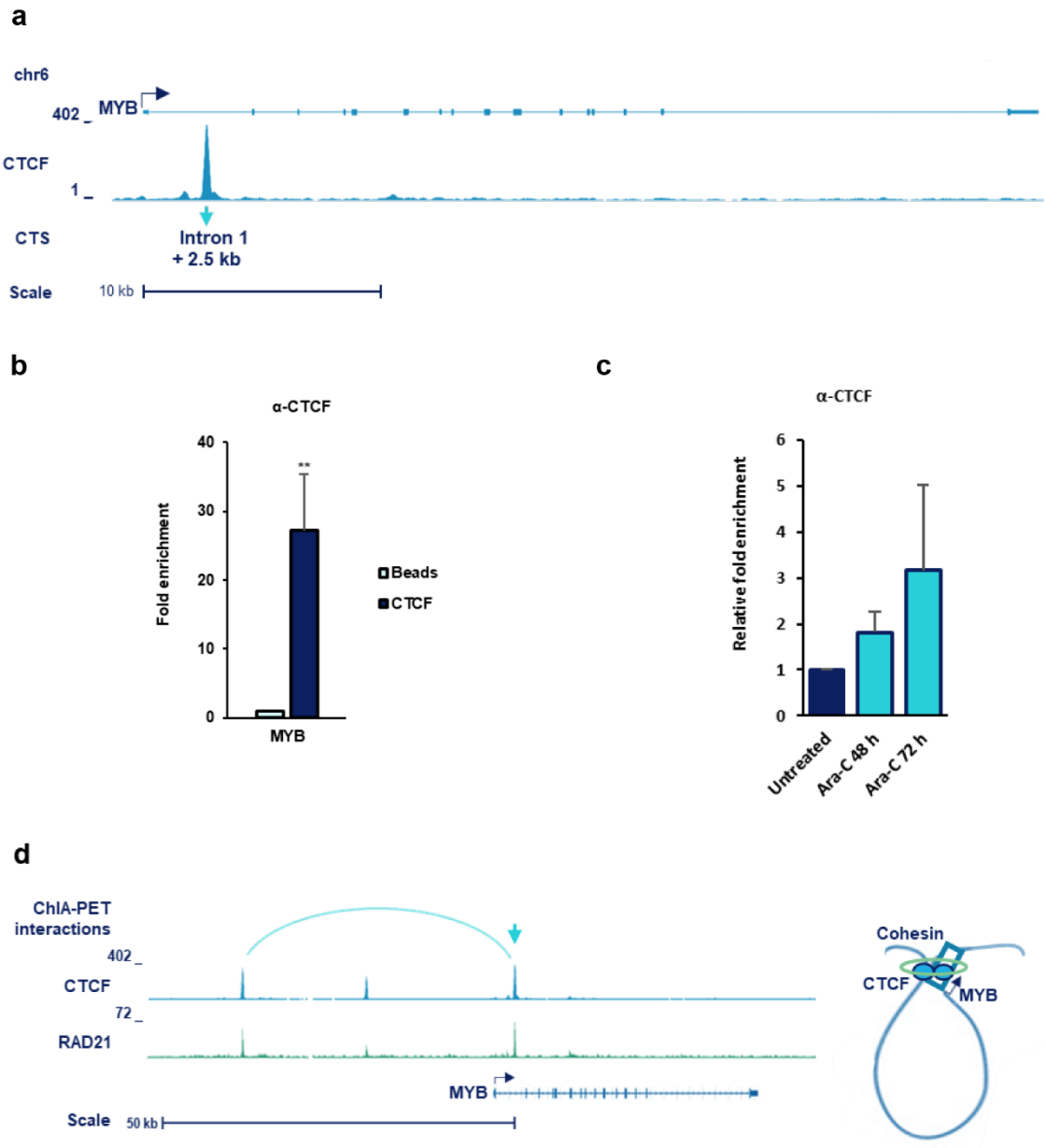

Figure 4.14. CTCF binding to MYB gene. *a) ENCODE analysis showing ChIP-seq profile of CTCF for MYB gene in chromosome 6. CTCF binding site is shown (blue arrow). b) ChIP analysis showing the binding of CTCF to the MYB CTS in K562 cells. The fold enrichment of the target sequence was determined as indicated in Materials and Methods section. Each value was normalized with respect to the beads (no-antibody). Bars indicate mean ± s.e.m of eight independent experiments; significance difference (**,p<0.01) from the beads. c) ChIP analysis showing the binding of CTCF to the MYB CTS in K562 cells upon treatment with with 1 μM Ara-C for the indicated times. Each value was normalized with respect to the untreated cells. Bars indicate mean ± s.e.m of eight independent experiments. d) ChIA-PET interaction from the MYB CTS (blue arrow) is shown as a blue arc. ChIP-seq profiles of CTCF and RAD21 (left) and representation of possible loop (right) are shown. CTCF, blue balls; Cohesin (RAD21), green circle; genes, blue boxes.*

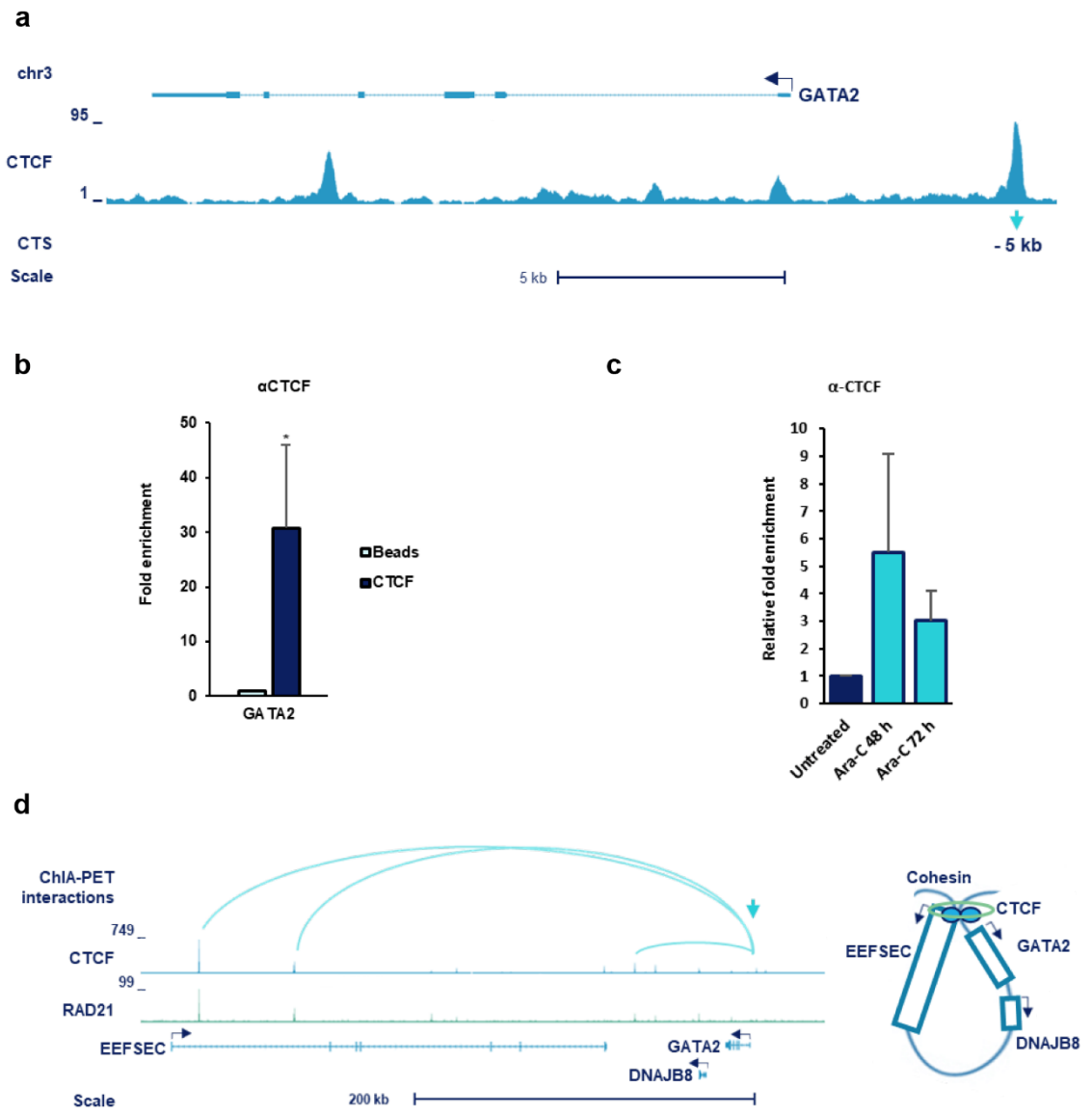

Figure 4.15. CTCF binding to GATA2 gene. *a) ENCODE analysis showing ChIP-seq profile of CTCF for GATA2 gene in chromosome 3. CTCF binding site is shown (blue arrow). b) ChIP analysis showing the binding of CTCF to the GATA2 CTS in K562 cells. The fold enrichment of the target sequence was determined as indicated in Materials and Methods section. Each value was normalized with respect to the beads (no-antibody). Bars indicate mean ± s.e.m of five independent experiments; significance difference (*,p<0.05) from the beads. c) ChIP analysis showing the binding of CTCF to the GATA2 CTS in K562 cells upon treatment with with 1 μM Ara-C for the indicated times. Each value was normalized with respect to the untreated cells. Bars indicate mean ± s.e.m of four to five independent experiments; significance difference (*,p<0,05) from the untreated cells. d) ChIA-PET interactions from the GATA2 CTS (blue arrow) are shown as blue arcs. ChIP-seq profiles of CTCF and RAD21 (left) and representation of possible loop (right) are shown. CTCF, blue balls; Cohesin (RAD21), green circle; genes, blue boxes.*

From the ENCODE ChIA-PET data we analyzed the possible interactions that are formed around *GATA2* gene. We observed three loops which could be formed between the analyzed CTS upstream *GATA2* and three CTS located downstream *GATA2* gene (**Figure 4.15d**). The different loops contain *GATA2* gene and *DNAJB8* gene (encoding a heat shock protein). The biggest one contain the *EEFSEC* gene (a translation factor necessary for the incorporation of selenocysteine into proteins).

HEY1

HEY1 (Hairy/enhancer-of-split related with YRPW motif protein 1) is a transcription factor that maintain an undifferentiated state of erythroid precursor cells. HEY1 interacts with GATA-1 and represses its transcriptional activation (Elagib et al., 2004). ENCODE analysis showed a CTCF binding site in the Exon 5 of *HEY1* gene (**Figure 4.16a, blue arrow**).

ChIP assays in untreated K562 cells showed a high CTCF occupancy in *HEY1* CTS (**Figure 4.16b**). We then analyzed how CTCF binding changed upon induction of erythroid differentiation (**Figure 4.16c**). After 72 hours of treatment with Ara-C, a significant increase of CTCF binding to Exon 5 of HEY1 was observed.

From the ENCODE ChIA-PET data we analyzed the possible interactions that are formed around *HEY1* gene. We observed a loop formed between the analyzed CTS in exon 5 of *HEY1* and a CTS located upstream *HEY1* gene (**Figure 4.16d**). The loop also contains the *MRPS28* gene (a component of the mitochondrial ribosome small subunit).

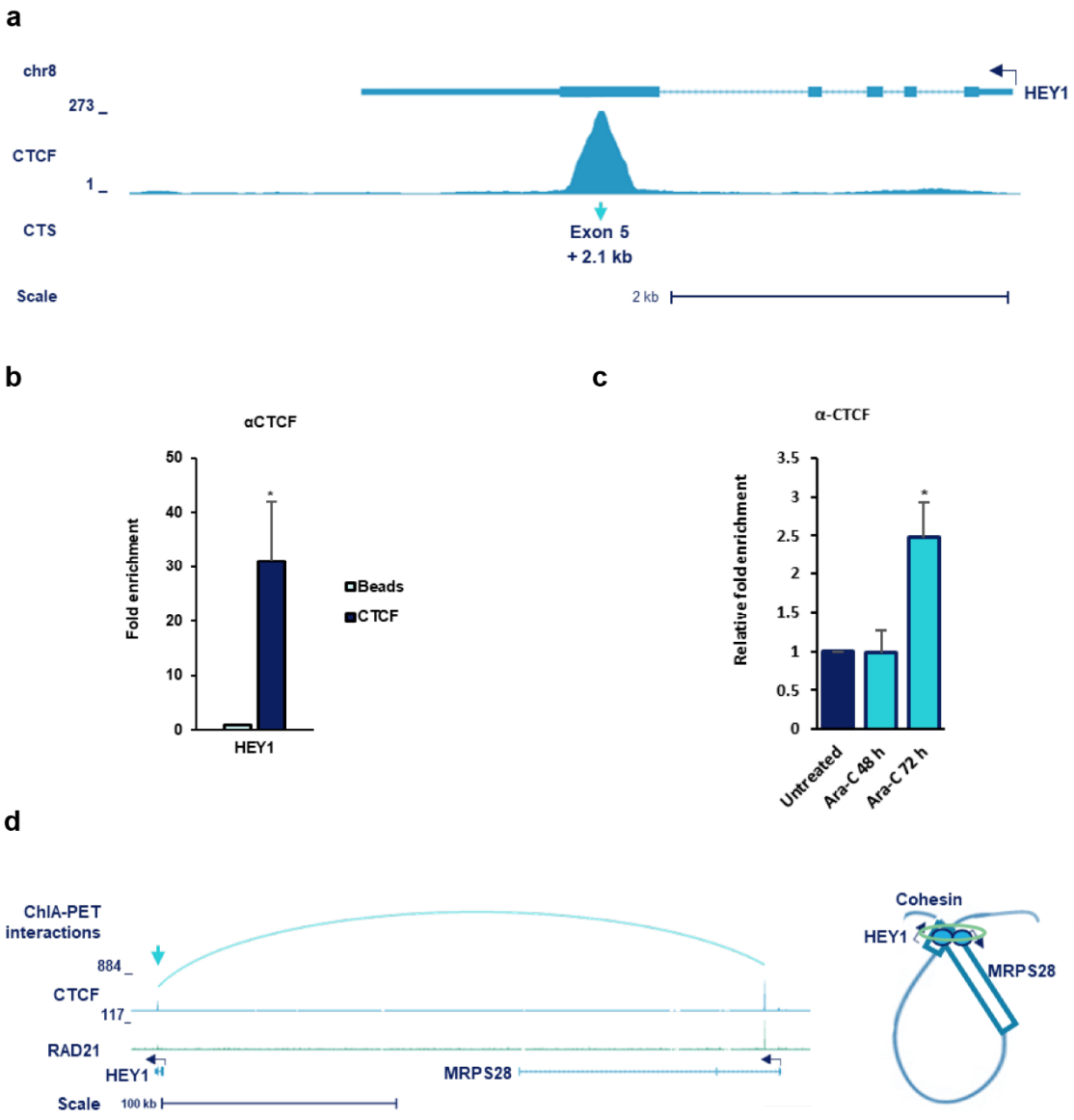

Figure 4.16. CTCF binding to HEY1 gene. *a) ENCODE analysis showing ChIP-seq profile of CTCF for HEY1 gene in chromosome 8. CTCF binding site is shown (blue arrow). b) ChIP analysis showing the binding of CTCF to the HEY1 CTS in K562 cells. The fold enrichment of the target sequence was determined as indicated in Materials and Methods section. Each value was normalized with respect to the beads (no-antibody). Bars indicate mean ± s.e.m of four independent experiments; significance difference (*,p<0.05) from the beads. c) ChIP analysis showing the binding of CTCF to the HEY1 CTS in K562 cells upon treatment with with 1 μM Ara-C for the indicated times. Each value was normalized with respect to the untreated cells. Bars indicate mean ± s.e.m of four independent experiments; significance difference (*,p<0,05) from the untreated cells. d) ChIA-PET interaction from the HEY1 CTS (blue arrow) is shown as a blue arc. ChIP-seq profiles of CTCF and RAD21 (left) and representation of possible loop (right) are shown. CTCF, blue balls; Cohesin (RAD21), green circle; genes, blue boxes.*

LMO2

LMO2 (LIM domain-only protein 2) is a non DNA-binding component of the CEN protein complex (see Introduction). LMO2 controls the erythroid lineage via activation of an erythroid-specific gene expression program and belongs to the core erythroid network (Chambers and Rabbitts, 2015). ENCODE analysis indicated a CTCF binding site 34 kb downstream of the *LMO2* gene (**Figure 4.17a, blue arrow**).

The CTCF binding site found downstream *LMO2* was analyzed in K562 cells. ChIP experiments confirmed a high occupancy of CTCF at the predicted CTS (**Figure 4.17b**). We also analyzed the binding of CTCF to *LMO2* CTS upon induction of erythroid differentiation with Ara-C (**Figure 4.17c**) and observed that Ara-C treatment slightly increased CTCF binding to *LMO2* upon differentiation.

From the ENCODE ChIA-PET data we analyzed the possible interactions that are formed around *LMO2* gene. We observed four possible loops which are formed between the analyzed CTS downstream *LMO2* and a CTS located upstream *LMO2* gene (**Figure 4.17d**). All the loops contain *LMO2* gene.

KLF1

KLF1 (Erythroid Krüppel-like factor 1) is a master erythroid transcription factor that belongs to the core erythroid network. KLF1 is essential during terminal erythroid differentiation and activation of adult β-globin expression (Gnanapragasam and Bieker, 2017). A possible CTCF binding site at Exon 2 of *KLF1* gene was found after the analysis of the ENCODE data (**Figure 4.18a, blue arrow**).

To analyzed CTCF binding to Exon 2 of *KLF1*, we performed ChIP assays in K562 cells. ChIP results confirmed a high CTCF binding to the *KLF1* CTS (**Figure 4.18b**). We analyzed the binding of CTCF upon induction of erythroid differentiation with Ara-C (**Figure 4.18c**). The results indicated that Ara-C treatment for 72 hours increased CTCF binding to *KLF1* Exon 2.

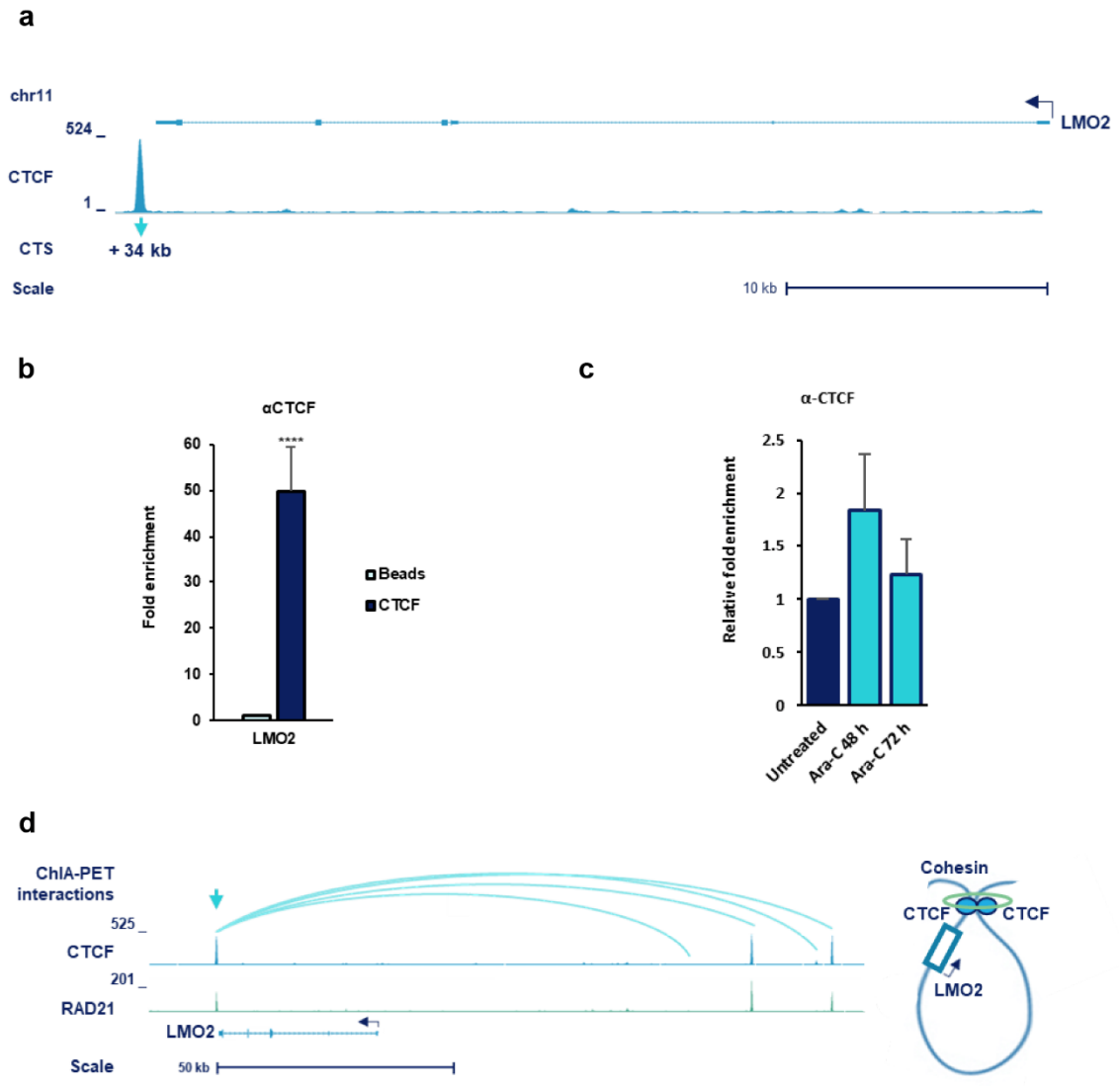

Figure 4.17. CTCF binding to LMO2 gene. *a) ENCODE analysis showing ChIP-seq profile of CTCF for LMO2 gene in chromosome 11. CTCF binding site is shown (blue arrow). b) ChIP analysis showing the binding of CTCF to the LMO2 CTS in K562 cells. The fold enrichment of the target sequence was determined as indicated in Materials and Methods section. Each value was normalized with respect to the beads (no-antibody). Bars indicate mean ± s.e.m of eight independent experiments; significance difference (****,p<0.0001) from the beads. c) ChIP analysis showing the binding of CTCF to the LMO2 CTS in K562 cells upon treatment with with 1 μM Ara-C for the indicated times. Each value was normalized with respect to the untreated cells. Bars indicate mean ± s.e.m of eight independent experiments. d) ChIA-PET interactions from the LMO2 CTS (blue arrow) are shown as blue arcs. ChIP-seq profiles of CTCF and RAD21 (left) and representation of possible loop (right) are shown. CTCF, blue balls; Cohesin (RAD21), green circle; genes, blue boxes.*

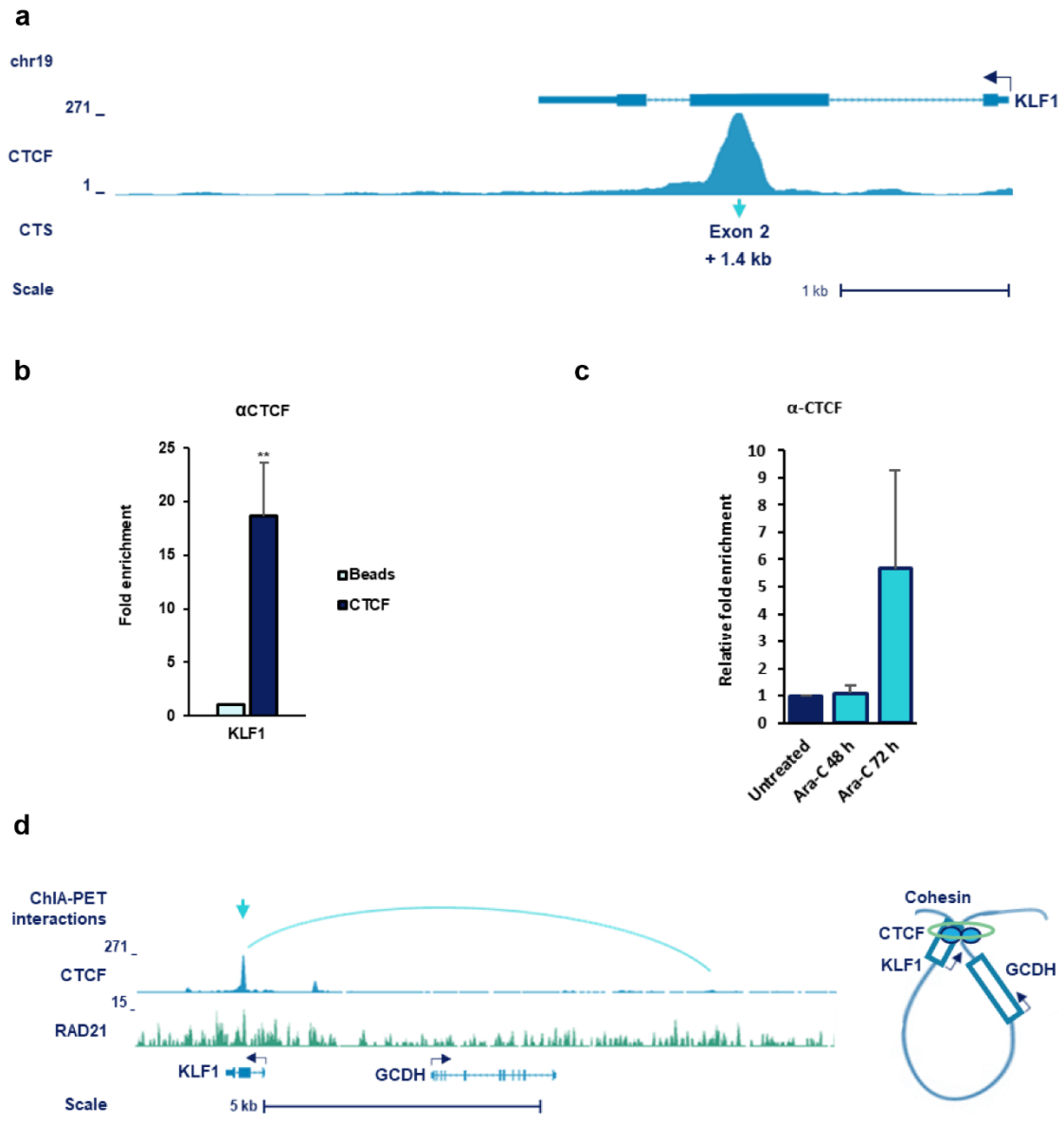

Figure 4.18. CTCF binding to KLF1 gene. *a) ENCODE analysis showing ChIP-seq profile of CTCF for KLF1 gene in chromosome 19. CTCF binding site is shown (blue arrow). b) ChIP analysis showing the binding of CTCF to the KLF1 CTS in K562 cells. The fold enrichment of the target sequence was determined as indicated in Materials and Methods section. Each value was normalized with respect to the beads (no-antibody). Bars indicate mean ± s.e.m of eight independent experiments; significance difference (**,p<0.01) from the beads. c) ChIP analysis showing the binding of CTCF to the KLF1 CTS in K562 cells upon treatment with with 1 μM Ara-C for the indicated times. Each value was normalized with respect to the untreated cells. Bars indicate mean ± s.e.m of eight independent experiments. d) ChIA-PET interaction from the KLF1 CTS (blue arrow) is shown as a blue arc. ChIP-seq profiles of CTCF and RAD21 (left) and representation of possible loop (right) are shown. CTCF, blue balls; Cohesin (RAD21), green circle; genes, blue boxes.*

From the ENCODE ChIA-PET data we analyzed the possible interactions that are formed around *KLF1* gene. We observed a loop formed between the analyzed CTS in exon 2 of *KLF1* and a CTS located upstream *KLF1* gene (**Figure 4.18d**). The loop also contains the *GCDH* gene (glutaryl-CoA dehydrogenase).

NFE2L2

NFE2L2 (Nuclear Factor Erythroid like 2) is an erythroid transcription factor involved in the regulation of β-globin gene transcription (Andrews, 1998). ENCODE analysis revealed two CTSs in the Intron 1 of *NFE2L2* gene and we selected one of them for study CTCF binding (**Figure 4.19a, blue arrow**).

To confirm CTCF binding to Intron 1 of *NFE2L2*, ChIP assay was performed in K562 cells and high occupancy of CTCF at *NFE2L2*, was found (**Figure 4.19b**). We also analyzed the binding of CTCF to *NFE2L2* CTS upon induction of erythroid differentiation (**Figure 4.19c**). Ara-C treatment increased CTCF binding to *NFE2L2* upon differentiation.

From the ENCODE ChIA-PET data we analyzed the possible interactions that are formed around *NFE2L2* gene. We observed one loop formed between the analyzed CTS in intron 1 of *NFE2L2* and a CTS located downstream *NFE2L2* which also contains the *HNRNPA3* gene (involved in pre-mRNA splicing). A smaller loop was also formed with a CTS in the exon 1 of *NFE2L2* gene (**Figure 4.19d**).

TCF3

TCF3 (Transcription Factor 3 or E2A) factor is part of the core erythroid network and participates in terminal erythroid maturation and hemoglobin production (Tsiftsoglou et al., 2009). ENCODE analysis revealed a CTCF binding site around 23 kb upstream *TCF3* gene (**Figure 4.20a, blue arrow**).

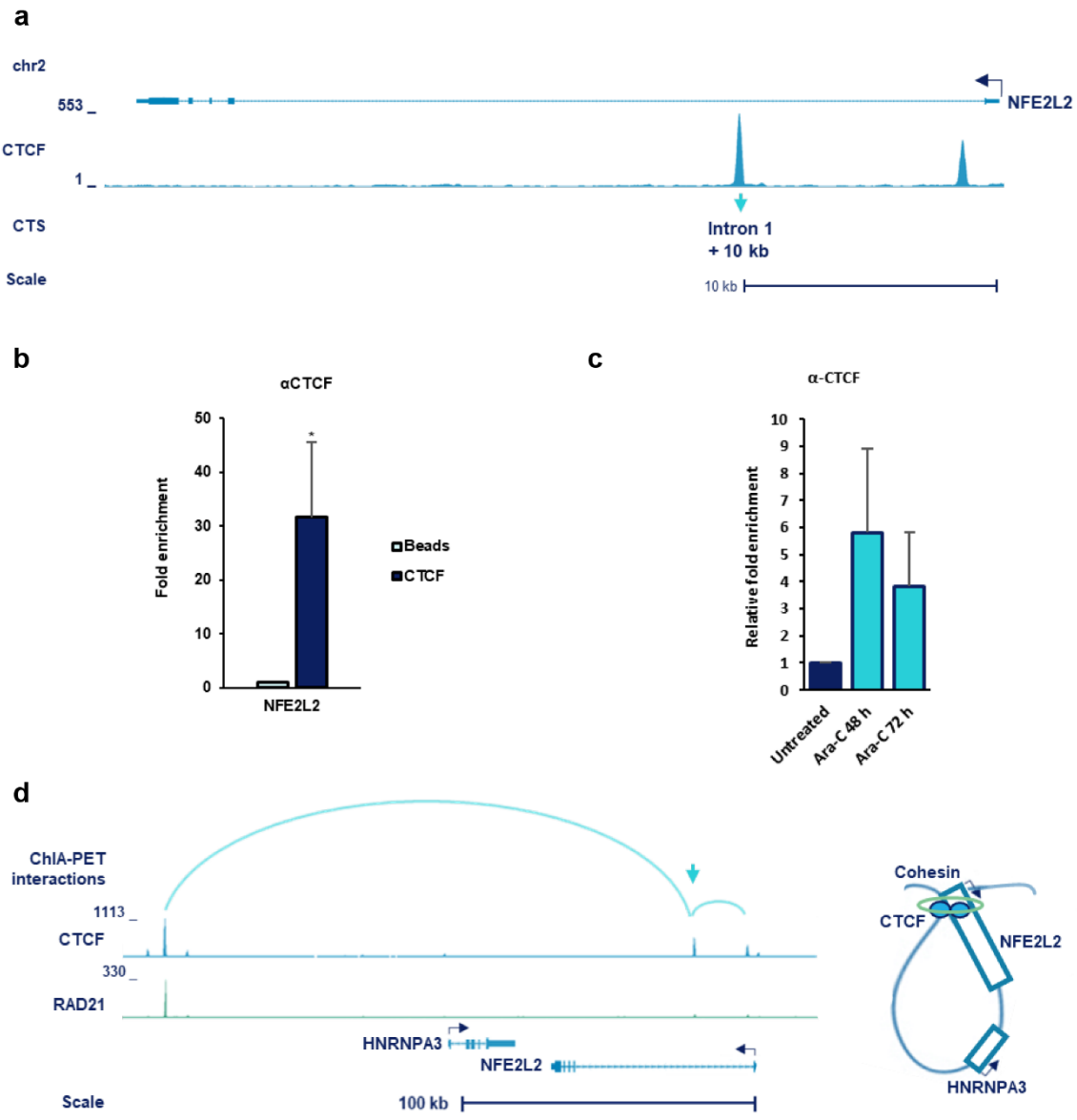

Figure 4.19. CTCF binding to NFE2L2 gene. *a) ENCODE analysis showing ChIP-seq profile of CTCF for NFE2L2 gene in chromosome 2. CTCF binding site is shown (blue arrow). b) ChIP analysis showing the binding of CTCF to the NFE2L2 CTS in K562 cells. The fold enrichment of the target sequence was determined as indicated in Materials and Methods section. Each value was normalized with respect to the beads (no-antibody). Bars indicate mean ± s.e.m of five independent experiments; significance difference (*,p<0.05) from the beads. c) ChIP analysis showing the binding of CTCF to the NFE2L2 CTS in K562 cells upon treatment with 1 μM Ara-C for the indicated times. Each value was normalized with respect to the untreated cells. Bars indicate mean ± s.e.m of four to five independent experiments; significance difference (***,p<0.001) from the untreated cells. d) ChIA-PET interactions from the NFE2L2 CTS (blue arrow) are shown as blue arcs. ChIP-seq profiles of CTCF and RAD21 (left) and representation of possible loop (right) are shown. CTCF, blue balls; Cohesin (RAD21), green circle; genes, blue boxes.*

CTCF occupancy was analyzed in K562 cells. ChIP experiments confirmed a significant CTCF binding upstream *TCF3* gene (**Figure 4.20b**). We also analyzed the binding of CTCF to *TCF3* CTS upon induction of erythroid differentiation with Ara-C (**Figure 4.20c**). We observed that Ara-C treatment slightly increased CTCF binding.

From the ENCODE ChIA-PET data we analyzed the possible interactions that are formed around *TCF3* gene. We observed seven loops formed between the analyzed CTS upstream *TCF3* and others CTSs around *TCF3* gene (**Figure 4.20d**). Four loops are formed with different CTSs located upstream *TCF3* gene and include the *ONECUT3* gene (a transitional activator) and *ATP883* gene (ATPase). Two loops are formed with CTSs located downstream *TCF3* gene and contains the *UQCR11* gene (a component of ubiquinol-cytochromo C reductase complex) and the *MBD3* gene (a transcriptional repressor). A smaller loop was also formed with a CTS in the exon 1 of *TCF3* gene (**Figure 4.20d**).

In conclusion, our results confirm a high occupancy of CTCF in all the analyzed CTSs to specific erythroid transcription factor genes. Additionally, when we induced erythroid differentiation with Ara-C, a tendency to increase in the binding of CTCF (non-significant in most cases) was found. These changes in the binding of CTCF are independent of the changes observed in the expression of these genes upon erythroid differentiation. ChIA-PET data suggest that CTCF, together with cohesins, is forming different long range interactions that could be important for the regulation of the studied erythroid genes.

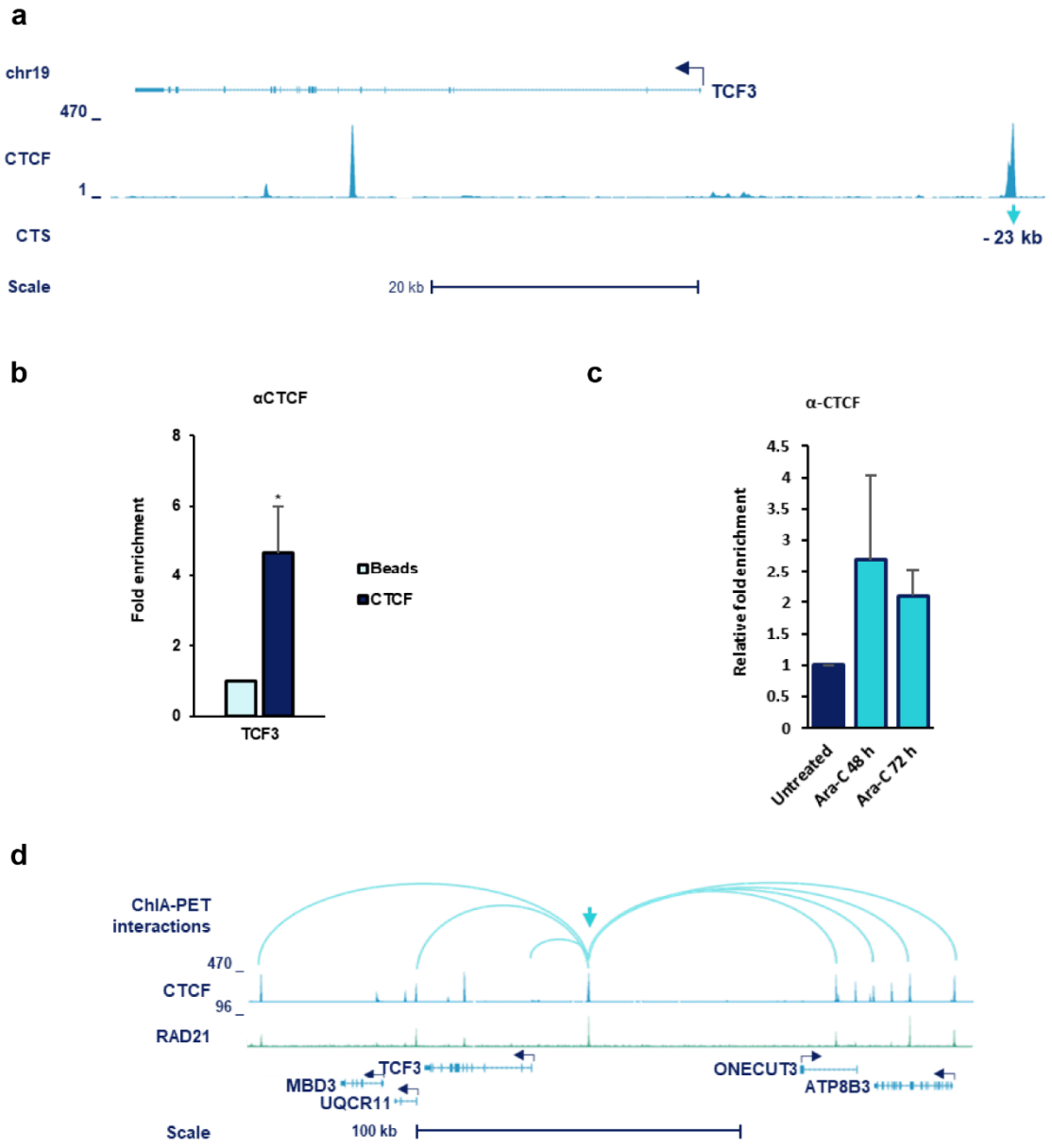

Figure 4.20. CTCF binding to TCF3 gene. *a) ENCODE analysis showing ChIP-seq profile of CTCF for TCF3 gene in chromosome 19. CTCF binding site is shown (blue arrow). b) ChIP analysis showing the binding of CTCF to the TCF3 CTS in K562 cells. The fold enrichment of the target sequence was determined as indicated in Materials and Methods section. Each value was normalized with respect to the beads (no-antibody). Bars indicate mean ± s.e.m of five independent experiments; significance difference (*,p<0.05) from the beads. c) ChIP analysis showing the binding of CTCF to the TCF3 CTS in K562 cells upon treatment with with 1 μM Ara-C for the indicated times. Bars indicate mean ± s.e.m of three to five independent experiments; significance difference (*,p<0.05) from the untreated cells. d) ChIA-PET interactions from the TCF3 CTS (blue arrow) are shown as blue arcs. ChIP-seq profiles of CTCF and RAD21 (left) and representation of possible loop (right) are shown. CTCF, blue balls; Cohesin (RAD21), green circle; genes, blue boxes.*

4.1.6. *MYC* regulation by CTCF

Since CTCF was first identified as a protein interacting with the CCCTC motif in the chicken c-*MYC* promoter (Lobanenkov et al., 1990), several studies reported *MYC* regulation by CTCF at different levels. In 1996, Fillipova et al, described that CTCF regulates negatively *MYC* expression and identified two constitutive CTCF-binding sites (site A and B) located in the first exon, close to the transcriptional start site of the *MYC* P2 promoter (Filippova et al., 1996). Also, it was described a constitutive CTCF binding site (site N), associated with a DNAse I hypersensitive region, termed MINE (MYC insulator element) (Gombert et al., 2003). In the last years, several studies have found a positive regulation of *MYC* by CTCF. It was described a super-enhancer mapping at -515 kb upstream *MYC* in colorectal cancer (Xiang et al., 2014). Also, a conserved enhancer-docking site located -2 kb upstream *MYC* transcription start site (Schuijers et al., 2018) and a distal enhancer cluster residing +1.8 Mb downstream *MYC* promoter (Hyle et al., 2019) have been recently reported.

Therefore, the previous results regarding *MYC* regulation by CTCF are controversial. In addition, the possible role of CTCF regulating *MYC* in the context of the erythroid differentiation has not been explored. To identify possible CTCF binding sites to *MYC* regulatory regions in our cellular model, we carried out and ENCODE analysis. We selected six possible CTSs, some of them previously described in different cellular models, such as the -515 kb upstream MYC, site N (-2 kb upstream), site A/B (exon 1) and site W (intron 1). Moreover, we selected two additional sites mapped at -335 kb and -10 kb upstream of *MYC* (**Figure 4.21a**).

To confirm the binding of CTCF, we performed chromatin immunoprecipitation (ChIP) assays in untreated K562 cells. In all the experiments, positive and negative controls were used in order to check that ChIP was working (see **Figure 4.12**). ChIP results indicated a high occupancy of CTCF in all the analyzed CTSs in the regulatory region of *MYC* gene, although the maximal signal was at the -10 kb site (**Figure 4.21b**).

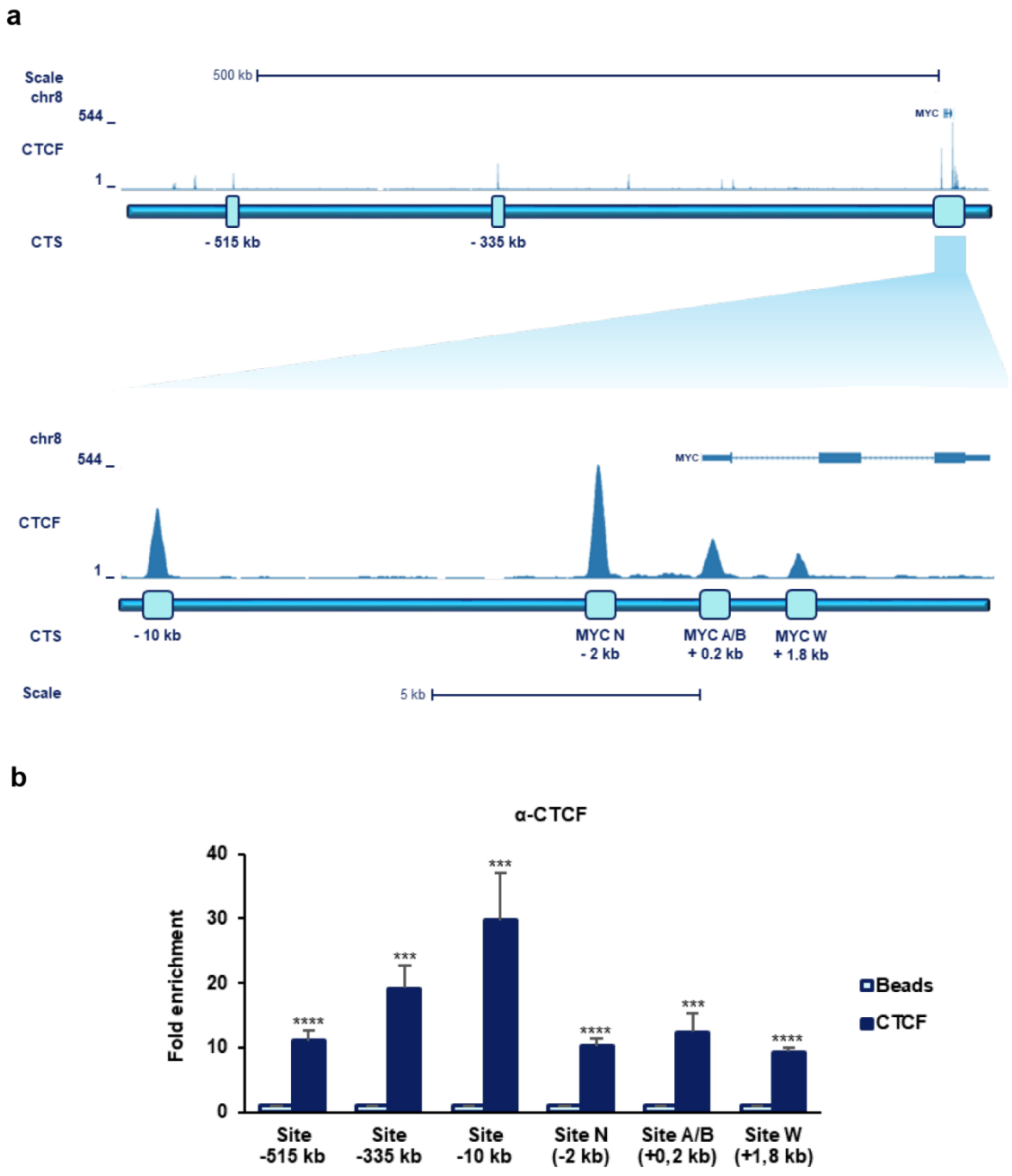

Figure 4.21. CTCF binding to MYC gene. *a) ENCODE analysis showing ChIP-seq profile of CTCF for MYC gene in chromosome 8 in K562 cell line. CTCF binding sites are shown (blue boxes). b) ChIP analysis showing the binding of CTCF to the MYC CTS in K562 cells. The fold enrichment of the target sequence was determined as indicated in Materials and Methods section. Each value was normalized with respect to the beads (no-antibody). Bars indicate mean ± s.e.m of four independent experiments; significance difference (***,p<0.001; ****,p<0.0001) from the beads.*

Once confirmed that CTCF is occupying the *MYC* gene regulatory regions, we analyzed the binding upon induction of erythroid differentiation. K562 cells

were treated with 1 μM Ara-C for 24, 48 and 72 hours or with 0.5 μM Imatinib for 24 and 48 hours. In general, CTCF occupancy upon differentiation increased with both treatments. Ara-C treatment slightly increased CTCF binding (**Figure 4.22a**). However, high occupancy of CTCF was observed with Imatinib treatment, except in Site -10 kb, where CTCF binding was maintained at short treatment times (**Figure 4.22b**).

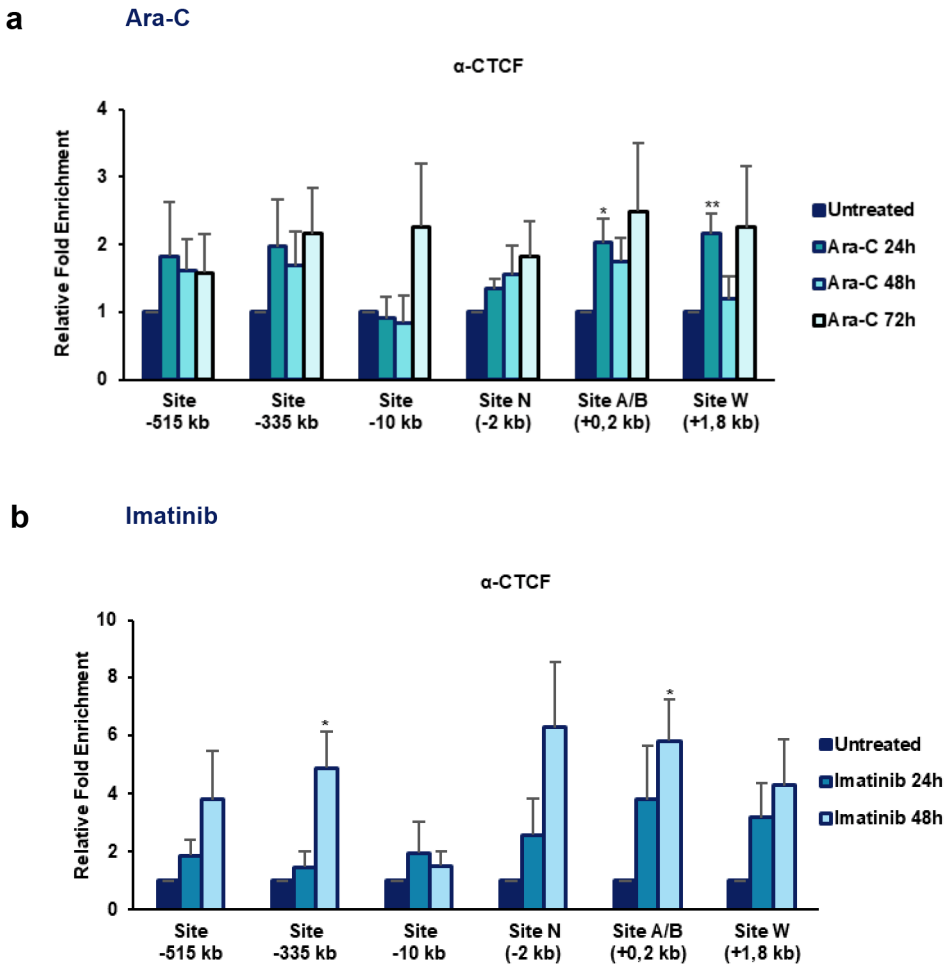

Figure 4.22. CTCF binding to MYC gene upon induction of erythroid differentiation. *ChIP analysis showing the binding of CTCF to the MYC CTSs in K562 cells upon treatment with with 1 μM Ara-C (a) or with 0.5 μM Imatinib for the indicated times (b). The fold enrichment of the target sequence was determined as indicated in Materials and Methods section. Each value was normalized with respect to the untreated cells. Bars indicate mean ± s.e.m of four independent experiments; significance difference (*,p<0.05;**,p<0.01) from the untreated cells.*

From the ENCODE ChIA-PET data we analyzed the possible interactions that are formed around the regulatory regions of *MYC* gene in K562 cells. We

observed a loop formed between the site -10 kb and a CTSs located around +928 kb downstream *MYC* gene (**Figure 4.23**). A second loop is formed between the *MYC* promoter and a CTS sited +1.9 Mb downstream *MYC* gene.

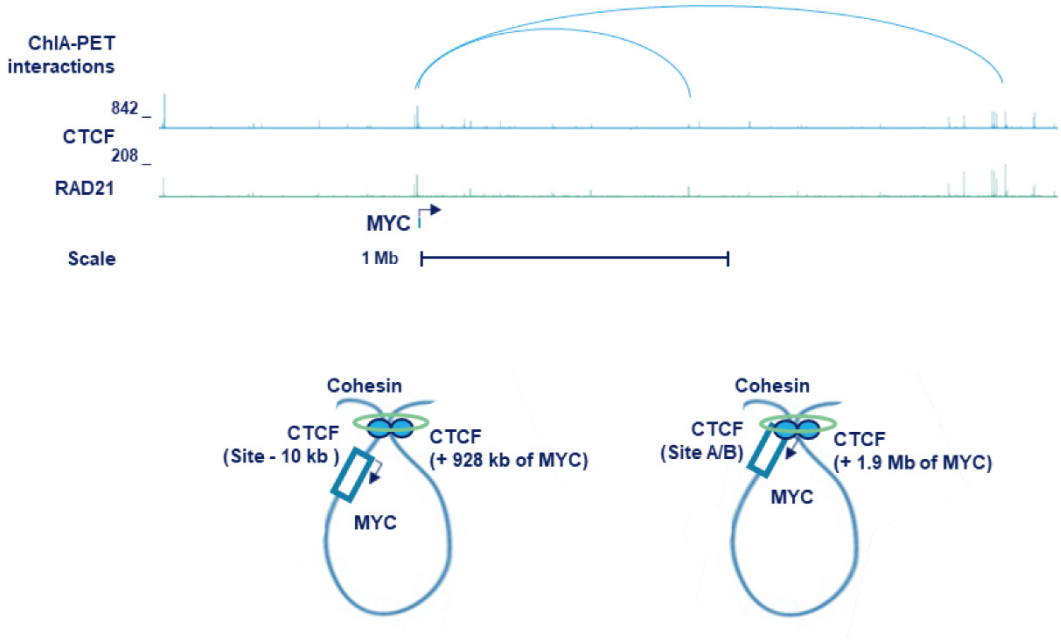

Figure 4.23. Putative interactions between MYC regulatory regions. *ChIA-PET interactions from MYC CTSs are shown in blue arcs. ChIP-seq profiles of CTCF and RAD21 are shown. Representation of two possible loops (bottom) are shown. CTCF, blue balls; Cohesin (RAD21), green circle; genes, blue boxes.*

Altogether, these results confirm CTCF binding to different regulatory regions of *MYC* gene and indicate a role of CTCF in MYC regulation. Moreover, during erythroid differentiation CTCF binding to *MYC* gene tends to increase, a process concomitant with the downregulation of MYC expression.

4.2. Effects of epigenetic drugs in B-cell lymphoma

CTCF is also involved in the regulation of lineage-specific gene expression in lymphoid cells. Our group has demonstrate that CTCF downregulation reduces *BCL6* expression and induces plasma cell differentiation. Moreover, CTCF regulates epigenetically BCL6 through the binding to the exon 1A of *BCL6* and this binding is associated with the presence of active histone marks and *BCL6* expression (Batlle-Lopez et al., 2015). Since BCL6 is heavily involved in lymphomas, we were then interested in the study the effects of epigenetic drugs potentially targeting BCL6.

Romidepsin is a histone deacetylase inhibitor that inhibits HDAC class I. It was approved by the FDA for the treatment of some T-cell lymphomas (Smolewski and Robak, 2017). We previously found that romidepsin induces apoptosis and differentiation, as well as BCL6 acetylation, in lymphoma cells (Cortiguera, MG, García-Gaipo, L et al submitted, see annex). On the other hand, JQ1 is a potent BET bromodomain inhibitor that is able to repress the expression of some genes such as *MYC* (Delmore et al., 2011).

Thus, the aim of this second part is to investigate the effects of romidepsin in combination with JQ1 in the treatment of different aggressive B-cell lymphoma cells. For that, we treated B-cell lymphoma cell lines from different origins (**Table 4.1**) with romidepsin and JQ1. A schematic representation of the experimental workflow is shown in **Figure 4.24**.

Table 4.1. B-cell lymphoma cell lines used in this work.

CELL LINE	ORIGIN	FISH			*BCL6* EXPRESSION
		BCL6	*MYC*	*BCL2*	
Ramos	Burkitt lymphoma; EBV negative	Normal	Rearrangement	Gain	+++
DG75	Burkitt lymphoma; EBV negative	Gain	Rearrangement	Normal	++
Raji	Burkitt lymphoma; EBV positive	Normal	Rearrangement	Normal	++
Toledo	GC-DLBCL	Gain and rearrangement	Gain	Normal	-

BCL6, BCL2 and *MYC* loci status and BCL6 expression of the different cell lines used was previously analyzed (MG Cortiguera, PhD Thesis 2017). These results are shown in **Table 4.1**.

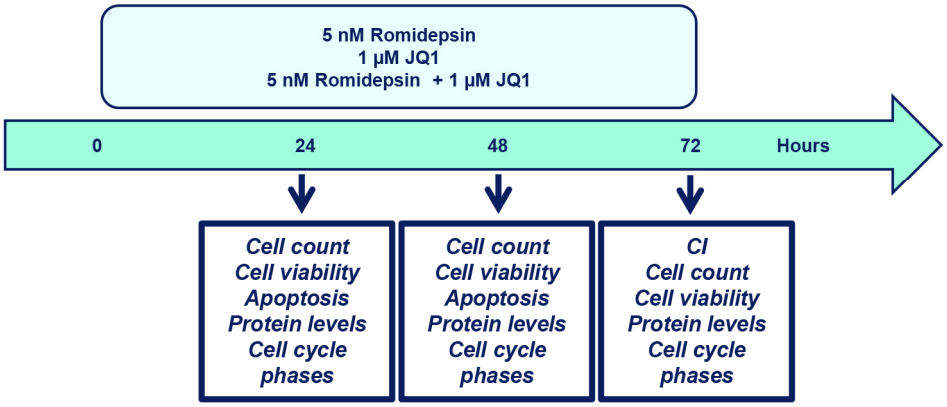

Figure 4.24. Experimental workflow for the analysis of epigenetic drugs in B-lymphomas. *Different human B-cell lymphoma cell lines were seeded (3x10^5 cells) and treated with 5 nM romidepsin and/or 1 µM JQ1 for 72 hours. Analysis performed at each time are shown.*

4.2.1. Romidepsin and JQ1 combination index

As a first approach, using different concentrations of romidepsin and JQ1 we generate a combination index plot (CI). Ramos, Raji and DG75 cells from Burkitt lymphoma were treated with different combinations of romidepsin and JQ1 for 72 hours. Metabolic activity was measured by WST-1 method and the combination index was obtained by the Chou-Talalay method (Chou and Talalay, 1984) (**Figure 4.15**). Synergistic effect (CI<1) was detected for Ramos, Raji and DG75 cell lines using different combinations of romidepsin and JQ1. For further experiments, we selected 5 nM romidepsin and 1 µM JQ1 that are doses close to the IC_{50} values (data not shown) where synergism was evident, especially in Ramos and Raji cells. Combined treatment of Toledo cells (from GC-DLBCL) did not showed a clear synergistic effect.

a

Ramos

Romid (nM)	JQ1 (μM)	Relative Metabolic Activity	Combination Index (CI)
0	0	1.00	
1.0	0.1	0.94	1.32
5.0	**1.0**	0.26	0.73
10.0	1.0	0.27	1.16
2.0	0.5	0.55	0.76
5.0	0.5	0.27	0.59
10.0	0.5	0.28	1.03
15.0	1.5	0.27	1.77

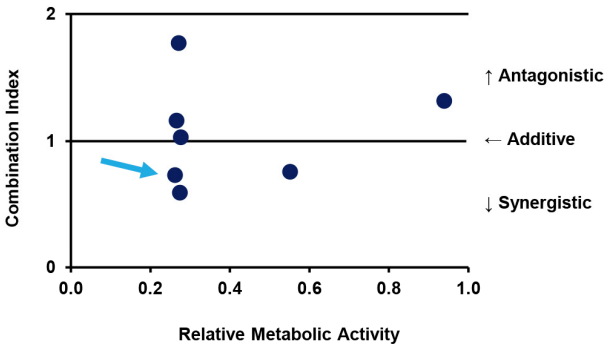

b

Raji

Romid (nM)	JQ1 (μM)	Relative Metabolic Activity	Combination Index (CI)
0	0	1.00	
1.0	0.1	0.57	0.80
5.0	**1.0**	0.29	0.50
10.0	1.0	0.29	0.99
2.0	0.5	0.29	0.20
5.0	0.5	0.29	0.52
10.0	0.5	0.28	0.98
15.0	1.5	0.28	1.40

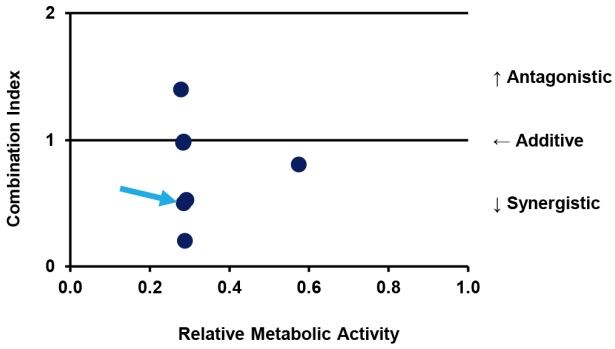

c

DG75

Romid (nM)	JQ1 (μM)	Relative Metabolic Activity	Combination Index (CI)
0	0	1.00	
1.0	0.1	0.50	0.14
5.0	**1.0**	0.46	0.90
10.0	1.0	0.49	1.34
2.0	0.5	0.50	0.52
5.0	0.5	0.46	0.60
10.0	0.5	0.40	0.68
15.0	1.5	0.38	1.22

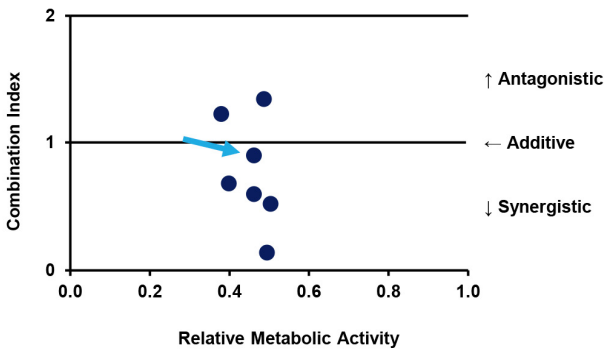

Figure 4.15. Romidepsin and JQ1 Combination Index (CI). *Lymphoma B-cells were seeded and treated with different combinations of romidepsin and JQ1 for 72 hours (left tables). Metabolic activity was measured by WST-1 assay and combination index (CI) was determine by Chou-Talalay method using CompuSyn software. Combination index plots for the combination of Romidepsin and JQ1 (right plots). CI<1 synergistic effect; CI=1 additive effect; CI>1 antagonistic effect. a) CI in Ramos cells. b) CI in Raji cells. c) CI in DG75 cells.*

4.2.2. Romidepsin and/or JQ1 decrease cell metabolic activity and inhibit cell proliferation

Once stablished the working concentration for the different treatments, alone or in combination (5 nM romidepsin and/or 1 μM JQ1) we analyzed the effect of the combination of romidepsin and JQ1 on metabolic activity and cell proliferation in Ramos, Raji, DG75 and Toledo cells.

Metabolic activity was measured using the WST-1 method which allows the quantification of cell viability. In general, results indicated that both treatments alone and their combination reduced metabolic activity in Ramos, Raji, DG75 and Toledo (**Figure 4.26**). Ramos cells were the most sensitive, showing a metabolic activity of 20% after treatment with 5 nM romidepsin + 1 μM JQ1, while Raji and Toledo showed around a 40% of metabolic activity. The less sensitive cells were DG75 which showed a 55% of metabolic activity. Similar results were obtained with treatment with romidepsin alone (around 25% in Ramos, 45% in Raji and Toledo and 65% in DG75) while the reduction was lower when cells were treated only with JQ1 (near 50% in Ramos and Toledo and 70% in Raji and DG75).

In addition, a reduction on cell proliferation was observed in cells treated with romidepsin or with JQ1 alone, being higher with romidepsin. The combination of treatments inhibited almost completely the proliferation in the four lymphoma cell lines (**Figure 4.27**).

All together, these results indicated that treatment with romidepsin and JQ1 reduced cell metabolic activity and proliferation of the lymphoma cell lines at different extent. Synergistic effect on cell proliferation was observed mainly in Ramos and Raji cells. For further experiments we focused in these two Burkitt lymphoma cell lines as well as in the DLBCL Toledo cells, for comparison.

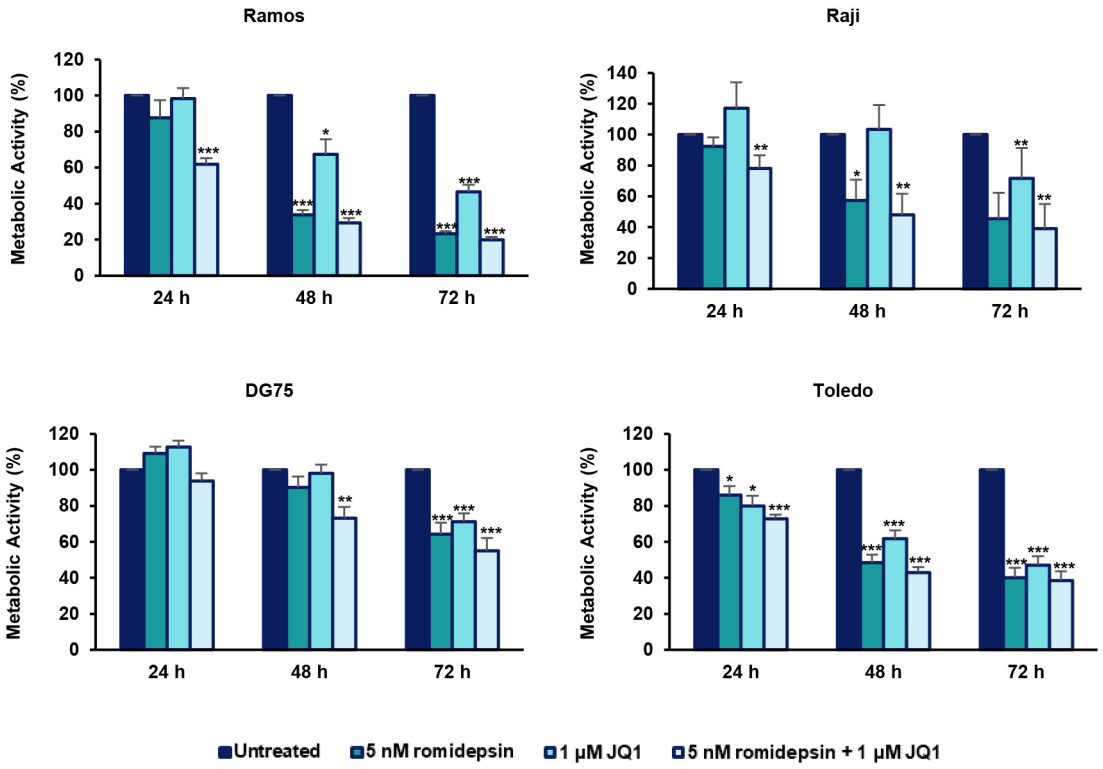

Figure 4.26. Romidepsin and JQ1 effect on metabolic activity. *Ramos, Raji, DG75 and Toledo cells were seeded and treated with 5 nM romidepsin and/or 1 μM JQ1 for 72 hours. Metabolic activity was measured at 24, 48 and 72 hours using WST-1 method. Untreated cells represented 100% of metabolic activity. Bars indicate mean ± s.e.m of four to five independent experiments; significance difference (*,p<0,05; **,p<0,01; ***,p<0,001) from the untreated cells.*

4.2.3. Romidepsin and JQ1 combined treatment induce apoptosis

To check if reduction of proliferation is the result of cell death or cell cycle arrest, trypan blue assay was carried out. A decrease in the percentage of viable cells was observed upon romidepsin treatment (alone or in combination with JQ1) in Ramos, Raji and Toledo while JQ1 alone does not induce cell death (**Figure 4.28**). These results suggested that treatment with romidepsin, but not JQ1, is causing cell death in B-cell lymphoma cell lines.

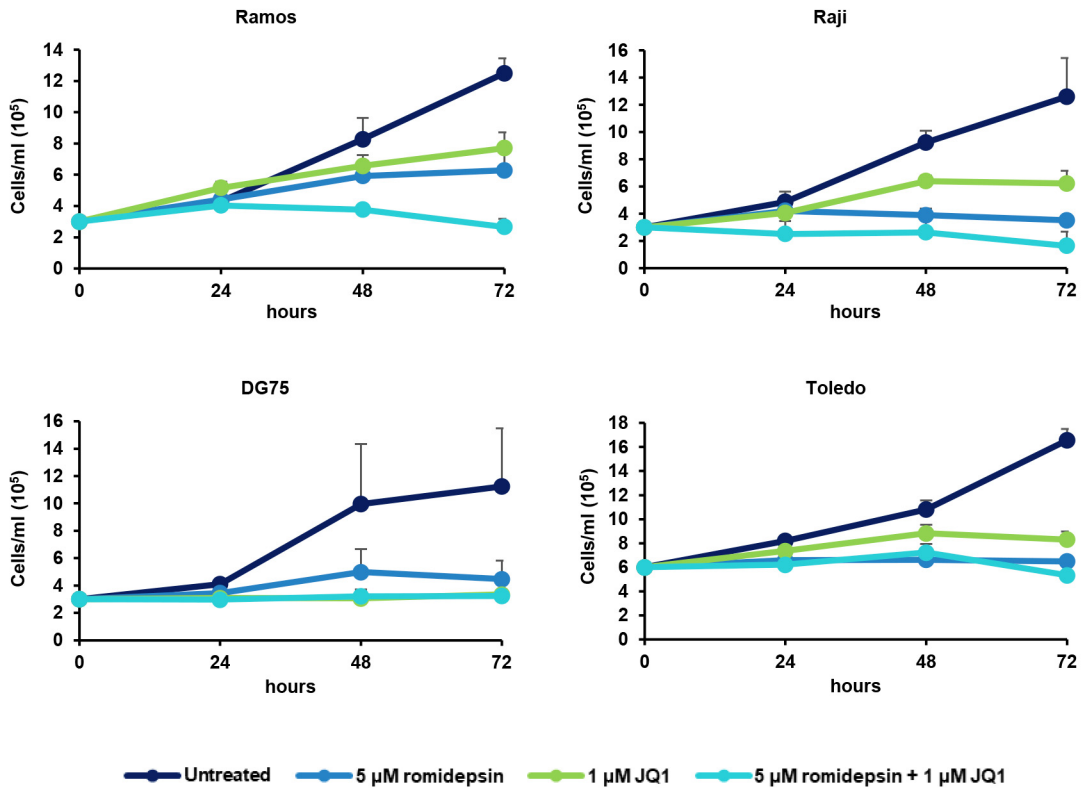

Figure 4.27. Romidepsin and JQ1 effect on cell proliferation. *Cell proliferation curves for Ramos, Raji, DG75 and Toledo cells. Cells were seeded and treated with 5 nM romidepsin and/or 1 μM JQ1. Cells were counted at 24, 48 and 72 hours. Bars indicate mean ± s.e.m of two to four independent experiments.*

To confirm if treatments with romidepsin were causing cell death, we performed Annexin-V assay to measure early apoptosis (**Figure 4.29**). As we expected, cells treated with JQ1 do not die by apoptosis, while romidepsin treatment increased the percentage of annexin-V positive cells mainly in Ramos and Toledo cells (60% and 90% respectively). Interestingly, treatment with romidepsin + JQ1 strongly increased the percentage of positive cells in Ramos and Raji (94% and 66% respectively). In Toledo cells, the increase in the percentage of annexin-V positive cells with the combined treatment was similar than with romidepsin alone.

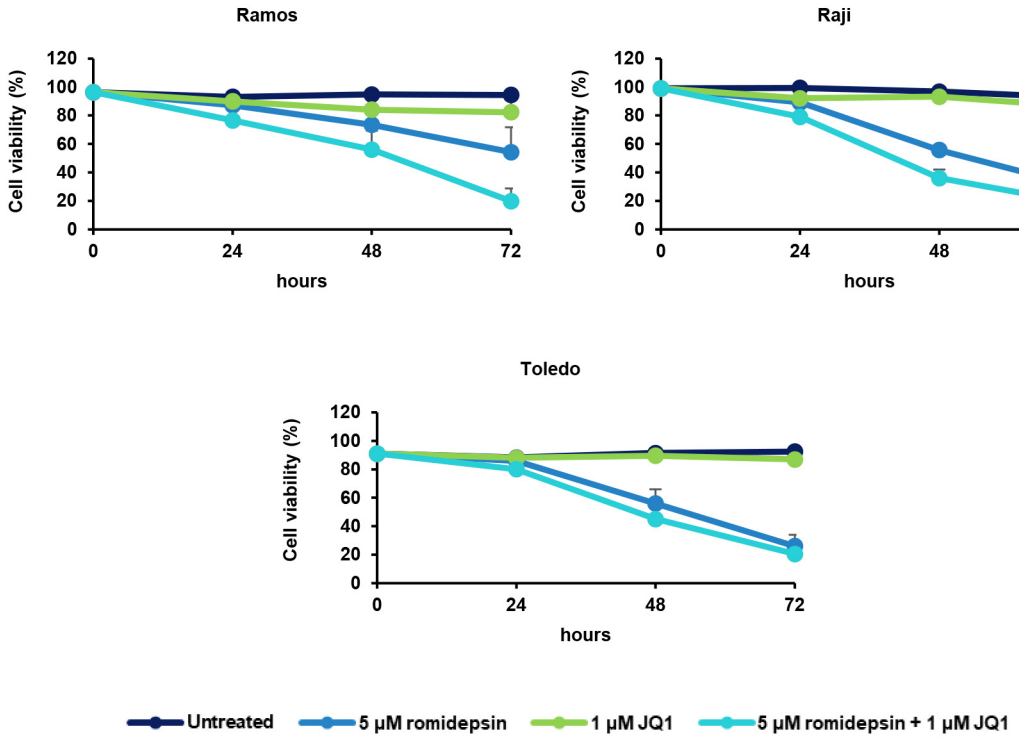

Figure 4.28. Romidepsin and JQ1 effect on cell viability. *Number of viable cells for Ramos, Raji and Toledo cells. Cells were seeded and treated with 5 nM romidepsin and/or 1 μM JQ1. Cells were stained with Trypan blue and counted at 24, 48 and 72 hours. Bars indicate mean ± s.e.m of two to four independent experiments.*

Cleavage of PARP1 protein (a nuclear poly (ADP-ribose) polymerase) is used as an apoptosis marker. Induction of apoptosis was analyzed by western-blot (**Figure 4.30**). High levels of cleaved PARP1 were found in Ramos cells upon treatment with romidepsin and JQ1 for 24 and 48 hours, while upon treatment with romidepsin alone, cleaved PARP1 was not detected until 48 hours. Similar results were found in Toledo cells at 48 hours. In Raji cells, cleaved PARP1 was only found with the combination treatment, in full agreement with the annexin V assays shown above. These results indicate a synergistic effect of romidepsin and JQ1 in the induction of apoptosis in the analyzed lymphoma cells.

BCL-xL is a member of the BCL2 family proteins which are known to regulate the intrinsic apoptotic pathway. BCL-xL is a protein with anti-apoptotic functions. Protein levels were analyzed by western-blot upon treatments (**Figure 4.30**Figure

4.). BCL-xL decreased in Ramos cells upon romidepsin and JQ1 treatment. Higher reduction was observed in Raji and Toledo cells.

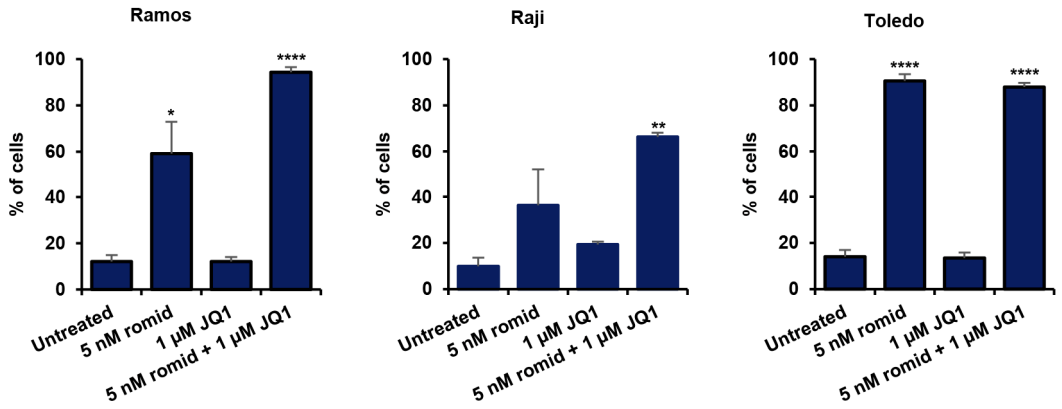

Figure 4.29. Romidepsin and JQ1 effect on apoptosis. *Annexin-V assay performed in Ramos, Raji and Toledo cells. Cells were seeded and treated with 5 nM romidepsin and/or 1 μM JQ1 for 48 hours. Bars indicate mean ± s.e.m of two or three independent experiments; significance difference (*,p<0,05; **,p<0,01; ****,p<0,0001) from the untreated cells.*

Finally, levels of γH2AX were also analyzed by western-blot (**Figure 4.30**). γH2AX is a marker of DNA damage response. Interestingly, we found a strong increase in γH2AX protein levels upon treatment with romidepsin and JQ1 in all cell lines.

Altogether these results demonstrated that romidepsin and JQ1 combined treatment induces apoptosis in lymphoma B-cells. Our results indicate a significant synergistic effect of romidepsin and JQ1 on apoptotic cell death.

4.2.4. Romidepsin and JQ1 induce cell cycle arrest

Germinal center B-cells are highly proliferating cells which exit the cell cycle and stop proliferation in order to be able to differentiate into plasma cells (Basso and Dalla-Favera, 2015). Based on this, we aimed to analyze the cell cycle distribution in Ramos, Raji and Toledo cell lines upon treatment with romidepsin and/or JQ1.

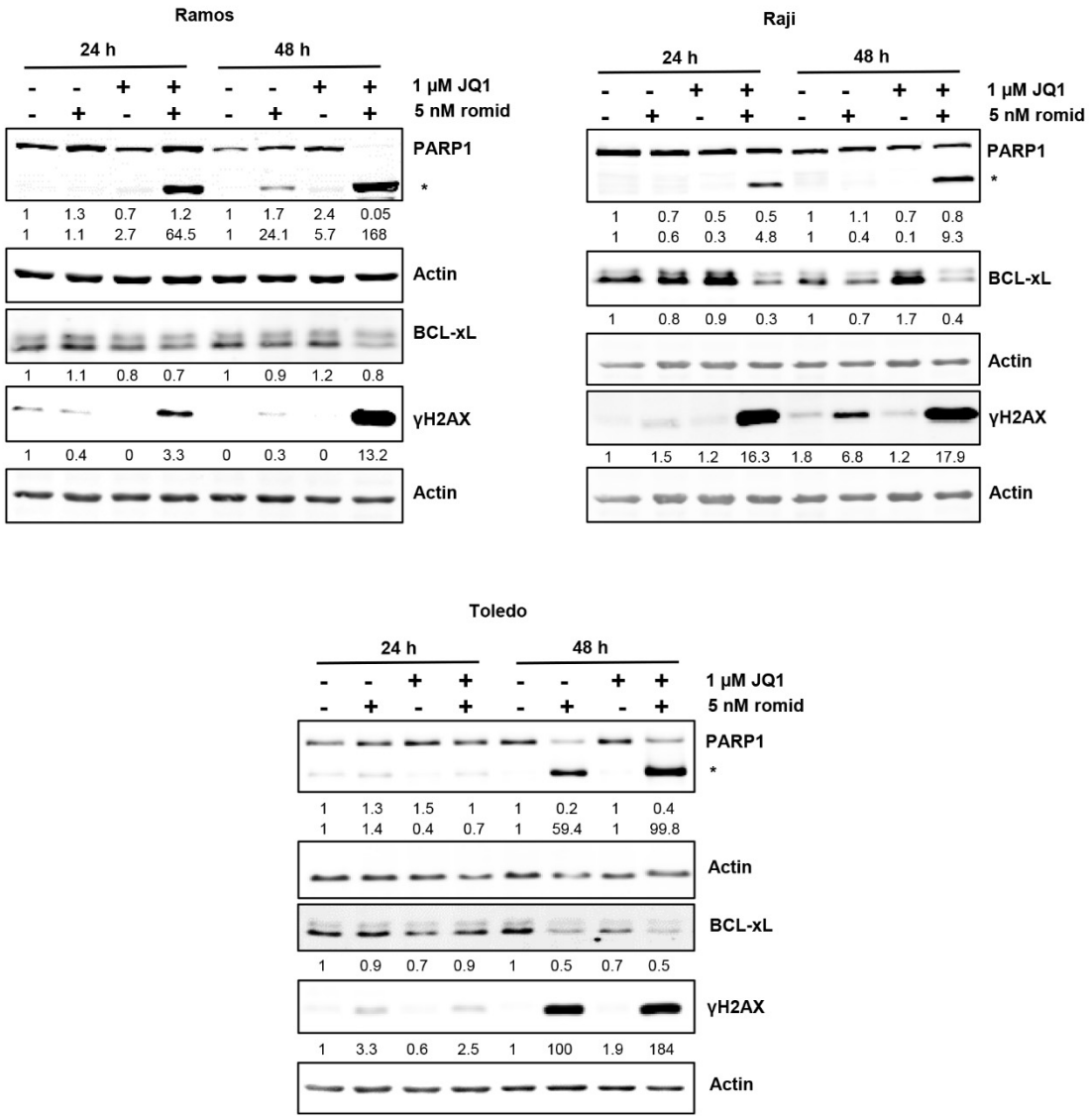

Figure 4.30. PARP1, BCL-xL and γ-H2AX levels upon treatment with romidepsin and JQ1. *Western blot showing PARP1, cleaved PARP1 (*), BCL-xL and γH2AX protein levels in Ramos, Raji and Toledo cells treated with romidepsin and/or JQ1 for 24 and 48 hours. Actin was used as loading control. Densitometry values are shown at the bottom, normalized to the control.*

First, we analyzed the fraction of cells in the sub G_0/G_1 phase of the cell cycle which is also an indicative of cell death. Romidepsin and JQ1 treatment increased the percentage of cells in sub G_0/G_1 in Ramos, Raji and Toledo cells (62%, 64% and 42% respectively) (**Figure 4.31**). These results were consistent with cell viability and apoptosis results. Then, we analyzed the cell cycle distribution in the viable cells.

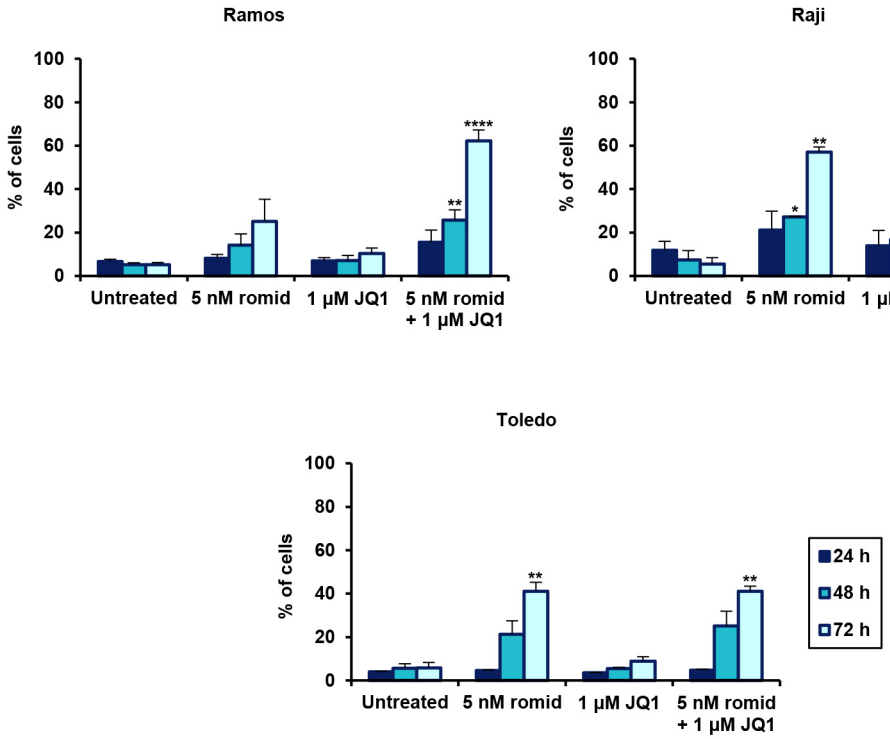

Figure 4.31. Sub G_0/G_1 fraction upon romidepsin and JQ1 treatment. *Sub G_0/G_1 fraction were analyzed by propidium iodide staining and flow cytometry analysis. Ramos, Raji and Toledo cells were treated with 5 nM romidepsin and/or 1 µM JQ1 for 24, 48 and 72 hours. Bars indicate mean ± s.e.m of two or three independent experiments; significance difference (*,p<0,05; **,p<0,01; ****,p<0,0001) from the untreated cells.*

In Ramos cells we found some accumulation of cells in G_0/G_1 phase, increasing from 42% to 55% and the corresponding reduction in the number of cells in S and G_2/M phases with romidepsin treatment. It is to note that the percentage of cells in each phase was calculated as a percentage from total viable cells. JQ1 treatment induced a strong accumulation of cells in G_0/G_1 phase, from 42% to 84%. Finally, upon treatment with romidepsin and JQ1, we observed an increased in the number of cells on G_0/G_1 phase, from 42% to 60% only at 24 hours of treatment. In Raji cells a slight accumulation of cells in G_0/G_1 phase was observed with romidepsin and combination treatment (from 51% to 60%) while JQ1 treatment induced an accumulation of more than 90% of cells in G_0/G_1 phase. Similar results were obtained in Toledo cells in which romidepsin and combination treatment induced an accumulation of cells in G_0/G_1 phase (from

62% to 71% and 75% respectively) and around 92% of cells were accumulated in G_0/G_1 phase upon JQ1 treatment (**Figure 4.32**).

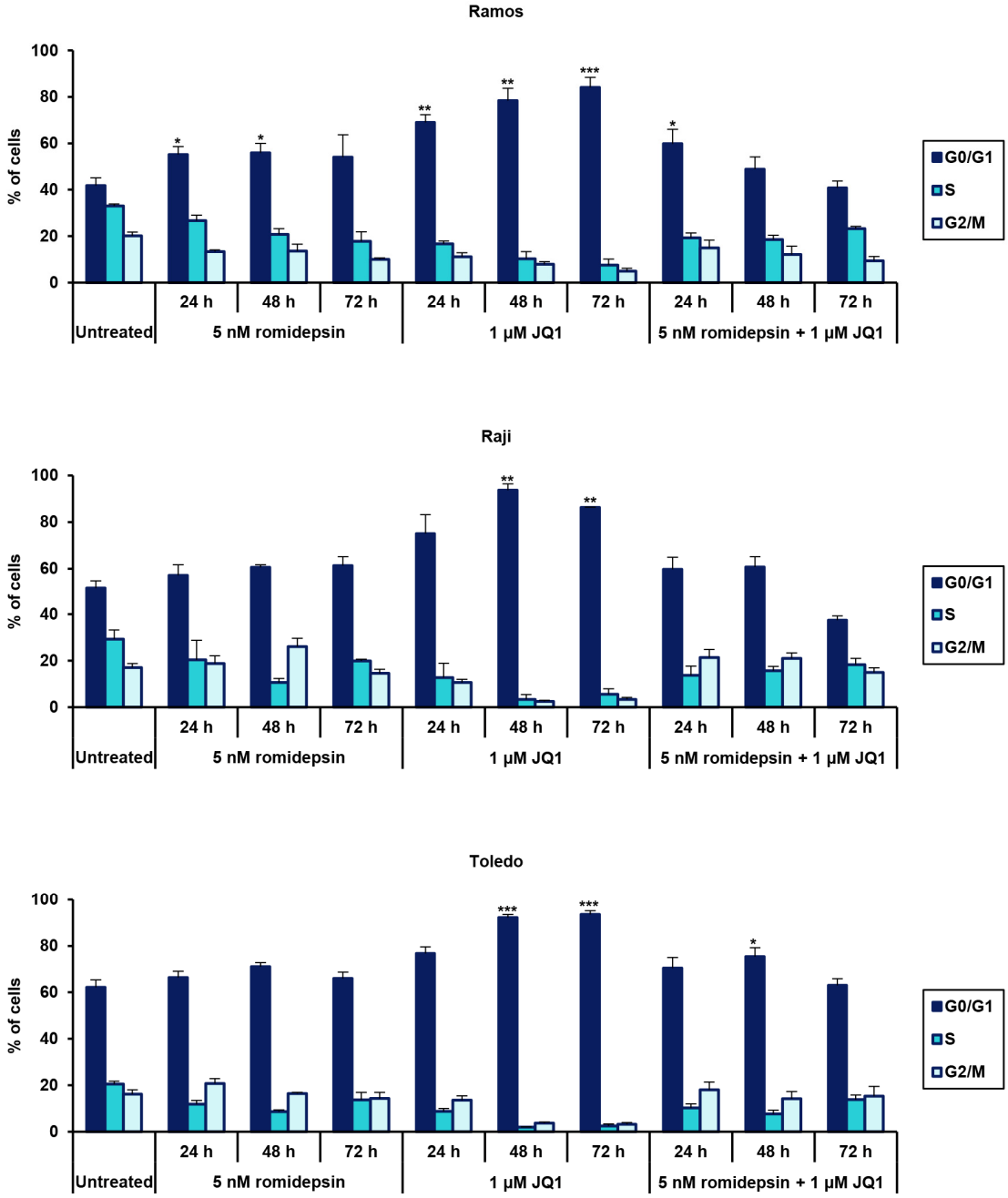

Figure 4.32. Romidepsin and JQ1 effect on cell cycle distribution. *Cell cycle assays were performed using propidium iodide staining and flow cytometry analysis. Ramos, Raji and Toledo cells were treated with 5 nM romidepsin and/or 1 μM JQ1 for 24, 48 and 72 hours. The percentage of cells in each phase was calculated as a percentage from total viable cells. Bars indicate mean ± s.e.m of two or three independent experiments; significance difference (*,p<0,05; **,p<0,01; ***,p<0,001) from the untreated cells.*

p21 and p27 belong to the *Cip/Kip* family of cyclin dependent kinase (*Cdk*) inhibitor proteins and have important functions in the regulation of cell cycle progression at G_1 and S phase (Besson et al., 2008). We analyzed their expression by western-blot in order to understand better the effect of romidepsin and JQ1 treatment in cell cycle (**Figure 4.33**). In Ramos cells, an increase in p21 protein levels was detected with the combination treatment after 24 hours. At longer times, synergistic effect was not evident maybe due to the high proportion of apoptotic cells. Levels of p27 was dramatically increased in Raji cells with romidepsin and JQ1 treatment. Finally, levels of p21 increased in Toledo cells. Overall, romidepsin and JQ1 treatment induce cell cycle arrest together with increase in p21 and/or p27 protein levels.

As it was previously describe, JQ1 induces transcriptional downregulation of MYC levels (Lovén et al., 2013). In order to confirm the effect of JQ1, MYC protein levels was analyzed by western-blot (**Figure 4.33**). The expected reduction in MYC levels was observed in Ramos, Raji and Toledo cell lines. Interestingly, romidepsin treatment also reduce MYC levels in all cell lines. Finally, the combination treatment completely downregulated MYC expression. Moreover, we analyzed the levels of cyclin A as a marker of proliferation and we observed a decrease in its expression in Ramos and Toledo cell lines (**Figure 4.33**).

Altogether, these results indicated that romidepsin and JQ1 treatment induces cell cycle arrest associated with increased p21 and/or p27 protein levels and MYC downregulation.

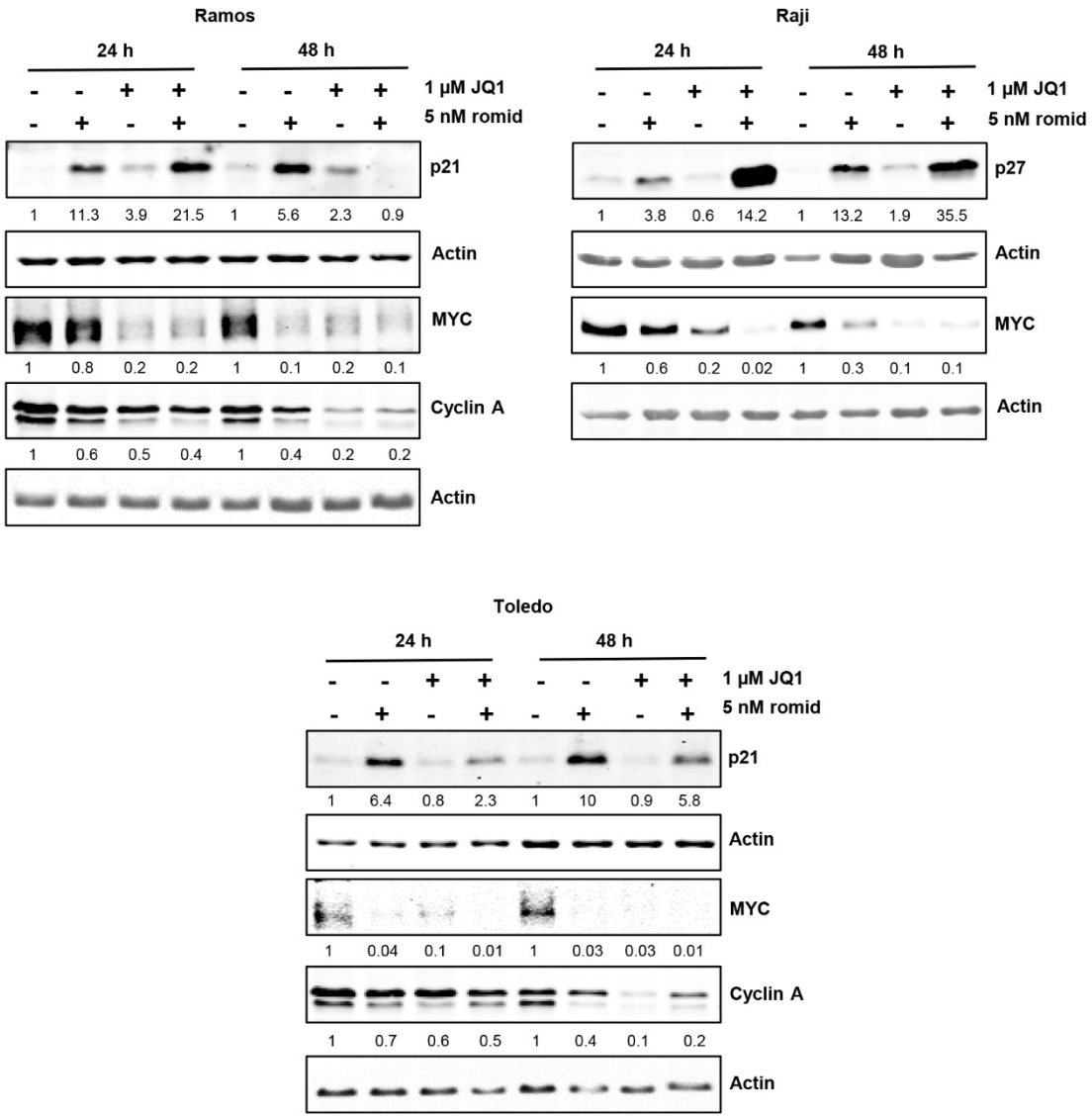

Figure 4.33. p21, p27, MYC and Cyclin A expression upon romidepsin and JQ1 treatment. *Western blot showing p21, p27, MYC and Cyclin A protein levels in Ramos, Raji and Toledo cells treated with romidepsin and/or JQ1 for 24 and 48 hours. Actin was used as loading control. Densitometry values are shown at the bottom, normalized to the control.*

4.2.5. Romidepsin and JQ1 induce *BCL6* downregulation and plasma cell differentiation

BCL6 is highly expressed in dark zone germinal center B-cells and its expression has to be downregulated in order to allow B-cells to exit the germinal center and to differentiate into plasma cells (Basso and Dalla-Favera, 2010). We analyzed the effect of romidepsin and JQ1 treatment on BCL6 expression in

different B-cell lymphoma cell lines (**Figure 4.34**). Combination treatment reduces BCL6 protein levels in all cell lines with basal expression of BCL6 (Ramos, Raji and DG75 from Burkitt lymphoma cells). BCL6 downregulation takes place after 24 hours of romidepsin and JQ1 treatment. Moreover, romidepsin and JQ1 alone also reduce BCL6 expression.

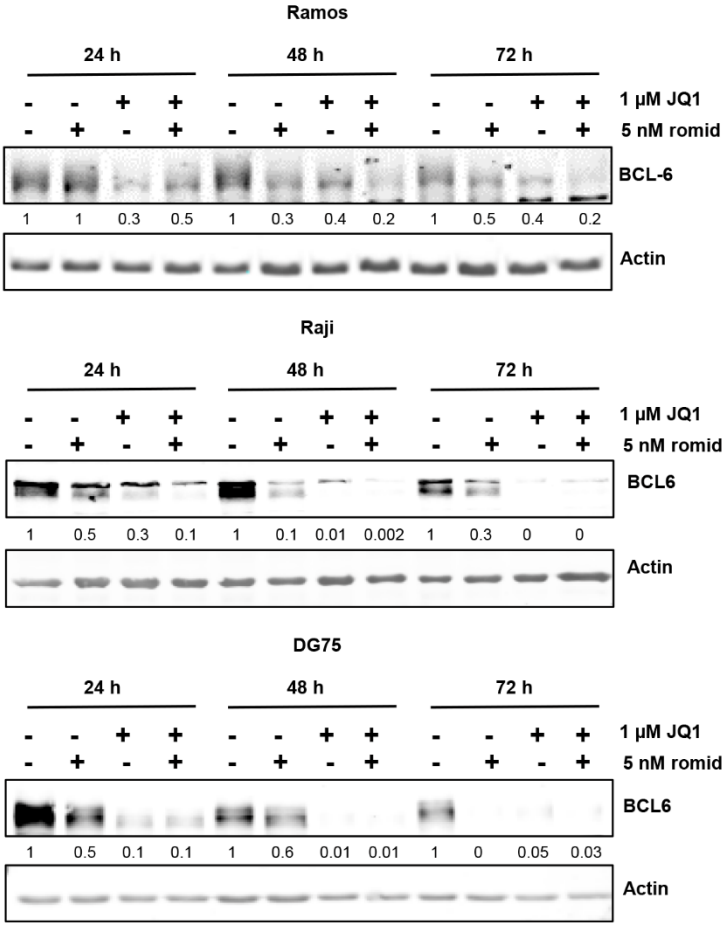

Figure 4.34. Romidepsin and JQ1 effect on BCL6 expression. *Western blot showing BCL6 protein levels in Ramos, Raji and DG75 cells treated with romidepsin and/or JQ1 for 24, 48 and 72 hours. Actin was used as loading control. Densitometry values are shown at the bottom, normalized to the control.*

A consequence of BCL6 downregulation is the induction of the expression of genes related with plasma cell differentiation such as BLIMP1 (Shaffer et al., 2004a). Western-blot analysis revealed that BLIMP1 levels were slightly increased in Ramos cells (**Figure 4.35**). Interestingly, in Toledo cells which do

not express BCL6, an increased in BLIMP1 levels was observed upon romidepsin and JQ1 treatment (**Figure 4.35**).

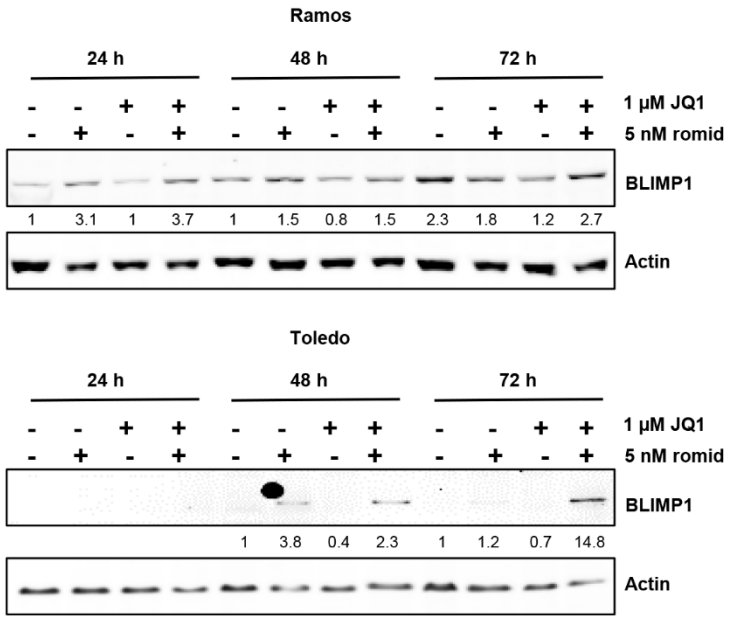

Figure 4.35. Romidepsin and JQ1 effect on plasma cell differentiation. *Western blot showing BLIPM1 protein levels in Ramos and Toledo cells treated with romidepsin and/or JQ1 for 24, 48 and 72 hours. Actin was used as loading control. Densitometry values are shown at the bottom, normalized to the control.*

These results together can indicate that romidepsin and JQ1 combined treatment induces plasma cell differentiation program probably by inhibiting BCL6 expression in B-cell lymphoma cells.

We can conclude that romidepsin and JQ1 combined treatment has a synergistic effect on apoptosis, cell cycle arrest and plasma cell differentiation. These results indicate that this drug combination could be effective in aggressive B-cell lymphoma treatment.

DISCUSSION

5. DISCUSSION

5.1. CTCF in the regulation of erythroid differentiation

Erythropoiesis is a dynamic and complex multistep process that involves differentiation and proliferation of hematopoietic stem cells to mature red blood cells. Different *in vitro* models are useful to study human erythroid differentiation from HSCs to erythrocytes. One of the most common cellular models are leukemia-derived cell lines such as K562 (Bianchi et al., 2000). Moreover, primary human erythroid cells purified from cord blood or from adult bone marrow are also used (Ronzoni et al., 2007).

The multipotent K562 cell line, which derives from a human chronic myeloid leukemia, has been widely used as cellular model to study the control of hematopoietic cell differentiation. This cell line, in response to specific differentiation inducers, can differentiate into different hematopoietic lineages. In particular, K562 cells can undergo erythroid differentiation when treated with different compounds such as, hemin (Rutherford et al., 1979), butyric acid (Gambari et al., 1986) and 5-azacytidine (Gambari et al., 1984). Furthermore, our group has described that erythroid differentiation can be induced in K562 cells by treatment with cytosine arabinoside (Ara-C) (Delgado et al., 1995) or Imatinib (Gomez-Casares et al., 2013). In this work, the induction of erythroid differentiation in K562 cells by Ara-C or Imatinib was confirmed by the inhibition of cell proliferation, increase number of hemoglobin producing cells and high expression of specific erythroid markers (γ-globin, ε-globin and GATA1).

CTCF was first described as a transcriptional regulator of *MYC* gene and our studies and others have shown that MYC plays an important role in erythropoiesis. Erythroid differentiation is accompanied with arrested cell proliferation and MYC downregulation. Our data confirmed that upon erythroid differentiation MYC mRNA and protein levels were significant reduced. These results are in agreement with the already reported data about MYC inhibition of erythroid cell differentiation induced by Ara-C in K562 cells (Delgado et al., 1995)

and inhibition of MYC activity enhances erythroid differentiation (Cañelles et al., 1997). Moreover, we observed a modest decrease in CTCF protein and mRNA levels upon induction of erythroid cell differentiation, as described (Delgado et al., 1999).

Human primary $CD34^+$ cells purified from cord blood of newborns were used as a more physiological model to study erythroid cell differentiation. $CD34^+$ cells are human hematopoietic stem/progenitor cells with the ability to differentiate into myeloid or lymphoid lineage. Erythropoietin (EPO) is an important cytokine primarily acting on erythroid precursors which is used to induce erythropoiesis in $CD34^+$ cells (Muta et al., 1994). In this work, erythroid differentiation of $CD34^+$ cells induced by EPO treatment, was confirmed by the presence of hemoglobin producing cells and changes in erythroid surface markers expression. Moreover, the upregulation in γ-globin and GATA1 protein levels confirmed the commitment to the erythroid lineage.

Therefore, our results confirmed that Ara-C and Imatinib induce erythroid cell differentiation in K562 cells and erythropoietin treatment in $CD34^+$ primary cells, as it was previously described.

5.1.1. CTCF downregulation inhibits erythroid cell differentiation

Previous results of our group revealed a differential expression and posttranslational modification of CTCF that was dependent on cellular differentiation pathways (Delgado et al., 1999). Also, we described that overexpression of CTCF in K562 cells promotes induced differentiation into the erythroid pathway (Torrano et al., 2005). These results suggest that CTCF could have a specific role in the regulation of erythroid differentiation. CTCF seems to be required for erythroid differentiation (Stadhouders et al., 2012) and for the chromatin dynamics of globin genes (Splinter et al., 2006). However, very little is known about the precise role of CTCF in erythropoiesis. For that reason, the aim of the first part of this Thesis is to get further insight into the regulation of erythroid cell differentiation by CTCF.

As a first approach, CTCF expression was downregulated via lentiviral transduction with shCTCF. We used two different systems to knock-down CTCF expression: a constitutive vector and a doxycycline-inducible system. With both systems we reduced CTCF expression about 60-80% depending on the experiment. K562 cells were infected and treated with Ara-C or Imatinib to test the CTCF effect on erythroid differentiation. We observed that CTCF downregulation slightly reduced cell proliferation which was also recently found (Bailey et al., 2018). A reduction in the percentage of hemoglobin producing cells and in the levels of erythroid markers (γ-globin, GATA1 and LMO2) demonstrates that CTCF downregulation inhibits erythroid cell differentiation in K562 cells. Similarly, Hou et al reported that CTCF knockdown reduced γ-globin transcription levels, however, no changes in GATA1 was observed in comparison with our results (Hou et al., 2010). Furthermore, upon induction of differentiation with Ara-C or Imatinib, the protein levels of erythroid markers as γ-globin, GATA1 and LMO2 did not increase when CTCF expression was reduced.

Our results obtained upon CTCF knockdown with both systems confirm that downregulation of CTCF inhibits the spontaneous and induced erythroid cell differentiation in K562 cells, indicating that CTCF is important for erythropoiesis. Furthermore, these results are in agreement with previous results from our lab describing that overexpression of CTCF in K562 cells increases erythroid cell differentiation (Torrano et al., 2005).

Using two different lentiviral systems we were able to reduce CTCF expression more than 50% in $CD34^+$ and then, tested EPO-mediated erythroid differentiation. CTCF depletion resulted in the impairment of erythroid differentiation, as assessed by a decrease in the percentage of hemoglobin producing cells, reduced number of $GYPA^+$ cells and a decrease in γ-globin and GATA1 protein levels. Colony forming unit assay also showed that CTCF downregulation dramatically reduced the number of erythroid colonies which confirms inhibition of erythroid differentiation in $CD34^+$ cells.

Taken together, our findings revealed that CTCF downregulation inhibits erythroid cell differentiation in leukemia K562 cells and in primary $CD34^+$ cells

and indicate an essential role of CTCF in the regulation of the differentiation along the erythroid pathway. A summary for CTCF knock-down effects on erythroid differentiation is shown in **Figure 5.1**.

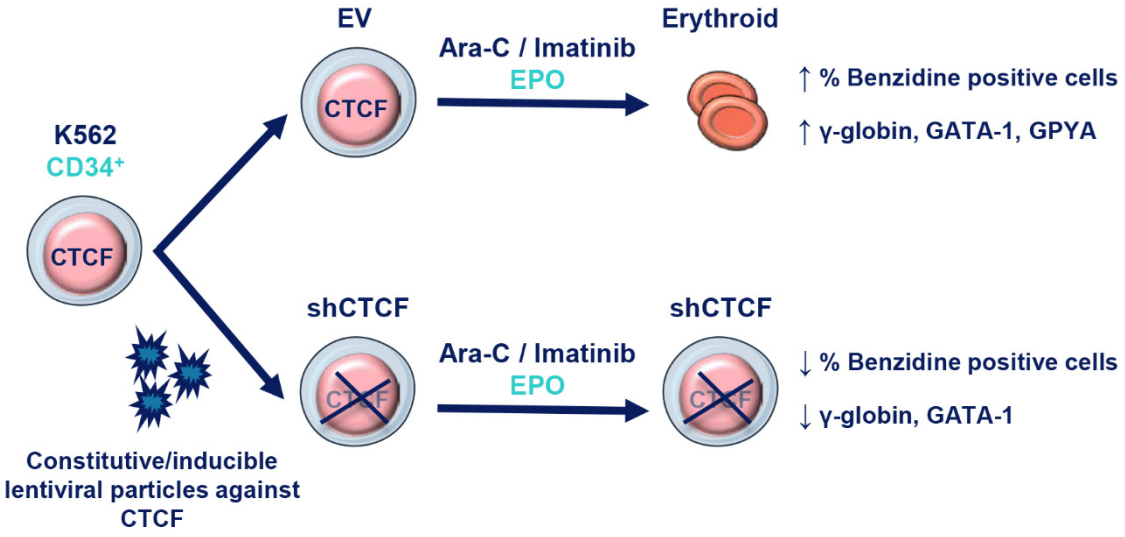

Figure 5.1. CTCF knock-down effects on erythroid cell differentiation. *Ara-C and Imatinib treatment induces erythroid cell differentiation in K562 cells and erythropoietin in CD34⁺ primary cells. Induction of erythropoiesis is confirmed by high levels of hemoglobinized cells and upregulation of γ-globin, GATA1 and LMO2 protein levels. On the other hand, CTCF downregulation inhibits erythroid cell differentiation induced by Ara-C and Imatinib or EPO in K562 and CD34⁺ cells. CTCF downregulation results in low levels of benzidine positive cells and downregulation of γ-globin and GATA1 protein levels.*

5.1.2. CTCF binding to erythroid transcription factor genes

Erythropoiesis is a developmental process regulated by different factors and transcriptional networks in a stage-specific manner (Tsiftsoglou et al., 2009). CTCF can directly regulate different hematopoietic and erythroid transcription factors. Also, CTCF may directly control the expression of different erythroid genes as globins (Cantor and Orkin, 2002). Furthermore, genomic studies in primary erythroid cells revealed that sites of CTCF and cohesin co-occupancy were enriched in gene promoters in hematopoietic stem cells and erythroid cells and these sites were associated with changes in chromatin architecture and gene expression during differentiation (Steiner et al., 2016).

Microarray-based expression profiling data from our group identified a number of erythroid genes which were up- or downregulated by CTCF (**Table 4.1**) (Torrano, V.; unpublished data). In this work, we hypothesized that CTCF could be regulating specific erythroid transcription factors genes and, therefore, we analyzed CTCF *in vivo* binding to the regulatory regions of selected erythroid genes and how the binding changes upon induction of erythroid differentiation in K562 cells. ENCODE platform (https://genome.ucsc.edu/) was used to identify possible CTCF binding sites to the regulatory regions of the erythroid genes and CTCF binding was confirmed by ChIP assays. Furthermore, we analyzed if our selected CTCF binding sites, together with cohesins, could participate in the formation of long-range interaction using the ENCODE data to find ChIA-PET (Chromatin Interaction PET) clusters.

A CTCF binding site was identified -43 kb upstream *ETS1* gene. The *ETS1* gene was first identified as the cellular precursor of the viral Ets1 oncogene, which induces erythroleukemia in chickens in association with v-Myb. ETS1 belongs to a large family of transcription factors with a crucial role in stem cell biology and tumorigenesis (Garrett-Sinha, 2013). ETS1 has been shown to be involved in the regulation of erythro/megakaryocytic lineage differentiation (Lulli et al., 2006). ETS1 expression must be downregulated during erythroid differentiation (Lulli et al., 2006) as we found by mRNA expression analysis upon induction of differentiation with Ara-C or Imatinib. CTCF binding to *ETS1* gene was confirmed by ChIP assay and, upon differentiation, we found that CTCF occupancy increased. These results could indicate that CTCF regulates negatively ETS1 expression, allowing erythroid cell differentiation to occur. Interestingly, the CTCF site identified is located between *ETS1* and *FLI1* (friend leukemia integration 1) another member of the ETS1 family. In human hematopoietic cell lines, FLI1 expression induced megakaryocyte and inhibits erythroid differentiation (Pereira et al., 1999). ENCODE ChIP-PET data revealed two possible interactions, containing *ETS1* gene, between *ETS1* upstream CTS and two CTCF sites located downstream *ETS1* (see **Figure 4.13**). These results allow us to hypothesize that CTCF could be acting as an insulator between *ETS1* gene and *FLI1* to regulate the expression of both genes.

MYB is a crucial transcription factor in hematopoiesis and erythropoiesis (Wang et al., 2018). *MYB* expression is tightly regulated and its deregulation is oncogenic; aberrant expression of MYB is found in human leukemias and lymphomas. MYB transcription factor has to be downregulated to allow erythropoiesis (Wang et al., 2018). In agreement, we found *MYB* downregulation upon induction of erythroid differentiation with Ara-C or Imatinib. We identify a possible CTCF binding site in the Intron 1 of *MYB* gene and we confirmed it by ChIP. Upon induction of differentiation, CTCF binding increase. Stadhouders et al, recently described CTCF binding to *MYB* intron 1 and reported that CTCF presence is required for high level MYB expression. Silencing CTCF results in a significant reduction of MYB transcription (Stadhouders et al., 2012) in agreement with our transcriptomic data. Moreover, ChIP-Seq and 3C-Seq studies show that the MYB-Hbs1l intergenic region harbors important regulatory elements that control *MYB* expression and these elements can bind with CTCF or with the CEN (GATA1, LDB1, TAL1 and KLF1 complex). An erythroid-specific pattern of interactions between a LDB1 complex binding site located -36 kb and -81 kb upstream *MYB* promoter and the CTCF binding site in intron 1 was also found (Stadhouders et al., 2012). Our ChIA-PET analysis showed a possible interaction between *MYB* CTCF binding site and a CTCF site located around upstream *MYB* gene which is consistent with the -36 kb site described by Stadhouders et al.

GATA factors are important regulators of erythropoiesis. GATA2 regulates proliferation and maintenance of hematopoietic stem cells and early progenitor cells. During erythroid differentiation its expression is repressed by GATA1 which is necessary for survival and terminal differentiation of erythroid progenitors (Moriguchi and Yamamoto, 2014). *GATA1* and *GATA2* expression is regulated by multiple transcription factors, including their own products (Kaneko et al., 2010). We analyzed mRNA expression upon erythroid differentiation and we found GATA2 downregulation. Different CTCF binding sites were located -29 kb upstream and +21, +33, and +50 kb downstream of the GATA1 gene locus (Moriguchi et al., 2015) and *GATA2* is transactivated by the binding of GATA2 itself to multiple autoregulatory GATA sites located at -77, -3.9, -2.8, and -1.8 kb and the 4th intronic +9.5 kb (Moriguchi and Yamamoto, 2014). The -2.8 and -1.8

kb sites were previously described (Snow et al., 2011). The -2.8 kb site confers maximal GATA2 expression in the undifferentiated stage while the -1.8 kb site maintains GATA2 repression in differentiate stages (Snow et al., 2011). In this study, we identified a CTCF binding site around -5 kb upstream *GATA2* gene and we confirmed CTCF binding by ChIP assay. Upon induction of erythroid differentiation with Ara-C we observed an increase of CTCF occupancy. These results could indicate that CTCF is regulating negatively *GATA2* expression upon differentiation. Moreover, ChIA-PET data revealed that *GATA2* upstream CTCF site participate in the formation of different interactions between three CTCF sites located downstream *GATA2*.

Another erythroid transcription factor whose expression has to be downregulated in order to allow erythroid differentiation is HEY1. HEY1 expression in primary hematopoietic progenitors inhibited erythroid differentiation (Elagib et al., 2004). We found a CTCF binding site in the exon 5 and we confirmed CTCF binding. ChIP analysis upon induction of differentiation with Ara-C reveals increased binding of CTCF to the CTS. ChIA-PET data shown a possible interaction between *HEY1* exon 5 and an upstream CTCF site. These results together could indicate a negative regulatory function of CTCF by the formation of a loop with *HEY1* gene.

LMO2 transcription factor also plays an important role in erythropoiesis. LMO2 is a non DNA-binding component of the core erythroid network which controls the erythroid lineage via activation of erythroid-specific genes (Sincennes et al., 2016). LMO2 levels has to be upregulated during erythroid cell differentiation as we confirmed by RT-qPCR. Our results also revealed that upon CTCF downregulation LMO2 protein levels were reduced, indicating a possible role of CTCF in LMO2 regulation. According to ENCODE data, we identified a CTCF binding site +34 kb downstream *LMO2* TSS. We confirmed CTCF binding by ChIP assay and upon induction of erythroid differentiation with Ara-C a slightly increased in the binding was observed. ChIA-PET data shown that our CTCF site of interest could be interacting with different regions upstream *LMO2* gene and forming loops which include *LMO2*. LMO2 expression is regulated by different upstream and downstream distal regulatory regions and they also identified

several CTCF/RAD21 bound regions throughout the LMO2 upstream region (Bhattacharya et al., 2012). Furthermore, it was described that silent genes are protected by insulated neighborhoods from active enhancers located outside the neighborhood, as happen with LMO2 which are located within a CTCF-CTCF loop (D Hnisz et al., 2016). These results could indicate that CTCF is forming a loop which allows LMO2 silencing.

KLF1 is also crucial for the induction of erythroid differentiation and for the activation of β-globin expression (Gnanapragasam and Bieker, 2017). KLF1 directly or indirectly regulates most genes involved in the terminal stages of erythropoiesis (Gnanapragasam and Bieker, 2017). KLF1 expression is upregulated upon induction of differentiation as we observed by RT-qPCR. A CTCF binding site at Exon 2 was found and CTCF binding was confirmed by ChIP. Upon induction of differentiation with Ara-C, CTCF binding to Exon 2 of *KLF1* increases which suggest that CTCF is involved in the positive regulation of KLF1 expression. ENCODE CTCF ChIA-PET data for K562 cells shown an interaction among our CTCF site at exon 2 of *KLF1* and a CTCF site upstream *KLF1* which included *GCDH* gene. These results could suggest that CTCF enhances *KLF1* transcription during erythroid differentiation, since the increase in occupancy of CTCF results in increased expression of KLF1. Moreover, CTCF binding to *KLF1* exon 2 could be regulating the *GCDH* gene. Despite there is no information in the literature about *KLF1* regulation by CTCF, it was recently described that KLF1, together with GATA1, participate in the generation of active chromatin structure at CTCF binding sites in the β-globin gene, facilitating the binding of CTCF to them and activating β-globin gene transcription (Kang et al., 2017). These could indicate that CTCF binding to *KLF1* could be important for the upregulation of KLF1 expression and indirectly for the β-globin gene expression.

Another erythroid transcription factor which is also involved in the regulation of β-globin expression is NFE2L2. NFE2L2 participates in the defense mechanism against oxidative stress of red blood cells (Andrews, 1998). ENCODE analysis revealed two CTCF binding sites in the Intron 1 of *NFE2L2* gene. We confirmed CTCF binding to the one located at +10 kb downstream TSS and upon

induction of erythroid differentiation with Ara-C the binding changes indicating a regulatory function of CTCF. Up to now, not much information is available on how NFE2L2 is regulated at the transcriptional level. ENCODE CTCF ChIA-PET data shown that our CTS of interest could be interacting with a CTCF site downstream *NFE2L2* gene and also with the other CTCF site located in the Intron 1. We can suggest that CTCF allows the interaction of enhancer elements with *NFE2L2* gene.

The last analyzed erythroid gene was TCF3 which is essential for terminal erythroid differentiation and hemoglobin production. TCF3 also forms part of the core erythroid network (Tsiftsoglou et al., 2009). A CTCF binding site was found around -23 kb upstream *TCF3* gene and CTCF binding was confirmed by ChIP assays. Moreover, upon induction of erythroid differentiation CTCF occupancy changes. Compared with the few information available about the regulation of TCF3 in erythropoiesis, much more is known about its role in B-cells. For example, it was described that CTCF together with TCF3 participate in B-cell development (Ebert et al., 2011). ENCODE ChIA-PET data shown that the analyzed CTCF site could form several interactions with other CTCF sites located upstream or downstream *TCF3* gene. These results can suggest that CTCF could be forming different long range interactions important for the regulation of TCF3 and also for other genes which are inside the interaction. Moreover, our CTCF binding site can be acting as an insulator element.

To summarize, CTCF binds to different regulatory regions of a number of erythroid transcription factors. Moreover, CTCF binding participates in the formation of long range interactions that could be important for the regulation of the expression of erythroid genes. Upon induction of erythroid differentiation with Ara-C, CTCF binding changes. These changes in the binding of CTCF are independently of the changes in the expression levels of these genes upon erythroid differentiation. Similar results were found by Ouboussad et al when they analyzed CTCF binding to different myeloid transcription factors (Ouboussad et al., 2013). They observed that CTCF enrichment changes during macrophage differentiation but they cannot correlate it with the changes in myeloid gene expression. These results could be related with the dual role of CTCF as a

transcriptional activator or repressor. This lack of correlation between gene expression and CTCF occupancy could be explained by the fact that CTCF function is modulated by neighboring DNA binding factors (Weth and Renkawitz, 2011) or by different post-translational modifications which affects CTCF function without changing DNA binding (Klenova et al., 2001; Torrano et al., 2006; Yu et al., 2004).

5.1.3. MYC regulation by CTCF

MYC can be regulated at different levels such as promoters, enhancers, transcription factors and chromatin state. CTCF was first described as a protein which interacts with chicken *MYC* promoter (Lobanenkov et al., 1990). Several studies reported that CTCF can bind to MYC regulatory elements and regulate MYC expression at different levels. Firstly, it was described that CTCF regulates negatively MYC expression by the binding to its promoter (Filippova et al., 1996). However, in the last years it was also described a positive regulation of MYC by CTCF (Xiang et al., 2014). Therefore, results about *MYC* regulation by CTCF are controversial. Analysis of the ENCODE data identifies six possible CTCF binding sites to *MYC* regulatory regions. Some of them were previously described in different cellular models. In this work, we analyze MYC regulation by CTCF in the context of erythroid differentiation.

ENCODE data in K562 cells revealed two possible CTCF binding sites located upstream MYC gene, one located at -515 kb and other at -335 kb. Both sites were previously described in colorectal cancer. Xiang et al found that CCAT1-L, a colorectal cancer specific long non-coding RNA, is transcribed from a locus -515 kb upstream of MYC and participates in MYC regulation and in the formation of long-range chromatin interactions. Their studies revealed the formation of an interaction between site -515 and *MYC* promoter and also between site -335 and -515 and between site -335 and *MYC* promoter. In addition, they observed specific enrichment of CTCF at sites -515, -335 and *MYC* promoter and CTCF knockdown disrupts these loops and reduces MYC expression (Xiang et al., 2014). The -335 site was previously described by Pomerantz et al. They showed a long-range physical interaction between *MYC*

promoter and the rs6983267 SNP region, which is located -335 kb upstream *MYC*, in colorectal cancer cell lines (Pomerantz et al., 2009). They suggested that this region is part of a cis-regulatory enhancer element for *MYC* gene and promotes MYC expression. Similar results were also obtained by Tuupanen et al (Tuupanen et al., 2009). Our results show that CTCF binds to the -515 kb and to the -335 kb regions upstream MYC in K562 cells. This interaction has not been previously described in hematopoietic cells. We could suggest that CTCF participate in the formation of loops between MYC and both sites in our cellular model, however, ENCODE ChIA-PET data in K562 cells do not revealed a possible interaction between these sites and *MYC* promoter.

We also confirmed CTCF binding at two additional sites located -10 kb and -2 kb (named Site N) upstream *MYC* gene. Although there is not relevant information about the site -10 kb, the site N has been thoroughly investigated. Gombert et al described the *MYC* insulator element (MINE) which is located in a conserved region around -2 kb upstream *MYC* P2 promoter at the intersection of transcriptionally active and inactive chromatin (Gombert et al., 2003). They observed that MINE provides two functional activities, enhancer-blocking and barrier activities. In addition, they confirmed that CTCF constitutively binds to the MINE element and *MYC* promoter region (Gombert et al., 2003). These results allows us to suggest that in our cellular model CTCF acts as an insulator element by the binding to MYC site N. Recently, Schuijers et al identified a high number or interactions between a conserved CTCF binding site (site N) and diverse super-enhancers within a +2.8 Mb MYC TAD (topologically associating domain). They defined this site as a CTCF dependent enhancer docking site necessary for high levels of MYC expression (Schuijers et al., 2018).

MYC promoter region also harbors CTCF binding sites. We selected one located in the exon 1 which contains MYC P1 and P2 promoters (named Site A/B) and one site located in the intron 1 (named Site W). CTCF binding to both sites was confirmed by ChIP assays. Site A/B was previously described by Filippova et al. They found a constitutive CTCF binding site A located close to the MYC P2 promoter and a CTCF binding site B close to MYC P1 promoter (Filippova et al., 1996). Mutations in P2 promoter CTCF binding site resulted in increased gene

activity and also CTCF suppressed *MYC* promoter activity which suggested that CTCF is a repressor of MYC expression (Filippova et al., 1996). However, Gombert et al revealed that CTCF is required for normal MYC expression and deletion of sites N and A results in reduced MYC expression which is inconsistent with the role of CTCF as a MYC repressor (Gombert and Krumm, 2009).

Finally, ENCODE ChIA-PET data in K562 cells revealed two possible long range interactions between different CTCF binding sites. The first one are formed between the site -10 kb and a CTCF binding site located around +928 kb downstream. The second interaction are between the *MYC* promoter and a CTCF binding site located around +1.9 Mb downstream. These second interaction could be related with the one described by Hyle et al. In their studies, they described an interaction between *MYC* promoter and a distal enhancer cluster located around +1.8 Mb downstream *MYC* (Hyle et al., 2019).

Our results confirm that CTCF binds to different regulatory regions of *MYC* gene allowing MYC expression in K562 cells. Then, we analyzed the binding upon induction of erythroid differentiation with Ara-C or Imatinib. We observed that CTCF binding increased with both treatments and upon induction of erythroid differentiation, MYC expression is downregulated. These results suggested that CTCF binding could repress MYC expression during erythroid differentiation.

In summary, analyzing different CTCF-binding sites to the regulatory regions of *MYC* gene, we confirm the ability of CTCF to bind to regions near transcription start sites, exons, introns and in intergenic regions and also the essential function of CTCF in the orchestration of long range chromatin interactions (Phillips and Corces, 2009). These results together indicate that CTCF may mediate transcriptional activation, suppression and insulation through its ability to form chromatin loops and regulate *MYC* expression. We can conclude that transcriptional regulation of *MYC* gene depends of long-distance CTCF dependent enhancer-promoter interactions.

Taken together these results, a proposed model for CTCF binding to erythroid transcription factor genes and *MYC* regulatory regions is shown in **Figure 5.2**.

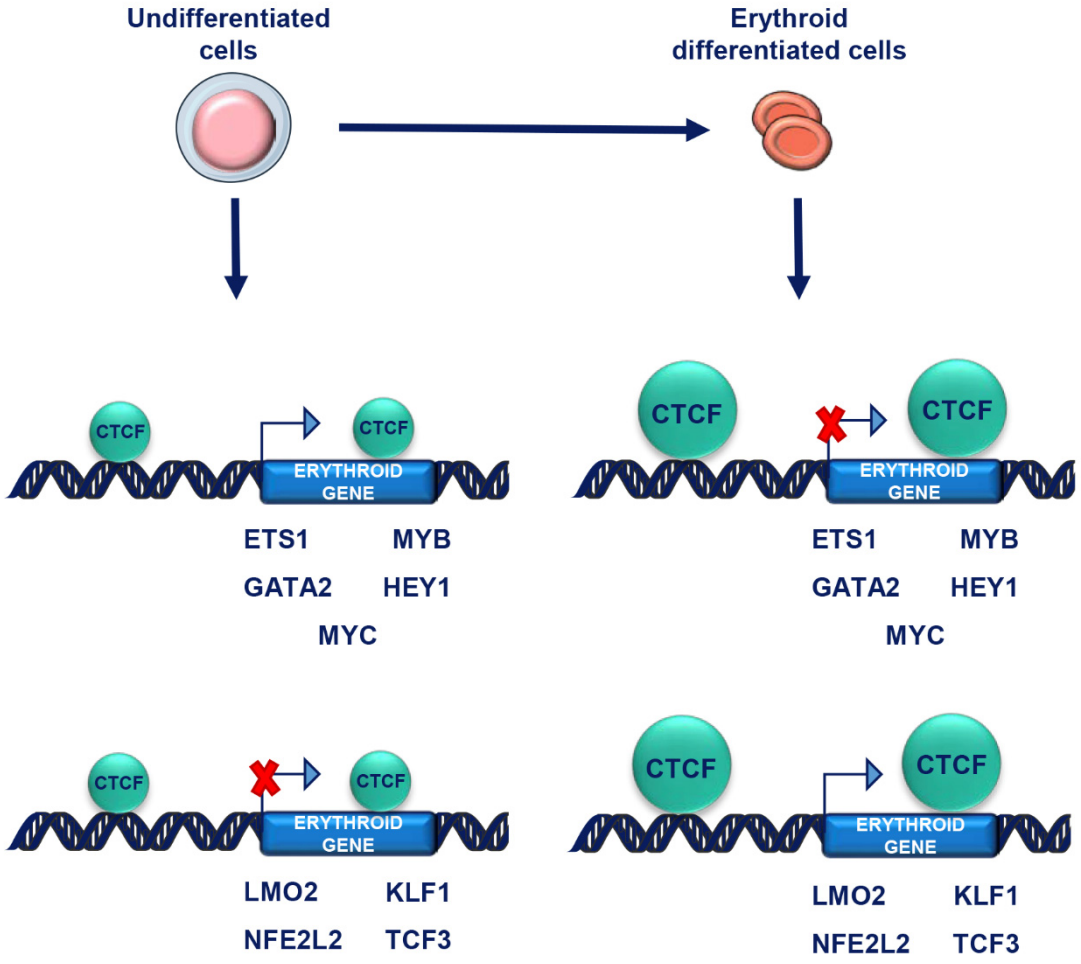

Figure 5.2. Proposed model for CTCF binding to erythroid transcription factors genes and MYC regulatory regions. *CTCF binds to the regulatory regions of different erythroid transcription factor genes and MYC gene in undifferentiated cells. Genes which inhibit erythroid cell differentiation as ETS1, MYB, GATA2 and HEY1 are expressed while genes which induce erythropoiesis such as LMO2, KLF1, NFE2L2 and TCF3 are inhibited. MYC is also expressed in an undifferentiated state. Upon induction of erythroid cell differentiation, CTCF binding increases and ETS1, MYB, GATA2 HEY1 and MYC expression is downregulated, while LMO2, KLF1, NFE2L2 and TCF3 expression is induced.*

5.2. Romidepsin and JQ1 effect on aggressive B-cell lymphoma

Epigenetic modifications are potentially reversible which make them important therapeutic targets. Histone deacetylases and BET bromodomains are related with epigenetic regulation of gene expression via histone acetylation. HDAC erases acetylation from histones while BET proteins recognized acetylated residues on histones and regulates gene transcription. Treatments combining HDAC inhibitors with BET inhibitors have shown promising results in multiple cancer types (Borbely et al., 2015; Enssle et al., 2018; Hölscher et al., 2018). Romidepsin is a histone deacetylase inhibitor that inhibits HDAC class I and it was approved by the FDA for the treatment of some T-cell lymphomas (Smolewski and Robak, 2017). On the other hand, JQ1 is a potent BET bromodomain inhibitor that is able to repress the expression of some genes such as *MYC* (Delmore et al., 2011). MYC deregulation is prevalent in lymphomas and is associated to a worse prognosis in lymphomas derived from the germinal center (Nguyen et al., 2017).

We have previously demonstrated that romidepsin treatment induces apoptosis, cell cycle arrest and plasma cell differentiation in lymphoma B-cells (Cortiguera, MG and Garcia-Gaipo, L submitted, see annex). In the second part of this work we investigate the effects of a combination treatment with romidepsin and JQ1 in the treatment of B-lymphoma cells.

5.2.1. Romidepsin and JQ1 treatment induces apoptosis and cell cycle arrest.

In this study we observed that romidepsin or JQ1, either alone or in combination, can inhibit cell viability and proliferation in different lymphoma B-cells. In general, the combination of romidepsin with JQ1 was more efficient in inhibiting cell proliferation than treatments alone. Similar results were also observed in other cancer types (Hölscher et al., 2018; Liu et al., 2019).

Our results showed that romidepsin and JQ1 acted synergistically to reduce cell viability in lymphoma B-cells. That reduction was accompanied by strong induction of apoptosis observed by the high increase in the percentage of annexin-V positive cells and PARP protein cleavage in Ramos, Raji and Toledo cells. As we expected from our previous results, romidepsin alone induced significantly apoptosis in Ramos and Toledo cells but not in Raji cells (Cortiguera, MG and Garcia-Gaipo, L; unpublished data). These results are also in agreement with studies showing that romidepsin induces apoptosis in some Burkitt lymphoma cells but not in others (Ierano et al., 2013). In contrast, JQ1 treatment alone did not induce apoptosis in any cell line analyzed but only proliferation arrest at the concentrations used here. Similar JQ1 effects on apoptosis have been reported in urothelial carcinoma and rhabdomyosarcoma (Enssle et al., 2018; Hölscher et al., 2018).

Induction of apoptosis is tightly controlled by different pro- and anti-apoptotic proteins of the BCL2 family (Czabotar et al., 2014). We observed a reduction in the levels of the anti-apoptotic protein BCL-xL, which is in agreement with apoptosis induction. The pro-apoptotic effects of romidepsin treatment can be strongly increased in combination therapy with JQ1. These results are consistent with recent studies showing that romidepsin and JQ1 in combination therapy induces cell death in different cancer types such us CTCL, testicular cancer and urothelial carcinoma (Hölscher et al., 2018; Jostes et al., 2017; Zhao et al., 2019). Moreover, treatments combining different HDAC inhibitors and BET inhibitors also induce apoptosis in rhabdomyosarcoma or gallbladder cancer (Enssle et al., 2018; Liu et al., 2019).

Interestingly, our results showed a strong increased in phosphorylated H2AX histone (γH2AX, a marker of DNA damage repair) upon treatment with romidepsin and JQ1 in all the analyzed cell lines. HDAC inhibitors cause hyperacetylation of histones while BET inhibitors block the interaction of acetylated histones with BET proteins. When histones are hyperacetylated a more open chromatin state takes place which makes DNA more susceptible to damage (Georgoulis et al., 2017). Previous studies have shown that HDAC inhibitors induced DNA damage and apoptosis (Frew et al., 2009; Y. Zhang et al.,

2004; Zhang et al., 2006). So this could explain our results. Indeed, we have also observed an increased in γH2AX protein levels with romidepsin treatment alone.

B-cells are highly proliferating cells that must stop proliferation in order to differentiate into plasma cells (Basso and Dalla-Favera, 2015). As we have observed a reduction on cell proliferation, we also investigated the effect of romidepsin and JQ1 treatment on the cell cycle. Flow cytometry analysis showed that the combination of treatments induced a higher Sub G_0/G_1 fraction than either drug on its own in lymphoma B-cells. These results were in agreement with the induction of apoptosis. Cell cycle distribution showed some accumulation of cells in G_0/G_1 phase upon treatment with romidepsin and JQ1. This accumulation was accompanied by an increased in p21 protein levels in Ramos and Toledo cells and in p27 levels in Raji cells. At longer times, the synergistic effect between romidepsine and JQ1 was not evident presumably due to the high proportion of apoptotic cells. Interestingly, a recent study also described cell cycle arrest in G_0/G_1 phase upon treatment with JQ1 and the HDAC inhibitor SAHA (Zhao et al., 2019). Cell cycle arrest in G_0/G_1 phase was observed with JQ1 treatment alone (Enssle et al., 2018; Fiskus et al., 2014; Jostes et al., 2017; Shao et al., 2014) or with romidepsin treatment (Cortiguera, MG et al; submitted, see annex).

JQ1 was described as a compound that has potent antiproliferative effects via downregulation of MYC expression in hematologic and non-hematologic malignancies (Delmore et al., 2011; Lovén et al., 2013). In this work, downregulation in MYC protein levels was observed in Ramos, Raji and Toledo cell lines. Combination treatment with romidepsin and JQ1 synergistically reduced MYC expression in all lymphoma B-cell lines and symergisticalluy indiced proliferation arrest. It was previously reported a synergistic activity of JQ1 and romidepsin associated with highly reduction in MYC protein levels in urothelial carcinoma cells (Hölscher et al., 2018).

5.2.2. Romidepsin and JQ1 treatment reduces BCL6 expression and induces plasma cell differentiation.

BCL6 is the master regulator of germinal center reaction by inhibiting the expression if genes involved in apoptosis, cell cycle and plasma cell differentiation (Shaffer et al., 2000). BCL6 is expressed in Burkitt lymphoma and some DLBCL (Basso and Dalla-Favera, 2015). In this study, we analyzed the effect of romidepsin and JQ1 treatment on BCL6 expression. In BCL6 expressing cell lines (Ramos, Raji and DG75) we observed a reduction on BCL6 expression upon romidepsin treatment, as we expected from previous results of our group that demonstrated that romidepsin treatment reduced BCL6 expression in B-cell lymphoma cell lines (Cortiguera, MG et al; submitted, see annex). JQ1 treatment alone also reduced BCL6 expression. A recent study showed that BCL6 expression was downregulated following treatment with JQ1 in Double/Triple-Hit lymphomas (Li et al., 2019). They found that BET inhibition directly regulated BCL6 transcription via decreasing BRD4 binding to the promoter region of *BCL6* (Li et al., 2019). It was also described a decrease of BCL6 expression upon JQ1 treatment in mouse B-cells (F. Gao et al., 2015). Combination treatment with romidepsin and JQ1 inhibits BCL6 expression more profoundly than treatments alone.

One important function of BCL6 is to inhibit the expression of plasma cell transcription factors to maintain the germinal center phenotype and prevent cell differentiation (Basso and Dalla-Favera, 2010; Shaffer et al., 2004a). BCL6 is a transcriptional repressor of plasma cell differentiation genes such as *PRDM1* (BLIMP1 protein) (Basso and Dalla-Favera, 2010). Our results showed an increase in BLIMP1 protein levels upon romidepsin and JQ1 treatment in Ramos (BCL6 expressing cell line) and Toledo (non-BCL6 expressing cell line). These results together with the downregulation of BCL6 expression in Ramos cells indicated that combination treatment may induce plasma cell differentiation. JQ1 treatment alone did not increase BLIMP1 levels although BCL6 expression was downregulated. Consistently, a recent study described that inhibition if BRD4 with

JQ1 led to the inhibition of germinal center B-cell differentiation via downregulation of BCL6 expression (F. Gao et al., 2015).

Taken together our results, we proposed a model for romidepsin and JQ1 effects on B-cell lymphoma cells, shown in **Figure 5.3**.

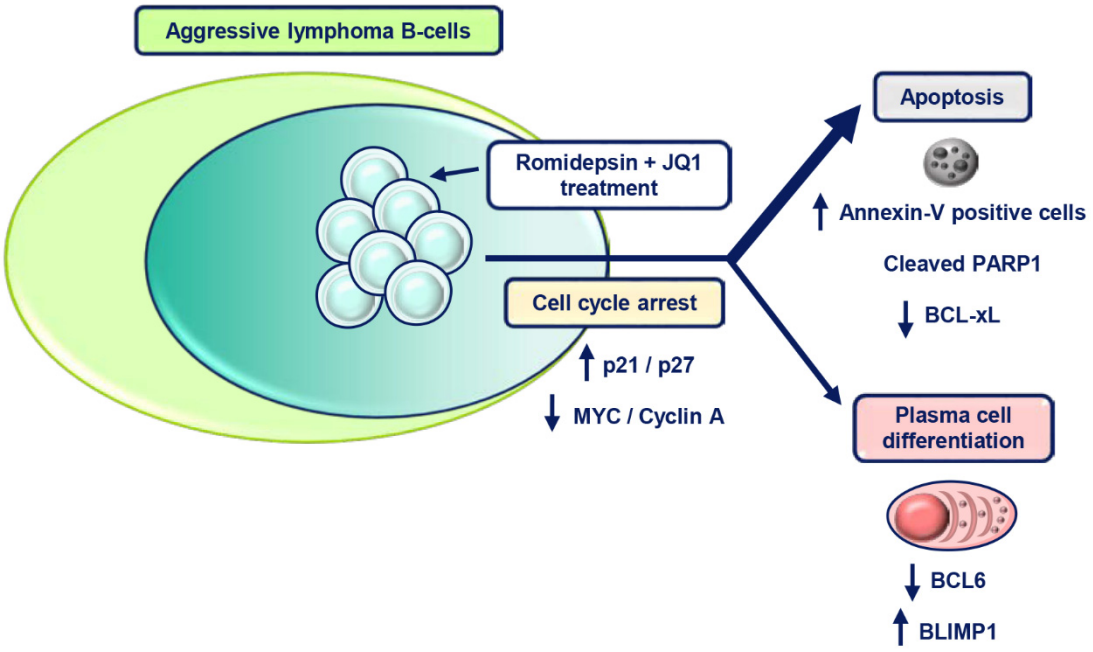

Figure 5.3. Proposed model for romidepsin and JQ1 effects on lymphoma B-cells. *Romidepsin and JQ1 treatment induces cell cycle arrest accompanied with increased levels of p21 or p27 and MYC and cyclin A downregulation. A huge number of cells die by apoptosis as shown by the positive annexin-V staining, cleavage of PARP protein and a decrease in BCL-xL levels. Finally, downregulation of BCL6 together with increase on PRDM1/BLIMP1 indicate plasma cell differentiation.*

In summary, we conclude that combination treatment with romidepsin and JQ1 synergistically induces apoptosis, cell cycle arrest and plasma cell differentiation by inhibiting BCL6 expression in B-cell lymphoma cells. Moreover, combination treatment is more effective than each treatment alone which suggests that JQ1 potentiates romidepsin effects. Our results indicate that the romidepsin and JQ1 combination could be effective in aggressive B-cells lymphoma treatment.

CONCLUSIONS

6. CONCLUSIONS

Erythroid cell differentiation: regulation by the CTCF factor

1. CTCF downregulation inhibits erythroid cell differentiation induced by Ara-C and Imatinib in K562 cells.
2. CTCF downregulation inhibits erythroid cell differentiation induced by erythropoietin in primary $CD34^+$ cells.
3. CTCF binds to the regulatory regions of important erythroid transcription factor genes and the binding increases upon induction of erythroid differentiation.
4. CTCF binds to *MYC* gene regulatory regions and the binding increases upon induction of erythroid differentiation.
5. CTCF binding participates in the formation of long-range interactions.
6. CTCF binding to transcription factor genes is correlated with their functions in the modulation of erythroid differentiation.
7. We propose that CTCF plays an essential role in erythroid differentiation through the direct regulation of crucial transcription factors.

B-cell differentiation and lymphoma: regulation by epigenetic drugs

8. Treatment with romidepsin and JQ1 reduces cell metabolic activity and cell proliferation in B-cell lymphoma cell lines.
9. Romidepsin and JQ1 combined treatment strongly induces apoptosis in lymphoma B-cells.
10. Treatment with romidepsin and JQ1 induces cell cycle arrest associated with increased p21 or p27 protein levels and MYC downregulation.
11. Romidepsin and JQ1 combination treatment induces plasma cell differentiation by inhibiting BCL6 expression in B-cell lymphoma cells.
12. Romidepsin and JQ1 have synergistic effects, showing a potential role for the treatment of aggressive B-cell lymphomas.

REFERENCES

7. REFERENCES

Acosta JC, Ferrandiz N, Bretones G, Torrano V, Blanco R, Richard C, O'Connell B, Sedivy J, Delgado MD, Leon J. 2008. Myc inhibits p27-induced erythroid differentiation of leukemia cells by repressing erythroid master genes without reversing p27-mediated cell cycle arrest. *Mol Cell Biol* **28**:7286–7295.

Ahuja N, Sharma AR, Baylin SB. 2016. Epigenetic Therapeutics: A New Weapon in the War Against Cancer. *Annu Rev Med* **67**:73–89. doi:10.1146/annurev-med-111314-035900

Albajar M, Gómez-Casares MT, Llorca J, Mauleon I, Vaqué JP, Acosta JC, Bermúdez A, Donato N, Delgado MD, León J. 2011. MYC in Chronic Myeloid Leukemia : Induction of Aberrant DNA Synthesis and Association with Poor Response to Imatinib. *Cancer Genes and Genomics* **9**:564–576. doi:10.1158/1541-7786.MCR-10-0356

Ali MA, El-bab F, Hend A, Matboli M, Tarek M, Reda M, Kamal KM, Nouh M, Ashry AM, El-Bab AF, Mesalam HA, Shafei AE-S, Abdel-Rahman O. 2017. Epigenetic regulation of immune checkpoints : another target for cancer immunotherapy ? *Immunotherapy* **9**:99–108. doi:10.2217/imt-2016-0111

Alizadeh AA, Eisen MB, Davis RE, Ma C, Lossos IS, Rosenwald A, Boldrick JC, Sabet H, Tran T, Yu X, Powell JI, Yang L, Marti GE, Moore T, Hudson Jr. J, Lu L, Lewis DB, Tibshirani R, Sherlock G, Chan WC, Greiner TC, Weisenburger DD, Armitage JO, Warnke R, Levy R, Wilson W, Grever MR, Byrd JC, Botstein D, Brown PO, Staudt LM. 2000. Distinct types of diffuse large B-cell lymphoma identified by gene expression profiling. *Nature* **403**:503–511. doi:10.1038/35000501

Allis CD, Berger SL, Cote J, Dent S, Jenuwien T, Kouzarides T, Pillus L, Reinberg D, Shi Y, Shiekhattar R, Shilatifard A, Workman J, Zhang Y. 2007. New Nomenclature for Chromatin-Modifying Enzymes. *Cell* **131**:633–636.

Alvarez-Dominguez JR, Hu W, Yuan B, Shi J, Park SS, Gromatzky AA, Oudenaarden A Van, Lodish HF. 2014. Global discovery of erythroid long noncoding RNAs reveals novel regulators of red cell maturation. *Blood* **123**:570–581. doi:10.1182/blood-2013-10-530683.The

Anderson MA, Huang D, Roberts A. 2014. Targeting BCL2 for the Treatment of Lymphoid Malignancies. *Semin Hematol* **51**:219–227. doi:10.1053/j.seminhematol.2014.05.008

Andrews NC. 1998. Molecules in focus the NF-E2 transcription factor. *Int J Biochem Cell Biol* **30**:429–432. doi:10.1016/S1357-2725(97)00135-0

Arzate-Mejía RG, Recillas-Targa F, Corces VG. 2018. Developing in 3D: the role of CTCF in cell differentiation. *Development* **145**:dev137729. doi:10.1242/dev.137729

Aulmann S, Bläker H, Penzel R, Rieker RJ, Otto HF, Sinn HP. 2003. CTCF gene mutations in invasive ductal breast cancer. *Breast Cancer Res Treat* **80**:347–352. doi:10.1023/A:1024930404629

Azzouzi I, Schmugge M, Speer O. 2012. MicroRNAs as components of regulatory networks controlling erythropoiesis. *Eur J Haematol* **89**:1–9. doi:10.1111/j.1600-0609.2012.01774.x

Bailey CG, Metierre C, Feng Y, Baidya K, Filippova GN, Loukinov DI, Lobanenkov V V, Semaan C, Rasko JE. 2018. CTCF Expression is Essential for Somatic Cell Viability and Protection Against Cancer. *Int J Mol Sci* **19**. doi:10.3390/ijms19123832

Baniahmad A, Steiner C, Kohne AC, Renkawitz R. 1990. Modular Structure of a Chicken Lysozyme Sirwet : Invohrement of an Unusual Thyroid Hormone Receptor Binding

Site. *Cell* **61**:505–514.

Bannard O, Cyster JG. 2017. Germinal centers: programmed for affinity maturation and antibody diversification. *Curr Opin Immunol* **45**:21–30. doi:10.1016/j.coi.2016.12.004

Bannister AJ, Kouzarides T. 2011. Regulation of chromatin by histone modifications. *Cell Res* **21**:381–395. doi:10.1038/cr.2011.22

Barbarotta L, Hurley K. 2015. Romidepsin for the Treatment of Peripheral T-Cell Lymphoma. *J Adv Pr Oncol* **6**:22–36.

Barminko J, Reinholt B, Baron MH. 2015. Development and differentiation of the erythroid lineage in mammals. *Dev Comp Immunol* **58**:18–29. doi:10.1016/j.dci.2015.12.012

Barski A, Cuddapah S, Cui K, Roh TY, Schones DE, Wang Z, Wei G, Chepelev I, Zhao K. 2007. High-resolution profiling of histone methylations in the human genome. *Cell* **129**:823–837.

Basso K, Dalla-Favera R. 2015. Germinal centres and B cell lymphomagenesis. *Nat Rev Immunol* **15**:172–184. doi:10.1038/nri3814

Basso K, Dalla-Favera R. 2010. BCL6. master regulator of the germinal center reaction and key oncogene in B Cell lymphomagenesis, 1st ed, Advances in Immunology. Elsevier Inc. doi:10.1016/S0065-2776(10)05007-8

Basso K, Saito M, Sumazin P, Margolin AA, Wang K, Lim WK, Kitagawa Y, Schneider C, Alvarez MJ, Califano A, Dalla-Favera R. 2010. Integrated biochemical and computational approach identifies BCL6 direct target genes controlling multiple pathways in normal germinal center B cells. *Blood* **115**:975–984. doi:10.1182/blood-2009-06-227017

Bates SE, Eisch R, Ling A, Rosing D, Turner M, Pittaluga S, Prince HM, Kirschbaum MH, Allen SL, Zain J, Geskin LJ, Joske D, Popplewell L, Cowen EW, Jaffe ES, Nichols J, Kennedy S, Steinberg SM, Liewehr DJ, Showe LC, Steakley C, Wright J, Fojo T, Litman T, Piekarz RL. 2015. Romidepsin in peripheral and cutaneous T-cell lymphoma: mechanistic implications from clinical and correlative data. *Br J Haematol* **170**:96–109. doi:10.1111/bjh.13400

Batlle-Lopez A, Cortiguera MG, Rosa-Garrido M, Blanco R, Del Cerro E, Torrano V, Wagner SD, Delgado MD. 2015. Novel CTCF binding at a site in exon1A of BCL6 is associated with active histone marks and a transcriptionally active locus. *Oncogene* **34**:246–256. doi:10.1038/onc.2013.535

Begley CG, Green AR, Article R. 1999. The SCL Gene : From Case Report to Critical Hematopoietic Regulator. *Blood* **93**:2760–2770.

Bell AC, Felsenfeld G. 2000. Methylation of a CTCF-dependent boundary controls imprinted expression of the Igf2 gene [see comments]. *Nature* **405**:482–485.

Bell AC, West AG, Felsenfeld G. 1999. The Insulator Activity of CTCF The Protein CTCF Is Required for the Enhancer Blocking Activity of Vertebrate Insulators. *Cell* **158**:387–396.

Bereshchenko OR, Gu W, Dalla-Favera R. 2002. Acetylation inactivates the transcriptional repressor BCL6. *Nat Genet* **32**:606–613.

Bergström R, Savary K, Morén A, Guibert S, Heldin CH, Ohlsson R, Moustakas A. 2010. Transforming growth factor β promotes complexes between Smad proteins and the CCCTC-binding factor on the H19 imprinting control region chromatin. *J Biol Chem* **285**:19727–19737. doi:10.1074/jbc.M109.088385

Besson A, Dowdy SF, Roberts JM. 2008. CDK Inhibitors: Cell Cycle Regulators and Beyond. *Dev Cell* **14**:159–169. doi:10.1016/j.devcel.2008.01.013

Bhattacharya A, Chen CY, Ho S, Mitchell JA. 2012. Upstream distal regulatory elements contact the Lmo2 promoter in mouse erythroid cells. *PLoS One* **7**:e52880. doi:10.1371/journal.pone.0052880

Bianchi E, Zini R, Salati S, Tenedini E, Norfo R, Tagliafico E, Manfredini R, Ferrari S. 2010. c-myb supports erythropoiesis through the transactivation of KLF1 and LMO2 expression. *Blood* **116**:99–111. doi:10.1182/blood-2009-08-238311

Bianchi N, Ongaro F, Chiarabelli C, Gualandi L, Mischiati C, Bergamini P, Gambari R. 2000. Induction of erythroid differentiation of human K562 cells by cisplatin analogs. *Biochem Pharmacol* **60**:31–40. doi:10.1016/S0006-2952(00)00297-5

Bickmore WA. 2013. The Spatial Organization of the Human Genome. *Annu Rev Genomics Hum Genet* **14**:67–84. doi:10.1146/annurev-genom-091212-153515

Bollig N, Brustle A, Kellner K, Ackermann W, Abass E, Raifer H, Camara B, Brendel C, Giel G, Bothur E, Huber M, Paul C, Elli A, Kroczek RA, Nurieva R, Dong C, Jacob R, Mak TW, Lohoff M. 2012. Transcription factor IRF4 determines germinal center formation through follicular T-helper cell differentiation. *Proc Natl Acad Sci* **109**:8664–8669. doi:10.1073/pnas.1205834109

Borbely G, Haldosen LA, Dahlman-Wright K, Zhao C. 2015. Induction of USP17 by combining BET and HDAC inhibitors in breast cancer cells. *Oncotarget* **6**:33623–33635. doi:10.18632/oncotarget.5601

Bouilloux F, Cohet N, Guyot B, Vainchenker W. 2008. EKLF restricts megakaryocytic differentiation at the benefit of erythrocytic differentiation. *Blood* **112**:576–584. doi:10.1182/blood-2007-07-098996.The

Braikia F-Z, Oudinet C, Haddad D, Oruc Z, Orlando D, Dauba A, Le Bert M, Khamlichi AA. 2017. Inducible CTCF insulator delays the IgH 3′ regulatory region-mediated activation of germline promoters and alters class switching. *Proc Natl Acad Sci* **114**:6092–6097. doi:10.1073/pnas.1701631114

Bresnick EH, Katsumura KR, Lee HY, Johnson KD, Perkins AS. 2012. Master regulatory GATA transcription factors: Mechanistic principles and emerging links to hematologic malignancies. *Nucleic Acids Res* **40**:5819–5831. doi:10.1093/nar/gks281

Burcin M, Arnold R, Lutz M, Kaiser B, Runge D, Lottspeich F, Filippova GN, Lobanenkov V V, Renkawitz R. 1997. Negative protein 1, which is required for function of the chicken lysozyme gene silencer in conjunction with hormone receptors, is identical to the multivalent zinc finger repressor CTCF. *Mol Cell Biol* **17**:1281–1288. doi:10.1128/mcb.17.3.1281

Bushey AM, Ramos E, Corces VG. 2009. Three subclasses of a Drosophila insulator show distinct and cell type-specific genomic distributions. *Genes Dev* **23**:1338–1350. doi:gad.1798209 [pii] 10.1101/gad.1798209

Calado DP, Sasaki Y, Godinho SA, Pellerin A, Sleckman BP, Alborán IM De, Janz M, Rodig S, Rajewsky K. 2014. MYC is essential for the formation and maintenance of germinal centers. *Nat Immunol* **13**:1092–1100. doi:10.1038/ni.2418.MYC

Canela A, Maman Y, Jung S, Wong N, Callen E, Day A, Kieffer-Kwon KR, Pekowska A, Zhang H, Rao SSP, Huang SC, Mckinnon PJ, Aplan PD, Pommier Y, Aiden EL, Casellas R, Nussenzweig A. 2017. Genome Organization Drives Chromosome Fragility. *Cell* **170**:507–521. doi:10.1016/j.cell.2017.06.034

Cañelles M, Delgado MD, Hyland KM, Lerga A, Richard C, Dang C V., León J. 1997.

Max and inhibitory c-Myc mutants induce erythroid differentiation and resistance to apoptosis in human myeloid leukemia cells. *Oncogene* **14**:1315–1327. doi:10.1038/sj.onc.1200948

Cantor AB, Orkin SH. 2002. Transcriptional regulation of erythropoiesis: An affair involving multiple partners. *Oncogene* **21**:3368–3376. doi:10.1038/sj.onc.1205326

Cardenas MG, Oswald E, Yu W, Xue F, MacKerell Jr. AD, Melnick AM. 2017. The Expanding Role of the BCL6 Oncoprotein as a Cancer Therapeutic Target. *Clin Cancer Res* **23**:885–893. doi:10.1158/1078-0432.CCR-16-2071

Cattoretti G, Chang CC, Cechova K, Zhang J, Ye BH, Falini B, Louie DC, Offit K, Chaganti RS, Dalla-Favera R. 1995. BCL-6 protein is expressed in germinal-center B cells. *Blood* **86**:45–53.

Celik H, Kramer A, Challen GA. 2016. DNA methylation in normal and malignant hematopoiesis. *Int J Hematol* **103**:617–626. doi:10.1007/s12185-016-1957-7

Chambers J, Rabbitts TH. 2015. LMO2 at 25 years: A paradigm of chromosomal translocation proteins. *Open Biol* **5**. doi:10.1098/rsob.150062

Chang C-C, Ye BH, Chaganti RSK, Dalla-Favera R. 1996. BCL-6, a POZ/zinc-finger protein, is a sequence-specific transcriptional repressor. *Proc Natl Acad Sci* **93**:6947–6952. doi:10.1073/pnas.93.14.6947

Chao W, Huynh KD, Spencer RJ, Davidow LS, Lee JT. 2002. CTCF, a candidate trans-acting factor for X-inactivation choice. *Science (80-)* **295**:345–347.

Chen D, Lei EP. 2019. Function and regulation of chromatin insulators in dynamic genome organization. *Curr Opin Cell Biol* **58**:61–68. doi:10.1016/j.ceb.2019.02.001

Chen H, Tian Y, Shu W, Bo X, Wang S. 2012. Comprehensive identification and annotation of cell type-specific and ubiquitous CTCF-binding sites in the human genome. *PLoS One* **7**. doi:10.1371/journal.pone.0041374

Chen K, Liu J, Heck S, Chasis JA, An X, Mohandas N. 2009. Resolving the distinct stages in erythroid differentiation based on dynamic changes in membrane protein expression during erythropoiesis. *Proc Natl Acad Sci* **106**:17413–17418. doi:10.1073/pnas.0909296106

Cheng X, Blumenthal RM. 2008. Mammalian DNA Methyltransferases: A Structural Perspective. *Structure* **16**:341–350. doi:10.1016/j.str.2008.01.004

Chernukhin I, Shamsuddin S, Kang SY, Bergstrom R, Kwon YW, Yu W, Whitehead J, Mukhopadhyay R, Docquier F, Farrar D, Morrison I, Vigneron M, Wu SY, Chiang CM, Loukinov D, Lobanenkov V, Ohlsson R, Klenova E. 2007. CTCF interacts with and recruits the largest subunit of RNA polymerase II to CTCF target sites genome-wide. *Mol Cell Biol* **27**:1631–1648.

Chernukhin I V, Shamsuddin S, Robinson AF, Carne AF, Paul A, El-Kady AI, Lobanenkov V V, Klenova EM. 2000. Physical and functional interaction between two pluripotent proteins, the Y-box DNA/RNA-binding factor, YB-1, and the multivalent zinc finger factor, CTCF. *J Biol Chem* **275**:29915–29921.

Chou T-C. 2010. Drug Combination Studies and Their Synergy Quantification Using the Chou-Talalay Method. *Cancer Res* **70**:440–446. doi:10.1158/0008-5472.CAN-09-1947

Chou T-C, Talalay P. 1984. Quantitative analysis of dose-effect relationships: the combined effects of multiple drugs or enzyme inhibitors. *Adv Enzyme Regul* **22**:27–55. doi:10.1016/0065-2571(84)90007-4

Cobaleda C, Jochum W, Busslinger M. 2007. Conversion of mature B cells into T cells

by dedifferentiation to uncommitted progenitors. *Nature* **449**:473–477. doi:10.1038/nature06159

Coiffier B, Thieblemont C, Van Den Neste E, Lepeu G, Plantier I, Castaigne S, Lefort S, Marit G, Macro M, Sebban C, Belhadj K, Bordessoule D, Fermé C, Tilly H. 2010. Long-term outcome of patients in the LNH-98.5 trial, the first randomized study comparing rituximab-CHOP to standard CHOP chemotherapy in DLBCL patients: a study by the Groupe d'Etudes des Lymphomes de l'Adulte. *Blood* **116**:2040–2045. doi:10.1182/blood-2010-03-276246.An

Constantinescu SN, Ghaffari S, Lodish HF. 1999. The erythropoietin receptor: Structure, activation and intracellular signal transduction. *Trends Endocrinol Metab* **10**:18–23. doi:10.1016/S1043-2760(98)00101-5

Coppola JA, Cole MD. 1986. Constitutive c-myc oncogene expression blocks mouse erythroleukaemia cell differentiation but not commitment. *Nature* **320**:760–763. doi:10.1038/320760a0

Cortiguera MG, Batlle-López A, Albajar M, Delgado MD, Leon J. 2015. MYC as therapeutic target in leukemia and lymphoma. *Blood Lymphat Cancer Targets Ther* **5**:75–91.

Cortiguera Ruiz MG. 2017. Epigenetic regulation of BCL6 in aggresive B-cell lymphoma: role of CTCF chromatin regulator and effects of a histone deacetylase inhibitor. *Dr Thesis*.

Crombie JL, Armand P. 2019. Diffuse Large B-Cell Lymphoma and High-Grade B-Cell Lymphoma: Genetic Classification and Its Implications for Prognosis and Treatment. *Hematol Oncol Clin North Am* **33**:575–585. doi:10.1016/j.hoc.2019.03.001

Cuddapah S, Jothi R, Schones DE, Roh TY, Cui K, Zhao K. 2009. Global analysis of the insulator binding protein CTCF in chromatin barrier regions reveals demarcation of active and repressive domains. *Genome Res* **19**:24–32.

Czabotar PE, Lessene G, Strasser A, Adams JM. 2014. Control of apoptosis by the BCL-2 protein family: Implications for physiology and therapy. *Nat Rev Mol Cell Biol*. doi:10.1038/nrm3722

Da Silva Almeida AC, Abate F, Khiabanian H, Martinez-Escala E, Guitart J, Tensen CP, Vermeer MH, Rabadan R, Ferrando A, Palomero T. 2015. The mutational landscape of cutaneous T cell lymphoma and Sézary syndrome. *Nat Genet* **47**:1465–1470. doi:10.1038/ng.3442

De Braekeleer M, Morel F, Le Bris MJ, Herry A, Douet-Guilbert N. 2005. The MLL gene and translocations involving chromosomal band 11q23 in acute leukemia. *Anticancer Res* **25**:1931–1944.

De La Rosa-Velazquez IA, Rincon-Arano H, Benitez-Bribiesca L, Recillas-Targa F. 2007. Epigenetic regulation of the human retinoblastoma tumor suppressor gene promoter by CTCF. *Cancer Res* **67**:2577–2585.

De La Rosa-Velázquez IA, Rincón-Arano H, Benítez-Bribiesca L, Recillas-Targa F. 2007. Epigenetic regulation of the human retinoblastoma tumor suppressor gene promoter by CTCF. *Cancer Res* **67**:2577–2585. doi:10.1158/0008-5472.CAN-06-2024

De Silva NS, Klein U. 2015. Dynamics of B cells in germinal centres. *Nat Rev Immunol* **15**:137–148. doi:10.1038/nri3804

de Wit E, Vos ESM, Holwerda SJB, Valdes-Quezada C, Verstegen MJAM, Teunissen H, Splinter E, Wijchers PJ, Krijger PHL, de Laat W. 2015. CTCF Binding Polarity

Determines Chromatin Looping. *Mol Cell* **60**:676–684. doi:10.1016/j.molcel.2015.09.023

Defossez PA, Kelly KF, Filion GJ, Perez-Torrado R, Magdinier F, Menoni H, Nordgaard CL, Daniel JM, Gilson E. 2005. The human enhancer blocker CTC-binding factor interacts with the transcription factor Kaiso. *J Biol Chem* **280**:43017–43023.

Del Rosario BCDBC, Kriz AJAJ, Rosario A.M. Del, Anselmo A, Fry CJ, White FMFM, Sadreyev RIRI, Lee JTJT, Del Rosario Amanda M, Anselmo A, Frye CJ, White FMFM, Sadreyev RIRI, Lee JTJT. 2019. Exploration of CTCF post-translation modifications uncovers Serine-224 phosphorylation by PLK1 at pericentric regions during the G2/M transition. *Elife* **8**:1–29. doi:10.7554/elife.42341

Delgado MD, Chernukhin I V., Bigas A, Klenova EM, Leon J, León J. 1999. Differential expression and phosphorylation of CTCF, a c-myc transcriptional regulator, during differentiation of human myeloid cells. *FEBS Lett* **444**:5–10. doi:10.1016/S0014-5793(99)00013-7

Delgado MD, Leon J. 2010. Myc roles in hematopoiesis and leukemia. *Genes Cancer* **1**:605–616.

Delgado MD, Lerga A, Canelles M, Gomez-Casares MT, Leon J. 1995. Differential regulation of Max and role of c-Myc during erythroid and myelomonocytic differentiation of K562 cells. *Oncogene* **10**:1659–1665.

Delmore JE, Issa GC, Lemieux ME, Rahl PB, Shi J, Jacobs HM, Kastritis E, Gilpatrick T, Paranal RM, Qi J, Chesi M, Schinzel AC, McKeown MR, Heffernan TP, Vakoc CR, Bergsagel PL, Ghobrial IM, Richardson PG, Young RA, Hahn WC, Anderson KC, Kung AL, Bradner JE, Mitsiades CS. 2011. BET bromodomain inhibition as a therapeutic strategy to target c-Myc. *Cell* **146**:904–917. doi:10.1016/j.cell.2011.08.017

Dimopoulos K, Grønbæk K. 2019. Epigenetic therapy in hematological cancers. *Apmis* **127**:316–328. doi:10.1111/apm.12906

Dimopoulos K, Søgaard Helbo A, Fibiger Munch-Petersen H, Sjö L, Christensen J, Sommer Kristensen L, Asmar F, Hermansen NEU, O'Connel C, Gimsing P, Liang G, Grønbæk K. 2018. Dual inhibition of DNMTs and EZH2 can overcome both intrinsic and acquired resistance of myeloma cells to IMiDs in a cereblon-independent manner. *Mol Oncol* **12**:180–195. doi:10.1002/1878-0261.12157

Dixon JR, Selvaraj S, Yue F, Kim A, Li Y, Shen Y, Hu M, Liu JS, Ren B. 2012. Topological domains in mammalian genomes identified by analysis of chromatin interactions. *Nature* **485**:376–80. doi:10.1038/nature11082

Dmitrovsky E, Kuehl WM, Hollis GF, Kirsch IR, Bender TP, Segal S. 1986. Expression of a transfected human c-myconcogene inhibits differentiation of a mouse erythroleukaemia cell line. *Nature* **322**:748–750. doi:10.1038/322748a0

Docquier F, Kita GX, Farrar D, Jat P, O'Hare M, Chernukhin I, Gretton S, Mandal A, Alldridge L, Klenova E. 2009. Decreased poly(ADP-ribosyl)ation of CTCF, a transcription factor, is associated with breast cancer phenotype and cell proliferation. *Clin Cancer Res* **15**:5762–5771. doi:1078-0432.CCR-09-0329 [pii] 10.1158/1078-0432.CCR-09-0329

Dominguez-Sola D, Victora GD, Ying CY, Phan RT, Saito M, Dalla-Favera R, Nussenzweig MC. 2012. c-MYC is required for germinal center selection and cyclic re- entry. *Nat Immunol* **13**:1083–1091. doi:10.1038/ni.2428.c-MYC

Donohoe ME, Zhang LF, Xu N, Shi Y, Lee JT. 2007. Identification of a Ctcf Cofactor, Yy1, for the X Chromosome Binary Switch. *Mol Cell* **25**:43–56. doi:10.1016/j.molcel.2006.11.017

Dos Santos Ferreira AC, Fernandes RA, Kwee JK, Klumb CE. 2012. Histone deacetylase inhibitor potentiates chemotherapy-induced apoptosis through Bim upregulation in Burkitt's lymphoma cells. *J Cancer Res Clin Oncol* **138**:317–325. doi:10.1007/s00432-011-1093-y

Dulmovits BM, Hom J, Narla A, Mohandas N, Blanc L. 2017. Characterization, regulation, and targeting of erythroid progenitors in normal and disordered human erythropoiesis. *Curr Opin Hematol* **24**:159–166. doi:10.1097/MOH.0000000000000328

Dzierzak E, Philipsen S. 2013. Erythropoiesis: development and differentiation. *Cold Spring Harb Perspect Med* **3**:a011601. doi:10.1101/cshperspect.a011601

Ebert A, McManus S, Tagoh H, Medvedovic J, Salvagiotto G, Novatchkova M, Tamir I, Sommer A, Jaritz M, Busslinger M. 2011. The Distal VH Gene Cluster of the Igh Locus Contains Distinct Regulatory Elements with Pax5 Transcription Factor-Dependent Activity in Pro-B Cells. *Immunity* **34**:175–187. doi:10.1016/j.immuni.2011.02.005

El-Kady A, Klenova E. 2005. Regulation of the transcription factor, CTCF, by phosphorylation with protein kinase CK2. *FEBS Lett* **579**:1424–1434.

Elagib KE, Xiao M, Hussaini IM, Delehanty LL, Palmer LA, Racke FK, Birrer MJ, Shanmugasundaram G, McDevitt MA, Goldfarb AN. 2004. Jun Blockade of Erythropoiesis: Role for Repression of GATA-1 by HERP2. *Mol Cell Biol* **24**:7779–7794. doi:10.1128/mcb.24.17.7779-7794.2004

Engel N, Thorvaldsen JL, Bartolomei MS. 2006. CTCF binding sites promote transcription initiation and prevent DNA methylation on the maternal allele at the imprinted H19/Igf2 locus. *Hum Mol Genet* **15**:2945–2954. doi:10.1093/hmg/ddl237

Enssle JC, Boedicker C, Wanior M, Vogler M, Knapp S, Fulda S. 2018. Co-targeting of BET proteins and HDACs as a novel approach to trigger apoptosis in rhabdomyosarcoma cells. *Cancer Lett* **428**:160–172. doi:10.1016/j.canlet.2018.04.032

Esteller M. 2008. Epigenetics in cancer. *N Engl J Med* **358**:1148–1159. doi:358/11/1148 [pii] 10.1056/NEJMra072067

Fardi M, Solali S, Farshdousti Hagh M. 2018. Epigenetic mechanisms as a new approach in cancer treatment: An updated review. *Genes Dis* **5**:304–311. doi:10.1016/j.gendis.2018.06.003

Farrell CM, West AG, Felsenfeld G. 2002. Conserved CTCF insulator elements flank the mouse and human beta-globin loci. *Mol Cell Biol* **22**:3820–3831.

Filippova GN. 2008. Genetics and epigenetics of the multifunctional protein CTCF. *Curr Top Dev Biol* **80**:337–360.

Filippova GN, Fagerlie S, Klenova EM, Myers C, Dehner Y, Goodwin G, Neiman PE, Collins SJ, Lobanenkov V V. 1996. An exceptionally conserved transcriptional repressor, CTCF, employs different combinations of zinc fingers to bind diverged promoter sequences of avian and mammalian c-myc oncogenes. *Mol Cell Biol* **16**:2802–2813. doi:10.1128/mcb.16.6.2802

Filippova GN, Lindblom A, Meincke LJ, Klenova EM, Neiman PE, Collins SJ, Doggett NA, Lobanenkov V V. 1998. A widely expressed transcription factor with multiple DNA sequence specificity, CTCF, is localized at chromosome segment 16q22.1 Within one of the smallest regions of overlap for common deletions in breast and prostate cancers. *Genes Chromosom Cancer* **22**:26–36. doi:10.1002/(SICI)1098-2264(199805)22:1<26::AID-GCC4>3.0.CO;2-9

Filippova GN, Qi CF, Ulmer JE, Moore JM, Ward MD, Hu YJ, Loukinov DI, Pugacheva EM, Klenova EM, Grundy PE, Feinberg AP, Cleton-Jansen AM, Moerland EW, Cornelisse CJ, Suzuki H, Komiya A, Lindblom A, Dorion-Bonnet F, Neiman PE, Morse HC, Collins SJ, Lobanenkov V V. 2002. Tumor-associated zinc finger mutations in the CTCF transcription factor selectively alter its DNA-binding specificity. *Cancer Res* **62**:48–52.

Fiskus W, Sharma S, Qi J, Valenta JA, Schaub LJ, Shah B, Peth K, Portier BP, Rodriguez M, Devaraj SGT, Zhan M, Sheng J, Iyer SP, Bradner JE, Bhalla KN. 2014. Highly active combination of BRD4 antagonist and histone deacetylase inhibitor against human acute myelogenous leukemia cells. *Mol Cancer Ther* **13**:1142–1154. doi:10.1158/1535-7163.MCT-13-0770

Flavahan WA, Drier Y, Liau BB, Gillespie SM, Venteicher AS, Stemmer-Rachamimov AO, Suvà ML, Bernstein BE. 2016. Insulator dysfunction and oncogene activation in IDH mutant gliomas. *Nature* **529**:110–114. doi:10.1038/nature16490

Frew AJ, Johnstone RW, Bolden JE. 2009. Enhancing the apoptotic and therapeutic effects of HDAC inhibitors. *Cancer Lett* **280**:125–133. doi:10.1016/j.canlet.2009.02.042

Frontelo P, Manwani D, Galdass M, Karsunky H, Lohmann F, Gallagher PG, Bieker JJ. 2007. Novel role for EKLF in megakaryocyte lineage commitment. *Blood* **110**:3871–3880. doi:10.1182/blood-2007-03-082065

Fudenberg G, Imakaev M, Lu C, Goloborodko A, Abdennur N, Mirny LA. 2016. Formation of Chromosomal Domains by Loop Extrusion. *Cell Rep* **15**:2038–2049. doi:10.1016/j.celrep.2016.04.085

Fujiwara Y, Browne CP, Cunniff K, Goff SC, Orkin SH. 1996. Arrested development of embryonic red cell precursors in mouse embryos lacking transcription factor GATA-1. *Proc Natl Acad Sci* **93**:12355–12358. doi:10.1073/pnas.93.22.12355

Fukazawa H, Masumi A. 2012. The Conserved 12-Amino Acid Stretch in the Inter-Bromodomain Region of BET Family Proteins Functions as a Nuclear Localization Signal. *Biol Pharm Bull* **35**:2064–2068. doi:10.1248/bpb.b12-00527

Gambari R, Barbieri R, Buzzoni D, Bernardi F, Marchetti G, Amelotti F, Piva R, Viola L, Senno L del. 1986. Human leukemic K562 cells: suppression of hemoglobin accumulation by a monoclonal antibody to human transferrin receptor. *Biochim el Biophys Acta* **886**:203–213.

Gambari R, del Senno L, Barbieri R, Viola L, Tripodi M, Raschellà G, Fantoni A. 1984. Human leukemia K-562 cells: induction of erythroid differentiation by 5-azacytidine. *Cell Differ* **14**:87–97. doi:10.1016/0045-6039(84)90033-2

Gao F, Yang Y, Wang Z, Gao X, Zheng B. 2015. BRAD4 plays a critical role in germinal center response by regulating Bcl-6 and NF-κB activation. *Cell Immunol* **294**:1–8. doi:10.1016/j.cellimm.2015.01.010

Gao J, Chen YH, Peterson LAC. 2015. GATA family transcriptional factors: Emerging suspects in hematologic disorders. *Exp Hematol Oncol* **4**:1–7. doi:10.1186/s40164-015-0024-z

Garcia-Manero G, Gore SD, Kambhampati S, Scott B, Tefferi A, Cogle CR, Edenfield WJ, Hetzer J, Kumar K, Laille E, Shi T, MacBeth KJ, Skikne B. 2016. Efficacy and safety of extended dosing schedules of CC-486 (oral azacitidine) in patients with lower-risk myelodysplastic syndromes. *Leukemia* **30**:889–896. doi:10.1038/leu.2015.265

Garcia-Manero G, Griffiths EA, Roboz GJ, Busque L, Wells RA, Odenike O, Steensma DP, Yee KWL, Faderl S, Amrein PC, Michaelis LC, Kantarjian HM, Oganesian A,

Lowder JN, Azab M, Savona MR. 2017. A Phase 2 Dose-Confirmation Study of Oral ASTX727, a Combination of Oral Decitabine with a Cytidine Deaminase Inhibitor (CDAi) Cedazuridine (E7727), in Subjects with Myelodysplastic Syndromes (MDS). *Blood* **130**:4274 LP – 4274.

Garrett-Sinha LA. 2013. Review of Ets1 structure, function, and roles in immunity. *Cell Mol Life Sci* **70**:3375–3390. doi:10.1007/s00018-012-1243-7

Genta S, Pirosa MC, Stathis A. 2019. BET and EZH2 Inhibitors: Novel Approaches for Targeting Cancer. *Curr Oncol Rep* **21**. doi:10.1007/s11912-019-0762-x

Georgoulis A, Vorgias CE, Chrousos GP, Rogakou EP. 2017. Genome instability and γH2AX. *Int J Mol Sci* **18**:1–10. doi:10.3390/ijms18091979

Ghoshal K, Datta J, Majumder S, Bai S, Kutay H, Motiwala T, Jacob ST. 2005. 5-Aza-Deoxycytidine Induces Selective Degradation of DNA Methyltransferase 1 by a Proteasomal Pathway That Requires the KEN Box, Bromo-Adjacent Homology Domain, and Nuclear Localization Signal. *Mol Cell Biol* **25**:4727–4741. doi:10.1128/mcb.25.11.4727-4741.2005

Giani FC, Fiorini C, Wakabayashi A, Ludwig LS, Salem RM, Jobaliya CD, Regan SN, Ulirsch JC, Liang G, Steinberg-Shemer O, Guo MH, Esko T, Tong W, Brugnara C, Hirschhorn JN, Weiss MJ, Zon LI, Chou ST, French DL, Musunuru K, Sankaran VG. 2016. Targeted Application of Human Genetic Variation Can Improve Red Blood Cell Production from Stem Cells. *Cell Stem Cell* **18**:73–78. doi:10.1016/j.stem.2015.09.015

Ginder GD, Gnanapragasam MN, Mian OY. 2008. The Role of the Epigenetic Signal, DNA Methylation, in Gene Regulation During Erythroid Development. *Curr Top Dev Biol* **82**:85–116. doi:10.1016/S0070-2153(07)00004-X

Glozak MA, Sengupta N, Zhang X, Seto E. 2005. Acetylation and deacetylation of non-histone proteins. *Gene* **363**:15–23. doi:10.1016/j.gene.2005.09.010

Gnanapragasam MN, Bieker JJ. 2017. Orchestration of late events in erythropoiesis by KLF1/EKLF. *Curr Opin Hematol* **24**:183–190. doi:10.1097/MOH.0000000000000327

Gombert WM, Farris SD, Rubio ED, Morey-Rosler KM, Schubach WH, Krumm A. 2003. The c-myc Insulator Element and Matrix Attachment Regions Define the c-myc Chromosomal Domain. *Mol Cell Biol* **23**:9338–9348.

Gombert WM, Krumm A. 2009. Targeted deletion of multiple CTCF-binding elements in the human C-MYC gene reveals a requirement for CTCF in C-MYC expression. *PLoS One* **4**:1–8. doi:10.1371/journal.pone.0006109

Gomes NP, Espinosa JM. 2010. Gene-specific repression of the p53 target gene PUMA via intragenic CTCF – Cohesin binding. *Genes Dev* **24**:1022–1034. doi:10.1101/gad.1881010.Freely

Gomez-Casares MT, Garcia-Alegria E, Lopez-Jorge CE, Ferrandiz N, Blanco R, Alvarez S, Vaque JP, Bretones G, Caraballo JM, Sanchez-Bailon P, Delgado MD, Martin-Perez J, Cigudosa JC, Leon J. 2013. MYC antagonizes the differentiation induced by imatinib in chronic myeloid leukemia cells through downregulation of p27(KIP1.). *Oncogene* **32**:2239–2246. doi:10.1038/onc.2012.246

Gómez-Casares MT, García-Alegria E, López-Jorge CE, Ferrándiz N, Blanco R, Alvarez S, Vaqué JP, Bretones G, Caraballo JM, Sánchez-Bailón P, Delgado MD, Martín-Perez J, Cigudosa JC, León J. 2013. MYC antagonizes the differentiation induced by imatinib in chronic myeloid leukemia cells through downregulation of p27 KIP1. *Oncogene* **32**:2239–2246. doi:10.1038/onc.2012.246

Gomez-Velazquez M, Badia-Careaga C, Lechuga-Vieco AV, Nieto-Arellano R, Tena JJ, Rollan I, Alvarez A, Torroja C, Caceres EF, Roy A, Galjart N, Delgado-Olguin P, Sanchez-Cabo F, Enriquez JA, Gomez-Skarmeta JL, Manzanares M. 2017. CTCF counter-regulates cardiomyocyte development and maturation programs in the embryonic heart. *PLoS Genet* **13**:1–25. doi:10.1371/journal.pgen.1006985

Gore A V., Weinstein BM. 2016. DNA methylation in hematopoietic development and disease. *Exp Hematol* **44**:783–790. doi:10.1016/j.exphem.2016.04.013

Grant S, Easley C, Kirkpatrick P. 2007. Vorinostat. *Nat Rev Drug Discov* **6**:21–22. doi:10.1038/nrd2227

Gregor A, Oti M, Kouwenhoven EN, Hoyer J, Sticht H, Ekici AB, Kjaergaard S, Rauch A, Stunnenberg HG, Uebe S, Vasileiou G, Reis A, Zhou H, Zweier C. 2013. De novo mutations in the genome organizer CTCF cause intellectual disability. *Am J Hum Genet* **93**:124–131. doi:10.1016/j.ajhg.2013.05.007

Gregory T, Yu C, Ma A, Orkin SH, Blobel G a, Weiss MJ. 1999. GATA-1 and erythropoietin cooperate to promote erythroid cell survival by regulating bcl-xL expression. *Blood* **94**:87–96.

Grunstein M. 1997. Histone acetylation in chromatin structure and transcription. *Nature* **389**:349–352. doi:10.1038/38664

Guastafierro T, Cecchinelli B, Zampieri M, Reale A, Riggio G, Sthandier O, Zupi G, Calabrese L, Caiafa P. 2008. CCCTC-binding factor activates PARP-1 affecting DNA methylation machinery. *J Biol Chem* **283**:21873–21880. doi:M801170200 [pii] 10.1074/jbc.M801170200

Guo J, Li N, Han J, Pei F, Wang T, Lu D, Jiang J. 2018. DNA recognition patterns of the multi-zinc-finger protein CTCF: a mutagenesis study. *Acta Pharm Sin B* **8**:900–908. doi:10.1016/j.apsb.2018.08.007

Guo Y, Xu Q, Canzio D, Shou J, Li J, Gorkin DU, Jung I, Wu H, Zhai Y, Tang Y, Lu Y, Wu Y, Jia Z, Li W, Zhang MQ, Ren B, Krainer AR, Maniatis T, Wu Q. 2015. CRISPR Inversion of CTCF Sites Alters Genome Topology and Enhancer/Promoter Function. *Cell* **162**:900–910. doi:10.1016/j.cell.2015.07.038

Guo YA, Chang MM, Huang W, Ooi WF, Xing M, Tan P, Skanderup AJ. 2018. Mutation hotspots at CTCF binding sites coupled to chromosomal instability in gastrointestinal cancers. *Nat Commun* **9**:1–14. doi:10.1038/s41467-018-03828-2

Haarhuis JHI, van der Weide RH, Blomen VA, Yáñez-Cuna JO, Amendola M, van Ruiten MS, Krijger PHL, Teunissen H, Medema RH, van Steensel B, Brummelkamp TR, de Wit E, Rowland BD. 2017. The Cohesin Release Factor WAPL Restricts Chromatin Loop Extension. *Cell* **169**:693-707.e14. doi:10.1016/j.cell.2017.04.013

Han D, Chen Q, Shi J, Zhang F, Yu X. 2017. CTCF participates in DNA damage response via poly(ADP-ribosyl)ation. *Sci Rep* **7**:1–10. doi:10.1038/srep43530

Hancock AL, Brown KW, Moorwood K, Moon H, Holmgren C, Mardikar SH, Dallosso AR, Klenova E, Loukinov D, Ohlsson R, Lobanenkov V V, Malik K. 2007. A CTCF-binding silencer regulates the imprinted genes AWT1 and WT1-AS and exhibits sequential epigenetic defects during Wilms' tumourigenesis. *Hum Mol Genet* **16**:343–354.

Hanssen LLP, Kassouf MT, Oudelaar AM, Biggs D, Preece C, Downes DJ, Gosden M, Sharpe JA, Sloane-Stanley JA, Hughes JR, Davies B, Higgs DR. 2017. Tissue-specific CTCF-cohesin-mediated chromatin architecture delimits enhancer interactions and function in vivo. *Nat Cell Biol* **19**:952–961. doi:10.1038/ncb3573

Hark AT, Schoenherr CJ, Katz DJ, Ingram RS, Levorse JM, Tilghman SM. 2000. CTCF

mediates methylation-sensitive enhancer-blocking activity at the H19/Igf2 locus [see comments]. *Nature* **405**:486–489.

Hashimoto H, Wang D, Horton JR, Zhang X, Corces VG, Cheng X. 2017. Structural Basis for the Versatile and Methylation-Dependent Binding of CTCF to DNA. *Mol Cell* **66**:711-720.e3. doi:10.1016/j.molcel.2017.05.004

Hassler MR, Schiefer AI, Egger G. 2013. Combating the epigenome: Epigenetic drugs against non-Hodgkin's lymphoma. *Epigenomics* **5**:397–415. doi:10.2217/epi.13.39

Hattangadi SM, Wong P, Zhang L, Flygare J, Lodish HF. 2011. From stem cell to red cell: Regulation of erythropoiesis at multiple levels by multiple proteins, RNAs, and chromatin modifications. *Blood* **118**:6258–6268. doi:10.1182/blood-2011-07-356006

Hauser J, Grundström C, Kumar R, Grundström T. 2016. Regulated localization of an AID complex with E2A, PAX5 and IRF4 at the Igh locus. *Mol Immunol* **80**:78–90. doi:10.1016/j.molimm.2016.10.014

Heath H, Ribeiro de Almeida C, Sleutels F, Dingjan G, van de Nobelen S, Jonkers I, Ling KW, Gribnau J, Renkawitz R, Grosveld F, Hendriks RW, Galjart N. 2008. CTCF regulates cell cycle progression of alphabeta T cells in the thymus. *Embo J* **27**:2839–2850.

Hecht JL, Aster JC. 2000. Molecular Biology of Burkitt Lymphoma. *J Clin Oncol* **18**:3707–3721. doi:10.1007/978-1-4614-4313-1

Heinz S, Texari L, Hayes MGB, Urbanowski M, Chang MW, Givarkes N, Rialdi A, White KM, Albrecht RA, Pache L, Marazzi I, García-Sastre A, Shaw ML, Benner C. 2018. Transcription Elongation Can Affect Genome 3D Structure. *Cell* **174**:1522-1536.e22. doi:10.1016/j.cell.2018.07.047

Hnisz Denes, Day DS, Young RA. 2016. Insulated Neighborhoods: Structural and Functional Units of Mammalian Gene Control. *Cell* **167**:1188–1200. doi:10.1016/j.cell.2016.10.024

Hnisz D, Weintraub AS, Day DS, Valton AL, Bak RO, Li CH, Goldmann J, Lajoie BR, Fan ZP, Sigova AA, Reddy J, Borges-Rivera D, Lee TI, Jaenisch R, Porteus MH, Dekker J, Young RA. 2016. Activation of proto-oncogenes by disruption of chromosome neighborhoods. *Science (80-)* **351**:1454–1458. doi:10.1126/science.aad9024

Hoffmann AV, Higgs DR, Keeling DM, Mehta AB. 2016. Postgraduate Haematology, Seventh ed. ed.

Holliday R. 1987. The Inheritance of Epigenetic Defects. *Science (80-)* **238**:163–170.

Hölscher AS, Schulz WA, Pinkerneil M, Niegisch G, Hoffmann MJ. 2018. Combined inhibition of BET proteins and class I HDACs synergistically induces apoptosis in urothelial carcinoma cell lines. *Clin Epigenetics* **10**:1–14. doi:10.1186/s13148-017-0434-3

Hou C, Dale R, Dean A. 2010. Cell type specificity of chromatin organization mediated by CTCF and cohesin. *Proc Natl Acad Sci U S A* **107**:3651–3656. doi:10.1073/pnas.0912087107

Hsu SC, Gilgenast TG, Bartman CR, Edwards CR, Stonestrom AJ, Huang P, Emerson DJ, Evans P, Werner MT, Keller CA, Giardine B, Hardison RC, Raj A, Phillips-Cremins JE, Blobel GA. 2017. The BET Protein BRD2 Cooperates with CTCF to Enforce Transcriptional and Architectural Boundaries. *Mol Cell* **66**:102-116.e7. doi:10.1016/j.molcel.2017.02.027

Hu CCA, Dougan SK, McGehee AM, Love JC, Ploegh HL. 2009. XBP-1 regulates signal transduction, transcription factors and bone marrow colonization in B cells. *EMBO*

J **28**:1624–1636. doi:10.1038/emboj.2009.117

Hyle J, Zhang Y, Wright S, Xu B, Shao Y, Easton J, Tian L, Feng R, Xu P, Li C. 2019. Acute depletion of CTCF directly affects MYC regulation through loss of enhancer-promoter looping. *Nucleic Acids Res*. doi:10.1093/nar/gkz462

Ierano C, Chakraborty AR, Nicolae A, Bahr JC, Zhan Z, Pittaluga S, Bates SE, Robey RW. 2013. Loss of the proteins Bak and Bax prevents apoptosis mediated by histone deacetylase inhibitors. *Cell Cycle* **12**:2829–2838. doi:10.4161/cc.25914

Iglesias-Platas I, Court F, Camprubi C, Sparago A, Guillaumet-Adkins A, Martin-Trujillo A, Riccio A, Moore GE, Monk D. 2013. Imprinting at the PLAGL1 domain is contained within a 70-kb CTCF/cohesin-mediated non-Allelic chromatin loop. *Nucleic Acids Res* **41**:2171–2179. doi:10.1093/nar/gks1355

Imai Y, Maru Y, Tanaka J. 2016. Action mechanisms of histone deacetylase inhibitors in the treatment of hematological malignancies. *Cancer Sci* **107**:1543–1549. doi:10.1111/cas.13062

Ing-Simmons E, Seitan VC, Faure AJ, Flicek P, Caroll T, Dekker J, Fisher AG, Lenhard B, Merkenschlager M. 2015. Spatial enhancer clustering and regulation of enhancer-proximal genes by cohesin. *Genome Res* **25**:504–513. doi:10.1101/gr.184986.114.8

Ingley E, Tilbrook PA, Klinken SP. 2004. New insights into the regulation of erythroid cells. *IUBMB Life* **56**:177–184. doi:10.1080/15216540410001703956

Ishihara K, Oshimura M, Nakao M. 2006. CTCF-dependent chromatin insulator is linked to epigenetic remodeling. *Mol Cell* **23**:733–742.

Issa JPJ, Roboz G, Rizzieri D, Jabbour E, Stock W, O'Connell C, Yee K, Tibes R, Griffiths EA, Walsh K, Daver N, Chung W, Naim S, Taverna P, Oganesian A, Hao Y, Lowder JN, Azab M, Kantarjian H. 2015. Safety and tolerability of guadecitabine (SGI-110) in patients with myelodysplastic syndrome and acute myeloid leukaemia: A multicentre, randomised, dose-escalation phase 1 study. *Lancet Oncol* **16**:1099–1110. doi:10.1016/S1470-2045(15)00038-8

Iwasaki H, Akashi K. 2007. Hematopoietic developmental pathways: on cellular basis. *Oncogene* **26**:6687–6696.

Jeong M, Goodell MA. 2016. Noncoding Regulatory RNAs in Hematopoiesis, 1st ed, Current Topics in Developmental Biology. Elsevier Inc. doi:10.1016/bs.ctdb.2016.01.006

Ji P, Murata-Hori M, Lodish HF. 2011. Formation of mammalian erythrocytes: Chromatin condensation and enucleation. *Trends Cell Biol* **21**:409–415. doi:10.1016/j.tcb.2011.04.003

Ji X, Dadon DB, Powell BE, Fan ZP, Borges-Rivera D, Shachar S, Weintraub AS, Hnisz D, Pegoraro G, Lee TI, Misteli T, Jaenisch R, Young RA. 2016. 3D Chromosome Regulatory Landscape of Human Pluripotent Cells. *Cell Stem Cell* **18**:262–275. doi:10.1016/j.stem.2015.11.007

Jones PA. 2012. Functions of DNA methylation: Islands, start sites, gene bodies and beyond. *Nat Rev Genet* **13**:484–492. doi:10.1038/nrg3230

Jostes S, Nettersheim D, Fellermeyer M, Schneider S, Hafezi F, Honecker F, Schumacher V, Geyer M, Kristiansen G, Schorle H. 2017. The bromodomain inhibitor JQ1 triggers growth arrest and apoptosis in testicular germ cell tumours in vitro and in vivo. *J Cell Mol Med* **21**:1300–1314. doi:10.1111/jcmm.13059

Kaminskas E, Farrell AT, Wang Y-C, Sridhara R, Pazdur R. 2005. FDA Drug Approval Summary: Azacitidine (5-azacytidine, Vidaza™) for Injectable Suspension.

Oncologist **10**:176–182. doi:10.1634/theoncologist.2011-0227

Kanduri C, Pant V, Loukinov D, Pugacheva E, Qi CF, Wolffe A, Ohlsson R, Lobanenkov V V. 2000. Functional association of CTCF with the insulator upstream of the H19 gene is parent of origin-specific and methylation-sensitive. *Curr Biol* **10**:853–856.

Kaneko H, Shimizu R, Yamamoto M. 2010. GATA factor switching during erythroid differentiation. *Curr Opin Hematol* **17**:163–168. doi:10.1097/MOH.0b013e32833800b8

Kang Y, Kim YW, Kang J, Yun WJ, Kim A. 2017. Erythroid specific activator GATA-1-dependent interactions between CTCF sites around the beta-globin locus. *Biochim Biophys Acta Gene Regul Mech* **1860**:416–426. doi:10.1016/j.bbagrm.2017.01.013

Kantarjian HM, Roboz GJ, Kropf PL, Yee KWL, O'Connell CL, Tibes R, Walsh KJ, Podoltsev NA, Griffiths EA, Jabbour E, Garcia-Manero G, Rizzieri D, Stock W, Savona MR, Rosenblat TL, Berdeja JG, Ravandi F, Rock EP, Hao Y, Azab M, Issa JPJ. 2017. Guadecitabine (SGI-110) in treatment-naive patients with acute myeloid leukaemia: phase 2 results from a multicentre, randomised, phase 1/2 trial. *Lancet Oncol* **18**:1317–1326. doi:10.1016/S1470-2045(17)30576-4

Kapur R, Zhang L. 2001. A Novel Mechanism of Cooperation between c-Kit and Erythropoietin Receptor. *J Biol Chem* **276**:1099–1106. doi:10.1074/jbc.M005894200

Katainen R, Dave K, Pitkanen E, Palin K, Kivioja T, Valimaki N, Gylfe AE, Ristolainen H, Hanninen UA, Cajuso T, Kondelin J, Tanskanen T, Mecklin JP, Jarvinen H, Renkonen-Sinisalo L, Lepisto A, Kaasinen E, Kilpivaara O, Tuupanen S, Enge M, Taipale J, Aaltonen LA. 2015. CTCF/cohesin-binding sites are frequently mutated in cancer. *Nat Genet* **47**:818–821. doi:10.1038/ng.3335

Kazanets A, Shorstova T, Hilmi K, Marques M, Witcher M. 2016. Epigenetic silencing of tumor suppressor genes: Paradigms, puzzles, and potential. *Biochim Biophys Acta - Rev Cancer* **1865**:275–288. doi:10.1016/j.bbcan.2016.04.001

Kikuchi M, Miki T, Kumagai T, Fukuda T, Kamiyama R, Miyasaka N, Hirosawa S. 2000. Identification of negative regulatory regions within the first exon and intron of the BCL6 gene. *Oncogene* **19**:4941–4945.

Kim LK, Esplugues E, Zorca CE, Parisi F, Kluger Y, Kim TH, Galjart NJ, Flavell RA. 2014. Oct-1 Regulates IL-17 Expression by Directing Interchromosomal Associations in Conjunction with CTCF in T Cells. *Mol Cell* **54**:56–66. doi:10.1016/j.molcel.2014.02.004

Kim MJ, Civin CI, Kingsbury TJ. 2019. MicroRNAs as regulators and effectors of hematopoietic transcription factors. *Wiley Interdiscip Rev RNA* 1–22. doi:10.1002/wrna.1537

Kim S, Yu NK, Kaang BK. 2015. CTCF as a multifunctional protein in genome regulation and gene expression. *Exp Mol Med* **47**:e166. doi:10.1038/emm.2015.33

Kim TG, Kim S, Jung S, Kim M, Yang B, Lee MG, Kim HP. 2017. CCCTC-binding factor is essential to the maintenance and quiescence of hematopoietic stem cells in mice. *Exp Mol Med* **49**:e371. doi:10.1038/emm.2017.124

Kitano M, Moriyama S, Ando Y, Hikida M, Mori Y, Kurosaki T, Okada T. 2011. Bcl6 Protein Expression Shapes Pre-Germinal Center B Cell Dynamics and Follicular Helper T Cell Heterogeneity. *Immunity* **34**:961–972. doi:10.1016/j.immuni.2011.03.025

Kitchen NS, Schoenherr CJ. 2010. Sumoylation modulates a domain in CTCF that activates transcription and decondenses chromatin. *J Cell Biochem* **111**:665–675.

doi:10.1002/jcb.22751

Klenova E, Scott AC, Roberts J, Shamsuddin S, Lovejoy EA, Bergmann S, Bubb VJ, Royer HD, Quinn JP. 2004. YB-1 and CTCF differentially regulate the 5-HTT polymorphic intron 2 enhancer which predisposes to a variety of neurological disorders. *J Neurosci* **24**:5966–5973.

Klenova EM, Chernukhin I V, El-Kady A, Lee RE, Pugacheva EM, Loukinov DI, Goodwin GH, Delgado D, Filippova GN, Leon J, Morse 3rd HC, Neiman PE, Lobanenkov V V. 2001. Functional phosphorylation sites in the C-terminal region of the multivalent multifunctional transcriptional factor CTCF. *Mol Cell Biol* **21**:2221–2234.

Klenova EM, Nicolas RH, Paterson HF, Carne AF, Heath CM, Goodwin GH, Neiman PE, Lobanenkov V V. 1993. CTCF, a conserved nuclear factor required for optimal transcriptional activity of the chicken c-myc gene, is an 11-Zn-finger protein differentially expressed in multiple forms. *Mol Cell Biol* **13**:7612–7624. doi:10.1128/mcb.13.12.7612

Klug A, Schwabe JW. 1995. Protein motifs 5. Zinc fingers. *FASEB J* **9**:597–604. doi:10.1096/fasebj.9.8.7768350

Knutson SK, Wigle TJ, Warholic NM, Sneeringer CJ, Allain CJ, Klaus CR, Sacks JD, Raimondi A, Majer CR, Song J, Scott MP, Jin L, Smith JJ, Olhava EJ, Chesworth R, Moyer MP, Richon VM, Copeland RA, Keilhack H, Pollock RM, Kuntz KW. 2012. A selective inhibitor of EZH2 blocks H3K27 methylation and kills mutant lymphoma cells. *Nat Chem Biol* **8**:890–896. doi:10.1038/nchembio.1084

Ko M, An J, Pastor WA, Koralov SB, Rajewsky K, Rao A. 2015. TET proteins and 5-methylcytosine oxidation in hematological cancers. *Immunol Rev* **263**:6–21. doi:10.1111/imr.12239

Koesters C, Unger B, Bilic I, Schmidt U, Bluml S, Lichtenberger B, Schreiber M, Stockl J, Ellmeier W. 2007. Regulation of dendritic cell differentiation and subset distribution by the zinc finger protein CTCF. *Immunol Lett* **109**:165–174.

Koulnis M, Porpiglia E, Hidalgo D, Socolovsky M. 2014. Erythropoiesis: from molecular pathways to system properties. *Adv Exp Med Biol* **844**:37–58. doi:10.1007/978-1-4939-2095-2

Koury MJ. 2016. Tracking erythroid progenitor cells in times of need and times of plenty. *Exp Hematol* **44**:653–663. doi:10.1016/j.exphem.2015.10.007

Koury MJ. 2009. Red Cell Production and Kinetics. *Ross Princ Transfus Med Fourth Ed* 17–28. doi:10.1002/9781444303513.ch2

Koury MJ, Bondurant MC. 1988. Maintenance by erythropoietin of viability and maturation of murine erythroid precursor cells. *J Cell Physiol* **137**:65–74. doi:10.1002/jcp.1041370108

Kouzarides T. 2007. Chromatin Modifications and Their Function. *Cell* **128**:693–705. doi:10.1016/j.cell.2007.02.005

Kulczyńska K, Siatecka M. 2016. A regulatory function of long non-coding RNAs in red blood cell development. *Acta Biochim Pol* **63**:675–680. doi:10.18388/abp.2016_1351

Kung JT, Kesner B, An JY, Ahn JY, Cifuentes-Rojas C, Colognori D, Jeon Y, Szanto A, Del Rosario BC, Pinter SF, Erwin JA, Lee JT. 2015. Locus-specific targeting to the X-chromosome revealed by the RNA interactome of CTCF recruited in a locus-specific manner and implicates CTCF-RNA interactions in long-range chromosomal interactions. *Mol Cell January* **2212**:361–375. doi:10.1016/j.molcel.2014.12.006

Küppers R. 2005. Mechanisms of B-cell lymphoma pathogenesis. *Nat Rev Cancer*

5:251–262. doi:10.1038/nrc1589

Küppers R, Dalla-Favera R. 2001. Mechanisms of chromosomal translocations in B cell lymphomas. *Oncogene* **20**:5580–5594. doi:10.1038/sj.onc.1204640

Kuzmin I, Geil L, Gibson L, Cavinato T, Loukinov D, Lobanenkov V, Lerman MI. 2005. Transcriptional Regulator CTCF Controls Human Interleukin 1 Receptor-associated Kinase 2 Promoter. *J Mol Biol* **346**:411–422.

Larsson J, Karlsson S. 2005. The role of Smad signaling in hematopoiesis. *Oncogene* **24**:5676–5692. doi:10.1038/sj.onc.1208920

Lasko D, Cavenee W, Nordenskjöld M. 1991. Loss of Constitutional Heterozygosity in human cancer. *Annu Rev Genet* **25**:281–314. doi:10.1146/annurev.ge.25.120191.001433

Laubach JP, Moreau P, San-Miguel JF, Richardson PG. 2015. Panobinostat for the treatment of multiple myeloma. *Clin Cancer Res* **21**:4767–4773. doi:10.1158/1078-0432.CCR-15-0530

Lee CH, Melchers M, Wang H, Torrey TA, Slota R, Qi C-F, Kim JY, Lugar P, Kong HJ, Farrington L, van der Zouwen B, Zhou JX, Lougaris V, Lipsky PE, Grammer AC, Morse HC. 2006. Regulation of the germinal center gene program by interferon (IFN) regulatory factor 8/IFN consensus sequence-binding protein. *J Exp Med* **205**:1507–1507. doi:10.1084/jem.20051450051208c

Lee HZ, Kwitkowski VE, Del Valle PL, Ricci MS, Saber H, Habtemariam BA, Bullock J, Bloomquist E, Shen YL, Chen XH, Brown J, Mehrotra N, Dorff S, Charlab R, Kane RC, Kaminskas E, Justice R, Farrell AT, Pazdur R. 2015. FDA approval: Belinostat for the treatment of patients with relapsed or refractory peripheral T-cell lymphoma. *Clin Cancer Res* **21**:2666–2670. doi:10.1158/1078-0432.CCR-14-3119

Lee J, Krivega I, Dale RK, Dean A. 2017. The LDB1 Complex Co-opts CTCF for Erythroid Lineage-Specific Long-Range Enhancer Interactions. *Cell Rep* **19**:2490–2502. doi:10.1016/j.celrep.2017.05.072

Lee JS, Raja P, Pan D, Pesola JM, Coen DM, Knipe DM. 2018. CCCTC-Binding Factor Acts as a Heterochromatin Barrier on Herpes Simplex Viral Latent Chromatin and Contributes to Poised Latent Infection. *MBio* **9**:1–13. doi:10.1128/mbio.02372-17

Lee JY, Mustafa M, Kim CY, Kim MH. 2017. Depletion of CTCF in breast cancer cells selectively induces cancer cell death via p53. *J Cancer* **8**. doi:10.7150/jca.18818

Lerga A, Crespo P, Berciano M, Delgado MD, Canelles M, Cales C, Richard C, Ceballos E, Gutierrez P, Ajenjo N, Gutkind S, Leon J. 1999. Regulation of c-Myc and Max in megakaryocytic and monocytic-macrophagic differentiation of K562 cells induced by protein kinase C modifiers: c-Myc is down-regulated but does not inhibit differentiation. *Cell Growth Differ* **10**:639–654.

Ley TJ, Ding L, Walter MJ, McLellan MD, Lamprecht T, Larson DE, Kandoth C, Payton JE, Baty J, Welch J, Harris CC, Lichti CF, Townsend RR, Fulton RS, Dooling DJ, Koboldt DC, Schmidt H, Zhang Q, Osborne JR, Lin L, O'Laughlin M, McMichael JF, Delehaunty KD, McGrath SD, Fulton LA, Magrini VJ, Vickery TL, Hundal J, Cook LL, Conyers JJ, Swift GW, Reed JP, Alldredge PA, Wylie T, Walker J, Kalicki J, Watson MA, Heath S, Shannon WD, Varghese N, Nagarajan R, Westervelt P, Tomasson MH, Link DC, Graubert TA, DiPersio JF, Mardis ER, Wilson RK. 2010. DNMT3A Mutations in Acute Myeloid Leukemia. *N Engl J Med* **363**:2424–2433. doi:10.1056/NEJMoa1005143

Li E, Bestor TH, Jaenisch R. 1992. Targeted mutation of the DNA methyltransferase gene results in embryonic lethality. *Cell* **69**:915–926. doi:10.1016/0092-8674(92)90611-F

Li G, Zhou Q, Ruan Y, Cai L, Chang H, Hong P, Kolchanov NA, Kulakova E V. 2015. Chromatin Interaction Analysis with Paired-End Tag (ChIA-PET) sequencing technology and application. *BMC Genomics* **15**:1–10. doi:10.1186/1471-2164-15-s12-s11

Li T, Hu J-F, Qiu X, Ling J, Chen H, Wang S, Hou A, Vu TH, Hoffman AR. 2008. CTCF Regulates Allelic Expression of Igf2 by Orchestrating a Promoter-Polycomb Repressive Complex 2 Intrachromosomal Loop. *Mol Cell Biol* **28**:6473–6482. doi:10.1128/MCB.00204-08

Li W, Gupta SK, Han W, Kundson RA, Nelson S, Knutson D, Greipp PT, Elsawa SF, Sotomayor EM, Gupta M. 2019. Targeting MYC activity in double-hit lymphoma with MYC and BCL2 and/or BCL6 rearrangements with epigenetic bromodomain inhibitors. *J Hematol Oncol* **12**:1–13. doi:10.1186/s13045-019-0761-2

Lin K-I, Lin Y, Calame K. 2002. Repression of c-myc Is Necessary but Not Sufficient for Terminal Differentiation of B Lymphocytes In Vitro. *Mol Cell Biol* **20**:8684–8695. doi:10.1128/mcb.20.23.8684-8695.2000

Lin KI, Angelin-Duclos C, Kuo TC, Calame K. 2002. Blimp-1-dependent repression of Pax-5 is required for differentiation of B cells to immunoglobulin M-secreting plasma cells. *Mol Cell Biol* **22**:4771–4780.

Lipsick JS, Wang DM. 1999. Transformation by v-Myb. *Oncogene* **18**:3047–3055. doi:10.1038/sj.onc.1202745

Listowski MA, Heger E, Bogusławska DM, Machnicka B, Kuliczkowski K, Leluk J, Sikorski AF. 2013. MicroRNAs: Fine tuning of erythropoiesis. *Cell Mol Biol Lett* **18**:34–46. doi:10.2478/s11658-012-0038-z

Liu F, Wu D, Wang X. 2018. Roles of CTCF in conformation and functions of chromosome. *Semin Cell Dev Biol*. doi:10.1016/j.semcdb.2018.07.021

Liu S, Li F, Pan L, Yang Z, Shu Y, Lv W, Dong P, Gong W. 2019. BRD4 inhibitor and histone deacetylase inhibitor synergistically inhibit the proliferation of gallbladder cancer in vitro and in vivo. *Cancer Sci* 2493–2506. doi:10.1111/cas.14102

Lobanenkov V V, Nicolas RH, Adler V V, Paterson H, Klenova EM, Polotskaja A V, Goodwin GH. 1990. A novel sequence-specific DNA binding protein which interacts with three regularly spaced direct repeats of the CCCTC-motif in the 5'-flanking sequence of the chicken c-myc gene. *Oncogene* **5**:1743–53.

Lovén J, Hoke HA, Lin CY, Lau A, Orlando DA, Vakoc CR, Bradner JE, Lee TI, Young RA. 2013. Selective inhibition of tumor oncogenes by disruption of super-enhancers. *Cell* **153**:320–334. doi:10.1016/j.cell.2013.03.036

Lübbert M, Suciu S, Baila L, Rüter BH, Platzbecker U, Giagounidis A, Selleslag D, Labar B, Germing U, Salih HR, Beeldens F, Muus P, Pflüger KH, Coens C, Hagemeijer A, Schaefer HE, Ganser A, Aul C, De Witte T, Wijermans PW. 2011. Low-dose decitabine versus best supportive care in elderly patients with intermediate- or high-risk myelodysplastic syndrome (MDS) ineligible for intensive chemotherapy: Final results of the randomized phase III study of the european organisation for rese. *J Clin Oncol* **29**:1987–1996. doi:10.1200/JCO.2010.30.9245

Lulli V, Romania P, Morsilli O, Gabbianelli M, Pagliuca A, Mazzeo S, Testa U, Peschle C, Marziali G. 2006. Overexpression of Ets-1 in human hematopoietic progenitor cells blocks erythroid and promotes megakaryocytic differentiation. *Cell Death Differ* **13**:1064–1074. doi:10.1038/sj.cdd.4401811

Lutz M, Burke LJ, Barreto G, Goeman F, Greb H, Arnold R, Schultheiss H, Brehm A, Kouzarides T, Lobanenkov V, Renkawitz R. 2000. Transcriptional repression by the insulator protein CTCF involves histone deacetylases. *Nucleic Acids Res* **28**:1707–

1713.

MacPherson MJ, Beatty LG, Zhou W, Du M, Sadowski PD. 2009. The CTCF insulator protein is posttranslationally modified by SUMO. *Mol Cell Biol* **29**:714–725. doi:MCB.00825-08 [pii] 10.1128/MCB.00825-08

Magrath I. 2012. Epidemiology: Clues to the pathogenesis of Burkitt lymphoma. *Br J Haematol* **156**:744–756. doi:10.1111/j.1365-2141.2011.09013.x

Mahajan MC, Karmakar S, Newburger PE, Krause DS, Weissman SM. 2009. Dynamics of alpha-globin locus chromatin structure and gene expression during erythroid differentiation of human CD34(+) cells in culture. *Exp Hematol* **37**:1143-1156 e3. doi:10.1016/j.exphem.2009.07.001

Majumder P, Gomez JA, Boss JM. 2006. The human major histocompatibility complex class II HLA-DRB1 and HLA-DQA1 genes are separated by a CTCF-binding enhancer-blocking element. *J Biol Chem* **281**:18435–18443.

Mancini E, Sanjuan-Pla A, Luciani L, Moore S, Grover A, Zay A, Rasmussen KD, Luc S, Bilbao D, O'Carroll D, Jacobsen SE, Nerlov C. 2012. FOG-1 and GATA-1 act sequentially to specify definitive megakaryocytic and erythroid progenitors. *EMBO J* **31**:351–365. doi:10.1038/emboj.2011.390

Marino MM, Rega C, Russo R, Valletta M, Gentile MT, Esposito S, Baglivo I, De Feis I, Angelini C, Xiao T, Felsenfeld G, Chambery A, Pedone PV. 2019. Interactome mapping defines BRG1, a component of the SWI/SNF chromatin remodeling complex, as a new partner of the transcriptional regulator CTCF. *J Biol Chem* **294**:861–873. doi:10.1074/jbc.RA118.004882

Marshall AD, Bailey CG, Rasko JE. 2014. CTCF and BORIS in genome regulation and cancer. *Curr Opin Genet Dev* **24**:8–15. doi:10.1016/j.gde.2013.10.011

Mathur R, Sehgal L, Havranek O, Köhrer S, Khashab T, Jain N, Burger JA, Neelapu SS, Davis RE, Samaniego F. 2017. Inhibition of demethylase KDM6B sensitizes diffuse large B-cell lymphoma to chemotherapeutic drugs. *Haematologica* **102**:373–380. doi:10.3324/haematol.2016.144964

Méndez-Catalá CF, Gretton S, Vostrov A, Pugacheva E, Farrar D, Ito Y, Docquier F, Kita G-X, Murrell A, Lobanenkov V, Klenova E. 2013. A Novel Mechanism for CTCF in the Epigenetic Regulation of Bax in Breast Cancer Cells. *Neoplasia* **15**:898-IN14. doi:10.1593/neo.121948

Merkenschlager M, Nora EP. 2016. CTCF and Cohesin in Genome Folding and Transcriptional Gene Regulation. *Annu Rev Genomics Hum Genet* **17**:17–43. doi:10.1146/annurev-genom-083115-022339

Miller IJ, Bieker JJ. 1993. A novel, erythroid cell-specific murine transcription factor that binds to the CACCC element and is related to the Krüppel family of nuclear proteins. *Mol Cell Biol* **13**:2776–2786. doi:10.1128/mcb.13.5.2776

Miranda-Saavedra D, Gottgens B. 2008. Transcriptional regulatory networks in haematopoiesis. *Curr Opin Genet Dev* **18**:530–535.

Miyagawa SI, Kobayashi M, Konishi N, Sato T, Ueda K. 2000. Insulin and insulin-like growth factor I support the proliferation of erythroid progenitor cells in bone marrow through the sharing of receptors. *Br J Haematol* **109**:555–562. doi:10.1046/j.1365-2141.2000.02047.x

Momparler RL. 2003. Cancer epigenetics. *Oncogene* **22**:6479–6483. doi:10.1016/B978-0-12-375709-8.00032-0

Moore JM, Rabaia NA, Smith LE, Fagerlie S, Gurley K, Loukinov D, Disteche CM, Collins SJ, Kemp CJ, Lobanenkov V V, Filippova GN. 2012. Loss of maternal CTCF is

associated with peri-implantation lethality of Ctcf null embryos. *PLoS One* **7**:e34915. doi:10.1371/journal.pone.0034915

Moore KS, von Lindern M. 2018. RNA binding proteins and regulation of mRNA translation in erythropoiesis. *Front Physiol* **9**:1–17. doi:10.3389/fphys.2018.00910

Moriguchi T, Yamamoto M. 2014. A regulatory network governing Gata1 and Gata2 gene transcription orchestrates erythroid lineage differentiation. *Int J Hematol* **100**:417–424. doi:10.1007/s12185-014-1568-0

Moriguchi T, Yu L, Takai J, Hayashi M, Satoh H, Suzuki M, Ohneda K, Yamamoto M. 2015. The Human GATA1 Gene Retains a 5' Insulator That Maintains Chromosomal Architecture and GATA1 Expression Levels in Splenic Erythroblasts. *Mol Cell Biol* **35**:1825–1837. doi:10.1128/MCB.00011-15

Morin RD, Johnson NA, Severson TM, Mungall AJ, An J, Goya R, Paul JE, Boyle M, Woolcock BW, Kuchenbauer F, Yap D, Humphries RK, Griffith OL, Shah S, Zhu H, Kimbara M, Shashkin P, Charlot JF, Tcherpakov M, Corbett R, Tam A, Varhol R, Smailus D, Moksa M, Zhao Y, Delaney A, Qian H, Birol I, Schein J, Moore R, Holt R, Horsman DE, Connors JM, Jones S, Aparicio S, Hirst M, Gascoyne RD, Marra MA. 2010. Somatic mutations altering EZH2 (Tyr641) in follicular and diffuse large B-cell lymphomas of germinal-center origin. *Nat Genet* **42**:181–185. doi:10.1038/ng.518

Morin RD, Mendez-Lago M, Mungall AJ, Goya R, Mungall KL, Corbett RD, Johnson NA, Severson TM, Chiu R, Field M, Jackman S, Krzywinski M, Scott DW, Trinh DL, Tamura-Wells J, Li S, Firme MR, Rogic S, Griffith M, Chan S, Yakovenko O, Meyer IM, Zhao EY, Smailus D, Moksa M, Chittaranjan S, Rimsza L, Brooks-Wilson A, Spinelli JJ, Ben-Neriah S, Meissner B, Woolcock B, Boyle M, McDonald H, Tam A, Zhao Y, Delaney A, Zeng T, Tse K, Butterfield Y, Birol I, Holt R, Schein J, Horsman DE, Moore R, Jones SJM, Connors JM, Hirst M, Gascoyne RD, Marra MA. 2011. Frequent mutation of histone-modifying genes in non-Hodgkin lymphoma. *Nature* **476**:298–303. doi:10.1038/nature10351

Mukhopadhyay M, Teufel A, Yamashita T, Agulnick AD, Chen L, Downs KM, Schindler A, Grinberg A, Huang S-P, Dorward D, Westphal H. 2003. Functional ablation of the mouse Ldb1 gene results in severe patterning defects during gastrulation. *Development* **130**:495–505. doi:10.1242/dev.00225

Muta K, Krantz SB, Bondurant MC, Wickrema A. 1994. Distinct roles of erythropoietin, insulin-like growth factor I, and stem cell factor in the development of erythroid progenitor cells. *J Clin Invest* **94**:34–43. doi:10.1172/JCI117327

Muto A, Ochiai K, Kimura Y, Itoh-Nakadai A, Calame KL, Ikebe D, Tashiro S, Igarashi K. 2010. Bach2 represses plasma cell gene regulatory network in B cells to promote antibody class switch. *EMBO J* **29**:4048–4061. doi:10.1038/emboj.2010.257

Nakahashi H, Kwon KR, Resch W, Vian L, Dose M, Stavreva D, Hakim O, Pruett N, Nelson S, Yamane A, Qian J, Dubois W, Welsh S, Phair RD, Pugh BF, Lobanenkov V, Hager GL, Casellas R. 2013. A genome-wide map of CTCF multivalency redefines the CTCF code. *Cell Rep* **3**:1678–1689. doi:10.1016/j.celrep.2013.04.024

Nandakumar SK, Ulirsch JC, Sankaran VG. 2016. Advances in understanding erythropoiesis: Evolving perspectives. *Br J Haematol*. doi:10.1111/bjh.13938

Nera KP, Kohonen P, Narvi E, Peippo A, Mustonen L, Terho P, Koskela K, Buerstedde JM, Lassila O. 2006. Loss of Pax5 promotes plasma cell differentiation. *Immunity* **24**:283–293. doi:10.1016/j.immuni.2006.02.003

Neumann M, Heesch S, Schlee C, Schwartz S, Gökbuget N, Hoelzer D, Konstandin NP, Ksienzyk B, Vosberg S, Graf A, Krebs S, Blum H, Raff T, Brüggemann M, Hofmann

WK, Hecht J, Bohlander SK, Greif PA, Baldus CD. 2013. Whole-exome sequencing in adult ETP-ALL reveals a high rate of DNMT3A mutations. *Blood* **121**:4749–4752. doi:10.1182/blood-2012-11-465138

Nguyen L, Papenhausen P, Shao H. 2017. The Role of c-MYC in B-Cell Lymphomas: Diagnostic and molecular aspects. *Genes (Basel)* **8**:2–22. doi:10.3390/genes8040116

Niitsu N, Hayashi Y, Sugita K, Honma Y. 2001. Sensitization by 5-aza-2′-deoxycytidine of leukaemia cells with MLL abnormalities to induction of differentiation by all-trans retinoic acid and 1α,25-dihydroxyvitamin D3. *Br J Haematol* **112**:315–326. doi:10.1046/j.1365-2141.2001.02523.x

Nikinmaa M. 1997. Oxygen and carbon dioxide transport in vertebrate erythrocytes: an evolutionary change in the role of membrane transport. *J Exp Biol* **200**:369–380.

Nikoloski G, Langemeijer SMC, Kuiper RP, Knops R, Massop M, Tönnissen ERLTM, Van Der Heijden A, Scheele TN, Vandenberghe P, De Witte T, Van Der Reijden BA, Jansen JH. 2010. Somatic mutations of the histone methyltransferase gene EZH2 in myelodysplastic syndromes. *Nat Genet* **42**:665–667. doi:10.1038/ng.620

Nora EP, Goloborodko A, Valton A-L, Gibcus JH, Uebersohn A, Abdennur N, Dekker J, Mirny LA, Bruneau BG. 2017. Targeted Degradation of CTCF Decouples Local Insulation of Chromosome Domains from Genomic Compartmentalization. *Cell* **169**:930-944.e22. doi:10.1016/j.cell.2017.05.004

Nora EP, Lajoie BR, Schulz EG, Giorgetti L, Okamoto I, Servant N, Piolot T, Van Berkum NL, Meisig J, Sedat J, Gribnau J, Barillot E, Blüthgen N, Dekker J, Heard E. 2012. Spatial partitioning of the regulatory landscape of the X-inactivation centre. *Nature* **485**:381–385. doi:10.1038/nature11049

Nuez B, Michalovich D, Bygrave A, Ploemacher R, Grosveld F. 1995. Defective haematopoiesis in fetal liver resulting from inactivation of the EKLF gene. *Nature* **375**:316–318.

Nussenzweig A, Nussenzweig MC. 2010. Origin of chromosomal translocations in lymphoid cancer. *Cell* **141**:27–38. doi:10.1016/j.cell.2010.03.016

Ochiai K, Maienschein-Cline M, Simonetti G, Chen J, Rosenthal R, Brink R, Chong AS, Klein U, Dinner AR, Singh H, Sciammas R. 2013. Transcriptional Regulation of Germinal Center B and Plasma Cell Fates by Dynamical Control of IRF4. *Immunity* **38**:918–929. doi:10.1016/j.immuni.2013.04.009

Ohlsson R, Lobanenkov V, Klenova E. 2010. Does CTCF mediate between nuclear organization and gene expression? *Bioessays* **32**:37–50.

Ohlsson R, Renkawitz R, Lobanenkov V. 2001. CTCF is a uniquely versatile transcription regulator linked to epigenetics and disease. *Trends Genet* **17**:520–527. doi:10.1016/S0168-9525(01)02366-6

Okano M, Bell DW, Haber DA, Li E. 1999. Dnmt3a and Dnmt3b are essential for de novo methylation and mammalian development. *Cell* **99**:247–57.

Ong CT, Corces VG. 2014. CTCF: an architectural protein bridging genome topology and function. *Nat Rev Genet* **15**:234–246. doi:10.1038/nrg3663

Orkin SH, Zon LI. 2008. Hematopoiesis: an evolving paradigm for stem cell biology. *Cell* **132**:631–644.

Ouboussad L, Kreuz S, Lefevre PF. 2013. CTCF depletion alters chromatin structure and transcription of myeloid-specific factors. *J Mol Cell Biol* **5**:308–322. doi:10.1093/jmcb/mjt023

Pal S, Cantor AB, Johnson KD, Moran TB, Boyer ME, Orkin SH, Bresnick EH. 2004. Coregulator-dependent facilitation of chromatin occupancy by GATA-1. *Proc Natl Acad Sci* **101**:980–985. doi:10.1073/pnas.0307612100

Palis J. 2014. Primitive and definitive erythropoiesis in mammals. *Front Physiol* **5 JAN**:1–9. doi:10.3389/fphys.2014.00003

Palstra RJ, Tolhuis B, Splinter E, Nijmeijer R, Grosveld F, de Laat W. 2003. The beta-globin nuclear compartment in development and erythroid differentiation. *Nat Genet* **35**:190–194.

Pasqualucci L. 2019. Molecular pathogenesis of germinal center-derived B cell lymphomas. *Immunol Rev* **288**:240–261. doi:10.1111/imr.12745

Pasqualucci L, Dalla-Favera R. 2015. The Genetic Landscape of Diffuse Large B-Cell Lymphoma. *Semin Hematol* **52**:67–76. doi:10.1053/j.seminhematol.2015.01.005

Pasqualucci L, Dominguez-Sola D, Chiarenza A, Fabbri G, Grunn A, Trifonov V, Kasper LH, Lerach S, Tang H, Ma J, Rossi D, Chadburn A, Murty V V, Mullighan CG, Gaidano G, Rabadan R, Brindle PK, Dalla-Favera R. 2011. Inactivating mutations of acetyltransferase genes in B-cell lymphoma. *Nature* **471**:189–195. doi:10.1038/nature09730

Pasqualucci L, Migliazza A, Basso K, Houldsworth J, Chaganti RS, Dalla-Favera R. 2003. Mutations of the BCL6 proto-oncogene disrupt its negative autoregulation in diffuse large B-cell lymphoma. *Blood* **101**:2914–2923.

Pasqualucci L, Neumeister P, Goossens T, Nanjangud G, Chaganti RS, Kuppers R, Dalla-Favera R. 2001. Hypermutation of multiple proto-oncogenes in B-cell diffuse large-cell lymphomas. *Nature* **412**:341–346. doi:10.1038/35085588

Peña-Hernández R, Marques M, Hilmi K, Zhao T, Saad A, Alaoui-Jamali MA, del Rincon S V., Ashworth T, Roy AL, Emerson BM, Witcher M. 2015. Genome-wide targeting of the epigenetic regulatory protein CTCF to gene promoters by the transcription factor TFII-I. *Proc Natl Acad Sci* **112**:E677–E686. doi:10.1073/pnas.1416674112

Pereira R, Quang CT, Lesault I, Dolznig H, Beug H, Ghysdael J. 1999. FLI-1 inhibits differentiation and induces proliferation of primary erythroblasts. *Oncogene* **18**:1597–1608. doi:10.1038/sj.onc.1202534

Perkins A, Xu X, Higgs DR, Patrinos GP, Arnaud L, Bieker JJ, Philipsen S. 2016. Kruppeling erythropoiesis: an unexpected broad spectrum of human red blood cell disorders due to KLF1 variants. *Blood* **127**:1856–1862. doi:10.1182/blood-2016-01-694331

Perreault AA, Venters BJ. 2018. Integrative view on how erythropoietin signaling controls transcription patterns in erythroid cells. *Curr Opin Hematol* **25**:189–195. doi:10.1097/MOH.0000000000000415

Pevny L, Simon MC, Roberyson E, Klein WH, Tsai S-F, D´Agasti V, Orkin SH, Costantini F. 1991. Erythroid differentiation in chimaeric mice blocked by a targeted mutation in the gene for transcription factor GATA-1. *Nature* **349**:257–260.

Phan RT, Dalla-Favera R. 2004. The BCL6 proto-oncogene suppresses p53 expression in germinal-centre B cells. *Nature* **432**:635–639.

Phan RT, Saito M, Basso K, Niu H, Dalla-Favera R. 2005. BCL6 interacts with the transcription factor Miz-1 to suppress the cyclin-dependent kinase inhibitor p21 and cell cycle arrest in germinal center B cells. *Nat Immunol* **6**:1054–1060. doi:ni1245 [pii] 10.1038/ni1245

Phillips-Cremins JE, Sauria MEG, Sanyal A, Gerasimova TI, Lajoie BR, Bell JSK, Ong CT, Hookway TA, Guo C, Sun Y, Bland MJ, Wagstaff W, Dalton S, McDevitt TC,

Sen R, Dekker J, Taylor J, Corces VG. 2013. Architectural protein subclasses shape 3D organization of genomes during lineage commitment. *Cell* **153**:1281–1295. doi:10.1016/j.cell.2013.04.053

Phillips JE, Corces VG. 2009. CTCF: Master Weaver of the Genome. *Cell* **137**:1194–1211. doi:10.1016/j.cell.2009.06.001

Pomerantz MM, Ahmadiyeh N, Jia L, Herman P, Verzi MP, Doddapaneni H, Beckwith CA, Chan JA, Hills A, Davis M, Yao K, Kehoe SM, Lenz HJ, Haiman CA, Yan C, Henderson BE, Frenkel B, Barretina J, Bass A, Tabernero J, Baselga J, Regan MM, Manak JR, Shivdasani R, Coetzee GA, Freedman ML. 2009. The 8q24 cancer risk variant rs6983267 shows long-range interaction with MYC in colorectal cancer. *Nat Genet* **41**:882–884. doi:10.1038/ng.403

Porcher C, Chagraoui H, Kristiansen MS. 2017. SCL/TAL1: A multifaceted regulator from blood development to disease. *Blood* **129**:2051–2060. doi:10.1182/blood-2016-12-754051

Porcher C, Swat W, Rockwell K, Fujiwara Y, Alt FW, Orkin SH. 1996. The T cell leukemia oncoprotein SCL/tal-1 is essential for development of all hematopoietic lineages. *Cell* **86**:47–57. doi:10.1016/S0092-8674(00)80076-8

Prickett AR, Barkas N, McCole RB, Hughes S, Amante SM, Schulz R, Oakey RJ. 2013. Genome-wide and parental allele-specific analysis of CTCF and cohesin DNA binding in mouse brain reveals a tissue-specific binding pattern and an association with imprinted differentially methylated regions. *Genome Res* **23**:1624–1635. doi:10.1101/gr.150136.112

Prochownik E V., Kukowska J. 1986. Deregulated expression of c-myc by murine erythroleukaemia cells prevents differentiation. *Nature* **322**:848–850. doi:10.1038/322848a0

Qin HT, Li HQ, Liu F. 2017. Selective histone deacetylase small molecule inhibitors: recent progress and perspectives. *Expert Opin Ther Pat* **27**:621–636. doi:10.1080/13543776.2017.1276565

Ramadoss M, Mahadevan V. 2018. Targeting the cancer epigenome: synergistic therapy with bromodomain inhibitors. *Drug Discov Today* **23**:76–89. doi:10.1016/j.drudis.2017.09.011

Ranuncolo SM, Polo JM, Dierov J, Singer M, Kuo T, Greally J, Green R, Carroll M, Melnick A. 2007. Bcl-6 mediates the germinal center B cell phenotype and lymphomagenesis through transcriptional repression of the DNA-damage sensor ATR. *Nat Immunol* **8**:705–714. doi:ni1478 [pii] 10.1038/ni1478

Ranuncolo SM, Polo JM, Melnick A. 2008. BCL6 represses CHEK1 and suppresses DNA damage pathways in normal and malignant B-cells. *Blood Cells Mol Dis* **41**:95–99. doi:S1079-9796(08)00041-7 [pii] 10.1016/j.bcmd.2008.02.003

Renaud S, Loukinov D, Bosman FT, Lobanenkov V, Benhattar J. 2005. CTCF binds the proximal exonic region of hTERT and inhibits its transcription. *Nucleic Acids Res* **33**:6850–6860. doi:33/21/6850 [pii] 10.1093/nar/gki989

Renda M, Baglivo I, Burgess-Beusse B, Esposito S, Fattorusso R, Felsenfeld G, Pedone P V. 2007. Critical DNA Binding Interactions of the Insulator Protein CTCF. *J Biol Chem* **282**:33336–33345. doi:10.1074/jbc.m706213200

Revilla IDR, Bilic I, Vilagos B, Tagoh H, Ebert A, Tamir IM, Smeenk L, Trupke J, Sommer A, Jaritz M, Busslinger M. 2012. The B-cell identity factor Pax5 regulates distinct transcriptional programmes in early and late B lymphopoiesis. *EMBO J* **31**:3130–3146. doi:10.1038/emboj.2012.155

Ronzoni L, Bonara P, Rusconi D, Frugoni C, Libani I, Cappellini MD. 2007. Erythroid differentiation and maturation from peripheral CD34(+) cells in liquid culture: Cellular and molecular characterization. *Blood Cells Mol Dis*.

Rosa-Garrido M, Ceballos L, Alonso-Lecue P, Abraira C, Delgado MD, Gandarillas A. 2012. A cell cycle role for the epigenetic factor CTCF-L/BORIS. *PLoS One* **7**:e39371. doi:10.1371/journal.pone.0039371

Rosa-Garrido M, Chapski DJ, Vondriska TM. 2018. Epigenomes in Cardiovascular Disease. *Circ Res* **122**:1586–1607. doi:10.1161/CIRCRESAHA.118.311597

Rutherford TR, Clegg JB, Weatherall DJ. 1979. K562 human leukaemic cells synthesise embrionic haemoglobin in response to haemin. *Nature* **280**:164–165.

Sado T. 2004. De novo DNA methylation is dispensable for the initiation and propagation of X chromosome inactivation. *Development* **131**:975–982. doi:10.1242/dev.00995

Saldaña-Meyer R, González-Buendía E, Guerrero G, Narendra V, Bonasio R, Recillas-Targa F, Reinberg D. 2014. CTCF regulates the human p53 gene through direct interaction with its natural antisense transcript, Wrap53. *Genes Dev* **28**:723–734. doi:10.1101/gad.236869.113

Sanada C, Xavier-Ferrucio J, Lu YC, Min E, Zhang PX, Zou S, Kang E, Zhang M, Zerafati G, Gallagher PG, Krause DS. 2016. Adult human megakaryocyte-erythroid progenitors are in the CD34+CD38mid fraction. *Blood* **128**:923–933. doi:10.1182/blood-2016-01-693705

Sawado T, Igarashi K, Groudine M. 2001. Activation of -major globin gene transcription is associated with recruitment of NF-E2 to the -globin LCR and gene promoter. *Proc Natl Acad Sci* **98**:10226–10231. doi:10.1073/pnas.181344198

Schmitz R, Ceribelli M, Pittaluga S, Wright G, Staudt LM. 2014. Oncogenic Mechanisms in Burkitt Lymphoma. *Cold Spring Harb Perspect Med* **4**:1–14.

Schmitz R, Young RM, Ceribelli M, Jhavar S, Xiao W, Zhang M, Wright G, Shaffer AL, Hodson DJ, Buras E, Liu X, Powell J, Yang Y, Xu W, Zhao H, Kohlhammer H, Rosenwald A, Kluin P, Müller-Hermelink HK, Ott G, Gascoyne RD, Connors JM, Rimsza LM, Campo E, Jaffe ES, Delabie J, Smeland EB, Ogwang MD, Reynolds SJ, Fisher RI, Braziel RM, Tubbs RR, Cook JR, Weisenburger DD, Chan WC, Pittaluga S, Wilson W, Waldmann TA, Rowe M, Mbulaiteye SM, Rickinson AB, Staudt LM. 2012. Burkitt lymphoma pathogenesis and therapeutic targets from structural and functional genomics. *Nature* **490**:116–120. doi:10.1038/nature11378

Schuijers J, Manteiga JC, Weintraub AS, Day DS, Zamudio A V, Hnisz D, Lee TI, Young RA. 2018. Transcriptional Dysregulation of MYC Reveals Common Enhancer-Docking Mechanism. *Cell Rep* **23**:349–360. doi:10.1016/j.celrep.2018.03.056

Schwartz YB, Pirrotta V. 2008. Polycomb complexes and epigenetic states. *Curr Opin Cell Biol* **20**:266–273. doi:10.1016/j.ceb.2008.03.002

Seita J, Weissman IL. 2010. Hematopoietic stem cell: Self-renewal versus differentiation. *Wiley Interdiscip Rev Syst Biol Med* **2**:640–653. doi:10.1002/wsbm.86

Seitan VC, Faure AJ, Zhan Y, McCord RP, Lajoie BR, Ing-Simmons E, Lenhard B, Giorgetti L, Heard E, Fisher AG, Flicek P, Dekker J, Merkenschlager M. 2013. Cohesin-Based chromatin interactions enable regulated gene expression within preexisting architectural compartments. *Genome Res* **23**:2066–2077. doi:10.1101/gr.161620.113

Sekiya T, Murano K, Kato K, Kawaguchi A, Nagata K. 2017. Mitotic phosphorylation of CCCTC-binding factor (CTCF) reduces its DNA binding activity. *FEBS Open Bio* **7**:397–404. doi:10.1002/2211-5463.12189

Shaffer AL, Lin K-I, Kuo TC, Yu X, Hurt EM, Rosenwald A, Giltnane JM, Yang L, Zhao H, Calame K, Staudt LM. 2004a. Blimp-1 Orchestrates Plasma Cell Differentiation by Extinguishing the Mature B Cell Gene Expression Program. *Immunity* **17**:51–62. doi:10.1016/s1074-7613(02)00335-7

Shaffer AL, Shapiro-Shelef M, Iwakoshi NN, Lee A-H, Qian S-B, Zhao H, Yu X, Yang L, Tan BK, Rosenwald A, Hurt EM, Petroulakis E, Sonenberg N, Yewdell JW, Calame K, Glimcher LH, Staudt LM. 2004b. XBP1, downstream of Blimp-1, expands the secretory apparatus and other organelles, and increases protein synthesis in plasma cell differentiation. *Immunity* **21**:81–93.

Shaffer AL, Young RM, Staudt LM. 2012. Pathogenesis of Human B Cell Lymphomas. *Annu Rev Immunol* **30**:565–610. doi:10.1146/annurev-immunol-020711-075027

Shaffer AL, Yu X, He Y, Boldrick J, Chan EP, Staudt LM. 2000. BCL-6 represses genes that function in lymphocyte differentiation, inflammation, and cell cycle control. *Immunity* **13**:199–212.

Shahbazian MD, Grunstein M. 2007. Functions of Site-Specific Histone Acetylation and Deacetylation. *Annu Rev Biochem* **76**:75–100. doi:10.1146/annurev.biochem.76.052705.162114

Shao Q, Kannan A, Lin Z, Stack BC, Suen JY, Gao L. 2014. BET protein inhibitor JQ1 attenuates myc-amplified MCC tumor growth in vivo. *Cancer Res* **74**:7090–7102. doi:10.1158/0008-5472.CAN-14-0305

Shapiro-Shelef M, Lin K, Mcheyzer-Williams LJ, Liao J, Mcheyzer-Williams MG, Calame K. 2003. Blimp-1 Is Required for the Formation of Immunoglobulin Secreting Plasma Cells and Pre-Plasma Memory B Cells. *Immunity* **19**:607–620.

Shivdasani RA, Orkin SH. 1996. The Transcriptional Control of Hematopoiesis. *Blood* **87**:4025–4039. doi:DOI: 10.1645/GE-2366.1

Shivdasani RA, Orkin SH. 1995. Erythropoiesis and globin gene expression in mice lacking the transcription factor NF-E2. *Proc Natl Acad Sci* **92**:8690–8694. doi:10.1073/pnas.92.19.8690

Sincennes MC, Humbert M, Grondin B, Lisi V, Veiga DFT, Haman A, Cazaux C, Mashtalir N, Affar ELB, Verreault A, Hoang T. 2016. The LMO2 oncogene regulates DNA replication in hematopoietic cells. *Proc Natl Acad Sci U S A* **113**:1393–1398. doi:10.1073/pnas.1515071113

Smith KGC, Light A, O'Reilly LA, Ang S-M, Strasser A, Tarlinton D. 2000. bcl-2 Transgene Expression Inhibits Apoptosis in the Germinal Center and Reveals Differences in the Selection of Memory B Cells and Bone Marrow Antibody-Forming Cells. *J Exp Med* **191**:475–484. doi:10.1084/jem.191.3.475

Smolewski P, Robak T. 2017. The discovery and development of romidepsin for the treatment of T-cell lymphoma. *Expert Opin Drug Discov* **12**:859–873. doi:10.1080/17460441.2017.1341487

Snow JW, Trowbridge JJ, Johnson KD, Fujiwara T, Emambokus NE, Grass JA, Orkin SH, Bresnick EH, Dc W. 2011. Context-dependent function of ' ' GATA switch ' ' sites in vivo. *Blood* **117**:4769–4772. doi:10.1182/blood-2010-10-313031

Solary E, Bernard OA, Tefferi A, Fuks F, Vainchenker W. 2014. The Ten-Eleven Translocation-2 (TET2) gene in hematopoiesis and hematopoietic diseases. *Leukemia* **28**:485–496. doi:10.1038/leu.2013.337

Song S, Matthias PD. 2018. The transcriptional regulation of germinal center formation. *Front Immunol* **9**:1–9. doi:10.3389/fimmu.2018.02026

Song SH, Kim TY. 2017. CTCF, Cohesin, and Chromatin in Human Cancer. *Genomics*

Inf **15**:114–122. doi:10.5808/GI.2017.15.4.114

Soto-Reyes E, Recillas-Targa F. 2010. Epigenetic regulation of the human p53 gene promoter by the CTCF transcription factor in transformed cell lines. *Oncogene* **29**:2217–2227. doi:10.1038/onc.2009.509

Spangler R, Sytkowski AJ. 1992. c-myc is an erythropoietin early response gene in normal erythroid cells: Evidence for a protein kinase C-mediated signal. *Blood* **79**:52–57.

Splinter E, Heath H, Kooren J, Palstra RJ, Klous P, Grosveld F, Galjart N, de Laat W. 2006. CTCF mediates long-range chromatin looping and local histone modification in the beta-globin locus. *Genes Dev* **20**:2349–2354.

Stadhouders R, Thongjuea S, Andrieu-Soler C, Palstra RJ, Bryne JC, van den Heuvel A, Stevens M, de Boer E, Kockx C, van der Sloot A, van den Hout M, van Ijcken W, Eick D, Lenhard B, Grosveld F, Soler E. 2012. Dynamic long-range chromatin interactions control Myb proto-oncogene transcription during erythroid development. *EMBO J* **31**:986–999. doi:10.1038/emboj.2011.450

Stam M, Tark-Dame M, Fransz P. 2019. 3D genome organization: a role for phase separation and loop extrusion? *Curr Opin Plant Biol* **48**:36–46. doi:10.1016/j.pbi.2019.03.008

Stamatoyannopoulos G. 2005. Control of globin gene expression during development and erythroid differentiation. *Exp Hematol* **33**:259–271.

Steiner LA, Schulz V, Makismova Y, Lezon-Geyda K, Gallagher PG. 2016. CTCF and CohesinSA-1 Mark Active Promoters and Boundaries of Repressive Chromatin Domains in Primary Human Erythroid Cells. *PLoS One* **11**:e0155378. doi:10.1371/journal.pone.0155378

Sun S, Del Rosario BC, Szanto A, Ogawa Y, Jeon Y, Lee JT. 2013. XJpx RNA activates xist by evicting CTCF. *Cell* **153**:1537. doi:10.1016/j.cell.2013.05.028

Suzuki M, Kobayashi-Osaki M, Tsutsumi S, Pan X, Ohmori S, Takai J, Moriguchi T, Ohneda O, Ohneda K, Shimizu R, Kanki Y, Kodama T, Aburatani H, Yamamoto M. 2013. GATA factor switching from GATA2 to GATA1 contributes to erythroid differentiation. *Genes to Cells* **18**:921–933. doi:10.1111/gtc.12086

Suzuki N, Ohneda O, Takahashi S, Higuchi M, Mukai HY, Nakahata T, Imagawa S, Yamamoto M. 2002. Erythroid-specific expression of the erythropoietin receptor rescued its null mutant mice from lethality. *Blood* **100**:2279–2288. doi:10.1182/blood-2002-01-0124

Swerdlow SH, Campo E, Pileri SA, Harris NL, Stein H, Siebert R, Advani R, Ghielmini M, Salles GA, Zelenetz AD, Jaffe ES. 2016. The 2016 revision of the World Health Organization classification of lymphoid neoplasms. *Blood* **127**:2375–2390. doi:10.1182/blood-2016-01-643569

Szalaj P, Plewczynski D. 2018. Three-dimensional organization and dynamics of the genome. *Cell Biol Toxicol* **34**:381–404. doi:10.1007/s10565-018-9428-y

Tanimoto K, Sugiura A, Omori A, Felsenfeld G, Engel JD, Fukamizu A. 2003. Human beta-globin locus control region HS5 contains CTCF- and developmental stage-dependent enhancer-blocking activity in erythroid cells. *Mol Cell Biol* **23**:8946–8952.

Taylor JJ, Pape KA, Steach HR, Jenkins MK. 2015. Apoptosis and antigen affinity limit effector cell differentiation ofa single naïve B cell. *Science (80-)* **347**:784–787.

Tiffen JC, Bailey CG, Marshall AD, Metierre C, Feng Y, Wang Q, Watson SL, Holst J, Rasko JEJ. 2013. The cancer-testis antigen BORIS phenocopies the tumor suppressor CTCF in normal and neoplastic cells. *Int J Cancer* **133**:1603–1613.

doi:10.1002/ijc.28184

Torrano V, Chernukhin I, Docquier F, D'Arcy V, León J, Klenova E, Delgado MD. 2005. CTCF regulates growth and erythroid differentiation of human myeloid leukemia cells. *J Biol Chem* **280**:28152–28161. doi:10.1074/jbc.M501481200

Torrano V, Navascues J, Docquier F, Zhang R, Burke LJ, Chernukhin I, Farrar D, Leon J, Berciano MT, Renkawitz R, Klenova E, Lafarga M, Delgado MD. 2006. Targeting of CTCF to the nucleolus inhibits nucleolar transcription through a poly(ADP-ribosyl)ation-dependent mechanism. *J Cell Sci* **119**:1746–1759.

Tsai FY, Orkin SH. 1997. Transcription factor GATA-2 is required for proliferation/survival of early hematopoietic cells and mast cell formation, but not for erythroid and myeloid terminal differentiation. *Blood* **89**:3636–43.

Tsiftsoglou AS, Vizirianakis IS, Strouboulis J. 2009. Erythropoiesis: model systems, molecular regulators, and developmental programs. *IUBMB Life* **61**:800–830.

Tunyaplin C, Shaffer AL, Angelin-Duclos CD, Yu X, Staudt LM, Calame KL. 2004. Direct repression of prdm1 by Bcl-6 inhibits plasmacytic differentiation. *J Immunol* **173**:1158–65. doi:10.4049/jimmunol.173.2.1158

Tuupanen S, Turunen M, Lehtonen R, Hallikas O, Vanharanta S, Kivioja T, Björklund M, Wei G, Yan J, Niittymäki I, Mecklin JP, Järvinen H, Ristimäki A, Di-Bernardo M, East P, Carvajal-Carmona L, Houlston RS, Tomlinson I, Palin K, Ukkonen E, Karhu A, Taipale J, Aaltonen LA. 2009. The common colorectal cancer predisposition SNP rs6983267 at chromosome 8q24 confers potential to enhanced Wnt signaling. *Nat Genet* **41**:885–890. doi:10.1038/ng.406

Ueda H, Manda T, Matsumoto S, Mukumoto S, Nishigaki F, Kawamura I, Shimomura K. 1994. FR901228, a novel antitumor bicyclic depsipeptide produced by Chromobacterium violaceum. *J Antibiot (Tokyo)* **47**:315–323. doi:10.7164/antibiotics.47.315

Ulianov S V., Gavrilov AA, Razin S V. 2012. Spatial organization of the chicken beta-globin gene domain in erythroid cells of embryonic and adult lineages. *Epigenetics and Chromatin* **5**:1. doi:10.1186/1756-8935-5-16

Valadez-Graham V, Razin S V, Recillas-Targa F. 2004. CTCF-dependent enhancer blockers at the upstream region of the chicken alpha-globin gene domain. *Nucleic Acids Res* **32**:1354–1362.

van de Nobelen S, Rosa-Garrido M, Leers J, Heath H, Soochit W, Joosen L, Jonkers I, Demmers J, van der Reijden M, Torrano V, Grosveld F, Delgado MD, Renkawitz R, Galjart N, Sleutels F. 2010. CTCF regulates the local epigenetic state of ribosomal DNA repeats. *Epigenetics Chromatin* **3**:19. doi:10.1186/1756-8935-3-19

Vandermolen KM, McCulloch W, Pearce CJ, Oberlies NH. 2011. Romidepsin (Istodax, NSC 630176, FR901228, FK228, depsipeptide): A natural product recently approved for cutaneous T-cell lymphoma. *J Antibiot (Tokyo)* **64**:525–531. doi:10.1038/ja.2011.35

Victora GD, Nussenzweig MC. 2012. Germinal Centers. *Annu Rev Immunol* **30**:429–457. doi:10.1146/annurev-immunol-020711-075032

Vietri Rudan M, Barrington C, Henderson S, Ernst C, Odom DT, Tanay A, Hadjur S. 2015. Comparative Hi-C Reveals that CTCF Underlies Evolution of Chromosomal Domain Architecture. *Cell Rep* **10**:1297–1309. doi:10.1016/j.celrep.2015.02.004

Vikstrom I, Carotta S, Luthje K, Peperzak V, Jost PJ, Glaser S, Busslinger M, Bouillet P, Strasser A, Nutt SL, Tarlinton DM. 2010. Mcl-1 is essential for germinal center formation and B cell memory. *Science (80-)* **330**:1095–1099.

doi:10.1126/science.1191793

Vostrov AAAA, Quitschke WWW. 1997. The Zinc Finger Protein CTCF Binds to the APBβ Domain of the Amyloid β-Protein Precursor Promoter. *J Biol Chem* **272**:33353–33359. doi:10.1074/jbc.272.52.33353

Wan L-B, Pan H, Hannenhalli S, Cheng Y, Ma J, Fedoriw A, Lobanenkov V, Latham KE, Schultz RM, Bartolomei MS. 2008. Maternal depletion of CTCF reveals multiple functions during oocyte and preimplantation embryo development. *Development* **135**:2729–2738. doi:10.1242/dev.024539

Wang H, Maurano MT, Qu H, Varley KE, Gertz J, Pauli F, Lee K, Canfield T, Weaver M, Sandstrom R, Thurman RE, Kaul R, Myers RM, Stamatoyannopoulos JA. 2012. Widespread plasticity in CTCF occupancy linked to DNA methylation. *Genome Res* **22**:1680–1688. doi:10.1101/gr.136101.111

Wang Q, Zhong H. 2015. Epigenetic programming contributes to development of drug resistance in hematological malignancies. *Front Biosci* **20**:728–742. doi:10.2741/4333

Wang W, Horner DN, Chen WLK, Zandstra PW, Audet J. 2008. Synergy between erythropoietin and stem cell factor during erythropoiesis can be quantitatively described without co-signaling effects. *Biotechnol Bioeng* **99**:1261–1272. doi:10.1002/bit.21677

Wang X, Angelis N, Thein SL. 2018. MYB – A regulatory factor in hematopoiesis. *Gene* **665**:6–17. doi:10.1016/j.gene.2018.04.065

Warren AJ, Colledge WH, Carlton MBL, Evans MJ, Smith AJH, Rabbitts TH. 1994. The Oncogenic Cysteine-rich LIM domain protein Rbtn2 is essential for erythroid development. *Cell* **78**:45–57. doi:10.1016/0092-8674(94)90571-1

Weiss MJ, Orkin SH. 1995. Transcription factor GATA-1 permits survival and maturation of erythroid precursors by preventing apoptosis. *Proc Natl Acad Sci* **92**:9623–9627. doi:10.1073/pnas.92.21.9623

Welch JJ, Watts JA, Vakoc CR, Yao Y, Wang H, Hardison RC, Blobel GA, Chodosh LA, Weiss MJ. 2004. Global regulation of erythroid gene expression by transcription factor GATA-1. *Blood* **104**:3136–3147.

Wendt KS, Yoshida K, Itoh T, Bando M, Koch B, Schirghuber E, Tsutsumi S, Nagae G, Ishihara K, Mishiro T, Yahata K, Imamoto F, Aburatani H, Nakao M, Imamoto N, Maeshima K, Shirahige K, Peters JM. 2008. Cohesin mediates transcriptional insulation by CCCTC-binding factor. *Nature* **451**:796–801.

Weth O, Renkawitz R. 2011. CTCF function is modulated by neighboring DNA binding factors. *Biochem Cell Biol* **89**:459–468. doi:10.1139/o11-033

Witcher M, Emerson BM. 2009. Epigenetic silencing of the p16(INK4a) tumor suppressor is associated with loss of CTCF binding and a chromatin boundary. *Mol Cell* **34**:271–284.

Wozniak RJ, Bresnick EH. 2008. Epigenetic control of complex loci during erythropoiesis. *Curr Top Dev Biol* **82**:55–83.

Wutz G, Várnai C, Nagasaka K, Cisneros DA, Stocsits RR, Tang W, Schoenfelder S, Jessberger G, Muhar M, Hossain MJ, Walther N, Koch B, Kueblbeck M, Ellenberg J, Zuber J, Fraser P, Peters J-M. 2017. Topologically associating domains and chromatin loops depend on cohesin and are regulated by CTCF, WAPL, and PDS5 proteins. *EMBO J* **36**:3573–3599. doi:10.15252/embj.201798004

Xiang JF, Yin QF, Chen T, Zhang Y, Zhang XO, Wu Z, Zhang S, Wang HB, Ge J, Lu X, Yang L, Chen LL. 2014. Human colorectal cancer-specific CCAT1-L lncRNA

regulates long-range chromatin interactions at the MYC locus. *Cell Res* **24**:513–531. doi:10.1038/cr.2014.35

Xu D, Ma R, Zhang J, Liu Z, Wu B, Peng J, Zhai Y, Gong Q, Shi Y, Wu J, Wu Q, Zhang Z, Ruan K. 2018. Dynamic Nature of CTCF Tandem 11 Zinc Fingers in Multivalent Recognition of DNA As Revealed by NMR Spectroscopy. *J Phys Chem Lett* **9**:4020–4028. doi:10.1021/acs.jpclett.8b01440

Xu N, Donohoe ME, Silva SS, Lee JT. 2007. Evidence that homologous X-chromosome pairing requires transcription and Ctcf protein. *Nat Genet* **39**:1390–1396. doi:10.1038/ng.2007.5

Xue K, Gu JJ, Zhang Q, Mavis C, Hernandez-Ilizaliturri FJ, Czuczman MS, Guo Y. 2016. Vorinostat, a histone deacetylase (HDAC) inhibitor, promotes cell cycle arrest and re-sensitizes rituximab- and chemo-resistant lymphoma cells to chemotherapy agents. *J Cancer Res Clin Oncol* **142**:379–387. doi:10.1007/s00432-015-2026-y

Ye BH, Cattoretti G, Shen Q, Zhang J, Hawe N, de Waard R, Leung C, Nouri-Shirazi M, Orazi A, Chaganti RS, Rothman P, Stall AM, Pandolfi PP, Dalla-Favera R. 1997. The BCL-6 proto-oncogene controls germinal-centre formation and Th2-type inflammation. *Nat Genet* **16**:161–170.

Yin M, Wang J, Wang M, Li X, Zhang M, Wu Q, Wang Y. 2017. Molecular mechanism of directional CTCF recognition of a diverse range of genomic sites. *Cell Res* **27**:1365–1377. doi:10.1038/cr.2017.131

Ying CY, Dominguez-Sola D, Fabi M, Lorenz IC, Hussein S, Bansal M, Califano A, Pasqualucci L, Basso K, Dalla-Favera R. 2013. MEF2B mutations lead to deregulated expression of the oncogene BCL6 in diffuse large B cell lymphoma. *Nat Immunol* **14**:1084–1092. doi:10.1038/ni.2688

Yu W, Ginjala V, Pant V, Chernukhin I, Whitehead J, Docquier F, Farrar D, Tavoosidana G, Mukhopadhyay R, Kanduri C, Oshimura M, Feinberg AP, Lobanenkov V, Klenova E, Ohlsson R. 2004. Poly(ADP-ribosyl)ation regulates CTCF-dependent chromatin insulation. *Nat Genet* **36**:1105–1110.

Yusufzai TM, Tagami H, Nakatani Y, Felsenfeld G. 2004. CTCF tethers an insulator to subnuclear sites, suggesting shared insulator mechanisms across species. *Mol Cell* **13**:291–298.

Zhang J, Ding L, Holmfeldt L, Wu G, Heatley SL, Payne-Turner D, Easton J, Chen X, Wang J, Rusch M, Lu C, Chen SC, Wei L, Collins-Underwood JR, Ma J, Roberts KG, Pounds SB, Ulyanov A, Becksfort J, Gupta P, Huether R, Kriwacki RW, Parker M, McGoldrick DJ, Zhao D, Alford D, Espy S, Bobba KC, Song G, Pei D, Cheng C, Roberts S, Barbato MI, Campana D, Coustan-Smith E, Shurtleff SA, Raimondi SC, Kleppe M, Cools J, Shimano KA, Hermiston ML, Doulatov S, Eppert K, Laurenti E, Notta F, Dick JE, Basso G, Hunger SP, Loh ML, Devidas M, Wood B, Winter S, Dunsmore KP, Fulton RS, Fulton LL, Hong X, Harris CC, Dooling DJ, Ochoa K, Johnson KJ, Obenauer JC, Evans WE, Pui CH, Naeve CW, Ley TJ, Mardis ER, Wilson RK, Downing JR, Mullighan CG. 2012. The genetic basis of early T-cell precursor acute lymphoblastic leukaemia. *Nature* **481**:157–163. doi:10.1038/nature10725

Zhang R, Burke LJ, Rasko JE, Lobanenkov V, Renkawitz R. 2004. Dynamic association of the mammalian insulator protein CTCF with centrosomes and the midbody. *Exp Cell Res* **294**:86–93.

Zhang Y, Adachi M, Zhao X, Kawamura R, Imai K. 2004. Histone deacetylase inhibitors FK228, N-(2-aminophenyl)-4-[N-(pyridin-3-yl-methoxycarbonyl)amino-methyl]benzamide and m-carboxycinnamic acid bis-hydroxamide augment radiation-induced cell death in gastrointestinal adenocarcinoma cells. *Int J Cancer*

110:301–308. doi:10.1002/ijc.20117

Zhang Y, Adachi M, Zou H, Hareyama M, Imai K, Shinomura Y. 2006. Histone deacetylase inhibitors enhance phosphorylation of histone H2AX after ionizing radiation. *Int J Radiat Oncol Biol Phys* **65**:859–866. doi:10.1016/j.ijrobp.2006.03.019

Zhao L, Okhovat JP, Hong EK, Kim YH, Wood GS. 2019. Preclinical Studies Support Combined Inhibition of BET Family Proteins and Histone Deacetylases as Epigenetic Therapy for Cutaneous T-Cell Lymphoma. *Neoplasia* **21**:82–92. doi:10.1016/j.neo.2018.11.006

Zheng H, Xie W. 2019. The role of 3D genome organization in development and cell differentiation. *Nat Rev Mol Cell Biol*. doi:10.1038/s41580-019-0132-4

Zlatanova J, Caiafa P. 2009. CTCF and its protein partners: divide and rule? *J Cell Sci* **122**:1275–1284. doi:10.1242/jcs.039990

Zuin J, Dixon JR, van der Reijden MIJA, Ye Z, Kolovos P, Brouwer RWW, van de Corput MPC, van de Werken HJG, Knoch TA, van IJcken WFJ, Grosveld FG, Ren B, Wendt KS. 2014. Cohesin and CTCF differentially affect chromatin architecture and gene expression in human cells. *Proc Natl Acad Sci* **111**:996–1001. doi:10.1073/pnas.1317788111

RESUMEN EN CASTELLANO

8. RESUMEN EN CASTELLANO

8.1. Introducción

CTCF es una proteína del tipo “dedos de zinc” que puede unirse a un amplio rango de secuencias diana usando diferentes combinaciones de sus dedos de zinc. CTCF fue inicialmente descrito como un represor transcripcional del oncogén c-*MYC* de pollo (Filippova et al., 1996). CTCF está implicado en muchas funciones reguladoras entre las que se incluyen activación o represión transcripcional de numerosos genes, unión a secuencias “insulator” para impedir el avance de la heterocromatina o bloqueando la acción de “enhancers” y organizador global de la cromatina (Arzate-Mejía et al., 2018; Kim et al., 2015; Xu et al., 2018). Mutaciones en los dedos de zinc del domino de unión al DNA de CTCF o mutaciones en los sitios diana de unión de CTCF, se relacionan frecuentemente con la desregulación de CTCF y el desarrollo de tumores (Filippova et al., 2002; Katainen et al., 2015). Además, CTCF participa en la regulación epigenética de numerosos genes implicados en cáncer como *MYC* o *BCL6*.

La eritropoyesis es el proceso de diferenciación de las células madre hematopoyéticas en diferentes progenitores eritroides para finalmente dar lugar a los eritrocitos maduros. Es un proceso altamente regulado y controlado por numerosas citoquinas y factores de crecimiento como eritropoyetina o SCF y factores de transcripción específicos, entre ellos GATA1, GATA2, MYB o KLF1 (Dzierzak and Philipsen, 2013; Nandakumar et al., 2016). Además, el factor de transcripción MYC también participa en la regulación de la diferenciación eritroide (Delgado and Leon, 2010). Entre todas las funciones en las que está involucrado CTCF también se encuentra la regulación de la eritropoyesis. Resultados previos de nuestro grupo han demostrado que la sobreexpresión de CTCF induce la diferenciación eritroide en células K562 (Torrano et al., 2005). Diferentes estudios describen que la unión de CTCF es necesaria para la transcripción de genes eritroides (Kang et al., 2017).

Los centros germinales son estructuras dinámicas dentro de los ganglios linfáticos y son esenciales para la formación de anticuerpos de alta afinidad. Histológicamente se dividen en dos zonas, la zona oscura y la zona clara. La zona oscura contiene células B altamente proliferativas que sufren hipermutación somática de las inmunoglobulinas mientras que la zona clara las células B se seleccionan dependiendo de su afinidad por el antígeno para sobrevivir, volver a la zona oscura o diferenciar a célula B de memoria o células plasmáticas (Bannard and Cyster, 2017; Basso and Dalla-Favera, 2015). Una compleja red de factores de transcripción regula el equilibrio entre los procesos que tienen lugar en el centro germinal. BCL6 es un represor transcripcional indispensable para la generación del centro germinal linfoide. Su expresión tiene que ser reducida para que las células B abandonen el centro germinal y diferencien a células plasmáticas (Song and Matthias, 2018). Los linfomas agresivos, como el linfoma de Burkitt o el linfoma difuso de célula grande derivan de las células B del centro germinal (Swerdlow et al., 2016). Los tratamientos convencionales para los linfomas agresivos no son muy efectivos por lo que es importante identificar estrategias novedosas para su tratamiento, como las terapias epigenéticas.

Los mecanismos epigenéticos están involucrados en la regulación de la expresión génica y en el control de numerosos procesos biológicos. Sus alteraciones pueden generar expresión génica aberrante. La desregulación epigenética es frecuente en células cancerosas (Ahuja et al., 2016). A diferencia de las mutaciones genómicas, las alteraciones epigenéticas son potencialmente reversibles mediante el uso de fármacos, por lo que la terapia con fármacos epigenéticos tiene un enorme potencial para el tratamiento del cáncer (Ahuja et al., 2016). Recientemente, se han realizado estudios con resultados prometedores en los que se combinan inhibidores de HDAC con inhibidores de bromodominios BET (Ramadoss and Mahadevan, 2018). La romidepsina es un inhibidor de histonas deacetilasa (HDACi) aprobado por la FDA para el tratamiento de algunos linfomas de células T, pero su efecto sobre los linfomas de células B y sobre la regulación de BCL6 no se ha investigado a fondo (Bates et al., 2015). Por otro lado, JQ1 es un inhibidor de bromodominios BET que reprime la expresión de algunos genes como por ejemplo MYC (Delmore et al.,

2011). La desregulación de MYC es prevalente en linfomas y se asocia a un peor pronóstico en linfomas derivados del centro germinal (Nguyen et al., 2017).

8.2. Objetivos

El objetivo general de la primera parte de este trabajo es estudiar la función de CTCF en la regulación de la diferenciación eritroide en células hematopoyéticas humanas. Para ello establecimos los siguientes objetivos:

1. Analizar los efectos del silenciamiento de CTCT en la diferenciación eritroide de células K562.
2. Explorar el papel de CTCF en la diferenciación de células primarias $CD34^+$.
3. Identificar factores de transcripción eritroides regulados por CTCF.
4. Estudiar la unión de CTCF a regiones reguladores de factores de transcripción eritroides durante la inducción de la diferenciación eritroide.
5. Analizar la unión de CTCF a las regiones reguladores de *MYC*.

Por otro lado, el objetivo general de la segunda parte de este trabajo es investigar los efectos de la romidepsina en combinación con JQ1 en el tratamiento de linfoma de células B agresivos. Para ello se establecieron los siguientes objetivos:

1. Estudiar los efectos del tratamiento combinado de romidepsina y JQ1 en proliferación celular, apoptosis y ciclo celular.
2. Analizar el efecto del tratamiento con romidepsina y JQ1 en la expresión de BCL6 y en la diferenciación de células B.

8.3. Resultados y discusión

8.3.1. Función de CTCF en el control de la diferenciación eritroide

Para estudiar el papel de CTCF en la diferenciación eritroide silenciamos la expresión de CTCF (mediante vectores lentivirales constitutivos pLKO-shCTCF) en células K562 e indujimos la diferenciación a linaje eritroide con Ara-C o Imatinib. El silenciamiento de CTCF redujo el porcentaje de células bencidina positivas (indicativo de células diferenciadas conteniendo hemoglobina) y la expresión de genes eritroides (γ-globina, GATA1 y LMO2) en comparación con las células no silenciadas. Estos resultados indican que la inhibición de CTCF puede inhibir la diferenciación eritroide. Para confirmar estos resultados, utilizamos un sistema inducible por doxiciclina para inhibir CTCF (pTRIPZ-shCTCF). Los resultados obtenidos fueron similares a los observados al inhibir CTCF con el vector constitutivo. Todos estos resultados demuestran que CTCF tiene un papel fundamental en la eritropoyesis ya que su silenciamiento inhibe la diferenciación eritroide inducida por Ara-C e Imatinib en células K562.

Como un modelo más fisiológico de estudio utilizamos células primarias $CD34^+$ purificadas a partir de sangre de cordón umbilical de recién nacidos. Silenciamos la expresión de CTCF (mediante vectores lentivirales pLKO-shCTCF) en células $CD34^+$ y las tratamos con eritropoyetina para inducir la diferenciación eritroide. Observamos que la inhibición de CTCF reduce el porcentaje de células bencidina positivas, la expresión de genes eritroides (γ-globina y GATA1) e inhibe la formación de colonias en comparación con las células no silenciadas. Estos resultados se confirmaron inhibiendo CTCF mediante el sistema inducible por doxiciclina. Al igual que con el sistema constitutivo observamos que la inhibición de CTCF disminuye el porcentaje de células diferenciadas en comparación con las células no silenciadas. Todos estos resultados indican que el silenciamiento de CTCF inhibe la diferenciación eritroide en células madre hematopoyéticas primarias y corroboran el papel de CTCF en la eritropoyesis.

Resultados previos de nuestro grupo identificaron una serie de genes relacionados con la diferenciación eritroide que parecían estar regulados por CTCF. Seleccionamos genes que inhiben la diferenciación eritroide (*ETS1, GATA2, HEY1* y *MYB*) y genes que inducen la diferenciación eritroide (*KLF1*, *LMO2*, *NFE2L2* y *TCF3*) y realizamos un análisis mediante la base de datos ENCODE para localizar posibles sitios de unión de CTCF a las regiones reguladoras de esos genes. Analizamos la unión de CTCF mediante ensayos de inmunoprecipitación de cromatina (ChIP) en células K562. Los resultados obtenidos revelaron un elevado enriquecimiento de CTCF en todos los sitios analizados de los diferentes genes eritroides.

Para estudiar si la unión de CTCF a los diferentes genes eritroides varia durante la inducción de la diferenciación eritroide, tratamos células K562 con Ara-C para inducir la diferenciación eritroide. El siguiente paso fue analizar la unión de CTCF a los genes eritroides seleccionados después de la inducción de la diferenciación eritroide mediante ChIP. Los resultados obtenidos indican que la unión de CTCF en los diferentes sitios analizados aumenta durante la diferenciación eritroide independientemente del aumento o disminución de la expresión del correspondiente gen. Estos resultados se podrían relacionar con el doble papel de CTCF como activador o represor transcripcional.

Finalmente, para analizar si la expresión de MYC está regulada por CTCF analizamos mediante la base de datos ENCODE, los posibles sitios de unión de CTCF a las regiones reguladoras de *MYC*. Encontramos varios posibles sitios de unión, algunos de ellos descritos previamente. Analizamos la unión de CTCF a los diferentes sitios de *MYC* mediante ensayos de inmunoprecipitación de cromatina (ChIP) en células K562. Los resultados obtenidos mostraron un alto enriquecimiento de CTCF en todos los sitios analizados. Una vez confirmada la unión de CTCF a los diferentes sitios de MYC, analizamos si esa unión variaba durante la diferenciación eritroide inducida por Ara-C e Imatinib. Los resultados obtenidos revelaron que la unión de CTCF a los diferentes sitios de MYC aumentaba durante la diferenciación eritroide. Dado que durante la diferenciación eritroide la expresión de MYC disminuye, el aumento de la unión

de CTCF a las regiones reguladoras de MYC puede indicar que CTCF regula negativamente la expresión de MYC durante la diferenciación eritroide.

8.3.2. Tratamiento epigenético de linfomas agresivos de células B

Para analizar los efectos del tratamiento combinado con los fármacos epigenéticos romidepsina (inhibidor de histona deacetilasa) y JQ1 (inhibidor de BRD4), tratamos diferentes líneas celulares de linfoma de células B (Ramos, Raji y DG75 procedentes de linfoma de Burkitt y Toledo de GCB-DLBCL). Estas líneas celulares presentan expresión desregulada de BCL6 y/o MYC. Tras el tratamiento analizamos la actividad metabólica (ensayo WST-1), proliferación celular (contaje celular), viabilidad (Trypan Blue), apoptosis (ruptura de PARP y expresión de genes de la familia de BCL2 por Western-Blot y Anexina-V por citometría de flujo), ciclo celular (citometría de flujo y expresión de MYC, p27, p21 y Ciclina-A) y la diferenciación de células B (expresión de BLC6 y BLIMP1).

Realizamos ensayos WST con diferentes combinaciones de ambos tratamientos para calcular el índice de combinación (CI). Las dosis seleccionadas para realizar los diferentes experimentos fueron 5 nM de romidepsina y 1 μM de JQ1, estas dosis tienen un efecto sinérgico (CI < 1) especialmente en Ramos y Raji.

Los resultados obtenidos indicaron que ambos tratamientos y su combinación reducen la actividad metabólica en Ramos, Raji, DG75 y Toledo. Resultados similares se obtuvieron con el tratamiento solo con romidepsina como con la combinación de romidepsina y JQ1, mientras que la reducción en la actividad metabólica observada fue menor cuando se trataron solo con JQ1. Además, observamos una reducción en la proliferación celular en células tratadas solo con romidepsina o con JQ1, siendo la reducción mayor con romidepsina. Sin embargo, la combinación de tratamientos inhibió casi completamente la proliferación celular en las cuatro líneas celulares estudiadas.

Por otro lado, observamos una disminución en el porcentaje de células viables con los tratamientos con romidepsina (sola o en combinación con JQ1)

en Ramos, Raji y Toledo. Este resultado se relaciona con el aumento del porcentaje de células anexina-V positivas con la combinación de tratamientos y con el tratamiento solo con romidepsina en Ramos, Raji y Toledo, siendo el aumento mucho mayor con el tratamiento combinado. La inducción de la apoptosis se confirmó mediante la ruptura del PARP1 y el descenso de los niveles de la proteína antiapoptótica BCL-xL observados por Western-Blot. Además, la combinación de tratamientos indujo la expresión del marcador de respuesta a daño al ADN γH2AX. Estos resultados indican un efecto sinérgico en apoptosis entre la romidepsina y el JQ1 en las líneas celulares de linfoma B Ramos, Raji y Toledo.

También analizamos el efecto de la combinación de romidepsina y JQ1 en el ciclo celular. El análisis por citometría de flujo mostro una ligera acumulación de células en la fase G_0/G_1 del ciclo celular en Ramos, Raji y Toledo con la combinación de tratamientos al igual que con el tratamiento con romidepsina sola, por el contrario, el tratamiento con JQ1 si provocó parada del ciclo celular en fase G_0/G_1. Sin embargo, al analizar la expresión de p27 y p21 por Western-Blot observamos un aumento en su expresión en todas las líneas analizadas. Además, el descenso en los niveles de MYC y de Ciclina-A observados confirman que la combinación de romidepsina y JQ1 provocan parada del ciclo celular en líneas celulares de linfoma de células B.

Finalmente, en las líneas celulares que expresan BCL6 (Ramos, Raji y Dg75) observamos una reducción de la expresión de BCL6 a nivel de proteína con los tratamientos solos y con la combinación, siendo más pronunciada con el tratamiento combinado, mientras que los niveles de BLIMP1 aumentaron ligeramente en Ramos. Además, en Toledo, una línea celular que no expresa BCL6, también observamos un aumento de la expresión de BLIMP1 con la combinación de tratamientos. Estos resultados indican que el tratamiento combinado de romidepsina con JQ1 induce diferenciación a célula plasmática.

En resumen, el tratamiento combinado de romidepsina y JQ1 induce sinérgicamente apoptosis, parada del ciclo celular y diferenciación de célula plasmáticas en células de linfoma de células B. Además, el tratamiento

combinado es más efectivo que cada tratamiento individual, lo que sugiere que JQ1 potencia los efectos de la romidepsina. Nuestros resultados indican que el tratamiento combinado de romidepsina y JQ1 podría ser efectivo en el tratamiento de linfomas de células B.

8.4. Conclusiones

1. El silenciamiento de CTCF inhibe la diferenciación eritroide inducida por Ara-C e Imatinib en células K562.
2. El silenciamiento de CTCF inhibe la diferenciación eritroide inducida por eritropoyetina en células primarias $CD34^+$.
3. CTCF se une a las regiones reguladoras de factores de trascripción eritroides. La unión de CTCF participa en la formación de interacciones
4. La unión de CTCF a genes eritroides aumenta durante la inducción de la diferenciación eritroide.
5. CTCF se une a las regiones reguladoras de *MYC* y la unión aumenta durante la inducción de la diferenciación eritroide.
6. La unión de CTCF a factores de transcripción se relaciona con sus funciones en la regulación de la diferenciación eritroide.
7. Proponemos que CTCF tiene un papel esencial en la diferenciación eritroide a través de la regulación directa de factores de transcripción.
8. El tratamiento con romidepsina y JQ1 reduce la actividad metabólica y la proliferación celular en líneas celulares de linfoma de células B.
9. La combinación de romidepsina y JQ1 induce fuertemente apoptosis en linfoma de células B.
10. El tratamiento con romidepsina y JQ1 induce parada del ciclo celular acompañado con un incremento en los niveles de p21 o p27 y la reducción de la expresión de MYC.
11. La combinación de romidepsina y JQ1 induce diferenciación a célula plasmática y la reducción de la expresión de BCL6 en células de linfoma de células B.
12. Romidepsina y JQ1 tienen un efecto sinérgico mostrando un importante papel para el tratamiento de linfomas agresivos de células B.

PUBLICATIONS

SREP-18-47112

Title

Suppression of BCL6 function by HDAC inhibitor mediated acetylation and chromatin modification enhances BET inhibitor effects in B-cell lymphoma cells

Author names and Addresses

María G. Cortiguera[1,2,4], Lorena García-Gaipo[1,4], Simon D. Wagner[3], Javier León[1], Ana Batlle-López[2*] and M. Dolores Delgado[1*].

[1]Instituto de Biomedicina y Biotecnología de Cantabria (IBBTEC) CSIC-Universidad de Cantabria, and Dpt. of. Biología Molecular, Universidad de Cantabria, Santander, Spain.

[2]Servicio de Hematologia, Hospital Marqués de Valdecilla-IDIVAL, Santander, Spain.

[3]Leicester Cancer Research Centre and Ernest and Helen Scott Haematological Research Unit, University of Leicester, Leicester LE1 7HB, UK

[4]Both authors contributed equally to this work

***Corresponding authors**

Prof. M. Dolores Delgado, Instituto de Biomedicina y Biotecnología de Cantabria (IBBTEC) c/Albert Einstein 22, 39011 Santander, Spain.

Tel: 34 942-201998. Email: maria.delgado@unican.es

Dr. Ana Batlle-López, Servicio de Hematologia, Hospital Marqués de Santander, Spain.

Tel: 34-942-202520. Email: mana.batlle@scsalud.es

Abstract

Multiple genetic aberrations in the regulation of BCL6, including in acetyltransferase genes, occur in clinically aggressive B-cell lymphomas and lead to higher expression levels and activity of this transcriptional repressor. BCL6 is, therefore, an attractive target for therapy in aggressive lymphomas. In this study romidepsin, a potent histone deacetylase inhibitor (HDACi), induced apoptosis and cell cycle arrest in Burkitt and diffuse large B-cell lymphoma cell lines, which are model cells for studying the mechanism of action of BCL6. Romidepsin caused BCL6 acetylation at early timepoints inhibiting its function, while at later timepoints BCL6 expression was reduced and target gene expression increased due to chromatin modification. MYC contributes to poor prognosis in aggressive lymphoma. MYC function is reduced by inhibition of chromatin readers of the bromodomain and extra-terminal repeat (BET) family, which includes BRD4. The novel combination of romidepsin and JQ1, a BRD4 inhibitor was investigated and showed synergy. Collectively we suggest that the combination of HDACi and BRD4i should be pursued in further pre-clinical testing.

Introduction

Aggressive lymphomas such as diffuse large B-cell lymphoma (DLBCL) and Burkitt lymphoma (BL) are a heterogeneous group of disorders in terms of clinical behavior, biological characteristics and response to treatments [1]. Despite improvements in diagnosis and treatment, non-Hodgkins-lymphomas are still an important cause of morbidity and mortality worldwide. Combination of rituximab with anthracycline-based chemotherapy regimen, such as R-CHOP (Rituximab-cyclophosphamide, doxorubicin, vincristine and prednisone) is effective [2] but overall >40% of patients are not cured of their disease. Thus, it is important to identify new approaches to therapy. Aggressive lymphomas are often derived from germinal center B-cells. Germinal centers are dynamic structures within normal lymph nodes, where B-cells proliferate intensely and undergo somatic hypermutation [3], a process involving the production of DNA breaks that is essential for the formation of high affinity antibodies. Conditions within the germinal center are therefore believed to predispose to the formation of lymphomas [3]. There is a wealth of genetic evidence that BCL6 contributes to the survival of DLBCL and clinical evidence suggests that a proportion of BCL6 expressing DLBCL patients have poor clinical outcomes. The role of BCL6 in Burkitt lymphoma has not been investigated but it is expressed in all cases and is likely to contribute to proliferation and survival.

BCL6 is a master transcription factor that is essential for normal germinal center formation [4,5]. Enforced expression of BCL6 in mice is sufficient for the development of lymphomas [6]. Multiple genetic abnormalities leading to increased BCL6 expression have been described [7,8] and BCL6 is also involved in chromosomal translocations in ~25% of DLBCL [9]. Thus, modulation of *BCL6* expression could be a potential target for therapy in lymphomas. Indeed, BCL6 inhibition using specific inhibitors was able to produce apoptosis and cell cycle arrest of these cells [10,11] suggesting that BCL6 may be a promising therapeutic target in lymphoma [12].

We and others, have recently shown that epigenetic mechanisms are involved in *BCL6* regulation [13-15]. Histone deacetylase inhibitors (HDACi) are a novel class of antitumor agents that have shown very promising results for the treatment of a number of hematologic malignancies [16,17]. Regulation of the reversible acetylation status of an increasing number of non-histone proteins, many of them being proto-oncogenes, allows to modulate a number of essential cellular processes such as protein interactions, protein stability, apoptosis, cell proliferation and cell survival [18].

Particularly, HDAC inhibitors have been shown to inhibit BCL6 function by inducing its acetylation, which leads to de-repression of its target genes [19]. Romidepsin is an HDACi with high inhibitory activity for class I histone deacetylases that is approved by the FDA for the treatment of cutaneous T-cell lymphoma or refractory/relapsed peripheral T-cell lymphoma [20,21]. HDACi synergize with other agents including hypomethylating agents in pre-clinical models of DLBCL [22].

MYC translocations occur in 10-15% of DLBCL [1]. High expression of MYC, independent of the presence of chromosomal translocations involving MYC, is associated with poor clinical outcome in B-cell lymphoma [23,24]. There is interest in the bromodomain and extra-terminal (BET) family member BRD4, which recognizes acetylated histones and plays an essential role in the regulation of *MYC* expression [25]. BRD4 (bromodomain-containing protein-4) inhibitors [26] such as JQ1 are able to cause *MYC* oncogene downregulation in a variety of human cancers, including leukemia and lymphoma [27]. BET inhibitors are currently being used in clinical trials [28].

Promising data on combining HDACi with BRD4 inhibitors has been reported [17]. This combination has a specific rationale in DLBCL and BL as it potentially targets MYC in poor prognosis disease. Thus, the aim of this study was to investigate the effects of romidepsin alone or in combination with the BRD4 inhibitor, JQ1, in the treatment of aggressive lymphomas, and to identify the molecular mechanisms involved in its effects.

Results

Romidepsin promotes apoptosis in cells from agressive lymphomas

As a first approach, we measured cell proliferation (based on metabolic activity) upon romidepsin treatment to establish a dose-response assessment and to analyze the effect of the HDACi on proliferation at different time points (Figure 1a). Romidepsin was tested in different types of aggressive B-cell lymphoma cell lines: three Burkitt lymphoma cell lines (Raji, DG75 and Ramos), one GC-DLBCL (Toledo) and one ABC-DLBCL (Ly03) (see Supplementary Table S1).

At 48 h, Raji and DG75 cells showed little (10-20 %) reduction of metabolic activity (Figure 1a), even with the highest doses tested (10 nM). Ramos cells were the most sensitive, showing a metabolic reduction 50 % after treatment with romidepsin (5 nM) while both Toledo and Ly03, showed intermediate sensitivity. Very high doses of romidepsin inhibit almost completely the proliferation of all the lymphoma cell lines studied (not shown). Given that with 1 nM concentration did not show any significant

effect on the studied cell lines and 10 nM treatment resulted in cell death for the most sensitive cell lines, we chose 2 nM and 5 nM as optimal concentrations for further experiments.

To evaluate the effects of romidepsin on apoptosis, Annexin V binding was determined (Figure 1b). No significant cell death was observed for the metabolically less-sensitive cell lines Raji and DG75, while the sensitive cell lines Ramos, Toledo and Ly03, showed significant apoptosis induction after treatment with romidepsin (5 nM), (Figure 1b). The apoptotic effects of this drug were verified using the PARP1 cleavage assay. Cleaved PARP1 was found in the high and moderate sensitive cell lines (Ramos, Toledo and Ly03) but not in the less sensitive ones (Raji, DG75) (Figure 1c).

We next examined the effect of romidepsin on expression of some BCL2 family members (Figure 2). The intrinsic apoptotic pathway can be primarily activated by chemotherapeutic drugs and various studies support its role in HDACi mediated cell death [29]. In agreement with previous reports, BCL2 expression was neither observed in Ramos or DG75 in basal conditions [30,31] or upon treatment with romidepsin. There was little change in the level of BCL2 in Raji and Toledo while there was suppression in Ly03 (Figure 2a), confirming previous results indicating that romidepsin is able to induce apoptosis despite BCL2 expression [32]. Other pro-survival proteins were investigated: BCL-xL levels were high in basal conditions and were reduced upon treatment in the sensitive cell lines with the exception of Ly03 (Figure 2b), suggesting that downregulation of BCL-xL might be mediating romidepsin apoptotic effect on germinal center derived cells. Transient expression or little change was observed in MCL1 levels with romidepsin (Figure 2c). Interestingly, the pro-apoptotic protein BIM (Figure 2d), showed some increase with romidepsin in DLBCL cell lines (Toledo and Ly03), which was in agreement with the PARP1 cleavage pattern detected with romidepsin treatment.

Altogether, these results demonstrate that romidepsin can repress metabolic activity and induce variable levels of apoptosis associated with changes in expression of BCL2 family proteins that might be different upon the different subtypes of lymphomas.

Romidepsin induces cell cycle arrest accompanied with p21 and p27 up-regulation

Romidepsin has previously been shown to induce cell cycle arrest in cells from different tissues [21]. Based on this information, we aimed to analyze the cell cycle in cell lines with different responses to the HDACi (Figure 3a). The fraction of cells in the sub-G_0/G_1

phases of the cell cycle, indicative of cell death (inset in Figure 3a), fully agree with the apoptosis observed in the sensitive cells (Figure 1). In Raji cells we found a significant accumulation of cells in G_0/G_1, increasing from 50% to 80%, with a corresponding reduction in cells in S and G_2/M phases of the cell cycle. For DG75 and Ramos the accumulation in G_0/G_1 was smaller but still statistically significant. The cell population distribution in Toledo cell line was not substantially affected (Figure 3a).

Given the effects of HDACi on cell cycle arrest, we wonder whether the cell cycle inhibitors $p27^{Kip1}$ (p27) and $p21^{Cip1}$ (p21) were involved as has been reported for other HDACi [33]. We observed an increase of p21 protein levels in DG75 and Ramos cells treated with romidepsin (Figure 3b). The increase in p21 in Toledo cells was no so prominent, probably reflecting the lack of cell cycle arrest in these cells. Additionally, levels of p27 were dramatically increased in Raji, DG75 and Ramos in the presence of romidepsin (Figure 3b). There is, therefore, no clear agreement between protein levels of p21 and p27 and the clear block in G_1 phase that the drug provokes across all these cell lines (Figure 3a). Overall, romidepsin induces cell cycle arrest together with increase in p21 and p27 expression in Ramos, the most sensitive cell line.

Romidepsin provokes BCL6 downregulation and triggers plasma cell differentiation

BCL6 is a transcriptional repressor and one of the “master regulators” that controls the exit of the B-cells from the germinal centers in order to differentiate toward plasma cells [3]. To determine the effect of romidepsin on *BCL6* expression, we analyze the effect of this histone deacetylase inhibitor on several BL cell lines with different BCL6 expression levels (see Supplementary Table S1). Romidepsin reduced BCL6 mRNA (not shown) and protein levels (Figure 4a) in a dose and time dependent manner. In DG75, BCL6 downregulation takes place after 24 hours of romidepsin treatment either with 2 nM or 5 nM concentrations. In Raji and Ramos, reduced BCL6 levels were observed upon 48 to 72 hours of treatment. Romidepsin effects on *CCND2* (Cyclin D2), a direct target of BCL6 [34], were evaluated. We found a strong increase in the *CCND2* mRNA levels in Raji and DG75 in response to romidepsin, and a modest upregulation in Ramos cells (Figure 4b), supporting a functionally important downregulation of BCL6 by romidepsin.

BCL6 downregulation is essential for B-cells to leave the germinal center and to differentiate towards plasma cell. As a consequence of BCL6 downregulation, induction of target genes essential for B-cells to differentiate into plasma cells, such as *PRDM1* (BLIMP1), takes place. We analyzed *PRDM1* mRNA levels in the B-cell lymphoma cell

lines upon romidepsin treatment. The gene was upregulated in Raji, DG75 and Ramos cells (Figure 4c). No significant changes were detected in the non-GC Ly03 cell line (not shown). B-cells exit from germinal centers and plasma cell differentiation program not only requires changes in *BCL6* and *PRDM1* expression but also changes in other regulators such as *PAX5* and *XBP1* [3]. We chose the extensively used cell line model Ramos to study the modifications in the expression of these other genes. A clear increase in BLIMP1 protein levels was detected in Ramos cells upon romidepsin treatment (Figure 4d), accompanied by a decrease in *PAX5* and *XBP1* mRNA expression (Figure 4e). Finally, surface markers were analyzed by flow cytometry in Ramos cells. The induction of plasma cell differentiation was corroborated by the decrease of CD20 (B-cell marker) and the increase of CD138 (plasma cell marker) (Figure 4f).

Altogether these results indicate that romidepsin triggers differentiation towards plasma cell differentiation by inhibiting BCL6 expression and this is independent of apoptosis induced by romidepsin.

Romidepsin induces BCL6 acetylation

BCL6 regulation is critical for germinal center development. Acetylation inactivates BCL6 either under physiological conditions or induced by the histone deacetylase inhibitor trichostatin A [19]. Although we have shown that long-term romidepsin treatment downregulates BCL6, we wondered whether romidepsin was able to induce BCL6 acetylation at shorter times. Using Ramos germinal center cells as a model, we assayed BCL6 acetylation after romidepsin treatment. Acetylation was assessed by immunoprecipitation with an antibody against BCL6, followed by western blot employing an antibody widely demonstrated to recognize acetylated lysines in several transcription factors or an antibody against BCL6 (Figure 5a). We found increased BCL6 acetylation (3.9-fold) after 3 hours of romidepsin treatment and this acetylation remains after 6 hours of treatment, although to a lesser extent (2.1-fold) (Figure 5a top panel). Under all conditions there were approximately equal amounts of BCL6 in each immunoprecipitate (Figure 5a bottom panel). These results are similar to those previously reported using a different HDACi [19], demonstrating that romidepsin induces BCL6 acetylation.

Romidepsin effects on transcription and histone marks at the BCL6 locus

As previously described, BCL6 bound to the *BCL6* exon1A represses its own transcription [7,35,36]. To investigate if the acetylation of BCL6 induced by romidepsin had consequences for transcription from the BCL6 locus, we used luciferase reporter assay

in HEK-293T, a cell line that does not express BCL6 (Figure 5b). We prepared a luciferase reporter construct containing the BCL6 binding site in exon1A, designated as BCL6(exon1A)pGL3. This reporter was cotransfected with a BCL6 expression vector (pCDNA-BCL6). Low luciferase activity was detected in cells transfected with pCDNA-BCL6 in the absence of romidepsin due to the BCL6 negative autoregulation. Luciferase activity progressively increased with romidepsin in a dose-dependent manner (Figure 5b). Therefore, the negative regulation of BCL6 was counteracted by romidepsin, suggesting that the HDACi is inhibiting BCL6 negative autoregulation by acetylation.

We have previously demonstrated that the chromatin regulator CTCF epigenetically regulates *BCL6* by binding to *BCL6* exon1A [14]. In addition, we have observed that (at timepoints longer than 24 hours) romidepsin reduces BCL6 expression (Figure 4a). Therefore, we aimed to analyze the CTCF occupancy of the BCL6 exon1A in that context, using ChIP assays in Ramos cells. Results revealed CTCF binding to the BCL6 exon1A in the untreated cells, which strongly diminishes upon treatment with romidepsin (Figure 5c). Finally, we analyzed the effect of romidepsin on the local chromatin structure at exon1A. Ramos cells were treated with romidepsin and ChIP assays using antibodies against modified histones were performed. A reduction in the binding of the active histone mark H3Ac together with an enrichment of the H3K9me3 repressive histone was observed in the BCL6 exon1A when cells were treated with romidepsin (Figure 5d). Together these results indicate that romidepsin protects the BCL6 regulatory region against CTCF binding thus favoring the incorporation of repressive histone marks on BCL6 exon1A.

Collectively our results indicate that, at relatively short time-points, romidepsin inhibition of the BCL6 deacetylation presumably repress BCL6 function as shown by others [19] but increase transcription at the BCL6 locus. At longer time points, romidepsin modifies the local chromatin structure at the BCL6 locus to suppress transcription and consequently BCL6 protein levels, to de-repress transcription of BCL6 target genes.

Romidepsin and JQ1 synergistic effects on proliferation and apoptosis

We next aimed to analyze the effect of combined treatment of the epigenetic drugs romidepsin (HDACi) and JQ1 (BRD4i) in Ramos, a Burkitt lymphoma cell line. Cell viability analysis (WST-1 method) using different concentrations of both compounds were performed to generate combination index (CI) plot (Supplementary Table S2). For further experiments, we choose doses close to the IC_{50} values (5 nM romidepsin and 1 μM JQ1) where synergism (CI<1) was evident (Figure 6a). Growth curve analysis

confirmed the synergistic effect on cell proliferation (Figure 6b). Annexin V staining (Figure 6c) and cleaved PARP1 (Figure 6d) were strongly increased after 48h with the combination treatment, together with decreased levels of the antiapoptotic protein BCL-xL, indicating significant synergistic effect of romidepsin and JQ1 on apoptotic cell death. Interestingly, the combination treatment dramatically induced the expression of γH2AX (Figure 6d), a well-known marker of DNA damage response.

We also analyzed the effects of romidepsin and JQ1 on the cell cycle. Both compounds alone provoked cell cycle arrest and increased the expression of p21 (Figure 6e). A further increase in p21 levels was detected after 24 h with the combination treatment. At longer times, this synergistic effect was not evident presumably due to the high proportion of apoptotic cells (Figure 6c). The expected decrease in the cyclin A (as a marker of proliferation) and MYC levels was also observed (Figure 6e). Finally, we found downregulation of BCL6 expression that was more pronounced upon 48 h of combination treatment while BLIMP1 levels were slightly increased with both romidepsin and JQ1 (Figure 6f).

Similar results were obtained in the less sensitive Raji cells from BL (Figure 7) and, to a lesser extent in Toledo cells, a GC-DLBCL cell line (Supplementary Fig. S1). Clear synergistic effects of romidepsin and JQ1 in terms of apoptosis (PARP1 cleavage and γH2AX induction) (Figure 7b), cell cycle arrest (p27 induction, MYC downregulation) and plasmatic differentiation (BCL6 downregulation) (Figure 7c) were observed, indicating that the drugs combination could be effective in aggressive B cells lymphoma.

Discussion

Novel strategies for treatment of aggressive lymphomas are needed. DLBCL, one of the most frequent lymphomas in western countries will be refractory to anthracycline conventional treatments in a substantial proportion of cases. BCL6 is a key regulator of normal germinal center B-cells and is expressed in Burkitt lymphoma and some DLBCL. Transcription factors are attractive targets for therapy because they control programs of gene expression [37]. It is likely that the gene expression program controlled by BCL6 has important roles in driving cell cycle progression and proliferation in normal and malignant B-cells [34,38] in turn suggesting that BCL6 is an attractive target for these types of lymphomas [10,12]. Inhibition of BCL6 has indeed shown very promising results in preclinical studies [39]. Moreover, targeting BCL6 might not only be effective on germinal center derived lymphomas but also those ABC-DLBCL cases that express it [40]. However, generation of potent, drug-like inhibitors against BCL6 remains challenging.

We and others, have shown that different epigenetic mechanisms are involved in the modulation of BCL6 expression in the germinal center reaction [13,14]. Epigenetic modulators are an attractive and effective strategy in a number of malignancies [16]. Among them, more than ten histone deacetylase inhibitors have shown promising results in studies performed in different hematological malignances, including lymphomas [17,20,33]. HDACi can produce a variety of effects including induction of apoptosis, cell cycle arrest, induction of differentiation and regulation of immune responses, and these effects are exerted in a cell type specific manner [20,21,33,41]. Some of these effects are generated by the inhibition of activity of HDACs while others might be the consequence of modification of other cellular proteins by acetylation. In this study a number of BL derived cell lines were used to evaluate the effect of romidepsin, a potent HDACi that has been approved for treatment of different types of T cell lymphomas but its role on B cell lymphomas is yet not well known. BL shows high level BCL6 expression and BL cell lines have been used to elucidate many aspects of BCL6 action [34]. We also analyzed the effect of romidepsin in two GC-DLBCL and ABC-DLBCL cell lines, for comparison.

Romidepsin induced apoptosis in metabolically sensitive lymphoma B-cell lines. Several reports have shown a role for the mitochondrial apoptotic pathway in HDACi mediated apoptosis [20,41]. In some cases BCL2 or BCL-xL, which block the intrinsic apoptotic pathway, are able to overcome the effects of a number of HDACi. Therefore, a differential expression of the pro-apoptotic and the anti-apoptotic BCL2 family members might explain the varying response to romidepsin. In healthy B-cells, BCL2 expression is reduced when B-cells enter the germinal center reaction [42]. Although the basal expression of BCL2 was variable among the cells used in this study, no relationship between BCL2 expression and sensitiveness to romidepsin was observed. This is not surprisingly since romidepsin has been shown to induce apoptosis even in models overexpressing BCL2, but not in BCL-xL models [32]. Although down-regulation of BCL-xL does not imply an immediate death [42], the reduction in the anti-apoptotic BCL-xL in Ramos and Toledo cells compared to the unchanged levels observed in the DG75 insensitive cell line, imply that BCL-xL might be a good marker for monitoring romidepsin effect in germinal center cells. This is in agreement with previous studies showing how expression of BCL-xL might confer a drug resistance phenotype [43]. Interestingly, BIM was upregulated in both DLBCL (Toledo and Ly03) cells in the presence of romidepsin, which might explain the apoptosis observed in those cell lines, given that BIM plays a critical role in HDACi induced apoptosis [44,45]. In DG75 and Ramos cells, BIM levels are maintained while MCL1 protein transiently increases upon

romidepsin treatment. Since MCL1 is essential for the survival of plasma cells [46], this transient expression of MCL1 detected in response to romidepsin might be providing a short-term window to allow cells to differentiate into plasma cells and/or die by apoptosis.

It is known that GC B-cells stop proliferating in order to be able to differentiate into plasma cells. Accordingly, cell cycle arrest in G_0/G_1 phase was observed, together with the increase in p21 and p27, in most of the lymphoma cells analyzed upon exposure to romidepsin. This is line with previous reports showing, that accumulation of cycling dependent kinase inhibitors is a general effect shared by most of all the histone deacetylase inhibitors, when used on various malignancies [18,33].

In this study we have shown that romidepsin (i) induces BCL6 acetylation, which inhibits BCL6 negative autoregulation, and (ii) protects the BCL6 regulatory region against CTCF binding thus favouring the incorporation of repressive histone marks. In agreement, treatment of DLBCLs with other HDACi has been shown to induce hyperacetylation of BCL6, reactivation of repressed target genes and induction of apoptosis [19,47]. In our study, the romidepsin-mediated downregulation of BCL6 was also associated with plasma cell differentiation, as shown by induction of PRDM1 (BLIMP1) levels and the expression of plasma cell surface marker (CD138). In treated Ramos cells, *PAX5* mRNA levels were downregulated, PAX5 being necessary for B-cells to maintain their germinal center identity [48,49]. However, when we analyzed the expression of XBP1, a gene that acts downstream of PRDM1-BLIMP1, we found no upregulation, suggesting that romidepsin might be triggering a partial plasma cell differentiation program but is not sufficient for terminal plasma cell differentiation. Therefore, as expected the mature plasma cell phenotype was not completely reached because cell lines have limited differentiation capacity. The effects of romidepsin on lymphoma B cells are summarized in Figure 8.

Combination of HDACi with drugs targeting different cellular pathways are being used with promising results in a number of tumors including lymphomas [17,18]. Recently, combination treatments of HDAC and BET inhibitors have been described to have synergistic effects in different cancers [50-58]. In order to further improve the response of aggressive lymphoma cells, we explored the effects of romidepsin together with the BRD4 inhibitor JQ1. BRD4i inhibits *MYC* expression, frequently deregulated in hematopoietic malignancies [27,59]. Strong synergistic effect of romidepsin and JQ1 activating DNA-damage response and apoptotic cell death was found in Ramos cells (from BL) as assessed by γH2AX induction, annexin V binding and PARP1 cleavage. Notably, synergy in apoptosis and plasma cell differentiation was also found in the less

sensitive Raji (from BL) and Toledo (from GC-DLBCL) cells. In agreement with our results, two recent reports demonstrated synergistic effects of romidepsin and JQ1 in solid tumors [54,55]. This novel combination therapy can be useful to treat poor prognosis or non-responders low survival lymphoma patients.

In conclusion, our findings provide new insights into the molecular mechanisms of romidepsin effect on aggressive lymphomas: cell cycle arrest and induction of plasma differentiation is induced upon exposure to the drug and this effect appear to be related to the inhibition of BCL6 expression and function. Romidepsin also induces a variable apoptotic effect that is significantly increased upon treatment with the BET inhibitor JQ1, which reduces MYC function. Overall our data show a potential role for romidepsin and JQ1 combination for the treatment of aggressive and BCL6 expressing lymphomas.

Methods

Cell lines culture and drugs treatment

Raji, DG75, Ramos, Toledo and Ly03 B-cell lymphoma cell lines (origin and features in Supplementary Table S1) were grown in RPMI-1640 supplemented with 10% or 20% fetal calf serum (Lonza) under standard conditions [14] and confirmed to be mycoplasma free. *BCL6*, *MYC* and *BCL2* loci status in the studied cell lines were determined by FISH analysis (Supplementary Table S1).

Romidepsin was kindly provided by Celgene (Summit, NJ, USA). (+)-JQ1 was purchase from Cayman Chemical (Ann Arbor, MI, USA). Drugs were diluted in DMSO and stored at -20^{O} C. To study the effects of the drugs, exponentially growing cells were treated with the different drug concentrations for several time points, depending on the experiment and cell line.

Cell proliferation and viability assays

Cells were treated with different doses of romidepsin and/or JQ1 for up to 96 h. Cell proliferation and cell viability was measured using the Guava ViaCount reagent (Merck Millipore, Darmstadt, Germany) or the NucleoCounter system (Chemometec, Allerod, Denmark). Metabolic activity of cells was measured using the WST-1 method (Roche, Basilea, Switzerland) which allows the quantification of the number of viable cells by the cleavage of tetrazolium salt WST-1 to formazan dye. Romidepsin and JQ1 combination effects were determined using the combination index (CI) values, analyzed by the Chou-Talalay method using CompuSyn Software [60].

Cell cycle, apoptosis and differentiation analysis

Cell cycle analysis were performed using propidium iodide staining as previously described [61]. Cells were fixed with cold ethanol and resuspended in PBS-citrate Na-BSA containing RNase and propidium iodide. The stained cells were analyzed by flow cytometry (FACSDiva cytometer). Annexin V-PE Apoptosis detection Kit (Immunostep, Salamanca, Spain) was used for the detection of early apoptotic cells. Cells were treated with romidepsin and JQ1 for 24 and 48 h and Annexin V-binding was analyzed by flow cytometry (FACSDiva^{TM} software, BD biosciences, NJ, USA). The cleavage of poly(ADP-ribose)polymerase-1 (PARP1), indicative of apoptosis, was analyze by immunoblot.

Cell surface markers were analyzed in the Hematology Department of Hospital Marqués de Valdecilla to assess cells differentiation. After 72 h of culture in the presence of 5 nM romidepsin, cell surface markers were analyzed by flow cytometry using the BD FACSDiva flow-cytometer following standard procedures [62]. The conjugated antibodies used were: anti-CD20 PE (BD 345793) from BD Biosciences and anti-CD138 FITC (Rafer; Zaragoza, Spain, IQP 153F).

RNA analysis by Reverse transcription (RT) and polymerase chain reaction (PCR)

Total RNA was isolated by using the Trizol reagent (Invitrogen, Carlsbad, CA, USA). For reverse transcription, first-strand cDNA was synthesized from 1 µg of total RNA using the iScript cDNA Synthesis Kit (Bio-Rad, Hercules, CA, USA). Quantitative PCR was performed with a IQTM SyBR Green Supermix kit (Bio-Rad). mRNA expression was normalized to ribosomal protein S14 mRNA levels (primers shown in Supplementary Table S3). Results were analyzed by comparative ΔΔCt method and expressed as mean ± SEM of duplicate PCRs from at least two independent experiments.

Immunoblot and immunoprecipitation assays

Cells were lysed in lysis buffer (1% NP-40, 100 mM NaCl, 20 mM Tris-HCl pH 7.4, 10 mM NaF, 1 mM orthovanadate and protease and phosphatase inhibitors cocktail). Samples were sonicated and subjected to SDS-PAGE and immunoblot as described previously [63]. The antibodies used were: anti-actin (I-19, sc1616), anti-BCL6 (N-3, sc858), anti-PARP1 (H-250, sc7150), anti-CycA (H-432, sc751) from Santa Cruz Biotech. (Santa Cruz, CA, USA); anti-BCL-xL (ab7974) from Abcam (Cambrigde, UK); anti-BCL2 (2876), anti-BIM (C34C5), anti-MCL1 (4572), anti-BLIMP1 (C14A4), anti-GAPDH (14C10), anti-cMYC (9402S), anti-p27 (3686), anti-p21 (2947) from Cell

Signalling Tech. (Danvers, MA, USA); Anti-phospho-Histone H2A.X (Ser139) (05-636) from Millipore (Darmstadt, Germany). Blots were developed with secondary antibodies conjugated to IRDye680 or IRDye800 (Li-Cor Biosciences, LiCor, Lincoln, NE, USA) and immunocomplexes were detected with an Odyssey infrared-imaging system (Li-Cor Biosciences). Some blots were revealed with the ECL system (Bio-Rad).

Immunoprecipitations were performed essentially as described [64]. For detection of the endogenous acetylated BCL6, Ramos cells were lysed in lysis buffer (50 mM Tris-HCl, 250 mM NaCl, 1 % Nonidet P-40, 0.5 % deoxycholic acid, 0.1 % SDS) containing 1 µM romidepsin and protease inhibitors cocktail. Protein extracts were immunoprecipitated with 3 µg of a mouse monoclonal antibody against BCL6 (PG-B6P) or unspecific immunoglobulins used as a control (IgGs sc-2025), from Santa Cruz Biotech. Dynabeads-protein G-bound magnetic beads (Invitrogen) were used to capture protein-antibody immunocomplexes. Immunocomplexes were resolved by SDS-PAGE and analyzed by western blot with antibody against acetyl lysine (9441, Cell Signaling). The same filter was then incubated with an anti-BCL6 (N3, sc858) rabbit polyclonal antibody.

Luciferase reporter assays

HEK-293T cells were transiently transfected using polyethilenimine (PEI) transfection reagent (Polysciences Inc., Warrington, PA, USA) as previously described [14] and reporter experiments were performed essentially as described [19]. 0.3 µg of the pGL3-basic vector (Promega) or 0.35 µg of the BCL6(exon1)-pGL3 reporter vector [65] and 0.1 µg of the pRL-null vector (Promega) were cotransfected with pCDNA-BCL6 expression vector [14]. Cells were treated for 12 hours with different concentrations of romidepsin. Luciferase activities were measured 48 hours after transfection using the Dual-Glo Luciferase Reporter System (Promega, Madison, WI, USA) in a Luminometer TD 20/20 Turner Designs. For each determination, luciferase activity was calculated as the Firefly activity normalized by the Renilla activity. Luciferase activity in arbitrary units (a.u.) was shown as the increase in activation relative to the activity of the pGL3 vector alone and the maximum value for each condition was set to 100.

Chromatin immunoprecipitation (ChIP)

For ChIP experiments chromatin was prepared from Ramos cells treated with 5 mM romidepsin for 48 h. ChIP assays were performed using the Pierce Magnetic ChIP Kit (Thermo Fisher Scientific, Waltham, MA, USA) following the manufacturer's protocol. Cells were fixed in formaldehyde, lysed, treated with Micrococcal nuclease and sonicated using a Bioruptor UCD-200TM (Diagenode, Liège, Belgium). ChIP was

performed using ChIP-Grade Protein A/G Magnetic Beads coupled to different antibodies: anti-CTCF-Ab-1 (07-729) from Millipore, anti-CTCF (ab10571) from Abcam; anti-CTCF (612149) from BD and anti-H3acetylated (06-599) from Millipore; anti-H3K9me3 (ab8898) from Abcam. Real-time PCR of immunoprecipitated DNA was performed in duplicate with equal amounts of specific antibody immunoprecipitated sample, control (beads) and input. Primers used for ChIP assays corresponding to the BCL6 exon 1A (+257) were: 5'-GCACTCCCCCTCTTATGTCA-3' and 5'-GATTTGGAGGTTCCGGTTC-3' [14]. The comparative cycle threshold approach was used for the data analysis [14]. The signals were normalized to the inputs and the fold enrichment was calculated relative to the control sample (no-antibody). The values are the mean ± S.E.M. of two to six independent experiments. Normalization of histone marks was based on the ChIP-IT qPCR analysis kit (Active motif North America, Carlsbad, CA, USA).

Statistical analysis

Results were presented as the mean of two to four determinations with error bars representing the standard error of the mean. The significance of differences was determined by the unpaired Student's *t* test; a $p<0,05$ was considered to be statistically significant.

References

1 Swerdlow, S. H. *et al.* The 2016 revision of the World Health Organization classification of lymphoid neoplasms. *Blood* **127**, 2375-2390 (2016).

2 Coiffier, B. *et al.* Long-term outcome of patients in the LNH-98.5 trial, the first randomized study comparing rituximab-CHOP to standard CHOP chemotherapy in DLBCL patients: a study by the Groupe d'Etudes des Lymphomes de l'Adulte. *Blood* **116**, 2040-2045 (2010).

3 Basso, K. & Dalla-Favera, R. Germinal centres and B cell lymphomagenesis. *Nat Rev Immunol* **15**, 172-184 (2015).

4 Dent, A. L., Shaffer, A. L., Yu, X., Allman, D. & Staudt, L. M. Control of inflammation, cytokine expression, and germinal center formation by BCL-6. *Science* **276**, 589-592 (1997).

5 Ye, B. H. *et al.* The BCL-6 proto-oncogene controls germinal-centre formation and Th2-type inflammation. *Nat Genet* **16**, 161-170 (1997).

6 Cattoretti, G. *et al.* Deregulated BCL6 expression recapitulates the pathogenesis of human diffuse large B cell lymphomas in mice. *Cancer Cell* **7**, 445-455 (2005).

7 Pasqualucci, L. *et al.* Mutations of the BCL6 proto-oncogene disrupt its negative autoregulation in diffuse large B-cell lymphoma. *Blood* **101**, 2914-2923 (2003).

8 Hatzi, K. & Melnick, A. Breaking bad in the germinal center: how deregulation of BCL6 contributes to lymphomagenesis. *Trends Mol Med* **20**, 343-352 (2014).

9 Ye, B. H., Rao, P. H., Chaganti, R. S. & Dalla-Favera, R. Cloning of bcl-6, the locus involved in chromosome translocations affecting band 3q27 in B-cell lymphoma. *Cancer research* **53**, 2732-2735 (1993).
10 Cardenas, M. G. *et al.* The Expanding Role of the BCL6 Oncoprotein as a Cancer Therapeutic Target. *Clin Cancer Res* **23**, 885-893 (2017).
11 Wagner, S. D., Ahearne, M. & Ko Ferrigno, P. The role of BCL6 in lymphomas and routes to therapy. *Br J Haematol* **152**, 3-12 (2011).
12 Leeman-Neill, R. J. & Bhagat, G. BCL6 as a therapeutic target for lymphoma. *Expert opinion on therapeutic targets* **22**, 143-152 (2018).
13 Lai, A. Y. *et al.* DNA methylation prevents CTCF-mediated silencing of the oncogene BCL6 in B cell lymphomas. *The Journal of experimental medicine* **207**, 1939-1950 (2010).
14 Batlle-Lopez, A. *et al.* Novel CTCF binding at a site in exon1A of BCL6 is associated with active histone marks and a transcriptionally active locus. *Oncogene* **34**, 246-256 (2015).
15 Batlle-Lopez, A., Cortiguera, M. G. & Delgado, M. D. The epigenetic regulator CTCF modulates BCL6 in lymphoma. *Oncoscience* **2**, 783-784 (2015).
16 Dawson, M. A. & Kouzarides, T. Cancer epigenetics: from mechanism to therapy. *Cell* **150**, 12-27 (2012).
17 Ahuja, N., Sharma, A. R. & Baylin, S. B. Epigenetic Therapeutics: A New Weapon in the War Against Cancer. *Annual review of medicine* **67**, 73-89 (2016).
18 New, M., Olzscha, H. & La Thangue, N. B. HDAC inhibitor-based therapies: can we interpret the code? *Molecular oncology* **6**, 637-656 (2012).
19 Bereshchenko, O. R., Gu, W. & Dalla-Favera, R. Acetylation inactivates the transcriptional repressor BCL6. *Nat Genet* **32**, 606-613 (2002).
20 West, A. C. & Johnstone, R. W. New and emerging HDAC inhibitors for cancer treatment. *The Journal of clinical investigation* **124**, 30-39 (2014).
21 Bates, S. E., Robey, R. W. & Piekarz, R. L. CCR 20th Anniversary Commentary: Expanding the Epigenetic Therapeutic Portfolio. *Clin Cancer Res* **21**, 2195-2197 (2015).
22 Kalac, M. *et al.* HDAC inhibitors and decitabine are highly synergistic and associated with unique gene-expression and epigenetic profiles in models of DLBCL. *Blood* **118**, 5506-5516 (2011).
23 Aukema, S. M. *et al.* Biological characterization of adult MYC-translocation-positive mature B-cell lymphomas other than molecular Burkitt lymphoma. *Haematologica* **99**, 726-735 (2014).
24 Gupta, M. *et al.* Expression of Myc, but not pSTAT3, is an adverse prognostic factor for diffuse large B-cell lymphoma treated with epratuzumab/R-CHOP. *Blood* **120**, 4400-4406 (2012).
25 Delmore, J. E. *et al.* BET bromodomain inhibition as a therapeutic strategy to target c-Myc. *Cell* **146**, 904-917 (2011).
26 Filippakopoulos, P. *et al.* Selective inhibition of BET bromodomains. *Nature* **468**, 1067-1073 (2010).
27 Cortiguera, M. G., Batlle-López, A., Albajar, M., Delgado, M. D. & León, J. MYC as therapeutic target in leukemia and lymphoma. *Blood and Lymphatic Cancer: Targets and Therapy* **5**, 75-79 (2015).
28 Andrieu, G., Belkina, A. C. & Denis, G. V. Clinical trials for BET inhibitors run ahead of the science. *Drug discovery today. Technologies* **19**, 45-50 (2016).
29 Peart, M. J. *et al.* Novel mechanisms of apoptosis induced by histone deacetylase inhibitors. *Cancer research* **63**, 4460-4471 (2003).
30 Finke, J. *et al.* Expression of bcl-2 in Burkitt's lymphoma cell lines: induction by latent Epstein-Barr virus genes. *Blood* **80**, 459-469 (1992).
31 Ierano, C. *et al.* Loss of the proteins Bak and Bax prevents apoptosis mediated by histone deacetylase inhibitors. *Cell Cycle* **12**, 2829-2838 (2013).

32 Newbold, A. *et al.* Characterisation of the novel apoptotic and therapeutic activities of the histone deacetylase inhibitor romidepsin. *Mol Cancer Ther* **7**, 1066-1079 (2008).
33 Zain, J. & O'Connor, O. A. Targeting histone deacetyalses in the treatment of B- and T-cell malignancies. *Investigational new drugs* **28 Suppl 1**, S58-78 (2010).
34 Shaffer, A. L. *et al.* BCL-6 represses genes that function in lymphocyte differentiation, inflammation, and cell cycle control. *Immunity* **13**, 199-212 (2000).
35 Kikuchi, M. *et al.* Identification of negative regulatory regions within the first exon and intron of the BCL6 gene. *Oncogene* **19**, 4941-4945 (2000).
36 Wang, X., Li, Z., Naganuma, A. & Ye, B. H. Negative autoregulation of BCL-6 is bypassed by genetic alterations in diffuse large B cell lymphomas. *Proceedings of the National Academy of Sciences of the United States of America* **99**, 15018-15023 (2002).
37 Melnick, A. M., Adelson, K. & Licht, J. D. The theoretical basis of transcriptional therapy of cancer: can it be put into practice? *J Clin Oncol* **23**, 3957-3970 (2005).
38 Bunting, K. L. *et al.* Multi-tiered Reorganization of the Genome during B Cell Affinity Maturation Anchored by a Germinal Center-Specific Locus Control Region. *Immunity* **45**, 497-512 (2016).
39 Cerchietti, L. C. *et al.* A small-molecule inhibitor of BCL6 kills DLBCL cells in vitro and in vivo. *Cancer Cell* **17**, 400-411 (2010).
40 Cardenas, M. G. *et al.* Rationally designed BCL6 inhibitors target activated B cell diffuse large B cell lymphoma. *The Journal of clinical investigation* **126**, 3351-3362 (2016).
41 Bolden, J. E., Peart, M. J. & Johnstone, R. W. Anticancer activities of histone deacetylase inhibitors. *Nature reviews* **5**, 769-784 (2006).
42 Peperzak, V., Slinger, E., Ter Burg, J. & Eldering, E. Functional disparities among BCL-2 members in tonsillar and leukemic B-cell subsets assessed by BH3-mimetic profiling. *Cell Death Differ* **24**, 111-119 (2017).
43 Minn, A. J., Rudin, C. M., Boise, L. H. & Thompson, C. B. Expression of bcl-xL can confer a multidrug resistance phenotype. *Blood* **86**, 1903-1910 (1995).
44 Zhao, Y. *et al.* Inhibitors of histone deacetylases target the Rb-E2F1 pathway for apoptosis induction through activation of proapoptotic protein Bim. *Proceedings of the National Academy of Sciences of the United States of America* **102**, 16090-16095 (2005).
45 Ding, H. *et al.* Histone deacetylase inhibitors interrupt HSP90*RASGRP1 and HSP90*CRAF interactions to upregulate BIM and circumvent drug resistance in lymphoma cells. *Leukemia* **31**, 1593-1602 (2017).
46 Peperzak, V. *et al.* Mcl-1 is essential for the survival of plasma cells. *Nat Immunol* **14**, 290-297 (2013).
47 Amengual, J. E. *et al.* Sirtuin and pan-class I/II deacetylase (DAC) inhibition is synergistic in preclinical models and clinical studies of lymphoma. *Blood* **122**, 2104-2113 (2013).
48 Revilla, I. D. R. *et al.* The B-cell identity factor Pax5 regulates distinct transcriptional programmes in early and late B lymphopoiesis. *EMBO J* **31**, 3130-3146 (2012).
49 Nera, K. P. *et al.* Loss of Pax5 promotes plasma cell differentiation. *Immunity* **24**, 283-293 (2006).
50 Bhadury, J. *et al.* BET and HDAC inhibitors induce similar genes and biological effects and synergize to kill in Myc-induced murine lymphoma. *Proceedings of the National Academy of Sciences of the United States of America* **111**, E2721-2730 (2014).

51 Mazur, P. K. *et al.* Combined inhibition of BET family proteins and histone deacetylases as a potential epigenetics-based therapy for pancreatic ductal adenocarcinoma. *Nature medicine* **21**, 1163-1171 (2015).
52 Mishra, V. K. *et al.* Histone deacetylase class-I inhibition promotes epithelial gene expression in pancreatic cancer cells in a BRD4- and MYC-dependent manner. *Nucleic acids research* **45**, 6334-6349 (2017).
53 Enssle, J. C. *et al.* Co-targeting of BET proteins and HDACs as a novel approach to trigger apoptosis in rhabdomyosarcoma cells. *Cancer Lett* **428**, 160-172 (2018).
54 Jostes, S. *et al.* The bromodomain inhibitor JQ1 triggers growth arrest and apoptosis in testicular germ cell tumours in vitro and in vivo. *J Cell Mol Med* **21**, 1300-1314 (2017).
55 Holscher, A. S., Schulz, W. A., Pinkerneil, M., Niegisch, G. & Hoffmann, M. J. Combined inhibition of BET proteins and class I HDACs synergistically induces apoptosis in urothelial carcinoma cell lines. *Clinical epigenetics* **10**, 1 (2018).
56 Borbely, G., Haldosen, L. A., Dahlman-Wright, K. & Zhao, C. Induction of USP17 by combining BET and HDAC inhibitors in breast cancer cells. *Oncotarget* **6**, 33623-33635 (2015).
57 Heinemann, A. *et al.* Combining BET and HDAC inhibitors synergistically induces apoptosis of melanoma and suppresses AKT and YAP signaling. *Oncotarget* **6**, 21507-21521 (2015).
58 Loosveld, M. *et al.* Therapeutic targeting of c-Myc in T-cell acute lymphoblastic leukemia, T-ALL. *Oncotarget* **5**, 3168-3172 (2014).
59 Delgado, M. D., Albajar, M., Gomez-Casares, M. T., Batlle, A. & Leon, J. MYC oncogene in myeloid neoplasias. *Clinical & translational oncology : official publication of the Federation of Spanish Oncology Societies and of the National Cancer Institute of Mexico* **15**, 87-94 (2013).
60 Chou, T. C. & Talalay, P. Quantitative analysis of dose-effect relationships: the combined effects of multiple drugs or enzyme inhibitors. *Advances in enzyme regulation* **22**, 27-55 (1984).
61 Albajar, M. *et al.* MYC in chronic myeloid leukemia: induction of aberrant DNA synthesis and association with poor response to imatinib. *Molecular cancer research : MCR* **9**, 564-576 (2011).
62 Colorado, M. *et al.* Simultaneous cytomorphologic and multiparametric flow cytometric analysis on lymph node samples is faster than and as valid as histopathologic study to diagnose most non-Hodgkin lymphomas. *Am J Clin Pathol* **133**, 83-91 (2010).
63 Torrano, V. *et al.* Targeting of CTCF to the nucleolus inhibits nucleolar transcription through a poly(ADP-ribosyl)ation-dependent mechanism. *Journal of cell science* **119**, 1746-1759 (2006).
64 Caraballo, J. M. *et al.* High p27 protein levels in chronic lymphocytic leukemia are associated to low Myc and Skp2 expression, confer resistance to apoptosis and antagonize Myc effects on cell cycle. *Oncotarget* **5**, 4694-4708 (2014).
65 Papadopoulou, V., Postigo, A., Sanchez-Tillo, E., Porter, A. C. & Wagner, S. D. ZEB1 and CtBP form a repressive complex at a distal promoter element of the BCL6 locus. *The Biochemical journal* **427**, 541-550 (2010).

Acknowledgments

We acknowledge Mercedes Colorado and Andrés Insunza, from the flow cytometry area, Hematologic neoplastic diagnostic unit, from the Hospital Universitario Marqués de Valdecilla for assistance with the generation of Flow Cytometry data. We thank Rosa Blanco for expert technical assistance. We are grateful to Celgene for kindly provide romidepsin. The work was supported by grants SAF2014-53526-R and SAF2017-88026-R from MINECO, Spanish Government, to MDD and JL (partially funded by FEDER program from European Union). MGC was recipient of a "Marcos Fernández" fellowship from Leukemia and Lymphoma foundation. LGG was recipient of a FPI fellowship from Spanish Government.

Author Contributions

MGC and LGG performed experiments, acquired and analyzed data; SDW, JL, ABL and MDD were involved in conception, design and data interpretation; ABL and MDD wrote the manuscript. All authors read and approved the final version of the manuscript**.**

Competing interests

M. D. Delgado and A. Batlle-Lopez's work has been funded by Celgene. The other authors declare no potential competing interests.

Figure Legends

Figure 1. Romidepsin effect on B-cell lymphoma cells proliferation and apoptosis. (**a**) The indicated cell lines were treated with different concentrations of romidepsin and metabolic activity was determined using WST-1 method at the designated times. Untreated cells represented 100 % of metabolic activity. The data show the means ± s.e.m. of four measurements in two independent experiments. (**b**) Annexin-V staining to assess early apoptosis in B-cell lymphoma cells untreated (control) or cells treated with 5 nM romidepsin for 48 h. One representative experiment is shown for each cell line. The graphs on the right represent percentages of Annexin V positive cells. The data show the means ± s.e.m. of two or three independent experiments; significance difference (*,p<0,05) from the control untreated cells. (**c**) Western blot showing PARP1 and cleaved-PARP1 (indicated with an asterisk) in B-cell lymphoma cells treated with romidepsin at the indicated times and concentrations. Actin was used as loading control. The blots were cropped for improved clarity and the full-length blots were included in the Supplementary Information file.

Figure 2. BCL2 family protein expression upon romidepsin treatment. Western blot showing BCL2 (**a**), BCL-xL (**b**), MCL1 (**c**) and BIM (**d**) protein expression in B-cell lymphoma cells treated with 2 or 5 nM romidepsin for the indicated times. Actin or GAPDH were used as loading controls. Densitometry values are shown at the bottom, normalized to the control. The blots were cropped for improved clarity and the full-length blots were included in the Supplementary Information file.

Figure 3. Cell cycle distribution and cell cycle inhibitors expression in B-cell lymphoma cells in the presence of romidepsin. (**a**) Cell cycle assays were performed using propidium iodide staining and flow cytometry in the indicated cell lines. Cells were treated with 5 nM of romidepsin for the indicated times. The fraction of cells in each phase of the cell cycle was calculated as a percentage from the total viable population. The data show the means ± s.e.m. of two to four independent experiments; significance difference (*,p<0,05) from the control untreated cells. The inset show the fraction of cells in the sub-G_0/G_1 phase, indicative of cell death. (**b**) Western blot showing p21 and p27 protein expression in B-cell lymphoma cells treated with 2 or 5 nM romidepsin for the indicated times. Actin was used as loading control. Unspecific band is indicated (*).The blots were cropped for improved clarity and the full-length blots were included in the Supplementary Information file.

Figure 4. Romidepsin induces BCL6 downregulation and markers of the plasma cell differentiation program. (**a**) Western blot showing BCL6 protein expression in B-

cell lymphoma cells treated with 2 or 5 nM romidepsin for the indicated times. Actin was used as loading control. (**b**) RT-PCR showing CCND2 mRNA expression in B-cell lymphoma cells upon romidepsin treatment for the indicated times. mRNA levels were normalized to the ribosomal S14 expression. The data show the means ± s.e.m. of at least two independent experiments. (**c**) RT-PCR showing PRDM1 mRNA expression in B-cell lymphoma cells as in (b). (**d**) Western blot showing BLIMP1 protein expression levels in Ramos cells upon romidepsin treatment for the indicated times. (**e**) RT-PCR showing PAX5 and XBP1 mRNA expression levels in Ramos cells as in (b). (**f**) Surface markers CD20 and CD138 analyzed by flow cytometry in Ramos cells untreated (black) or treated with 5 nm romidepsin (grey) for 72 h.

Figure 5. Romidepsin effects on BCL6 acetylation, BCL6 autoregulation and local chromatin structure at the BCL6 exon1A. (**a**) Immunoprecipitation showing BCL6 acetylation. Immunoprecipitation of BCL6 protein in Ramos cells treated for 3 h and 6 h with 10 nM romidepsin. Total lysates were immunoprecipitated with anti-BCL6 antibodies, and the presence of acetylated BCL6 and total amount of BCL6 immunoprecipitated was detected by western blot. Densitometry values are shown at the bottom. Inputs are shown as controls. Immunoprecipitation of IgG was used as negative control. (**b**) Romidepsin effect on the negative autoregulation of BCL6 gene. Luciferase assay showing the effects of romidepsin on BCL6 exon1A regulatory region. HEK-293T cells were co-transfected with either pGL3 vector or with the BCL6 (exon1A)pGL3 reporter vector together with the indicated amount of pCDNA-BCL6 expression vector. pRL-null vector was used to normalize the transfection efficiency. Transfected cells were exposed to the indicated doses of romidepsin for 12 h and luciferase activity was determined 48 h after transfection. The data show the means ± s.e.m. of three measurements in three independent experiments. a.u., arbitrary units. BCL6 gene regulatory region indicating the BCL6 binding site (BCL6BS) is shown. (**c**) Romidepsin effect on CTCF *in vivo* binding to BCL6 exon1A. ChIP analysis with a mix of three anti-CTCF antibodies, showing the binding of this protein to the exon1A of BCL6. Chromatin was prepared from Ramos cells. Relative enrichment was quantified by real-time PCR. The fold enrichment was determined as indicated in Methods section. (**d**) Presence of histone marks at the BCL6 exon1A upon treatment with romidepsin. ChIP analysis with CTCF, H3Ac and H3K9me3 antibodies, showing the presence of these proteins at the exon1A of BCL6. Chromatin was prepared from Ramos cells treated with romidepsin. Relative enrichment was quantified by real-time PCR. The fold enrichment of a particular target sequence was determined as indicated in Methods section. Bottom panel shows typical PCR products after the ChIP assays.

The gels were cropped for improved clarity and the full-length gels were included in the Supplementary Information file.

Figure 6. Synergistic effects of romidepsin and JQ1 in Ramos B-cell lymphoma cells. (**a**) Combination index plot showing synergistic effect (arrow) of romidepsin (5 nM) plus JQ1 (1 μM) on the proliferation of Ramos cells. (**b**) Growth curves of Ramos cells untreated (Control) or treated with romidepsin and/or JQ1 for up to 72h. (**c**) Annexin-V staining to assess apoptosis in Ramos cells untreated (Control) or treated with romidepsin and/or JQ1 for 48 h. Results shown are the means ± s.e.m. of three experiments; significance difference (*,p<0,03; ***,p<0,001) from the control untreated cells. (**d**) Western blot showing cleaved PARP1 and BCL-xL and γH2AX protein levels in Ramos cells treated with romidepsin and/or JQ1 for the indicated times. Actin was used as loading control. Densitometry values are shown at the bottom, normalized to the control. (**e**) Western blot showing p21, MYC, and cyclin A protein levels in Ramos cells treated as above. (**f**) Western blot showing BCL6 and BLIMP1 protein levels in Ramos cells treated as above. The blots were cropped for improved clarity and the full-length blots were included in the Supplementary Information file.

Figure 7. Synergistic effects of romidepsin and JQ1 in Raji B-cell lymphoma cells. (**a**) Combination index plot showing synergistic effect (arrow) of romidepsin (5 nM) plus JQ1 (1 μM) on the proliferation of Raji cells. (**b**) Western blot showing cleaved PARP1 and BCL-xL and γH2AX protein levels in Raji cells treated with romidepsin and/or JQ1 for the indicated times. Actin was used as loading control. Densitometry values are shown at the bottom, normalized to the control. (**c**) Western blot showing p27, MYC and BCL6 protein levels in Raji cells treated as above. The blots were cropped for improved clarity and the full-length blots were included in the Supplementary Information file.

Figure 8. Proposed model for epigenetic drugs effect on B-cell lymphoma cells and BCL6 regulation. Romidepsin induces cell cycle arrest accompanied with increased levels of p27 and p21 in most lymphoma cells. The sensitive lymphoma B-cells undergo apoptosis as shown by cleavage of PARP1 and positive Annexin V staining. Downregulation of BCL6 and PAX5 together with increase on PRDM1 (BLIMP1) is also observed, and plasma cell differentiation program is initiated. Synergistic effect of romidepsin and JQ1 mainly in apoptosis induction (thicker line) is demonstrated. In B-cell lymphoma cells, CTCF is bound to BCL6 exon1A impairing BCL6 binding to its negative autoregulation site and is associated with marks representative of an open chromatin state (H3Ac). In the presence of romidepsin BCL6 is acetylated, CTCF is not longer bound to BCL6 exon1A and repressive histone marks

(H3K9me3) are incorporated. The consequent downregulation of BCL6 correlates with plasmatic differentiation as shown above.

Figure 1. Cortiguera et al.

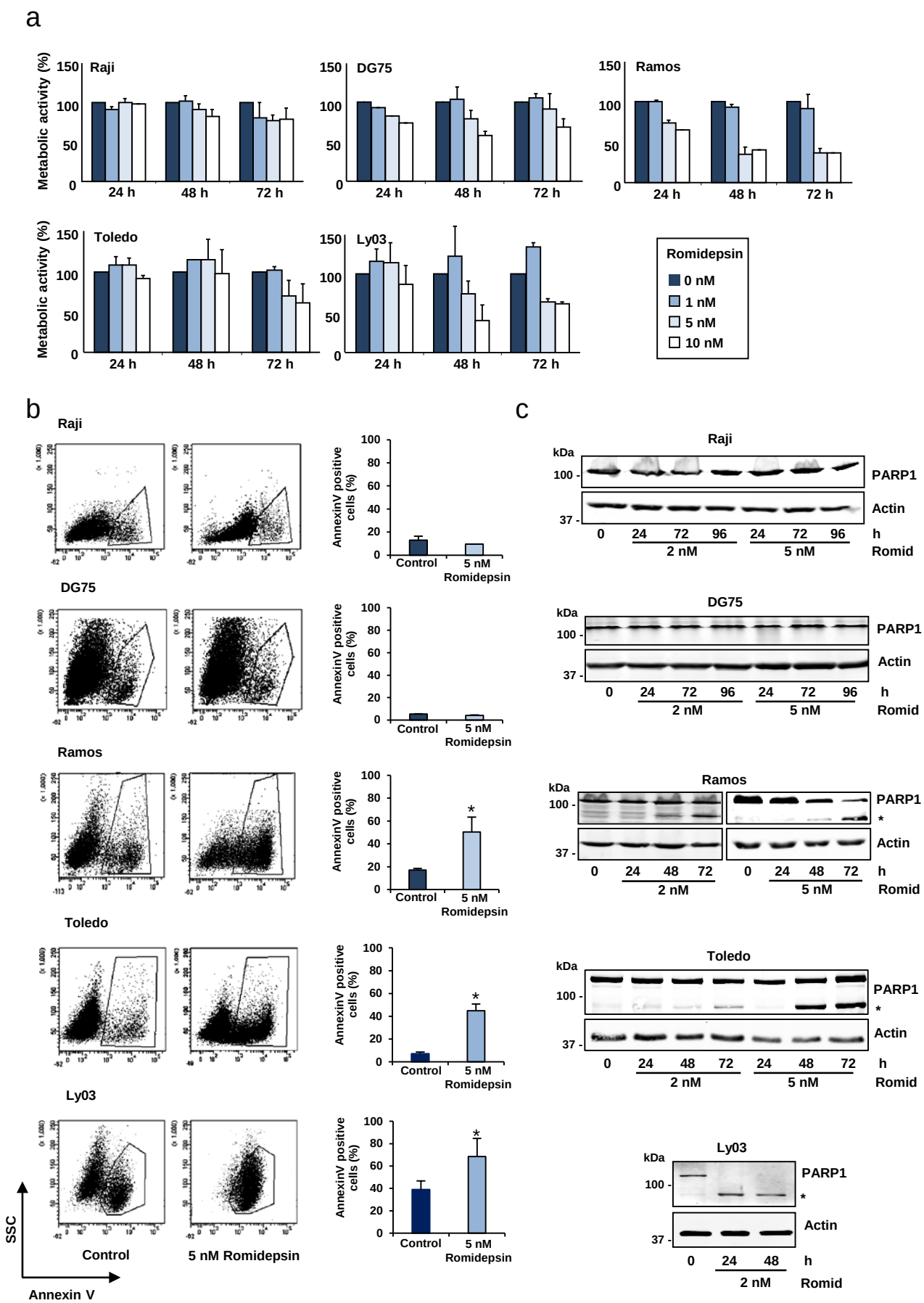

Figure 2. Cortiguera et al.

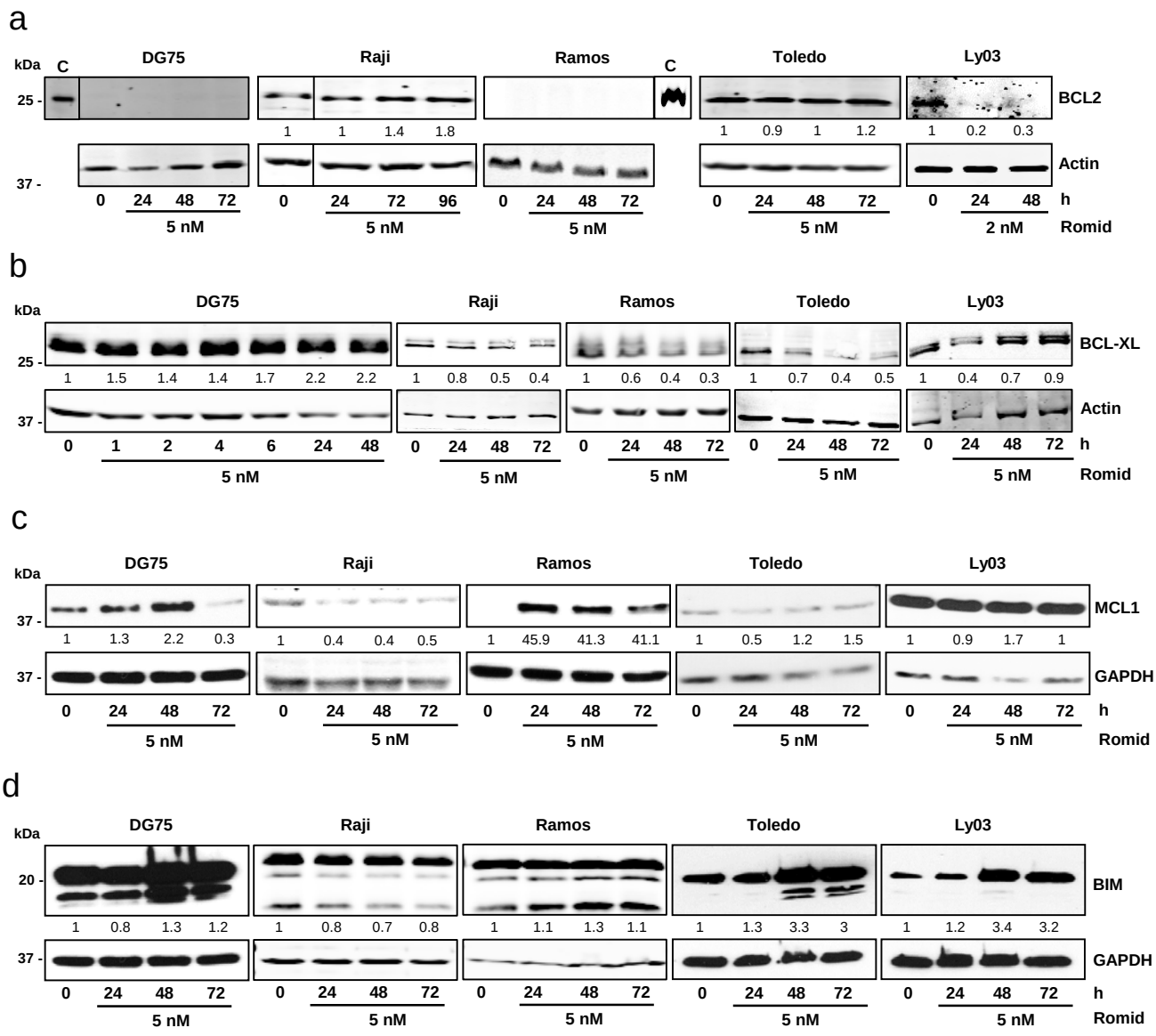

Figure 3. Cortiguera et al.

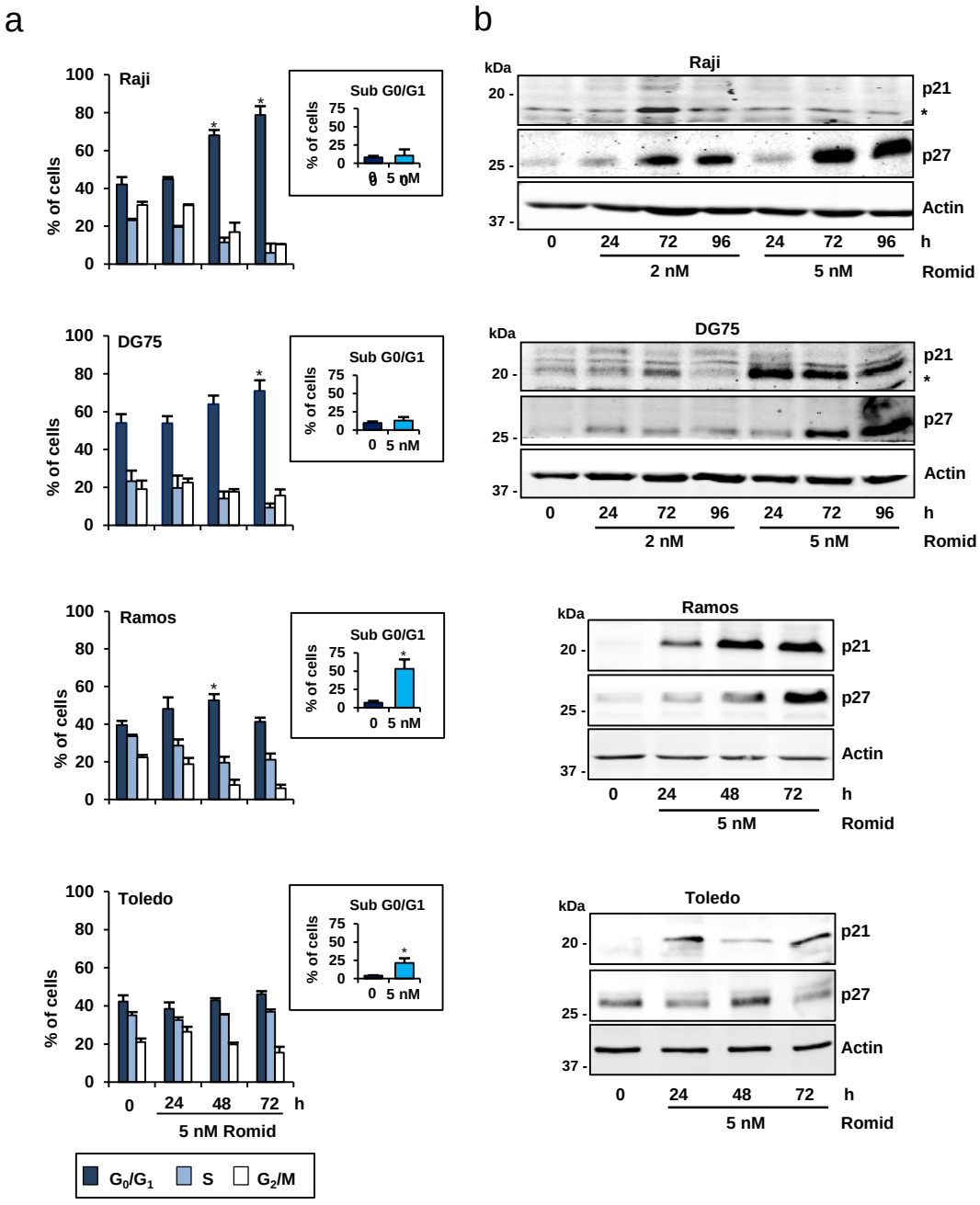

Figure 4. Cortiguera et al.

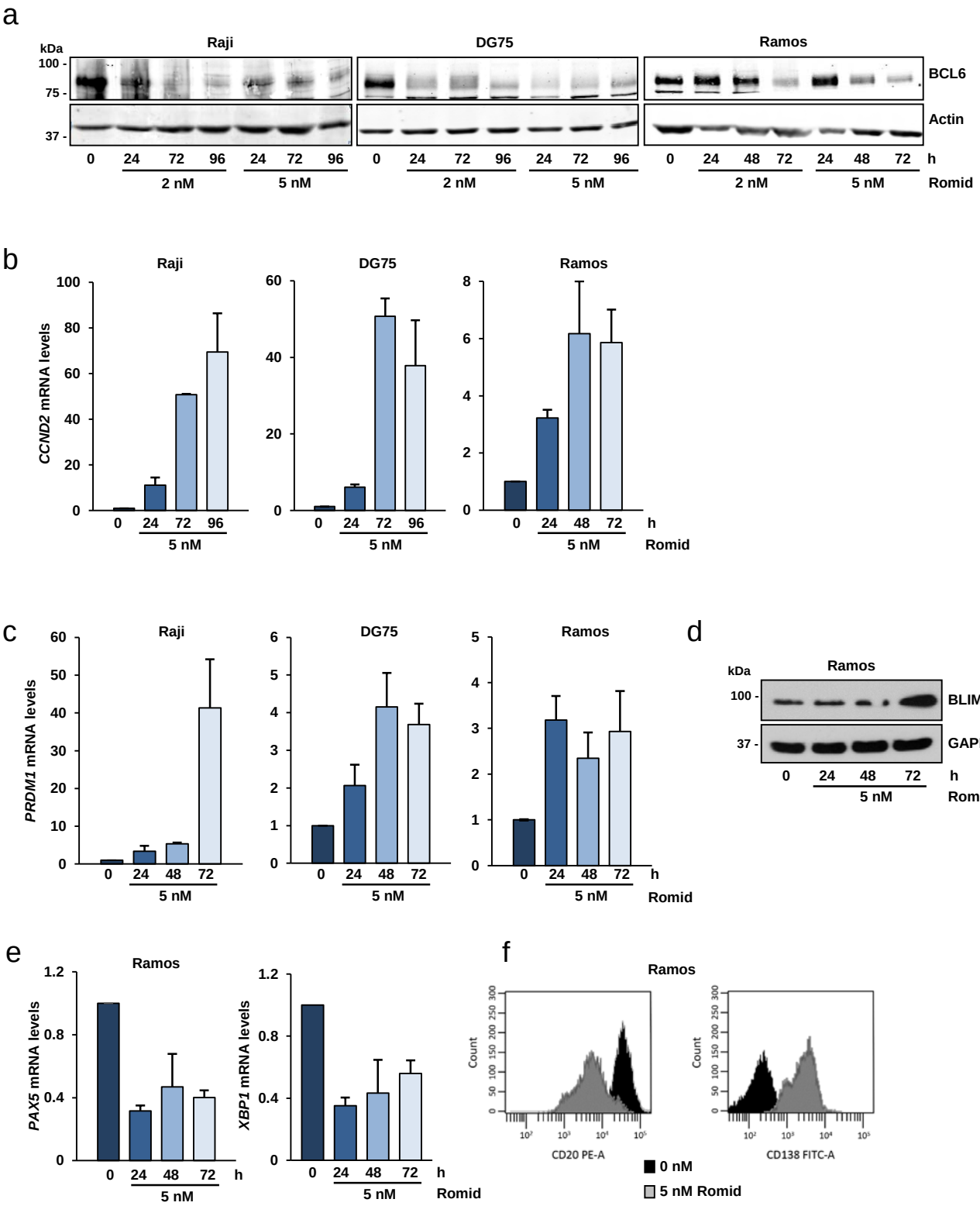

Figure 5. Cortiguera et al.

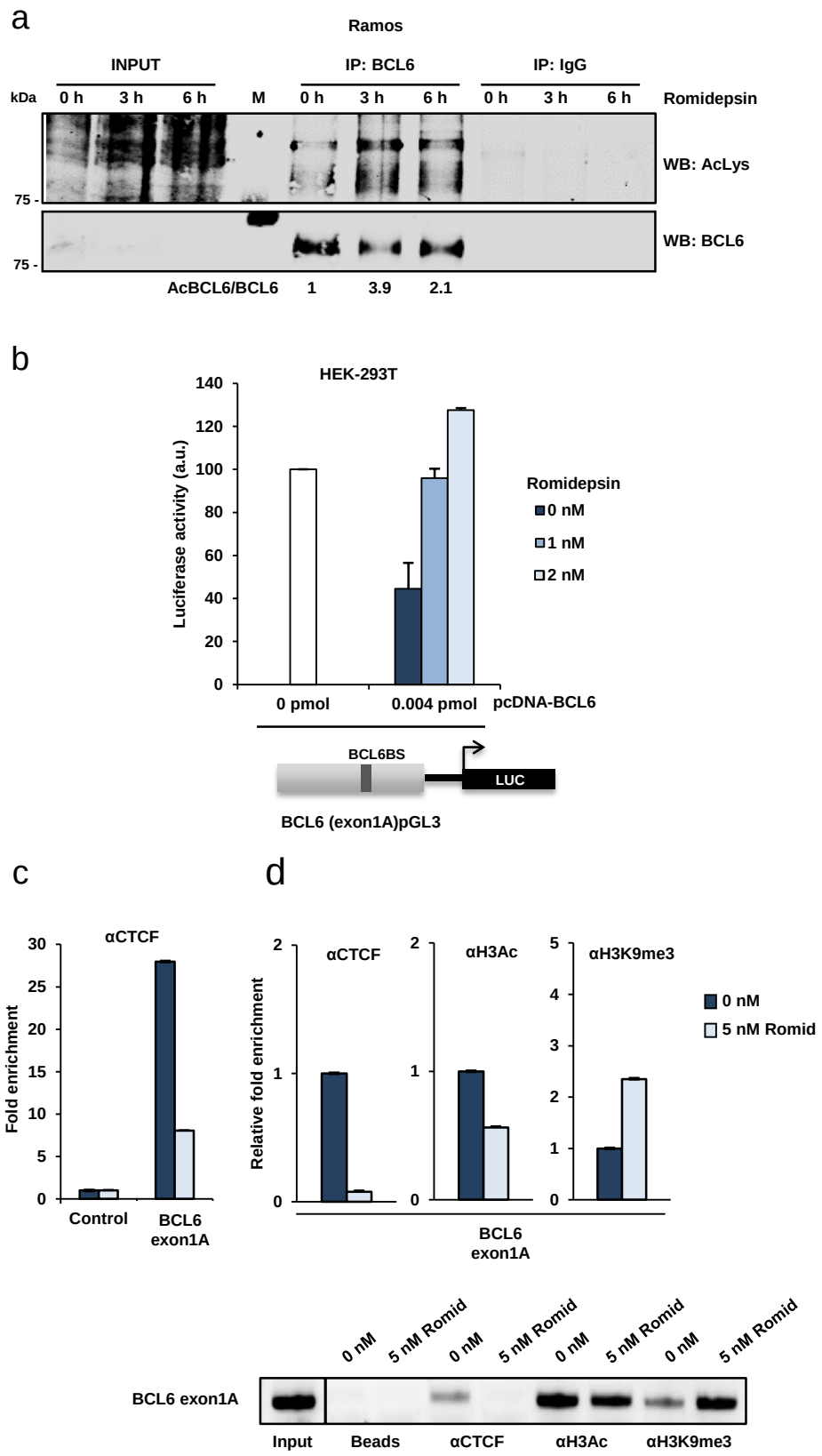

Figure 6. Cortiguera et al.

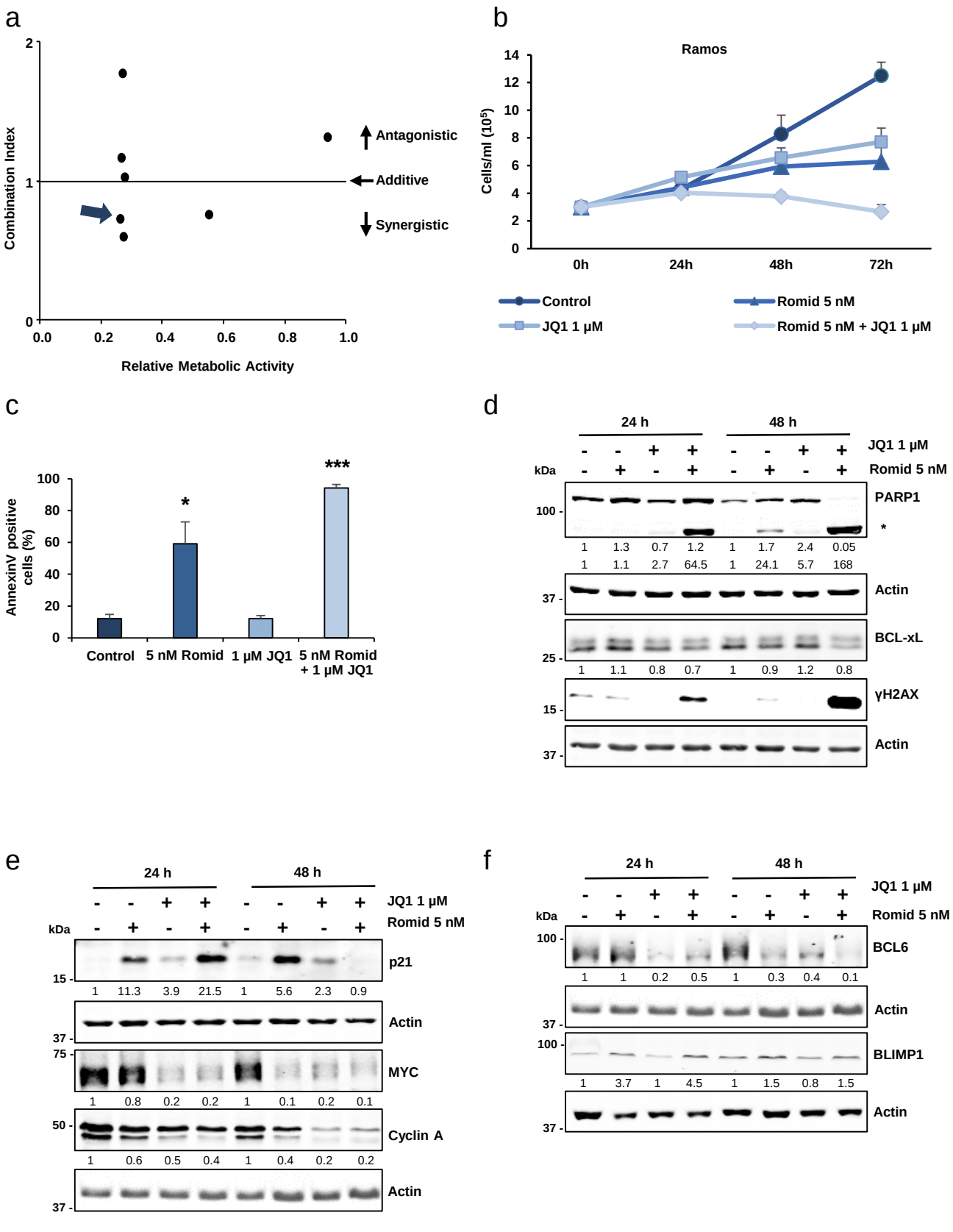

Figure 7. Cortiguera et al.

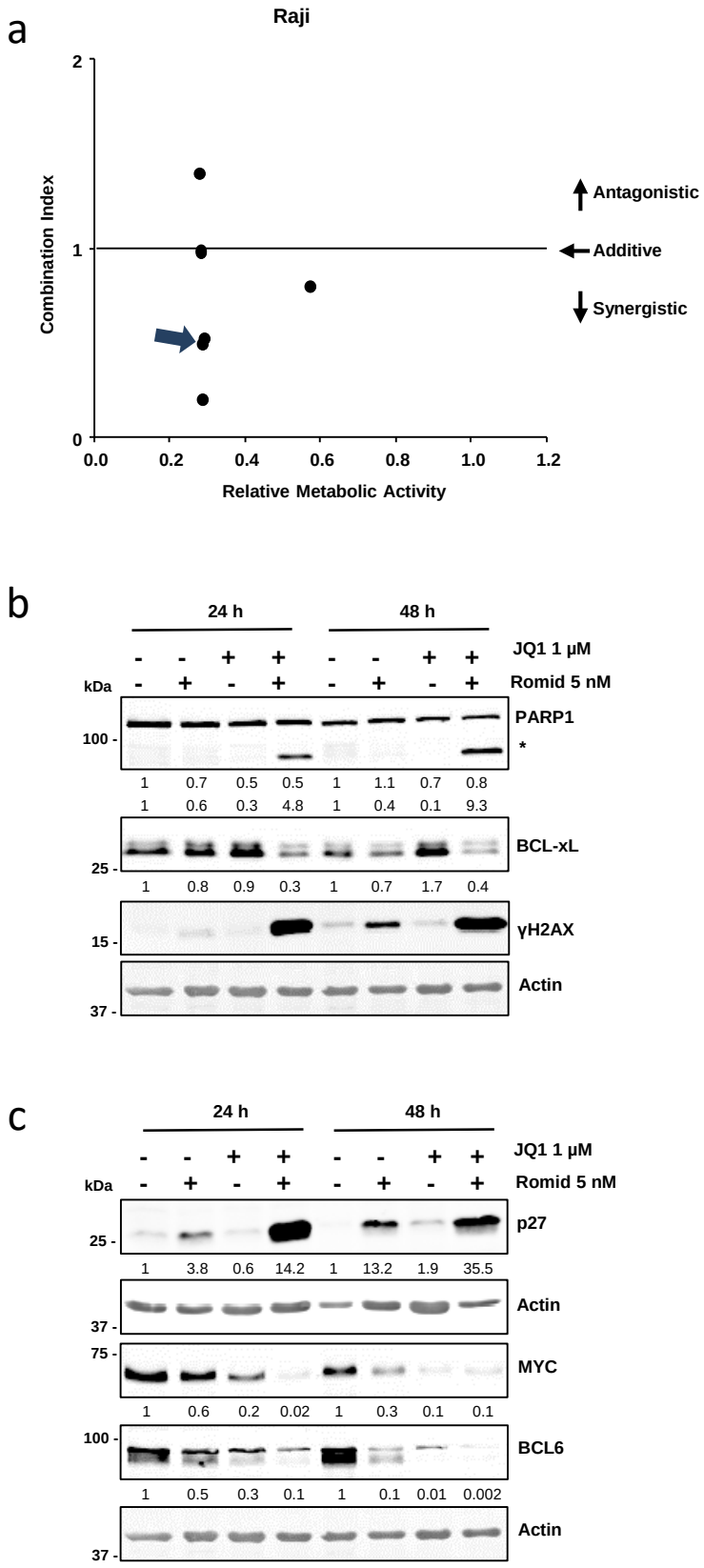

Figure 8. Cortiguera et al.

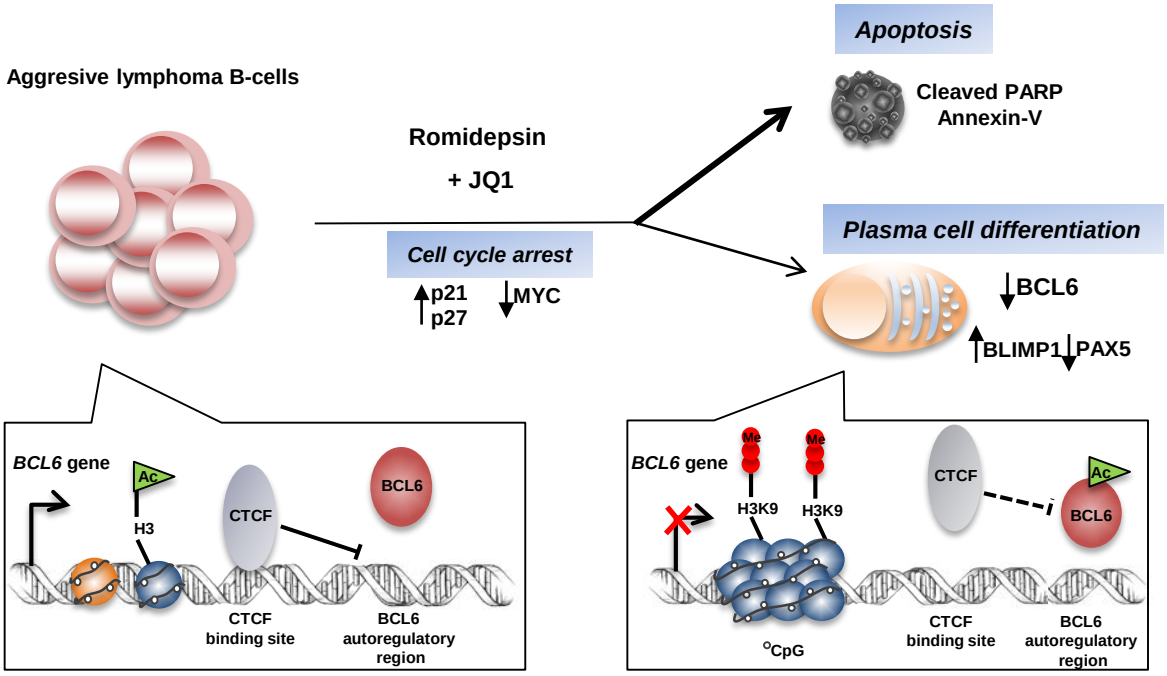

Supplementary Figure S1. Cortiguera et al.